



University of HUDDERSFIELD

University of Huddersfield Repository

Atallah, Suliman

Evaluation of Pharmacological Strategies Targeting the Glycolytic Phenotype of Cancer

Original Citation

Atallah, Suliman (2019) Evaluation of Pharmacological Strategies Targeting the Glycolytic Phenotype of Cancer. Doctoral thesis, University of Huddersfield.

This version is available at <http://eprints.hud.ac.uk/id/eprint/34928/>

The University Repository is a digital collection of the research output of the University, available on Open Access. Copyright and Moral Rights for the items on this site are retained by the individual author and/or other copyright owners. Users may access full items free of charge; copies of full text items generally can be reproduced, displayed or performed and given to third parties in any format or medium for personal research or study, educational or not-for-profit purposes without prior permission or charge, provided:

- The authors, title and full bibliographic details is credited in any copy;
- A hyperlink and/or URL is included for the original metadata page; and
- The content is not changed in any way.

For more information, including our policy and submission procedure, please contact the Repository Team at: E.mailbox@hud.ac.uk.

<http://eprints.hud.ac.uk/>

University of
HUDDERSFIELD

Evaluation of Pharmacological Strategies
Targeting the Glycolytic Phenotype of
Cancer

Suliman Atallah

A thesis submitted for the partial fulfilment of the
requirements for the degree of Doctor of Philosophy

The University of Huddersfield

April 2018

Abstract

The presence of hypoxia within tumours has significant biological and pharmacological implications leading to resistance to therapy and poor prognosis. The eradication of hypoxic cells has been a major goal for many years but despite decades of research, no hypoxia specific therapies have been approved for use in humans. The purpose of this thesis is to explore the possibility of targeting the glycolytic phenotype of cancers with the aim of specifically eradicating hypoxic cells.

Initial studies using a series of glycolytic inhibitors (3-bromopyruvate, 2-deoxyglucose and sodium oxamate) did not show hypoxia selectivity *in vitro* and in several cell lines, resistance under hypoxia (0.1% oxygen) occurred. In the case of the pyruvate dehydrogenase kinase 1 (PDK1) inhibitor dichloroacetate (DCA) however, hypoxia selectivity was observed *in vitro* but the magnitude of the sensitisation was much less than that of the hypoxia activated prodrug tirapazamine. Nevertheless, DCA did inhibit PDK1 leading to reduced phosphorylation of the pyruvate dehydrogenase complex and hypoxia selective cell kill.

These results questioned whether glucose was indeed important for the survival of hypoxic cells but studies where glucose was removed from culture media confirmed that glucose is required for the survival of hypoxic cells *in vitro*. Using this model, mannose was also shown to be an important monosaccharide that could support the growth of cells under hypoxia opening up a novel avenue for future research. Finally, a series of novel organometallic complexes based on the metal silver were explored as potential glycolytic inhibitors. The silver N-heterocyclic carbene Ag8 was shown to be a potent and selective inhibitor of lactate dehydrogenase A (LDH-A) leading to reduced export of lactate from cells. Ag8 has a complex mechanism of action with inhibition of LDH-A being a novel mechanism.

In conclusion, this study has demonstrated that targeting key enzymes in the glycolytic pathway does not generate hypoxia selective cytotoxic effects. This conclusion is surprising and reflects the complexity of targeting cellular metabolism. The identification of mannose as an important fuel for hypoxic cells opens up new avenues for research and the inhibition of LDH-A by organometallic complexes such as Ag8 requires further studies.

Acknowledgments

First I would like to thank my supervisor Prof. Roger Phillips and my co-supervisor Dr. Simon Allison. It was a great pleasure for me to do this research with you and that will remain a great memory for me. Thank you for all of your teaching, guidance and support all over my journey. Thank you for reviewing my thesis and for correcting the many spelling errors and for all the hours you spent helping me.

I would also like to thank my colleagues: Scott, Omar, Sam, Tsitsi and Hollie. Thank you for the understanding, your kindness and support. I also would like to thank, Urfan Sabir and James Rooney for their listening, their patience and processing a 'million' orders, all of which were urgent! I would like to say big thanks to my best friend Dionne Coburn who passed away after a short time fighting bladder cancer.

To Dad and Mom, that's it, we're at the end of studies! Thank you for your permanent presence at my side and for all the sacrifices you have made to allow me to get there. Thank you also for all the love you give me every day since I was born. And finally, a huge thank you to my love and my little two angels Besan and Malik, my reason for being. You have been there for four years to live my dream through me so thank you for your patience. It was not always easy, helping me to support myself to calm my anger and to dry my tears and smile at me as only you know how to. Thank you for your support and for always believing in me. You have been very patient and especially last two months, thank you very much. Anything I can write will never be enough to tell you how much I love you and how happy I am to be your husband.

Contents

Chapter.1: Introduction	1
1.1 Introduction	1
1.2 Treatment of Cancer.....	3
1.3 The hypoxic tumour microenvironment.....	5
1.4 Therapeutic implications of tumour hypoxia.....	7
1.5 Therapeutic strategies designed to target hypoxic cells.	9
1.6 Hypoxia activated prodrugs – concluding remarks.....	17
1.7 Biological implications of tumour hypoxia.	17
1.8 The glycolytic phenotype of cancer – an emerging hallmark of cancer.....	22
1.9 Aerobic Glycolysis (Warburg effect).....	23
1.10 Glutamine metabolism	25
1.11 Regulation of metabolic pathways	27
1.12 Key enzymes in the glycolytic pathway	31
1.13 Use of inhibitors to target key enzymes in tumour glycolysis.....	33
1.14 Cellular metabolism under hypoxic conditions.....	36
1.15 Rationale and aims of this study	40
Chapter 2:Materials and general methods	42
2.1 Materials	42
2.2 Cells and cell culture conditions.....	42
2.3 Recovery of cell lines from storage in liquid nitrogen.	43

2.4 Routine maintenance and sub-culturing of cells.....	44
2.5 Cell counting using a haemocytometer	44
2.6 Chemosensitivity studies.....	46
2.6.1 Validation of the MTT assay.....	46
2.6.2 Chemosensitivity studies under aerobic or hypoxic conditions.	47
2.6.3 Chemosensitivity studies using short-term drug exposures.	51
2.7 Cell assays.....	52
2.7.1 Quantification of cell number and viability	52
2.7.2 Induction of Apoptosis.....	52
2.8 Western blotting	53
2.8.1 Sample preparation.....	53
2.8.2 Measuring protein concentration (BCA assay)	54
2.8.3 SDS-PAGE electrophoresis	55
2.8.4 Electrophoretic transfer of proteins	56
2.8.5 Blocking and immune-detection	57
Chapter 3: Evaluation of metabolic inhibitors as hypoxia selective agents .	59
3.1 Introduction	59
3.2 Additional methods.....	60
3.2.1 High Performance Liquid Chromatography (HPLC)	60
3.3 Results	61
3.3.1 Validation of the MTT assay	61

3.3.2 Determine the different of cancer cells grown under aerobic and hypoxic condition.....	62
3.3.3 Response of a HCT116 p53 ^{+/+} cell line to tirapazamine	63
3.3.4 Response of a panel of cell lines to DCA	64
3.3.5 Hypoxia cytotoxicity ratios (HCR) and selectivity ratios (SR)	67
3.3.6 Response of colorectal cancer cells following short time exposure to DCA ...	69
3.3.7 Short time exposure for DCA against colorectal cancer cells	72
3.3.8 Determination of DCA stability by using HPLC analysis.....	74
3.3.9 Influence of different growth media on the response of HCT116 cells to DCA	77
3.3.10 Dose response of colorectal cancer cells to different glycolytic inhibitors under hypoxic and normoxic conditions	80
3.3.11 Dose response of ovarian cancer cells to AKT inhibitors under hypoxic and normoxic conditions.....	89
3.3.12 Western blot analysis of cellular PDH phosphorylation levels in response to DCA treatment	92
3.3.12.1 Bradford assay calibration curve	92
3.3.12.2 Immunoblots.....	93
3.3.13 Measurement of cell viability and mitochondrial membrane potential of cells treated with DCA under hypoxic and aerobic conditions.	98
3.3.14 Comparison of the effects of different DCA treatment	105
3.4 Discussion	109

Chapter 4: Investigation of alternative carbon sources as metabolic fuels

.....	114
4.1 Introduction.....	114
4.2 Materials and Methods	115
4.2.1 Cell culture.....	115
4.2.2 Influence of glucose deprivation on cell growth	116
4.2.3 The recovery of cells following glucose deprivation under aerobic and hypoxic conditions	117
4.2.4 Validation of the results obtained using the MTT assay using the sulforhodamine B (SRB) assay.....	117
4.2.5 Analysis of alternative carbon sources to glucose	118
4.2.6 Western blot analysis of mannose 6 phosphate isomerase and mannose monophosphate.....	119
4.2.7 Influence of glutamine on the survival of cells	119
4.2.8 The effect of 2DG and 968 on the survival of cells.	120
4.2.9 Measuring glucose level into cell culture medium.....	122
4.3 Results.....	122
4.3.1 Influence of glucose deprivation on cell growth	122
4.3.2 Validation of results using the SRB assay	130
4.3.3 Recovery of cell survival following glucose deprivation	131
4.3.4 Influence of oxygen tension and glucose concentration	133
4.3.5 Influence of different sugars on cell growth in vitro under aerobic and hypoxic	

conditions.	136
4.3.6 Comparison between the ability of glucose and mannose to support the growth of cells under hypoxic conditions.	141
4.3.7 Influence of mannose to support the growth of DLD1 and PSN1 cells under hypoxic conditions.	145
4.3.8 Influence of fructose and sucrose on the survival of HCT116 p53 ^{+/+} and HCT116 p53 ^{-/-} cells under aerobic and hypoxic conditions.	147
4.3.9 Influence of L-glutamine and glucose deprivation on cell survival under aerobic and hypoxic conditions.....	152
4.3.10 Influence of glucose and glutamine on cell sensitivity to the glutaminase inhibitor 968.	154
4.3.11 The influence of glucose deprivation on cell viability and the cell cycle ...	158
4.3.12 Assessment of glucose-free complete media for trace of glucose	159
4.3.13 Assessment of M6PI and PMM2 expression	163
4.4 Discussion	167
Chapter 5:Inhibition of glycolytic enzymes by silver complexes.	171
5.1 Introduction	171
5.2 Materials and Methods.....	172
5.2.1 Compounds.....	172
5.2.2 Inhibition of purified Rabbit muscle LDH.	172
5.2.3 Analysis of LDH-A and LDH-B activity in a panel of cell lines.	174
5.2.4 Determination of protein concentration using the Pierce BCA assay.....	175

5.2.5 Western blot analysis of LDH-A and LDH-B protein expression.	175
5.2.6 Inhibition of LDH-A and LDH-B in cell lysates.	177
5.2.7 Release of lactate from cell cultures.	177
5.2.8 Analysis of the effect of Ag8 on NAD(H) and NAD/NADH ratios.	178
5.2.9 Inhibition of hexokinase by silver complexes	179
5.3 Results	180
5.3.1 Inhibition of purified rabbit lactate dehydrogenase.	180
5.3.2 Specific activity of LDH-A and LDH-B in a panel of cell lines	181
5.3.3 Protein expression of LDH-A and LDH-B in a panel of cell lines	182
5.3.4 Inhibition of LDHA and LDH-B in cell lysates.	184
5.3.5 Release of lactate from cells in culture.	185
5.3.6 Effect of Ag8 on NAD, NADH, NAD(H) and the NAD/NADH ratio.	188
5.3.7 Inhibition of hexokinase by silver complexes	193
5.4 Discussion.	194
Chapter 6: General Discussion	196
Chapter 7. References	207

List of Figures

Figure 1.1: Estimated age-standardised rates per 100,000 of cancer incidence and mortality in 2012.

Figure 1.2: Age standardised incidence and mortality rates (per 100, 0000) in selected countries as determined by the IACR.

Figure1.3: Cartoon of the structural and functional differences between the capillary networks within normal and tumour tissue.

Figure1.4: Generalised scheme for the activation of hypoxia activated prodrugs.

Figure1.5: Chemical structure of nimorazole and general mechanism for the hypoxia selectivity of nitroimidazoles.

Figure1.6: Mechanism of action of tirapazamine

Figure 1.7: Mechanism of action of TH-302.

Figure 1.8: Mechanism of action of TH-4000.

Figure1.9: Chemical structure and mechanism of action of Apaziquone (EO9).

Figure1.11: Structure and mechanism of action of PR-104A.

Figure 1.12: Regulation of HIF-1a and protein signalling under normoxic and hypoxic conditions.

Figure 1.13: the impact of HIF-1 α on tumour cells under hypoxic conditions.

Figure 1.14: The emerging hallmarks of cancer.

Figure 1.15: Glucose metabolism in normal cells and tumour cells.

Figure 1.16: Metabolic pathway for the biosynthesis of lipids.

Figure 1.17: Regulation of cell metabolism in proliferating cancer cells.

Figure 1.18: Chemical structures of known inhibitors of glycolysis.

Figure 1.19: Metabolic adaptations of tumours cells to hypoxia.

Figure 1.20: summarizes metabolic coupling of aerobic tumour cells and hypoxic tumour cells within a tumour.

Figure 1.21: Overview of the compounds used in this thesis and their sites of action in the metabolic pathways.

Figure 2.1: Cell counting using the haemocytometer.

Figure 2.2: Schematic showing MTT validation experimental design.

Figure 2.3: Schematic of the plate layout used to assess chemosensitivity.

Figure 2.4: Typical layout of the plate for conducting the Pierce BCA protein assay.

Figure 2.5: Electro-blotting sandwich used during western blot.

Figure 3.1: Relationship between cell number and absorbance in the MTT assay.

Figure 3.2 Percentage of cell survival of untreated cancer cell line under aerobic and hypoxic condition

Figure 3.3: Response of HCT116 p53^{+/+} following a continuous 96-hour exposure to tirapazamine under aerobic and hypoxic conditions.

Figure 3.4: Response of HCT116 p53^{+/+}, HCT116 p53^{-/-}, HT-29 and BE following a continuous 96 hour exposure to DCA under aerobic and hypoxic conditions.

Figure 3.5: Response of PANC 10.05 , LS123 , SW48 and ARPE-19 following a continuous 96-hour exposure to DCA under aerobic and hypoxic conditions.

Figure 3.6: Graphical representation of the response of cells to DCA.

Figure 3.7: Response of HCT116 p53^{-/-}, HCT116 p53^{+/+}, BE and HT-29 following a one-hour exposure to DCA under aerobic and hypoxic conditions.

Figure 3.8: Influence of drug exposure time on the response of HT29 and HCT116 p53^{+/+} to DCA.

Figure 3.9: Standard calibration curve to measure stability of DCA in medium at 37°C, 5% CO₂ and humid conditions over a 24 hour period.

Figure 3.10: Calibration curve and representative chromatograms for the analysis of DCA.

Figure 3.11: Response of HCT116 p53^{+/+} and HCT116 p53^{-/-} to DCA (1-hour exposure) in DMEM and RPMI1640 media.

Figure 3.12: Response of HCT116 p53^{+/+} cells to 2-deoxy-glucose (2-DG), 3-bromopyruvate (3-BP), sodium oxamate and gossypol under aerobic and hypoxic conditions.

Figure 3.13: Response of HT-29 cells to 2-deoxy-glucose (2-DG), 3-bromopyruvate (3-BP), sodium oxamate and gossypol under aerobic and hypoxic conditions

Figure 3.14: Response of HCT116 p53^{-/-} cells to 2-deoxy-glucose (2-DG), 3-

bromopyruvate (3-BP), sodium oxamate and gossypol under aerobic and hypoxic conditions.

Figure 3.15: Response of BE cells to 2-deoxy-glucose (2-DG), 3-bromopyruvate (3-BP), sodium oxamate and gossypol under aerobic and hypoxic conditions.

Figure 3.16: Summary of all the HCR data generated using a panel of glycolytic inhibitors and cell lines.

Figure 3.17: Response of IGROV cells to PP-1 to PP-3 under aerobic and hypoxic conditions.

Figure 3.18: Bradford calibration curve that was used to determine the concentration of cell lysates.

Figure 3.19: Western blot analysis of HCT116 p53^{+/+} cells treated with different dose of DCA under hypoxic and aerobic conditions for 72 hours.

Figure 3. 20: Western blot analysis of HCT116 p53^{-/-} cells treated with a different dose of DCA under hypoxic and aerobic conditions for 72 hours.

Figure 3.21: Western blot analysis of β -actin of treated cells with a different dose of DCA under hypoxic and aerobic conditions for 72 hours.

Figure 3.22: Mitochondrial potential membrane of HCT116 p53^{+/+} cells treated with a range of DCA concentrations under aerobic conditions for 72 hours.

Figure 3.23: Mitochondrial potential membrane of HCT116 p53^{+/+} cells treated with a range of DCA concentrations under hypoxic conditions for 72hours.

Figure 3.24: Summary of the effects of DCA on mitochondrial potential membrane,

cell number and cell viability of HCT116 p53^{+/+} cells treated under aerobic and hypoxic conditions for 72hours.

Figure 3.25: Mitochondrial potential membrane of HT29 cells treated with a range of DCA concentrations under aerobic conditions for 72 hours.

Figure 3.26: Mitochondrial potential membrane of HT29 cells treated with a range of DCA concentrations under hypoxic conditions for 72 hours.

Figure 3.27: Summary of the effects of DCA on the mitochondrial potential membrane, cell number and cell viability of HT29 cells treated under aerobic and hypoxic conditions for 72hours.

Figure 3.28: Mitochondrial membrane potential of HCT116 p53^{+/+} cells exposed 75mM DCA for different time periods under aerobic conditions.

Figure 3.29: Mitochondrial membrane potential of HCTt116 p53^{+/+} cells exposed to 75mM DCA for different time periods under aerobic conditions.

Figure 3.30: Mitochondrial membrane potential and viability of HCT116 p53^{+/+} cells exposed to 75mM DCA for different time points under aerobic conditions.

Figure 3.31 Mitochondrial membrane potential and viability of HCT116 p53^{+/+} cells exposed to 75mM DCA for different time points under aerobic conditions.

Figure 3.32 Mitochondrial membrane potential and viability of HCT116 p53^{+/+} cells exposed to 75mM DCA for different time points under aerobic conditions.

Figure 4.1: Influence of glucose concentration on the survival of HCT116 p53^{+/+} cells.

Figure 4.2: Influence of glucose concentration on the survival of HCT116 p53^{-/-} cells.

Figure 4.3: Influence of glucose concentration on the survival of HT29 cells.

Figure 4.5: Influence of glucose concentration on the survival of DLD1 cells.

Figure 4.6: Influence of glucose concentration on the survival of PSN-1 cells¹²⁹.

Figure 4.7: Influence of glucose concentration on cell survival using the SRB assay.

Figure 4.9: Influence of oxygen tension and glucose concentration on HCT116p53^{+/+} cell survival.

Figure 4.10: Influence of oxygen tension and glucose concentration on HCT116p53^{-/-} cell survival.

Figure 4.11: Effect of replacing glucose with various sugars on the survival of HCT116^{+/+} cells under aerobic conditions.

Figure 4.12: Effect of replacing glucose with various sugars on the survival of HCT116^{+/+} cells under hypoxic conditions.

Figure 4.13: Effect of replacing glucose with various sugars on the survival of HCT116^{-/-} cells under aerobic conditions.

Figure 4.14: Effect of replacing glucose with various sugars on the survival of HCT116^{-/-} cells under hypoxic conditions.

Figure 4.15: Influence of glucose or mannose on the survival of cells under hypoxia (0.1% oxygen).

Figure 4.16: Influence of glucose or mannose on the survival of cells under hypoxia

(0.1% oxygen) .

Figure 4.17: Influence of glucose or mannose on the survival of cells under hypoxia (0.1% oxygen) .

Figure 4.18: Influence of mannose concentration on the survival of DLD1 cells.

Figure 4.19: Influence of fructose concentration on the survival of HCT116 p53^{+/+} cells.

Figure 4.20: Influence of fructose concentration on the survival of HCT116 p53^{-/-} cells.

Figure 4.21: Influence of sucrose concentration on the survival of HCT116 p53^{+/+} cells.

Figure 4.22: Influence of sucrose concentration on the survival HCT116 p53^{-/-} cells.

Figure 4.23: Influence of glucose and L-glutamine concentration on cell survival.

Figure 4.24: Response of HCT116 p53^{+/+} and HCT116 p53^{-/-} cells to glutaminase inhibitor 968.

Figure 4.25: Response of HCT116 p53^{+/+} and HCT116 p53^{-/-} to 968 (96-hours exposure) in high glucose DMEM.

Figure 4.26: Response to 968 in high glucose DMEM.

Figure 4.27: Cell Cycle analysis.

Figure 4.28: Cell viability, and determination of loss of mitochondrial membrane potential.

Figure 4.29: Cell viability, and determination of loss of mitochondrial membrane potential.

Figure 4.30: Western blot analysis of MPI.

Figure 4.31: Western blot analysis of MPI.

Figure 4.32: Summary of key metabolic pathways.

Figure 4.33: Schematic summarising mannose metabolism.

Figure 5.1: Chemical structures of silver complexes.

Figure 5.2: Inhibition of purified rabbit muscle lactate dehydrogenase by a series of silver complexes and cisplatin (CIS20).

Figure 5.3: Specific activities of LDH-A and LDH-B in a panel of cell lines.

Figure 5.4: Preliminary western blot analysis of LDH-A and LDH-B.

Figure 5.5: Inhibition of LDH-A and LDH-B and percentage activity .

Figure 5.6: Lactate calibration curves.

Figure 5.7: Release of lactate from HCT116 p53^{-/-} cells.

Figure 5.8: The effect of Ag8 on extracellular levels of lactate .

Figure 5.9: Calibration curves for NADH and NAD.

Figure 5.10: Validation of the NAD(H) assay.

Figure 5.11: Morphological effects of Ag8.

Figure 5.12: The effect of Ag8 on the levels of NAD and NADH

Figure 5.13: Inhibition of yeast hexokinase by silver complexes.

Figure 6.2: Metabolism of mannose.

List of Tables

Table 2.1 Concentrations and chemical structures of glycolysis inhibitors used to target the glycolytic pathway of colon cancer cells under hypoxic and aerobic conditions

Table 2. 2: List of primary and secondary antibodies.

Table 3.1: Response of a panel of cancer and non-cancer (ARPE19) cells following continuous exposure to DCA under aerobic and hypoxic (0.1% oxygen) conditions

Table 3.2: Response of cell lines following a one-hour exposure to DCA under aerobic and hypoxic conditions

Table 3.3: Response of HCT116 cells to DCA (1-hour exposure) under aerobic and hypoxic conditions in DMEM and RPMI 1640 culture media.

Table 3.4: Response of a panel of cells lines to glycolytic inhibitors under aerobic and hypoxic conditions (continuous 96-hour drug exposure)

Table 5.1: Recipe for making a 4% stacking gel and a 15% separating gel.

Abbreviations

ATP	Adenosine triphosphate
AQ4N	Banaxantrone
ATCC	American tissue culture collection
BSA	Bovine serum albumin
DCA	Dichloroacetate
DMEM	Dulbecco's modified eagle medium
DMSO	Dimethyl sulfoxide
EGFR	Epidermal growth factor receptor
EO9	Apaziquone
ECACC	European Collection of Authenticated Cell Cultures
FIH	Factor inhibiting HIF
FBS	Fetal Bovine serum
GLS	Glutaminase
GLUT	Glucose transporters
GBM	Glioblastoma
HRE	Hypoxia-responsive elements

HK	Hexokinase
HIF1	Hypoxia inducible factor 1
HPLC	High-performance liquid chromatography
HAPs	Hypoxia activated prodrugs
IACR	International Agency for Research on Cancer
LDH-A	Lactate dehydrogenase A
MTT	the 3-(4,5-dimethylthiazol-2-yl)-2,5-diphenyltetrazolium bromide
NHC	N-heterocyclic carbenes
NF-κB	Nuclear factor-kappa β
OXPHOS	Oxidative phosphorylation
PO₂	Oxygen partial pressure
PHD	Prolyl hydroxylases
PGM	Phosphoglycerate mutase
PDK1	Pyruvate dehydrogenase kinase 1
PI3K	Phosphoinositide 3-kinase pathway
PDH	Pyruvate dehydrogenase
PDK	Pyruvate dehydrogenase kinase
PDPs	Pyruvate dehydrogenase phosphatase

PIP3	Phosphorylated phosphatidylinositol 3
PFKFB3	6-phosphofructo-2-kinase
PBS	phosphate buffered saline
p53	p53 tumour suppressor gene
RPMI1640	Roswell Park Memorial Institute 1640
ROS	Reactive oxygen species
SCO2	Synthesis of cytochrome C oxidase 2
TH-4000	Tarloxotinib
TIGAR	TP53-induced glycolysis regulator
TH-302	Evofofamide
TPZ	Tirapazamine
VHL	Von Hippel Lindau protein
2DG	2-deoxy-D-glucose
3-BP	3-Bromopyruvate

Chapter 1

1.1 Introduction to the cancer problem.

Cancer is a disease defined by an uncontrolled cell growth. The disease is common and represents an important cause of mortality in the world. In 2012, the World Health Organisation estimated that 8.2 million deaths and 32.6 million people living with cancer (within 5 years of being diagnosed) in the same time period occurred worldwide from cancer with about 4.1 million new cancer cases. The International Agency for Research on Cancer (IACR) and the World Health Organisation have provided estimates of cancer incidence and mortality rates in different parts of the world for 2012 and these are summarised in figure 1.1

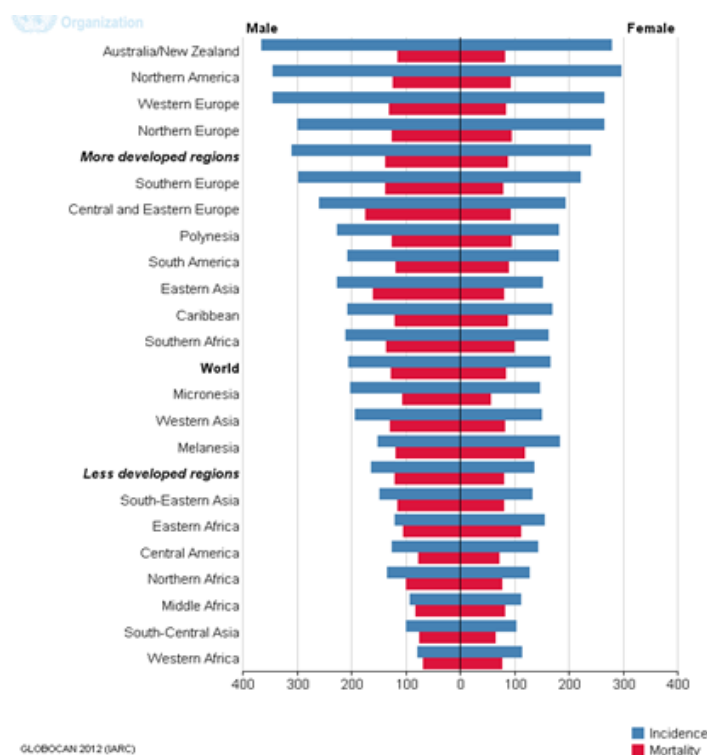


Figure 1.1 Estimated age-standardised rates per 100,000 of cancer incidence and mortality in 2012.

This figure was generated by the International Agency for Research on Cancer and full details of the report can be found elsewhere (www.globocan.iarc.fr). In total, the IACR estimated that there were 14.1million new cases of all cancer types in 2012, and there were also 8.2 million cancer deaths. There are clear geographical differences in both cancer incidence and mortality and whilst incidence is low in the less developed regions of the world, mortality rates are much higher reflecting poorer survival in these regions of the world.

In the UK, Cancer Research UK report that approximately 357,000 new cases of cancer were diagnosed in 2014 and of these, over half were breast, prostate, lung and bowel cancers. With regards to mortality in the UK in 2014, the estimated number of cancer related deaths was 163,000 with over half of these deaths being caused by lung, bowel, breast and prostate cancers (cancerresearchuk.org). Whilst the overall cancer burden both globally and in the UK remains a significant problem for healthcare providers, there is clear evidence that the 'war on cancer' is having an impact on mortality figures. This is illustrated in figure 1.2 which clearly demonstrates that whilst incidence is increasing, mortality rates are decreasing.

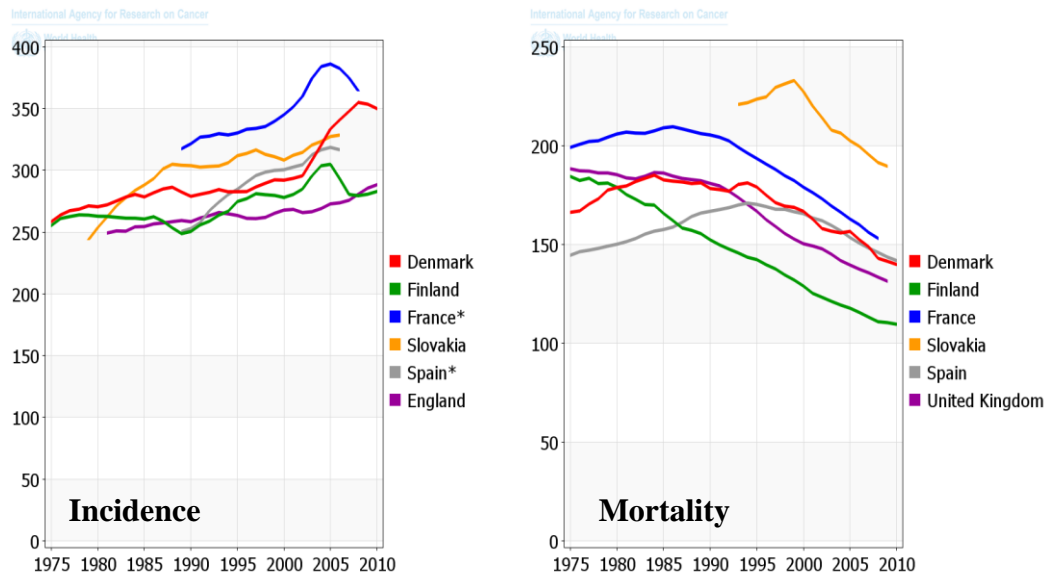


Figure 1.2 Age standardised incidence and mortality rates (per 100, 0000) in selected countries as determined by the IACR. Similar trends have been reported for other countries, full details of which can be found at www.globocan.iarc.fr

In summary, whilst the cancer problem remains a significant issue for society and incidence is indeed increasing, the decreased mortality rates demonstrate that significant progress is being made. Significant challenges nevertheless remain and the ‘war on cancer’ is being fought on many fronts. This includes avoidance of risks and therefore reducing incidence, early detection with the aim of detecting the disease before it has spread and the development of new therapeutics that selectively target key aspects of tumour biology.

1.2 Treatment of Cancer

Therapies available for the treatment of cancer typically include surgery, radiotherapy and chemotherapy. Cancer patients traditionally receive treatment depending on the type, grade and stage of cancer including how far it has spread at the time of the diagnosis. The recent emergence of targeted therapeutics and more

accessible methods of characterising genetic lesions in cancer offers the prospect of personalised medicine that's tailored to the needs of the individual (Ciardiello et al., 2014). This emerging field is under development and has the potential to change the way patients are treated in the clinic. Surgery is often used as the first treatment to remove the primary tumour and a margin of surrounding normal tissue. Surgery is often used in combination with radiotherapy which uses high energy radiation to cause damage to cancer cells. Cancer patients could receive external or internal radiotherapy, which might be before or after their surgery to decrease tumour growth and target the remaining tumour cells. Surgery and radiotherapy are successful modalities for treating localised tumours but once the tumour has spread beyond the primary site, a systemic based therapy is required. Chemotherapy is the term used to describe the use of drugs to kill cancer cells. These drugs may be administered via various routes but the majority are delivered to the tumour via the bloodstream and as such, they have the potential to target cancer cells anywhere in the body.

Chemotherapy for cancer can trace its origins back to nitrogen mustard derivatives of mustard gas used in the First World War. Since the pioneering studies of Gilman and Goodman in the 1940s, a number of drugs have been approved for use in humans (Goodman and Wintrobe, 1946). These drugs typically target the process of cell replication with alkylating agents, antimetabolites, anti-mitotic agents, anticancer antibiotics and others being widely described as 'classical' anticancer drugs (Goodman and Wintrobe, 1946). Whilst there have been considerable successes with the use of chemotherapy (typified by the use of cisplatin to treat testicular cancers), there are a number of significant limitations that remain significant

challenges to the successful treatment of cancers. The most significant barriers to successful treatment are toxicity to normal tissues and resistance to chemotherapy.

Whilst toxicity to normal tissues is dose limiting and can be life threatening, a major issue faced by chemotherapy is drug resistance. This problem affects just about all anticancer drugs, including the modern targeted drugs and is a major contributing factor to the mortality caused by cancer (Holohan et al., 2013). Usually the term drug resistance applies to acquired drug resistance where changes in target biochemistry (reduced expression, mutations in the target gene and protein for example), increased drug efflux, decreased drug uptake, detoxification and reduced cellular response to drug induced damage occur following exposure to chemotherapy (Housman et al., 2014). Since the seminal work of Thomlinson and Gray in the 1950s (Thomlinson and Gray, 1955, Dendy and Wardman, 2006), the role of the tumour microenvironment and hypoxia in particular in the therapy resistance phenotype has generated considerable interest. The adaptation of tumour cells to hypoxia and acidosis is now regarded as one of the driving forces behind tumour progression and metastasis as its association with tumour progression and a poor therapeutic outcome (Bertout et al., 2008, Brahimi-Horn et al., 2007). The development of therapeutic strategies designed to eradicate the hypoxic fraction of cells is therefore an important objective in cancer drug discovery.

1.3 The hypoxic tumour microenvironment

A key feature required for tumours to grow beyond a certain size (typically 1mm in diameter) is the establishment of a blood supply. As tumours progress, they undergo an 'angiogenic switch' leading to the production of growth factors that stimulate the

development of new blood vessels from existing blood vessels. This process is called angiogenesis and it is a recognised hallmark of cancer (Hanahan and Weinberg, 2000). The blood vessels that develop are however structurally and functionally different from the capillary network within normal tissues and these differences are summarised in figure 1.3

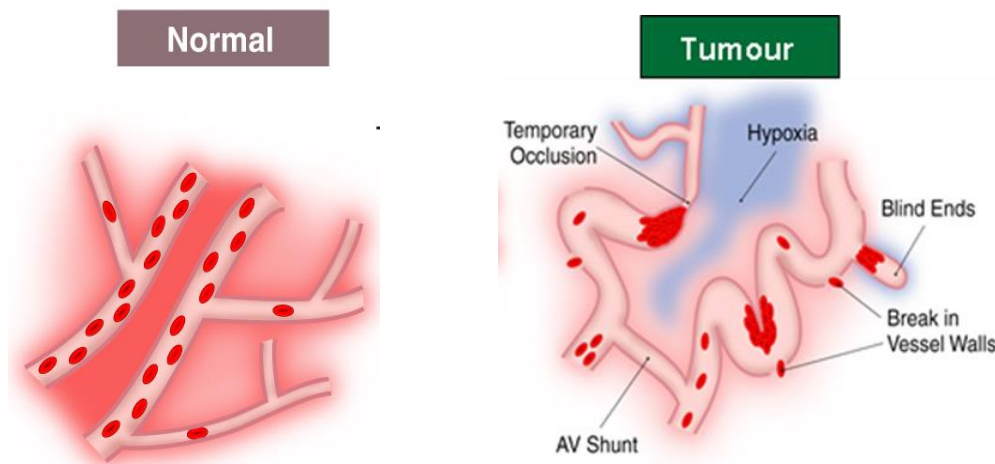


Figure 1.3 Cartoon of the structural and functional differences between the capillary networks within normal and tumour tissue. In contrast to normal tissues, the vascular network in tumours is poorly organised and structurally abnormal leading to regions that are poorly perfused with blood. This creates regions where oxygen tension is low (hypoxia) and it is associated with low extracellular pH, low nutrients and high levels of catabolites, all of which contribute to the hypoxic microenvironment (Brown and Giaccia, 1998).

In contrast to normal tissues where the capillary network is well organised and functionally efficient, the blood vessels in tumours are highly irregular, tortuous, have blind ends, premature linking of arterioles and venuoles (arterio-venous shunts), lack smooth muscle innervation, have abnormal pericyte coverage, have incomplete epithelial linings and basement membranes (Vaupel et al., 1989, Brown and Giaccia,

1998, Giaccia and Kastan, 1998). This results in a blood flow that is often poor, highly irregular and the vessels are 'leakier' leading to elevated interstitial fluid pressures within tumours (Heldin et al., 2004). All of these factors combine to generate a 'physiological' microenvironment within tumours, the severity of which increases as a function of distance from a supporting blood vessel (Quail and Joyce, 2013). This microenvironment is characterised by hypoxia, low extracellular pH, low nutrient status, low cell proliferation rates and high levels of catabolites but of these, hypoxia is the best studied. Numerous studies have demonstrated that hypoxia is a common feature in many if not all solid tumours although the extent and severity is highly heterogenous. The definition of hypoxia together with a summary of oxygen tensions measured in different tumours has recently been published (Grazia Cipolleschi et al., 2014). These studies clearly demonstrate that oxygen tensions within solid tumours is significantly lower than normal tissue with pancreatic and prostate cancers being profoundly hypoxic. The presence of hypoxia in tumours has both therapeutic and biological implications, details of which are reviewed below

1.4 Therapeutic implications of tumour hypoxia.

As stated previously, the seminal work of Thomlinson and Gray (Gray et al., 1953, Thomlinson and Gray, 1955) demonstrated that the presence of hypoxia in tumours contributed to resistance to radiotherapy. Radiation kills tumour cells either directly through DNA damage or indirectly via the formation of reactive oxygen species (ROS) which requires the presence of oxygen. Under hypoxic conditions (<0.4% oxygen), increased resistance to radiotherapy occurs and it is estimated that hypoxic cells are 3 fold less sensitive to radiotherapy compared to well oxygenated cells

(McKeown, 2014). There is now a substantial body of evidence demonstrating that hypoxia plays a role in resistance to radiotherapy in the clinic (Overgaard, 2011) with particularly significant effects observed in cervical cancer (Höckel et al., 1996), head and neck cancer (Brizel et al., 1999) and soft tissue sarcoma (Nordsmark et al., 2001). Resistance to radiotherapy is more complex than hypoxia alone but it nevertheless remains an important contributing factor to radio-resistance (Barker et al., 2015).

Similarly, the hypoxic microenvironment of tumours is associated with resistance to chemotherapy (Shannon et al., 2003). Resistance can occur via direct effects as drugs such as bleomycin require oxygen to generate free radicals capable of killing cells (Sikic, 1986). Indirect effects include barriers to drug delivery including elevated interstitial fluid pressure. Furthermore, the presence of hypoxia induces numerous adaptations at the cellular level leading to reduced efficacy of anticancer drugs (Harris, 2002). Many of these adaptations are mediated by the hypoxia inducible factor 1 (HIF) transcription factor, details of which are described below alongside other biological implications of tumour hypoxia.

1.5 Therapeutic strategies designed to target hypoxic cells.

Whilst the presence of hypoxic conditions within solid tumours is regarded as a problem (Barker et al., 2015), it paradoxically provides an opportunity for the development of novel therapeutic strategies designed to selectively kill hypoxic cells. One major strategy that has been explored over the past 40 years is the development of bioreductive or hypoxia activated prodrugs (HAPs). These are prodrugs that are designed to become active only under hypoxic conditions (Huttunen et al., 2011). HAPs are activated by one or two electron oxidoreductases to intermediates that have the ability to be converted back to the parent compound in the presence of oxygen. For example, the one-electron oxidoreductase mechanism is reversible in the presence of oxygen making the prodrug radical intermediate unstable. In the absence of oxygen, the intermediate is stabilised and can either be directly toxic to cells or undergo further reactions to generate a toxic product. The back oxidation of the prodrug radical can form superoxide in the presence of oxygen and this can be toxic to cells but in the absence of this oxygen, the prodrug radical produces highly cytotoxic products as it reduces and fragments further (Guise et al., 2014). In contrast, the two-electron reduction involves an irreversible mechanism and generally leads to a toxic metabolite that is oxygen independent with regards to its stability and activity. In this case, its activity is not dependent on oxygen but its selectivity is determined by the presence of elevated levels of two electron oxidoreductases in tumours (Figure 1.4) (Phillips, 2016).

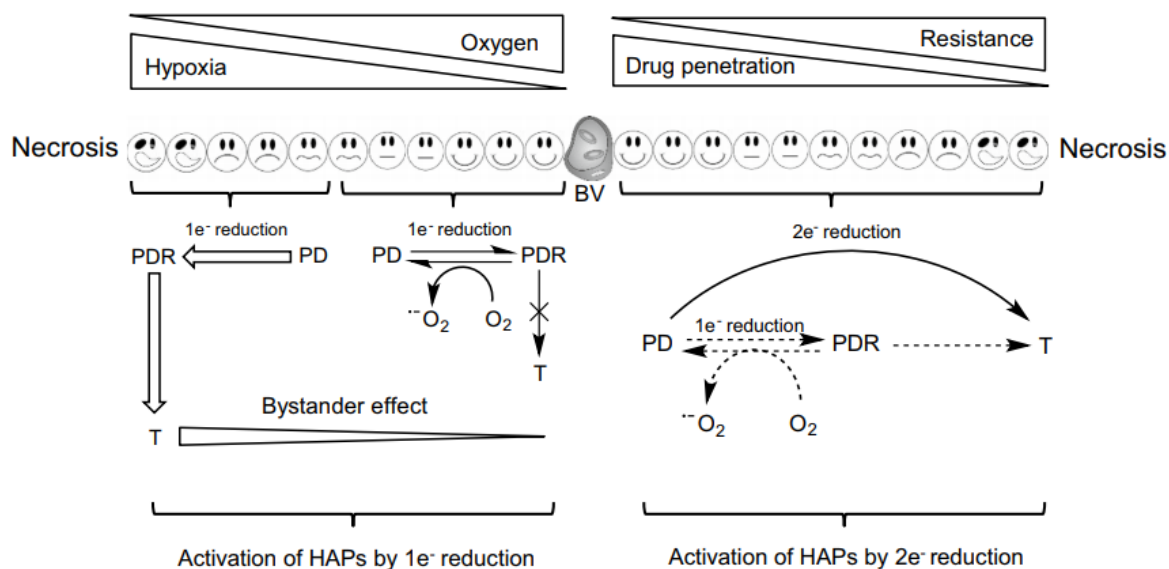


Figure 1.4 Generalised scheme for the activation of hypoxia activated prodrugs. This scheme depicts the general mechanisms by which HAPs are activated by one-electron and two-electron reductions in hypoxic and aerobic tumour cells. PD, PDR and T represent prodrug, prodrug radical and toxin respectively and BV denotes blood vessel in the diagram. The resistance and drug penetration notations in the diagram illustrate the role that the microenvironment plays in reducing delivery of cytotoxic drugs to hypoxic cells and the fact that these cells are generally resistant to chemotherapy (Phillips, 2016).

Numerous examples of chemical compounds that have been developed as HAPs have been described and these have been extensively reviewed elsewhere (Phillips, 2016, Guise et al., 2014). Briefly, the major classes/types of HAPs include:

(i) Nimorazole is structurally related to misonidazole and metronidazole and belongs to the class of 5-nitroimidazoles. Its chemical structure and a general mechanism for the activation of nitroimidazoles is presented in figure 1.5. It acts as a radiosensitizer and it is currently being evaluated in a phase III clinical trial (NIMRAD) in combination with radiotherapy study against head and neck cancer, laryngeal cancer and oral cancer (Cancer Research UK).

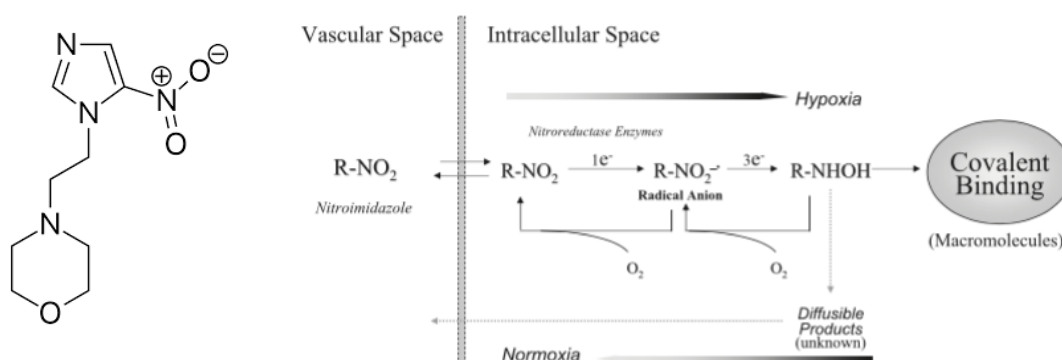


Figure 1.5 Chemical structure of nimorazole (left) and general mechanism for the hypoxia selectivity of nitroimidazoles (right). Once inside the cell, the prodrug is reduced by one electron reductases to intermediates that can be back oxidised to the parent compound in the presence of oxygen. In the absence of oxygen, further reduction takes place ultimately leading to DNA damage (Takasawa et al., 2008).

(ii) Tirapazamine (TPZ) is an aromatic N-oxide. Its mechanism of action is presented in figure 1.5 and following reduction by one electron reductases such as cytochrome P450, DNA damage is caused by spontaneous decay to generate an hydroxyl radical or an oxidising benzotriazinyl radical leading to inhibition of topoisomerase II (Brown and Wilson, 2004). In the presence of oxygen, the tirapazamine free radical is back oxidised to the parent compound and it is this that gives tirapazamine

hypoxia selective cytotoxic properties. Its efficacy in combination with radiotherapy and cisplatin chemotherapy was demonstrated with many hypoxic cell lines and with various in vivo studies on xenografts of human tumours (Brown and Wilson, 2004). Unfortunately, tirapazamine failed to demonstrate sufficient clinical evidence of efficacy (Jameson et al., 2010, Rischin et al., 2010).

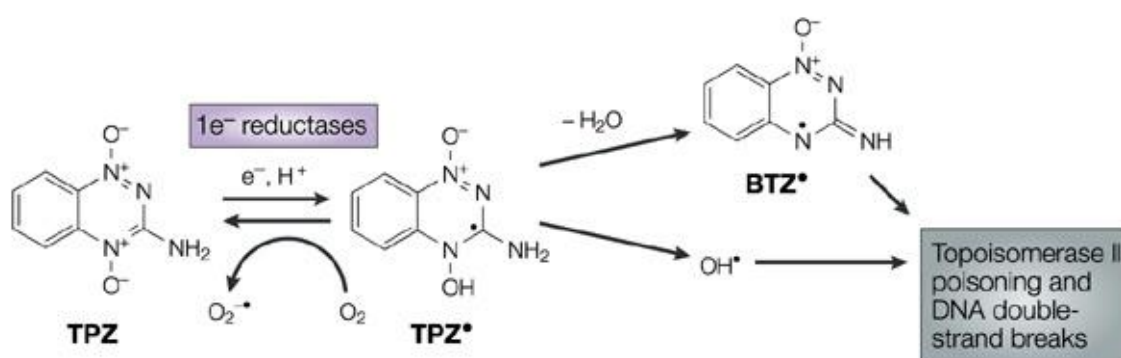


Figure 1.6 Mechanism of action of tirapazamine (Brown and Wilson, 2004)

(iii) Evofosfamide (TH-302) is a 2-nitroimidazole compound conjugated to a bromo-isophosphoramine mustard. Its mechanism of action is shown in figure 1.7 and it has been shown that its effectiveness is increased in hypoxic conditions compared to aerobic cells in vitro. This compound also targets hypoxic tumour cells in xenograft models of tumours in vivo and showed promise in phase II clinical trials (Borad et al., 2015). Unfortunately, the results of phase III clinical trials (MAESTRO trial) of TH-302 in combination with gemcitabine against pancreatic cancer and soft tissue sarcoma proved disappointing (Van Cutsem et al., 2016).

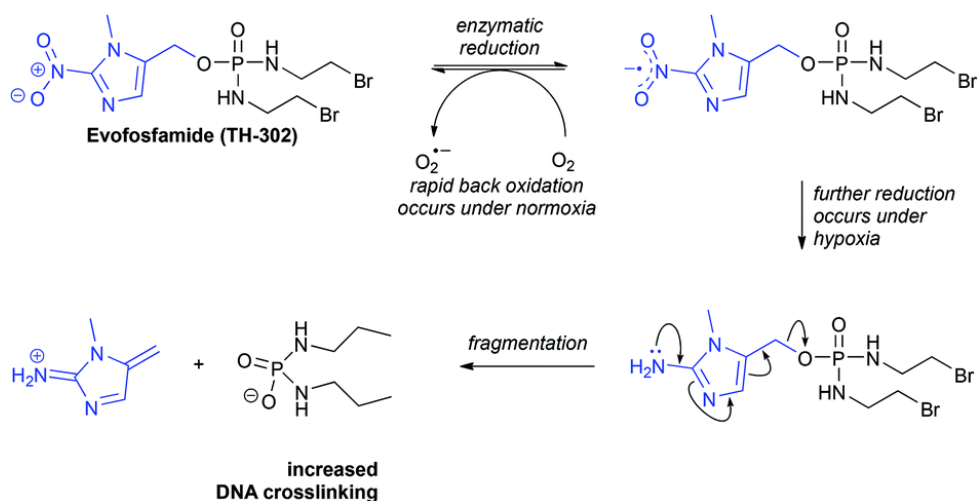


Figure 1.7 Mechanism of action of TH-302. In the absence of oxygen, the nitro group is reduced (and doesn't undergo redox cycling) resulting in stabilisation of reactive intermediates that subsequently fragment to release the active drug (O'Connor et al., 2015)

(iv) Tarloxotinib (TH-4000) is a prodrug that releases a potent tyrosine kinase inhibitor of the epidermal growth factor receptor (EGFR) under hypoxic conditions. Its structure and mechanism of action is illustrated in figure 1.8 and preclinical studies have shown it has efficacy against a number of experimental models including lung tumours. It is currently in Phase II clinical trials for the treatment of lung, head and neck cancer and melanoma.

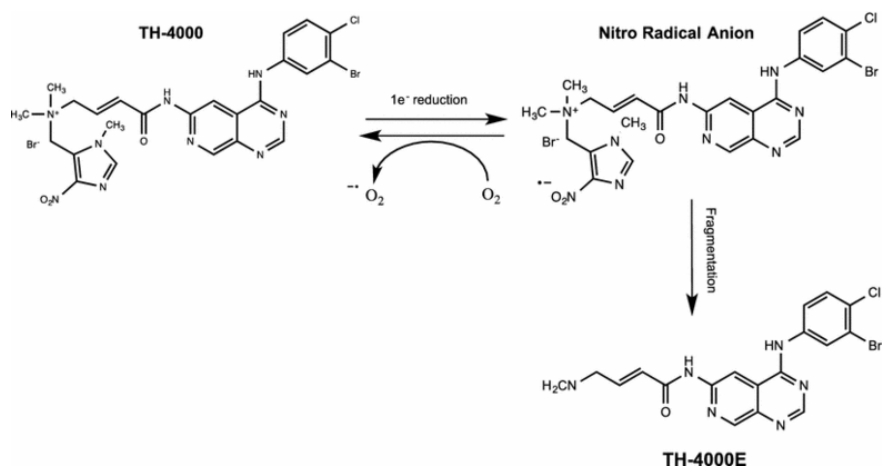


Figure 1.8 Mechanism of action of TH-4000. The potent EGFR inhibitor TH4000E is released from the prodrug by 1 electron reduction and lack of redox cycling in the absence of O_2 (Phillips, 2016).

(v) Apaziquone (EO9) is an indolequinone derivative of mitomycin C. This molecule is reduced by either one (such as cytochrome P450 reductase) or two electron reductases (such as NAD(P)H Quinone oxidoreductase 1, NQO1) and has the ability to target both hypoxic and aerobic tumours based on the relative amounts of one and two electron reductases in the tumour (Phillips, 2016). Its chemical structure and proposed mechanism of action is presented in figure 1.9. It has had a chequered history in the clinic but is currently in phase III clinical trials against superficial bladder cancer where it is administered intravesically as a loco-regional therapy (Phillips, 2016).

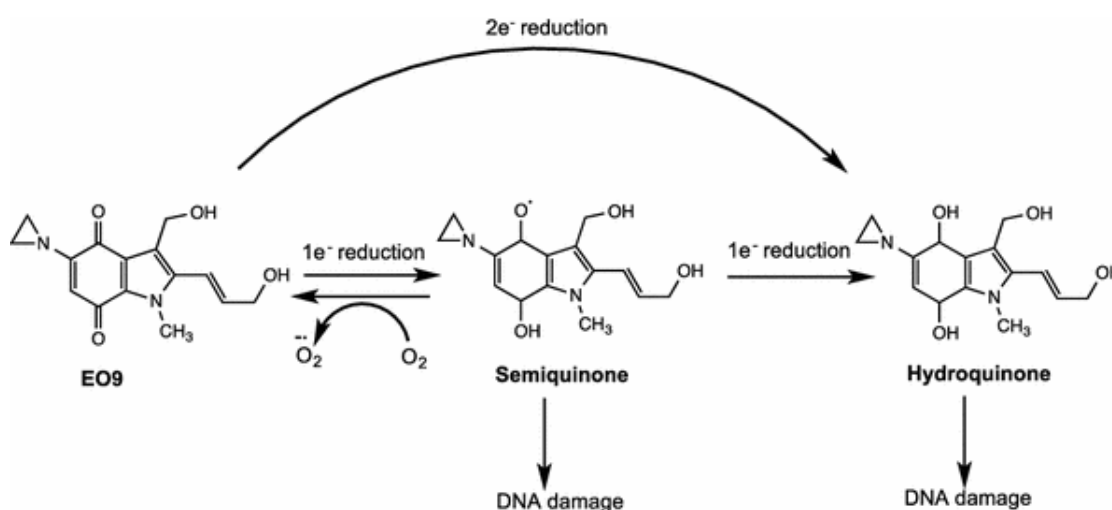


Figure 1.9 Chemical structure and mechanism of action of Apaziquone (EO9). Reduction of the quinone by one-electron oxidoreductases generates the semiquinone that undergoes redox cycling in the presence of oxygen. In the absence of oxygen, further reduction to the hydroquinone generates DNA damaging species. Two electron reduction is effectively oxygen independent and in this case, selectivity is determined by the expression of enzymes such as NQO1 in tumours (Phillips, 2016).

(vi) Banoxantrone (AQ4N) is an aliphatic N-oxide metabolized by cytochrome P450 and by the inducible NO synthase to AQ4, which is a potent topoisomerase II inhibitor. Its chemical structure and mechanism of action is presented in figure 1.10. The parent compound undergoes sequential two electron reduction to AQ4M and then AQ4 in a process that's inhibited by oxygen. AQ4 inhibits topoisomerase activity when hypoxic cells try to enter the cell cycle following reoxygenation caused by partner therapeutics killing the aerobic fraction. This molecule has shown antitumor, anti-metastatic and antiangiogenic effects in preclinical models of cancer in combination with radiotherapy and phase I clinical trials were promising (Albertella et al., 2008). AQ4N is currently not undergoing further clinical development because of commercial reasons but new analogues of AQ4N are being developed by OncoTherics.

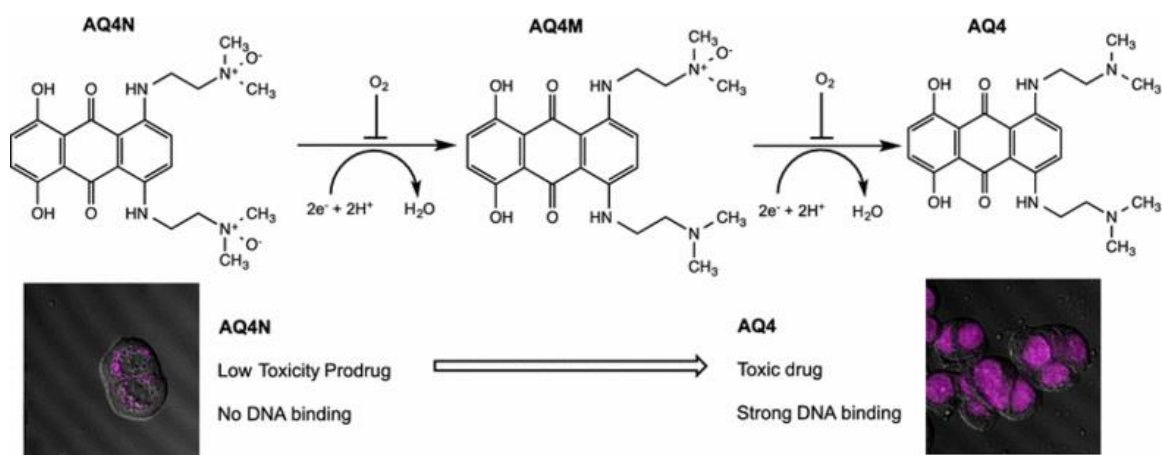


Figure 1.10 Chemical structure of AQ4N and reductive activation to the potent topoisomerase inhibitor AQ4 (Phillips, 2016). AQ4N is reduced by various cytochrome P450 isoforms to the mono-N-oxide (AQ4M) and subsequently AQ4. This process is inhibited by oxygen as it outcompetes AQ4N for the haem center within the CYP enzymes. The images represent cells treated with either AQ4N (showing no binding to the nucleus) or AQ4 (showing strong binding to the nucleus).

(vii) PR-104 is a nitro-aromatic 'pre-prodrug' and its structure and mechanism of action is outlined in figure 1.11. The initial reaction is removal of the phosphate group by phosphatases and this can occur in both aerobic and hypoxic cells. The product (PR-104A) is then metabolized to nitro radical intermediates which can be back oxidised to the non-toxic PR104A form. In the absence of oxygen, the nitro radical can be reduced further to generate the active products PR-104H and PR-104M. Reduction of PR-104A by aldo-ketoreductases (a two electron reduction step) bypasses the oxygen sensitive intermediate and can generate active metabolites under both aerobic and hypoxic conditions depending upon the enzymology of the tumour. PR-104A is undergoing clinical trials against acute myeloid leukaemia and acute lymphoblastic leukaemia (Konopleva et al., 2015).

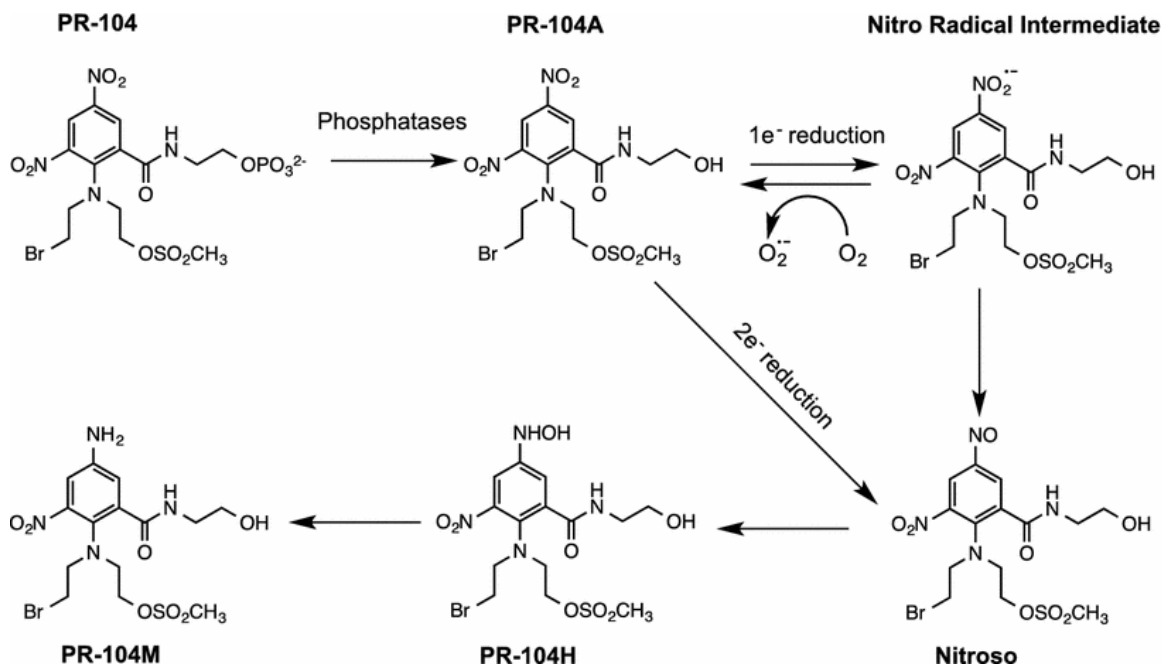


Figure 1.11 Structure and mechanism of action of PR-104A (Phillips, 2016)

1.6 Hypoxia activated prodrugs – concluding remarks

Whilst the concept underpinning the development of HAPs or bioreductive drugs is elegant and attractive, the disappointing outcome of nearly 40 years of research is that no new drugs that are specifically designed to eradicate hypoxic cells have successfully been approved for use in humans as yet. Numerous reasons for the failure of these compounds in clinical trials have been put forward and whilst the lack of success is frustrating, it has provided scientists with a wealth of knowledge that can be incorporated into the preclinical and clinical evaluation of the next generation of HAPs. As described above, new HAPs are currently in clinical trial but attention is switching to developing alternative approaches that are designed to exploit some of the biological features of hypoxic cells, details of which are covered in the following sections.

1.7 Biological implications of tumour hypoxia.

As stated above, hypoxia is a key feature of the tumour microenvironment and it affects the biological activity of tumour cells. Tumour hypoxia plays a significant role in tumour progression leading to tumours becoming more invasive, aggressive and resistant to therapeutic agents (Vaupel and Mayer, 2007). Unlike normal tissue, the tumour vasculature is of poor quality and does not allow a sufficient supply of oxygen to tumour cells that exist some distance away from a blood vessel (Brizel et al., 1999). The tumour regions are considered hypoxic when the oxygen partial pressure (PO₂) is close to or less than 10 mmHg (Harrison and Blackwell, 2004). These hypoxic zones have been found in a large number of human tumours including tumours of the breast, cervix, lungs, prostate, rectum, pancreas, colon, brain, and

melanoma (Yoshimura et al., 2004, Brown and Wilson, 2004, Vaupel and Mayer, 2007). Cells that reside in hypoxic areas have to adapt to these challenging conditions and the master regulator of these adaptations is the transcription factor hypoxia inducible factor 1 (HIF1).

Under hypoxic conditions, HIF1 becomes active and the key regulatory steps involved are presented in figure 1.12. HIF is complex heterodimeric protein composed of an α subunit that is sensitive to oxygen and a β subunit that is insensitive to oxygen. Under normoxic conditions, HIF-1 α has only a short half-life as prolyl hydroxylases (PHD) and factor inhibiting HIF (FIH) add hydroxyl groups to proline residues 402 and 564 (in the case of PHD) and asparagine 803 (in the case of FIH). Hydroxylated prolines 402 and 564 are targeted by the tumour suppressor von Hippel Lindau (VHL) which adds ubiquitin leading to proteosomal destruction (Martin, 2005; Maxwell, 1999). FIH adds hydroxyl groups to asparagine 803 and this prevents the binding of transcriptional co-activators (Poyya et al., 2017). PHDs and FIH are dioxygenases and do not work in the absence of oxygen and this leads to rapid intracellular accumulation of HIF-1 α (Klaassen et al., 2013). After translocation into the cell nucleus, HIF-1 α complexed to HIF-1 β to form active HIF1, then binds to specific DNA sequences called hypoxia-responsive elements leading to transcription of the corresponding target genes (Cay et al., 1992). Numerous human and veterinary studies have shown a correlation between the increased expression of HIF-1 in tumours and the malignancy of tumours (Majmundar et al., 2010). HIF-1 plays a key role in controlling how cells adapt to oxygen depletion and it triggers the expression of genes involved in angiogenesis, oxygen consumption, promotes the

glycolytic phenotype, supports cells that have a stem cell-like phenotype and selects for more aggressive, metastatic cells (Ahluwalia and S Tarnawski, 2012).

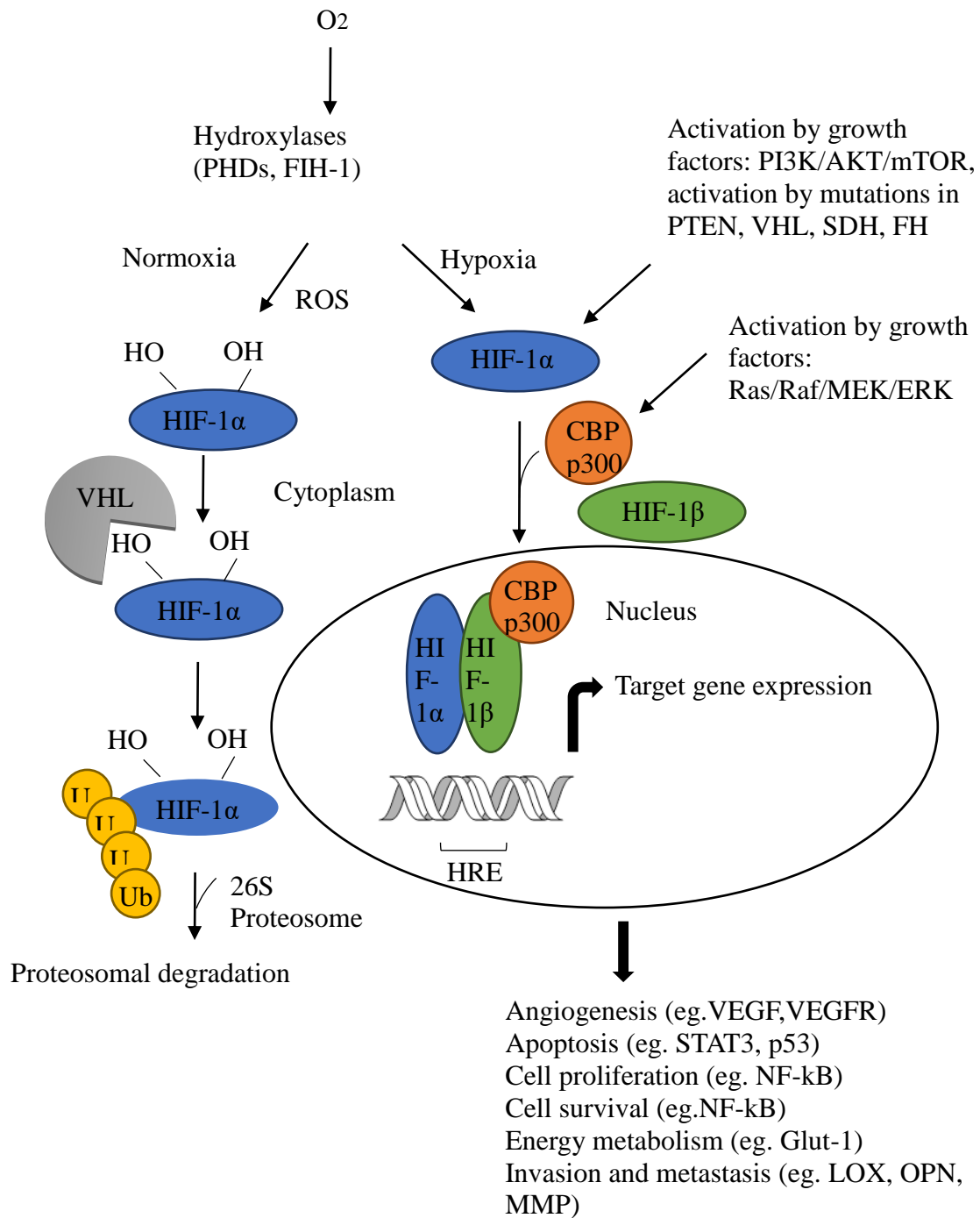


Figure 1.12 Regulation of HIF-1 α and protein signalling under normoxic and hypoxic conditions (Walsh et al., 2014).

HIF1 directly impacts upon a number of key biological processes and these are summarised in figure 1.13. Full details of its impact upon processes such as angiogenesis and cell survival can be found elsewhere (Walsh et al., 2014, Vaupel and Harrison, 2004) but the remainder of this chapter will focus on the effects of hypoxia and HIF1 on the metabolic phenotype of cancers. To place the effects of hypoxia on metabolism into context, the metabolic phenotype of cancer will be discussed first.

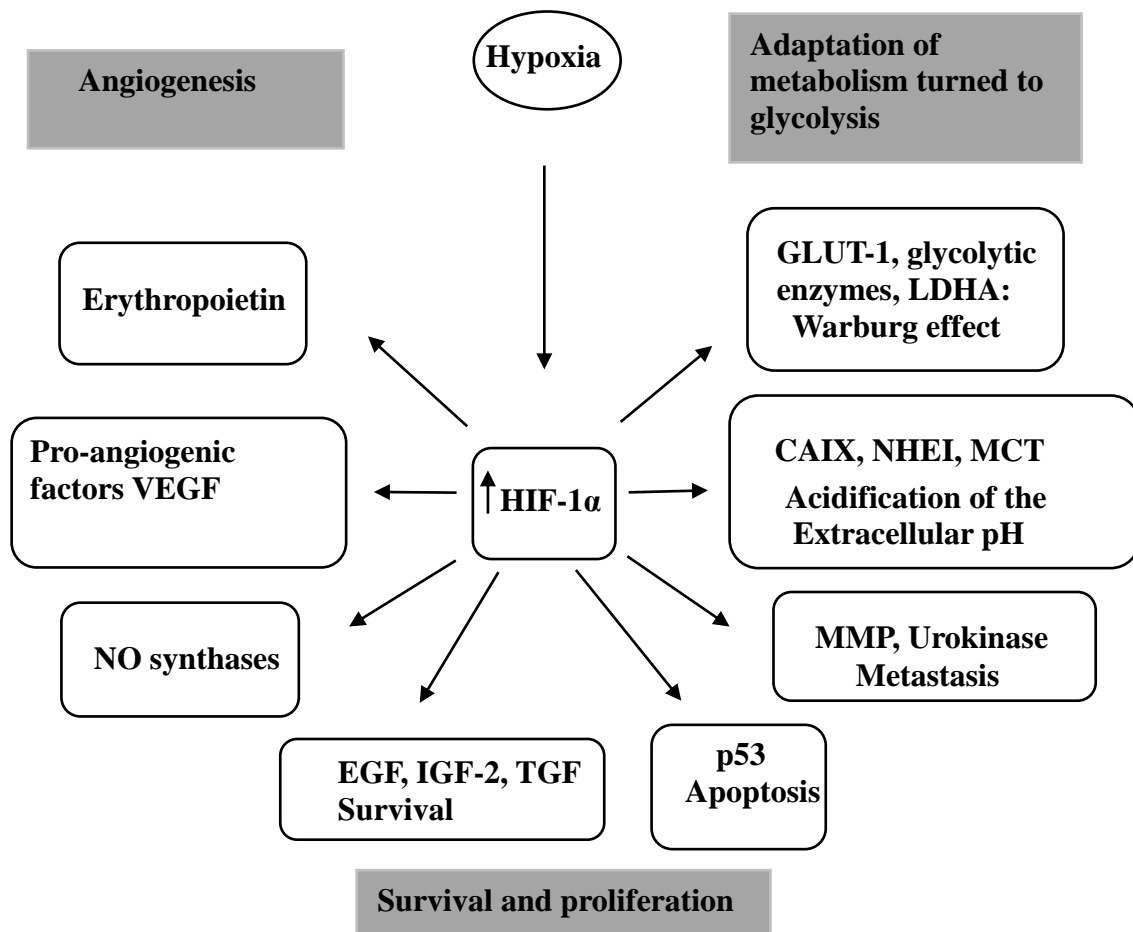


Figure 1.13 The impact of HIF-1 α on tumour cells under hypoxic conditions. Hypoxia causes stabilization of the factor HIF-1 α and this co-ordinates the expression of many genes involved in the response of tumour cells to hypoxia (Vaupel and Harrison, 2004).

1.8 The glycolytic phenotype of cancer – an emerging hallmark of cancer.

In 2000, Hanahan and Weinberg proposed the concept of "hallmarks of cancer" and they have identified six characteristics (abnormalities) that a normal cell acquires during the process of tumorigenesis. These include self-sufficiency in growth signals, the avoidance of growth inhibitory signals, the ability to invade and metastasize, replicative immortality, the induction of angiogenesis and resistance to cell death. Four additional features were added to this list in their updated version (Hanahan and Weinberg, 2011) and these included the emerging hallmarks of deregulated cellular energetics and avoidance of immune surveillance and the enabling characteristics of genomic instability and tumour-promoting inflammation (Figure 1.14).

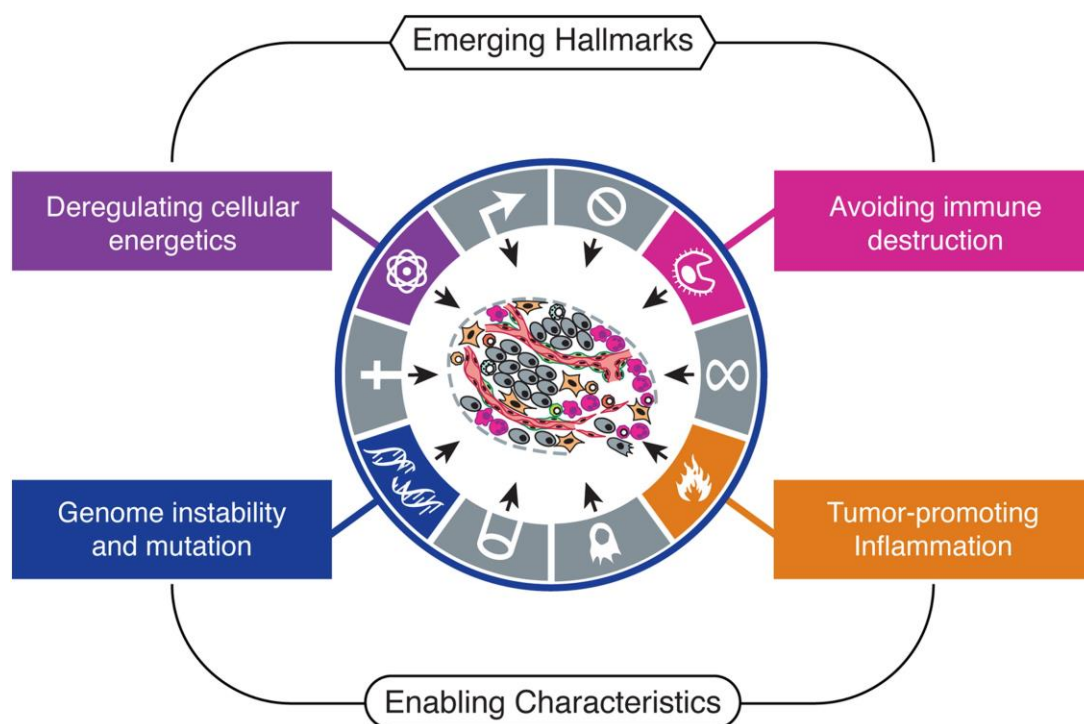


Figure1.14 The emerging hallmarks and enabling characteristics of cancer (Hanahan and Weinberg, 2011).

In their 2011 article, Hanahan and Weinberg acknowledge the growing scientific evidence of metabolic perturbation in cancers and that as cancers develop a metabolic switch from oxidative phosphorylation to aerobic glycolysis frequently takes place. This metabolic reprogramming is now recognised as a common feature of many types of cancer and in some cases, mutations in genes that govern the expression of key metabolic proteins have been associated with oncogenic events (DeBerardinis and Chandel, 2016). In addition, it is now known that many metabolic enzymes are under the control of oncogenes, tumour suppressor genes and key transcription factors such as HIF1. These facts make the metabolic phenotype of cancers interesting both biologically and because of the therapeutic opportunities it provides.

1.9 Aerobic Glycolysis (Warburg effect)

Like most cells, tumour cells use glucose as a major source of energy for growth and survival. In normal cells, mitochondrial aerobic respiration (oxidative phosphorylation) generates 90% of the energy for the cell in the form of adenosine triphosphate (ATP), whereas approximately 10% of the energy is produced by glycolysis. Therefore, glucose is completely catabolized via glycolysis and the citric acid cycle (Krebs cycle) and generates a large amount of ATP through the oxidative phosphorylation process. For one molecule of glucose, a total of 36 molecules of ATP are produced. When oxygen levels are reduced, glucose is metabolized to lactate in a process known as anaerobic glycolysis, producing 2 molecules of ATP per one molecule of glucose. In tumour cells, they undergo metabolic reprogramming to favour glycolysis and the production of lactate, even in the presence of oxygen

(figure 1.15). In a tumour, it is estimated that 85% of energy is generated by the glycolytic pathway despite the fact that oxidative phosphorylation is the most effective route for producing ATP (Jones and Bianchi, 2015, Vander Heiden et al., 2009). Tumour cells become glucose-dependent and its consumption is increased and this phenomenon is called the Warburg effect (figure.1.15).

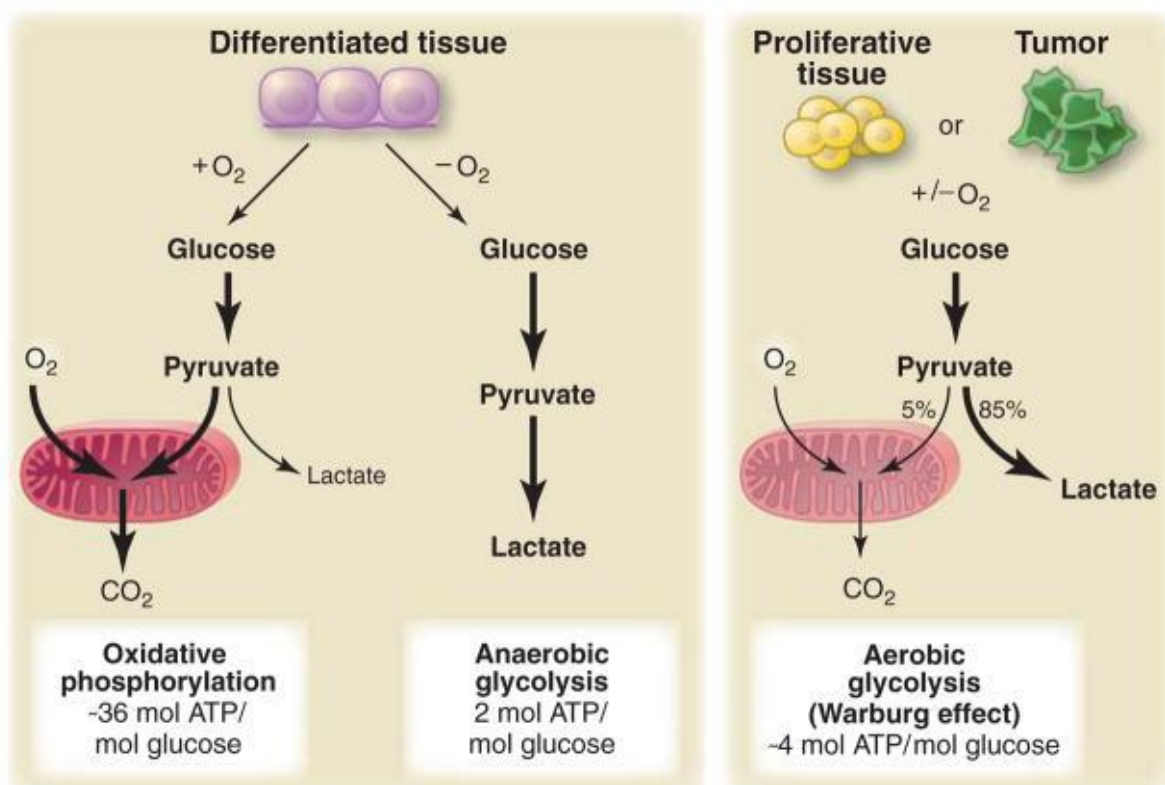


Figure 1.15 Glucose metabolism in normal cells and tumour cells. Normal cells undergo anaerobic glycolysis only in the absence of oxygen. Cancer cells however undergo aerobic glycolysis even in the presence of oxygen (Vander Heiden et al., 2009).

Nevertheless, even if the mitochondria seem to participate little in energy metabolism, it does not mean that the mitochondria are inactive. Indeed, it has been shown in a highly glycolytic glioblastoma lineage that the Krebs cycle in these cells is

intact and that mitochondria play a key role in anaplerotic reactions via the use of glutamine (DeBerardinis et al., 2007).

1.10 Glutamine metabolism

In order to divide, a cell must duplicate its genome and provide sufficient protein and lipids to create a new cell. For this purpose, the cell must use common extracellular nutrients such as glucose or glutamine and enter them into metabolic pathways that convert them into biosynthetic precursors. Alongside glycolysis, cancer cells are also heavily dependent upon glutamine and the process of glutaminolysis (Daye and Wellen, 2012). As illustrated in figure 1.16A, glutamine can be metabolised by glutaminase (GLS) to give glutamate and this can enter into the Krebs cycle via conversion to α -ketoglutarate. This can then be used to replenish the oxaloacetic acid required to drive the Krebs cycle and allows for key intermediates such as citrate to be used for lipid synthesis (DeBerardinis et al., 2007).

Alternative pathways are available as illustrated in figure 1.16B, the presence of hypoxia leads to the up-regulation of HIF1 and this in turn leads to an increased expression of pyruvate dehydrogenase kinase 1 (PDK1). PDK1 directly phosphorylates and inactivates the pyruvate dehydrogenase complex leading to reduced entry of acetyl CoA into the Krebs cycle. Under these conditions, lipid synthesis is still possible via the conversion of glutamine into citrate outside of the mitochondria as illustrated in figure 1.16B. This pathway is also possible in aerobic conditions in tumours where VHL function is lost (Anastasiou and Cantley, 2012).

1.11 Regulation of metabolic pathways associated with the Warburg effect.

The demonstration that various oncogenic mutations directly mediate the metabolic reprogramming seen in cancers has generated considerable interest amongst cancer biologists and the drug discovery community. Full details of the links between oncogenic drivers and metabolism are described in detail elsewhere (Vaupel and Harrison, 2004) and described briefly below and summarised in figure 1.17.

PI3K: A major regulator of metabolism is the phosphoinositide 3-kinase pathway (PI3K). PI3K regulates the level of phosphorylated phosphatidylinositol 3 (PIP3) and it can be activated by growth factors leading to activation of downstream client proteins such as Akt and mTOR (Franke, 2008, Auger et al., 1989). This activation is important for both cell proliferation and glucose metabolism. mTOR plays a key role in metabolism (Shimobayashi and Hall, 2014) where cell growth is promoted by the stimulation of de novo synthesis of lipids, nucleotides and proteins which represent key building blocks for cell proliferation. In addition to its role in providing biosynthetic precursors for cell growth, this signalling pathway regulates the entry of glucose into the cell and its use. It makes the cells dependent on a high flux of glucose via the activation of hexokinase or phosphofructokinase (Kohn et al., 1996, Hardie, 2012) (Deprez et al., 1997).

HIF1: As described above, HIF1 is a master regulator of cellular response to hypoxia in tumours (Clottes, 2005). HIF1 is a transcription factor involved in the regulation of the expression of many genes that control different cellular functions, such as angiogenesis, survival, invasion and metabolism (Lauzier et al., 2006). With regards to metabolism, HIF1 increases the expression of enzymes involved in glycolysis,

such as 6-phosphofructo-2-kinase (PFKFB3) (Obach et al., 2004) and aldolase A (Semenza et al., 1996). It also contributes to an increase in intracellular glucose by increasing the expression of glucose transporters (GLUT1 and GLUT3) which mediate glucose entry into the cell (Haase, 2006, Zapata-Morales et al., 2014, Song et al., 2009). HIF1 also reduces mitochondrial oxidative phosphorylation by blocking pyruvate entry into the mitochondria by inhibiting the conversion of pyruvate to acetyl-CoA by pyruvate dehydrogenase (PDH). HIF1 is a transcriptional activator of the pyruvate dehydrogenase kinase PDK1 which inactivates PDH enzymatic activity by phosphorylation (Kim and Dang, 2006, Kim et al., 2006).

AKT: AKT is an intracellular serine/threonine kinase and a downstream effector of the PI3K signalling pathway. It is activated through interaction with PIP3 at the cell membrane but can also be activated independent of PI3K activity. It is a key signalling molecule with over 100 reported cellular substrates. Akt signalling is associated with multiple cellular effects including regulation of cell survival, proliferation, protein synthesis and metabolism. In normal cells Akt, which functions as a proto-oncogene, participates in the regulation of the balance between cell survival and cell death (Riemenschneider et al., 2006). One of the features of cancer cells is disturbance of this balance resulting in uncontrolled cell proliferation and enhanced cell survival (Chen et al., 2001). Interestingly, oncogenic activation of AKT kinase does not necessarily increase proliferation of cancer cells in culture but has been shown to stimulate glycolysis in the presence of oxygen (Elstrom et al., 2004). AKT stimulates glucose consumption without changing the oxidative phosphorylation rate (Kim and Dang, 2006, Kim et al., 2006). Importantly, cancer cells overexpressing

AKT became dependent on glucose to survive and proliferate (Elstrom et al., 2004). The effects of AKT on growth and cell proliferation appear closely related to its impact on energy metabolism, particularly through the control of activation of mTORC1 (complex mammalian target of rapamycin 1). Abnormalities of the PI3K / AKT / mTOR pathway are important events leading to the development of a tumour (Riemenschneider et al., 2006).

MYC: The oncogene Myc targets many genes that are involved in the breakdown of glucose to pyruvate and finally to lactate (Le et al., 2010, Hsieh et al., 2015). These genes include Lactate dehydrogenase A (LDHA), the glucose transporter GLUT1, hexokinase 2, phosphofructokinase and enolase 1. Myc also induces breakdown of glutamine by stimulating glutaminase, which transforms glutamine into glutamate. Glutamate can be excreted or enter the Krebs cycle where it is transformed into α -ketoglutarate as described above. In cells that express the Myc oncogene, they can become dependent on glutamine and cells enter apoptosis when glutamine is removed from the culture media (Altman et al., 2016). Therefore, Myc promotes aerobic glycolysis and glutaminolysis in cancer cells thereby supporting the metabolic reprogramming observed in cancer cells (DeBerardinis et al., 2008b).

The tumour suppressor gene p53: P53 is involved in many cell processes and is widely regarded as the 'guardian of the genome' (Lane, 1992). The diverse functions of p53 range from cell cycle regulation to the control of apoptotic signalling pathways. It plays the role of 'controller' in the cell that can detect stressful situations and depending on the severity of the stress, it can direct the cell to repair, cell cycle arrest or undergo apoptosis (Balint and Vousden, 2001, Braithwaite et al., 2006).

More recent evidence has demonstrated that p53 participates in the regulation of cell respiration via disruption through transcriptional activation of Synthesis of cytochrome C oxidase 2 (SCO2) which is critical for the function of the cytochrome c oxidase complex and oxygen utilisation and suppresses glycolysis via TP53 Induced Glycolysis Regulatory Phosphatase (TIGAR) and phosphoglycerate mutase (PGM) (Matoba et al., 2006). In addition, wild type p53 reduces intracellular levels of glucose by inhibiting the expression of the glucose transporters GLUT1 and GLUT4 (Schwartzberg-Bar-Yoseph et al., 2004). P53 also inhibits the expression of pyruvate dehydrogenase kinase 2 which phosphorylates and inactivates the PDH complex that catalyses the conversion of pyruvate to acetyl-CoA (Contractor and Harris, 2012). Thus, the inactivation of p53 is directly linked to the metabolic reprogramming observed in cancer cells (Kroemer and Pouyssegur, 2008)

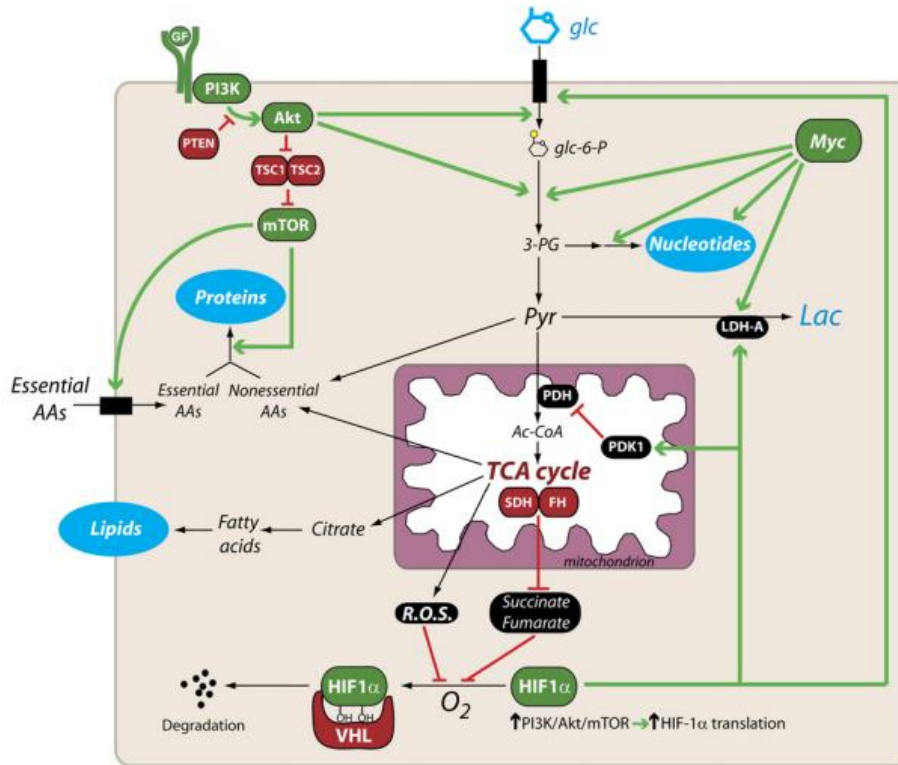


Figure 1.17 Regulation of cell metabolism in proliferating cancer cells (DeBerardinis et al., 2008a). The figure shows several key pathways that impact upon cell metabolism and are significant contributors to the Warburg effect. Constitutive activation of key pathways such as PI3K, AKT, mTOR, Myc, and HIF1 impact upon both glucose metabolism and the uptake of essential amino acids, all of which contribute to metabolic reprogramming in cancers.

1.12 Key enzymes in the glycolytic pathway

The metabolic enzymes frequently modified in cancer may be different depending on the presence of specific genetic abnormalities but despite this, three key enzymes play an important role in the glycolytic phenotype of cancer cells. These are hexokinase (HK), pyruvate dehydrogenase kinase (PDK) and lactate dehydrogenase A (LDHA), details of which are briefly outlined below.

Hexokinase (HK): There are two isoforms of HKs, HK1 which is highly expressed in tissues like the brain and HK2 which is overexpressed in a number of cancers such as glioblastoma multiforme (GBM) and is associated with a poor prognosis (Wolf et al., 2011). Decreasing the expression of HK2 restores oxidative metabolism of glucose and enhances cell sensitivity to cytotoxic insults (Aft et al., 2002, Pedersen, 2007). In addition, inhibition of HK2 expression in orthotopic GBM xenografts caused a significant decrease in proliferation and angiogenesis (Wolf et al., 2011). Experimental overexpression of HK2 in cancer cells *in vitro* resulting in increased glucose phosphorylation is associated with increased cellular proliferation (Ahn et al., 2009).

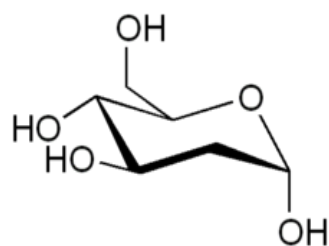
Pyruvate dehydrogenase kinase (PDK): As described earlier, PDK is a protein that participates in the regulation of the pyruvate dehydrogenase complex (PDH) responsible for the conversion of pyruvate to acetyl-CoA which then enters the Krebs cycle. The regulation of PDH is highly coordinated by phosphorylation and dephosphorylation cycles catalysed by PDK and pyruvate dehydrogenase phosphatases (PDPs) respectively. PDK exists in four isoforms (PDK1-PDK4) (Popov et al., 1997). These kinases are found deregulated in several diseases especially in cancers such as colon, kidney and lung cancers. The overexpression of PDK1 is associated with HIF-1 stabilization (Kim et al., 2006).

Lactate dehydrogenase (LDH): LDH is the enzyme in the glycolytic pathway that converts pyruvate to lactate either in the absence of oxygen (as is the case in normal cells) or in the presence of oxygen (aerobic glycolysis). LDH is encoded by 2 genes, the LDH-A gene (M-muscle) and the LDH-B gene (H-Heart). These 2 genes code for

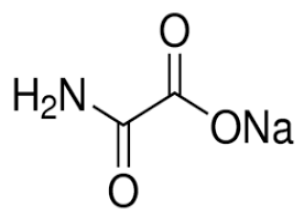
2 polypeptide chains called the M and H subunits. There are 5 isoforms of the LDH (Markert and Ursprung, 1962). LDH-1 isoform is composed of 4 H subunits and LDH-5 by 4 M subunits. LDH-5 is the most effective isoform to catalyse the conversion of pyruvate to lactate whereas LDH1 catalyses the conversion of lactate to pyruvate. In tumour cells that undergo aerobic glycolysis, increased glucose consumption leads to accumulation of lactate. This could lead to acidification of the tumour cell (intracellular pH would become acidic) but in order to maintain viability, lactate anions and H⁺ ions are pumped out of the cell into the extracellular space resulting in the extracellular pH decreasing whilst intracellular pH is maintained at 7.4. High expression of LDH-5 is a poor prognostic factor in several cancers (Shim et al., 1997, Koukourakis et al., 2003). Many studies also show that LDH-A expression is a marker of tumour aggression and resistance to certain treatments (Deichmann et al., 1999).

1.13 Use of inhibitors to target key enzymes in tumour glycolysis (Warburg effect)

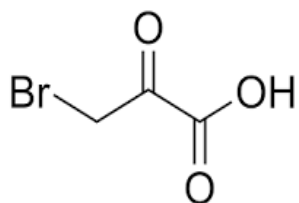
A number of small molecule inhibitors of glycolysis have been described in the literature and their chemical structures are presented in figure 1.18. Brief details of their pharmacological properties are also described below.



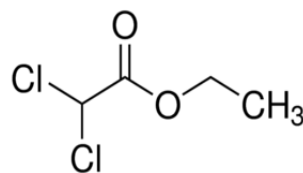
2-deoxy-D-glucose



Sodium oxamate



3-bromopyruvate



Dichloroacetate

Figure1. 18 Chemical structures of known inhibitors of glycolysis.

2-deoxy-D-glucose (2DG): 2-Deoxy-D-glucose differs from glucose by the presence of a hydrogen atom instead of a hydroxyl group on the C2 atom. The first step of glycolysis is the phosphorylation of glucose to glucose 6 phosphate by hexokinases. 2DG can also be phosphorylated by HK to generate 2DG-phosphate, which accumulates in the cell and inhibits HK and therefore glucose metabolism (Young, 1972). (Pelicano et al., 2006). At millimolar concentrations, 2DG induces a decrease in the levels of ATP and cell death (Brown, 1962). This compound has entered clinical trial programs for the treatment of cancer in combination with other agents and these studies have shown that up to 250 mg/kg, 2DG is safe. It has also been shown to increase the effect of radiation therapy in patients with cerebral tumours (Singh et al., 2005, Dwarakanath and Jain, 2009).

3-Bromopyruvate (3-BP): 3-Bromopyruvate is also an inhibitor of HK leading to a decrease in ATP and cell death (Pedersen, 2012, Nakano et al., 2011). The exact mechanism is not fully understood but it is thought that 3-BP may bind to sulfhydryl groups of the hexokinase that are responsible for its enzymatic activity (Davidescu et al., 2015). This inhibitor attacks the early stages of glycolysis and causes a strong ATP depletion, especially in tumour cells with mitochondrial defects (Xiao et al., 2013, Xu et al., 2005). Chen et al (2009) also demonstrated that 3-BP is able to dissociate mitochondrial bound Hexokinase (HK2 binds to mitochondrial VDAC channels) and induces apoptosis (Chen et al., 2009, Shoshan, 2012). Transport of 3-BP into tumour cells is via lactate transporters on the cell surface (Queirós et al., 2012). Correspondingly, Ko et al (2004) reported complete tumour response without side effects in rats after the intraperitoneal administration of 3-BP.

Dichloroacetate (DCA): This molecule is known to inhibit PDK and prevent pyruvate entering into the Krebs cycle (Bonnet et al., 2007). DCA is already used clinically for the treatment of mitochondrial genetic diseases (Kaufmann et al., 2006). It is an analogue of pyruvate and it enters the bloodstream quickly after oral intake giving it good bioavailability. This molecule is transported across cell membranes by the monocarboxylate transporters that normally carry lactate, pyruvate or ketone bodies. DCA decreases tumour growth *in vitro* and *in vivo* without affecting the normal cells (Li et al., 2012, Stacpoole et al., 1998). DCA obtained notoriety in the popular press following publications in Cancer Cell (Bonnet et al., 2007) and subsequently the New Scientist by Evangelos Michelakis of the University of Alberta claiming that DCA was a 'cheap, safe drug that kills most cancers' (Sanchez et al., 2013). Whilst this

generated considerable interest in the public domain, clinical trials have yet to prove it is effective at treating cancer.

Sodium Oxamate: Sodium oxamate is structurally similar to pyruvate and inhibits LDH-A competitively. The cell becomes depleted of NAD⁺ and glyceraldehyde-3-phosphate accumulates. Thereby more fructose-1,6-bisphosphate is obtained inhibiting phosphofructokinase and thus blocking glycolysis (Goldberg et al., 1965). In addition to inhibition of LDH-A, sodium oxamate inhibits aspartate aminotransferase. The authors were also able to show that sodium oxamate selectively inhibits the growth of MDA-MB-231 cells compared to normal human epithelial cells and also slowed tumour growth *in vivo* (Thornburg et al., 2008). The blockade of LDH-A by sodium oxamate also inhibited tumour growth (B cell-Lymphoma and pancreas) in a mouse model (Le et al., 2010). In chemo-resistant breast cancer cells, inhibition of LDH-A by sodium oxamate enhanced the cytotoxic potency of the chemotherapeutic agent Taxol (Zhou et al., 2010)

1.14 Cellular metabolism under hypoxic conditions.

To date, the majority of studies have focused on unravelling the metabolic phenotype of cancers in aerobic conditions with comparatively little attention being paid to the metabolic properties of hypoxic cells. The effect of hypoxia on cell metabolism has however been reviewed in detail elsewhere (Eales et al., 2016) and key features are outlined in figure 1.19.

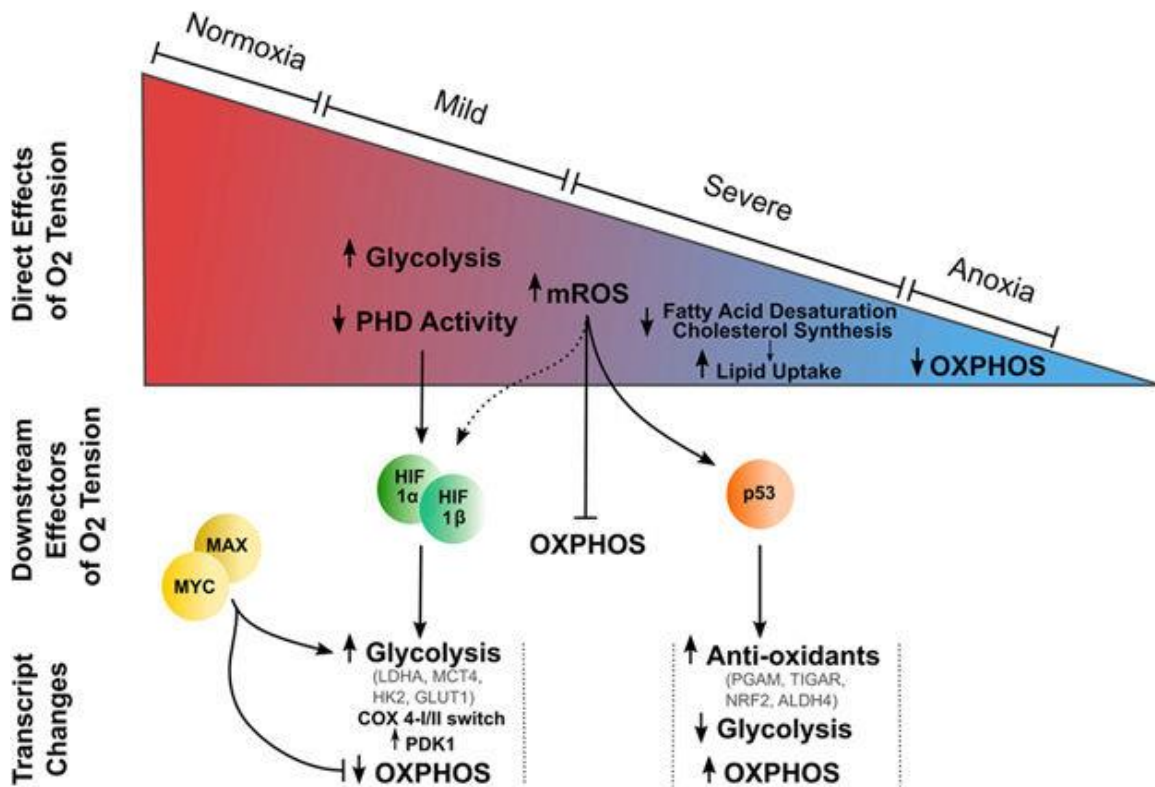


Figure1. 19 Metabolic adaptations of tumours cells to hypoxia (Eales et al., 2016).

As the oxygen tension inside tumours decreases, the majority of metabolic adaptations to hypoxia are mediated by HIF1. These include up-regulation of key glycolytic enzymes including HK and LDH-A and transporters such as Glut-1 (responsible for transporting glucose into the cell) and MCT4 (responsible for exporting lactate out of the cell). Cell proliferation can be reduced via the HIF1 dependent up-regulation of p21WAF1/CIP1 although there are other tumours where cell proliferation can still occur under hypoxia through mTOR related pathways (DeYoung et al., 2008). HIF1 can also reduce oxidative phosphorylation by changing subunits within cytochrome c oxidase complex (COX4-1 replaced with COX4-2) and increased expression of mitochondrial LON protease leads to degradation of the

COX4-1 subunit (Semenza, 2011). Another key change mediated by HIF1 is upregulation of PDK1 and suppression of PDH activity thereby reducing the flux of carbon into the Krebs cycle (Kim et al., 2006). In addition to increased glycolysis, hypoxic cells with high MYC expression have elevated glutamine metabolism and this could support cell proliferation under hypoxic conditions (Wise et al., 2008, DeBerardinis et al., 2007).

However, hypoxia is also known to induce cell apoptosis by reducing expression of the anti-apoptotic Bcl-2 gene or by activation of the P53 gene (Shimizu et al., 1995, Li et al., 1999). Normally, p53 contributes to genomic stability by inducing cell cycle arrest and cell death after DNA damage. In addition to this p53 participates in the regulation of metabolism. It controls glycolysis by activating the expression of TIGAR (TP53-induced glycolysis regulator), which reduces the level of intracellular fructose-2,6-bisphosphate (Bensaad et al., 2006). Moreover, p53 reduces the intracellular glucose by inhibiting glycolysis pathway. Therefore, Loss of p53 induces activation of the NF- κ B, it accelerates glycolysis in tumour cells (Kawauchi et al., 2008).

Recent studies have shown that a high carbon fraction of fatty acids in hypoxic cells is not derived from glucose or glutamine, and that hypoxic cells can use another source (exogenous acetate) to maintain the Krebs cycle. Acetate utilisation can support lipogenesis and sustain cell growth under hypoxic conditions (Bulusu et al., 2017, Kamphorst et al., 2014). A few years ago, Sonveaux et al identified that cancer cells can operate in oxidative mode producing energy from glucose and other oxidative fuels. In contrast, hypoxic cancer cells convert glucose to lactate to

produce energy. Sonveaux and colleagues also reported metabolic coupling between hypoxic and normoxic tumour cells with normoxic tumour cells oxidising lactate (generated through glycolysis by hypoxic cells) as a source of energy, which enables availability of glucose for hypoxic / glycolytic cancer cells to survive (Figure 1.20). This type of behaviour has been demonstrated in many human tumours (Sonveaux et al., 2008).

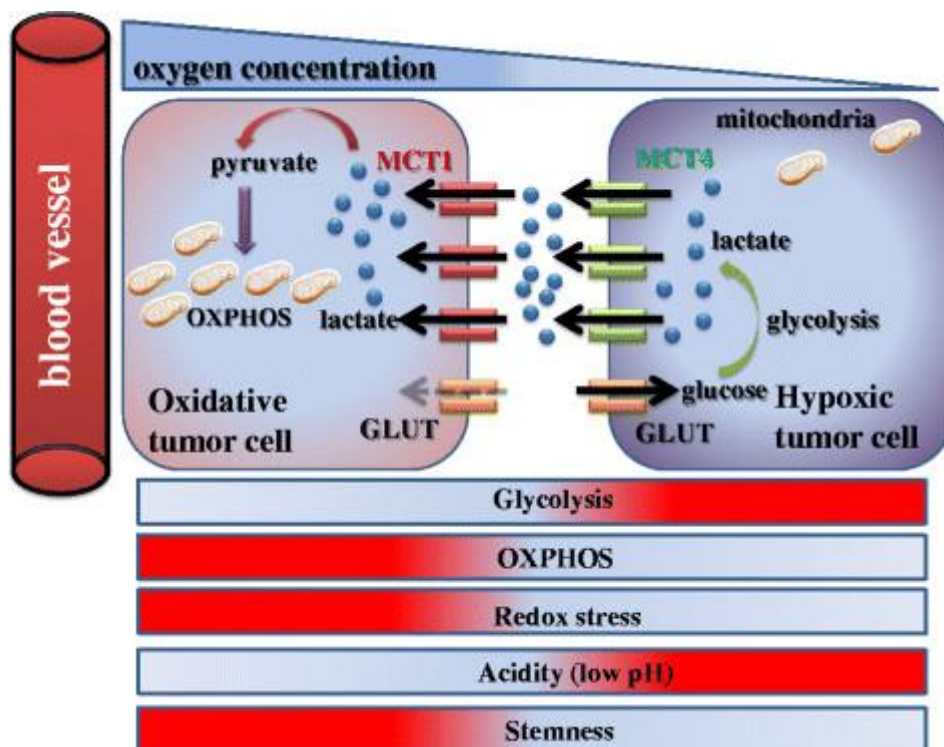


Figure 1.20 summarizes metabolic coupling of aerobic tumour cells and hypoxic tumour cells within a tumour (Yoshida, 2015).

1.15 Rationale and aims of this study

The altered metabolism of cancer cells was first described by Otto Warburg in the 1930s and is a specific and key feature of cancers. This emerging hallmark of cancers offers many therapeutic opportunities and this is particularly true in the context of the hypoxic microenvironment. The switch to a highly glycolytic phenotype under hypoxic conditions suggests that inhibitors of glycolysis should be preferentially active against hypoxic cells and this hypothesis will be tested in this thesis. In view of the failure of HAP technology to eradicate hypoxic cells, there is a clear need for new therapeutic approaches for targeting cancer cells in the hypoxic microenvironment.

The principle aim of this thesis therefore is to determine whether or not established inhibitors of cellular metabolism are preferentially active against hypoxic tumour cells compared to aerobic cells. The inhibitors used and the enzymes they inhibit are illustrated in figure 1.20. In addition, it is known that alternative carbon sources such as lactate and acetate can be used to support the growth of tumour cells and this thesis will also explore whether other sugars than glucose can serve as carbon sources to support the growth and/or survival of tumour cells under hypoxic conditions. Finally a series of novel organometallic complexes based on silver N-heterocyclic carbenes (NHC) will be investigated as potential inhibitors of key enzymes in the glycolytic pathway. The rationale for this is based on preliminary studies showing that silver NHC complexes can inhibit glycolysis (Allison et al 2017). It is not clear however where in the glycolytic pathway these inhibitors might work and therefore the aim of this phase of the project is to determine their ability to inhibit

enzymes such as HK, PFK and LDH-A.

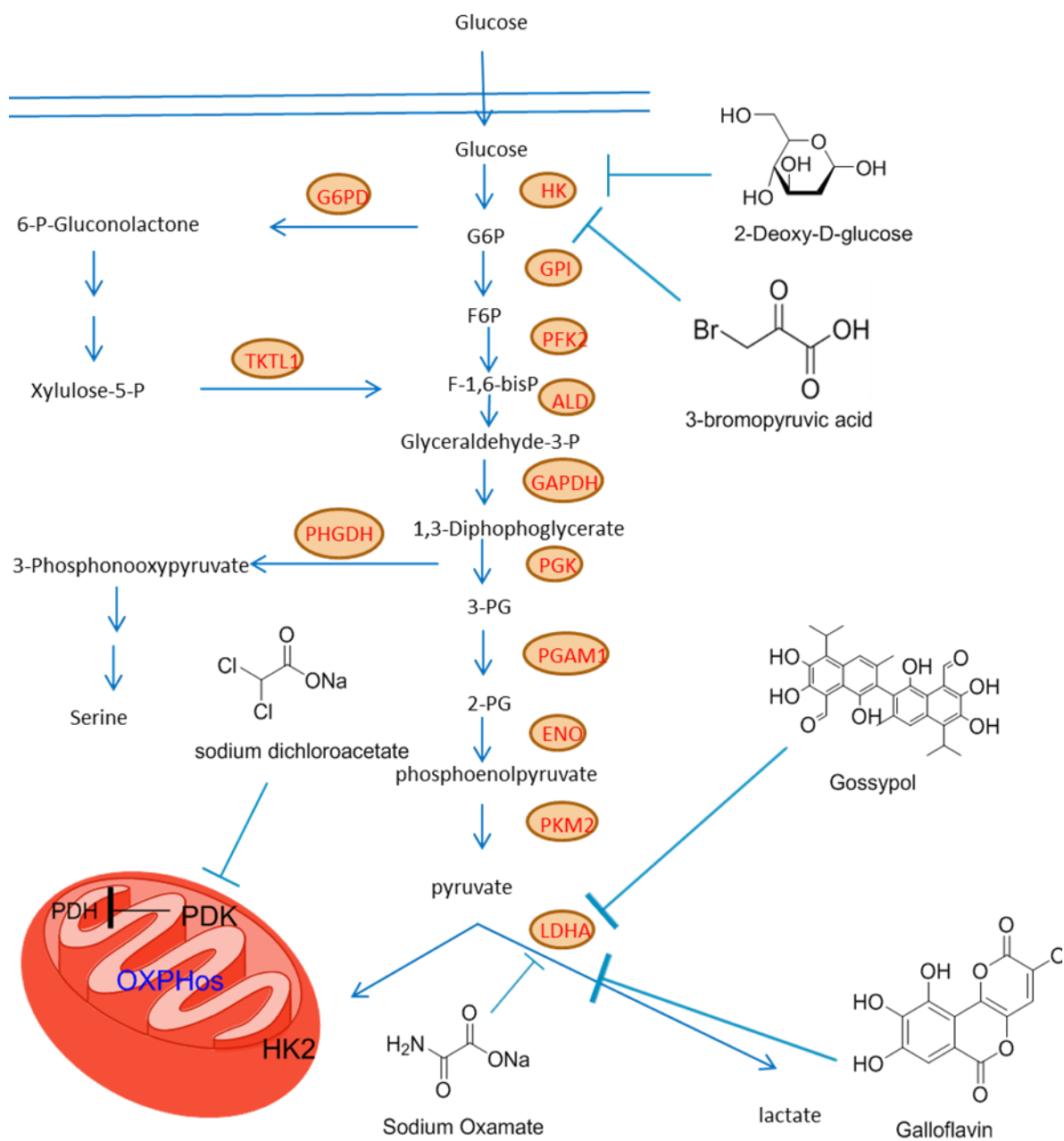


Figure 1.21 Overview of the compounds used in this thesis and their sites of action in the metabolic pathways.

Chapter 2

Materials and general methods

2.1 Materials

All chemicals were obtained from Sigma Aldrich unless otherwise stated. This includes: 3-bromopyruvate (3BP), 2-Deoxy-D-glucose (2DG), Sodium Oxamate, Gossypol, Sodium Dichloroacetate (DCA), Dulbecco's Modified Eagle Medium (DMEM), Sodium Pyruvate, Roswell Park Memorial Institute 1640 medium (RPMI 1640), Foetal Bovine Serum (FBS), L-glutamine, trypsin (0.05%)/EDTA (0.02%), Phosphate Buffered Saline (PBS) tablets, Tetrabutylammonium Sulfate, Dimethyl Sulphoxide (DMSO). MTT (3-(4,5-Dimethylthiazol-2-yl)-2,5-Diphenyltetrazolium Bromide) was obtained from Alfa Aesar chemicals. HPLC grade Acetonitrile was obtained from Fisher Scientific.

2.2 Cells and cell culture conditions

Unless otherwise stated, all cell lines were initially purchased from the American Type Culture Collection (ATCC) or the European Collection of Authenticated Cell Cultures (ECACC) and stored in the cell culture bank at the University of Huddersfield. These included the human colorectal cancer cell lines SW48, LS123, HT29, BE (obtained originally from Dr Tim Ward, Paterson Institute for Cancer Research, Manchester), HCT116 p53^{-/-} and HCT116 p53^{+/+} (both obtained from Professor Bert Vogelstein, Johns Hopkins University, Howard Hughes Medical Institute, USA). HT-29 and BE cells were maintained in RPMI 1640 supplemented with 10% FBS, 2mM L-glutamine and 1mM sodium pyruvate. HCT116 p53^{-/-},

HCT116 p53^{+/+} and SW48 cells were maintained in DMEM supplemented with 10% FBS, 2mM L-glutamine and 1mM sodium pyruvate. Similarly, human non-small cell lung cancer A549 cells were maintained in DMEM supplemented with 10% FBS, 2mM L-glutamine, and 1mM sodium pyruvate. The LS123 cell line was maintained in EMEM medium supplemented with 10% FBS, 2mM L-glutamine, and 1mM sodium pyruvate. The human pancreatic cancer cell line Panc10.05 was maintained in RPMI1460 with same supplements as above. Normal human retinal pigment epithelial (ARPE19) cells were cultured in DMEM/F12 supplemented with 10% FBS and 2mM L-glutamine. All cells were maintained as monolayer cultures at a constant temperature of 37°C in a CO₂ enriched (5%), humidified atmosphere.

2.3 Recovery of cell lines from storage in liquid nitrogen.

A frozen vial of each cell line suspended in freezing medium (10% DMSO, 20% FBS and 70% medium) was removed from liquid nitrogen storage. Cells were rapidly thawed and transferred into a sterile universal tube containing 5ml of pre-warmed medium. Following centrifugation at 800 rpm for 5 minutes, the supernatant was removed and the cell pellet gently re-suspended in fresh medium. The cells were plated into a T25 flask and incubated at 37°C in a humidified CO₂ enriched atmosphere. When the cells were 70-80% confluent, they were sub-cultured and placed into new culture vessels as described below.

2.4 Routine maintenance and sub-culturing of cells

All work was carried out in class II biological safety hoods under aseptic conditions. Medium from the cell culture flask was removed and cells were washed with 10ml of sterile PBS. After washing, PBS was removed and cells were detached from the flask by adding 3ml of 1X trypsin EDTA solution. The flask was returned to the incubator and allowed to incubate for approximately 5 minutes at 37°C or until the cells completely detached. Once detachment was complete, pre-warmed medium was added into the flask to stop the activity of trypsin. The cell suspension was collected from the flask and placed in a sterile universal tube (50ml falcon tubes) and centrifuged at 800 rpm for 5 minutes to pellet the cells. The supernatant was removed and the cell pellet was re-suspended in 10ml cell culture medium. The cells then were seeded into the appropriate sized flask to maintain the culture or used for experiments.

2.5 Cell counting using a haemocytometer

Both the haemocytometer and its coverslip were cleaned with 70% ethanol prior to adding the coverslip onto the haemocytometer slide. The coverslip was pressed firmly onto the haemocytometer until Newton rings appeared. Cells were trypsinised and the suspension of cells was mixed by gentle repeat pipetting. Subsequently, each side of the haemocytometer chamber was gently filled with approximately 10µl of cell suspension from the edge of the chamber. The cells were counted in the central chamber and the 4 corner chambers. Cells were counted in a total of 10 chambers and the average number of cells per chamber was determined. This was multiplied by 10^4 to obtain the number of cells/ml. The counting chambers and the

2.6 Chemosensitivity studies

2.6.1 Validation of the MTT assay

Briefly, the 3-(4,5-dimethylthiazol-2-yl)-2,5-diphenyltetrazolium bromide (MTT) assay is one of the most widely used colorimetric assays for measuring cellular response to drugs. It is a metabolic activity assay that relies on the conversion of MTT to a coloured formazan product by enzymes present in the mitochondria of cells (Marshall et al., 1995, Riss et al., 2016). Initial validation of the assay was based on determining the relationship between cell number and absorbance of the formazan product.

Cells (HT29, HCT116 p53^{+/+} and BE) were sub-cultured as described above and a cell suspension of 5.7×10^5 cells/ml was prepared. Cells were seeded into 96 well flat bottom plates with various numbers of cells per well as follows: To lane 1 (rows A to H), complete medium (200 μ l/well) was added to serve as a blank. To lane 2 (rows A to H), 200 μ l of cell suspension was added and to each subsequent lane, the volume of cell suspension added reduced by 20 μ l (figure 2.2). In all cases, the final volume in each well was made up to 200 μ l with complete medium. The cells were immediately treated with 20 μ l of MTT (5mg/ml) and incubated for 4 hours at 37 °C in humidified air with 5% CO₂. After the incubation period, medium was carefully removed and formazan crystals were dissolved with 150 μ l of DMSO. The optical density was then determined at 550 nm using a Tecan Infinite F50 microplate reader. The true absorbance of each lane was determined by subtracting the absorbance of the blank and this was plotted against cell number. The experiment was repeated three times for each cell line.

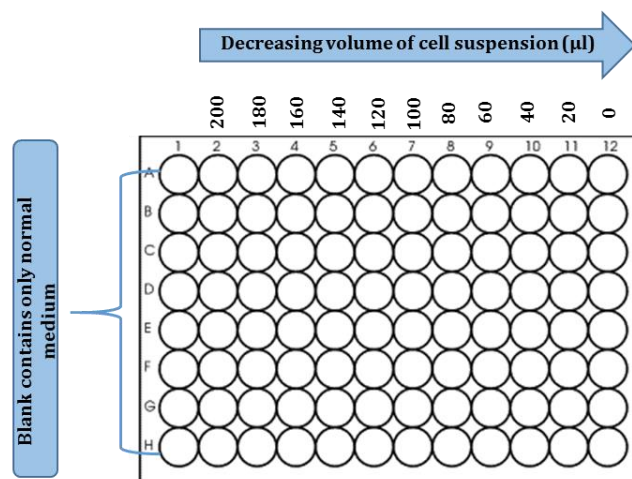


Figure 2.2 Schematic showing MTT validation experimental design, which is characterized by growing HT-29, HCT116 p53^{+/+} and BE cell lines on 96 well plates at different cell numbers per well. Cells were incubated for 4 hours with 20μl of MTT (5mg/ml). Lane 1 rows (A-H) treated as blank containing media only.

2.6.2 Chemosensitivity studies under aerobic or hypoxic conditions (continuous drug exposures).

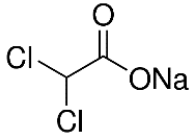
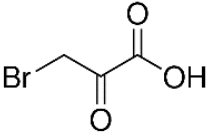
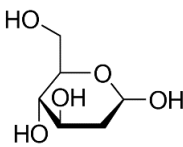
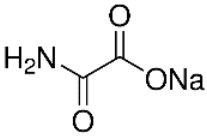
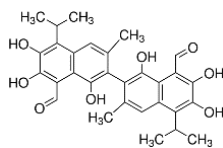
Cell survival of HT29, BE, HCT116 p53^{+/+}, HCT116 p53^{-/-}, PANC10.05, LS123, SW48 and ARPE19 cells following continuous exposure to a series of glycolytic/metabolic inhibitors was determined using the MTT assay. Cells were seeded into 96-well flat bottom plates at a final concentration of 2000 cells per well in appropriate culture medium. In addition, HCT116 p53^{+/+} and HCT116 p53^{-/-} cells were also seeded in RPMI 1640 medium to determine whether cellular response was influenced by the cell culture medium. For studies conducted under normoxia, plates were incubated under standard conditions of 37 °C in humidified air with 5% CO₂. For hypoxic conditions, plates were incubated in a H35 HypOxystation (Don Whitley

Scientific, Shipley, UK) which provides a stable atmosphere of humidified gases consisting of 5% CO₂, 0.1% oxygen with the remainder made up with nitrogen. The chamber is also heated to maintain a temperature of 37°C. In both cases, cells were seeded into 96well plates and incubated under normoxic or hypoxic conditions for 24 hours prior to drug exposure.

For drug exposure, medium was carefully removed from each well and replaced with medium containing a various concentration of inhibitor. Details of the inhibitors used and their preparation is presented in table 2.1. Plates were set up for each compound as follows; lane 1 (rows A to H) media only (200µl/well) to serve as the blank. Lane 2 (rows A to H) contained cells and culture medium with no drug (200µl/well) and this served as the control. Lanes 3 to 12 contained medium with different concentrations of drug with increments increasing as illustrated in figure 2.3. A range of drug concentrations was used for each inhibitor, details of which are specified in the results section of the thesis. In all cases, a 2-fold serial dilution strategy was used to prepare drug concentrations. Following the addition of drugs to wells (200µl/well), plates were incubated at 37°C for 96 hours before cell survival was assessed using the MTT assay. As described above, 20µl of 5mg/ml MTT solution was added to each well and allowed to incubate for 4hours in the incubator at 5% CO₂ and 37°C. The cells were processed as described above and cell survival was determined by dividing the true absorbance of the treated wells by the true absorbance of the controls (expressed as a percentage). Cell survival was plotted against drug concentration to generate a dose response curve and the IC₅₀ (concentration required to kill 50% of cells) was determined for each cell line and

treatment. All experiments were repeated a minimum of three times and the results were expressed as the mean \pm standard deviation. In the case of gossypol where the compound was dissolved in DMSO, stock solutions were prepared at 50mM in DMSO and stored at -20°C. The final concentration of DMSO used to treat cells was 0.2% (v/v). This concentration of DMSO was not toxic to cells following a 96 hour exposure. All other procedures were identical to the ones described above.

Table2. 1 Concentrations and chemical structures of glycolysis inhibitors used to target the glycolytic pathway of colon cancer cells under hypoxic and aerobic conditions.

Inhibitor	Molecular Weight	Chemical Structure	Concentration (stock solution)	Solvent
DCA	150.92		500mM	Medium
3BP	166.96		350μM	Medium
2DG	164.16		16mM	Medium
Sodium oxamate	111.03		100mM	Medium
Gossypol	518.55		100 μM	DMSO

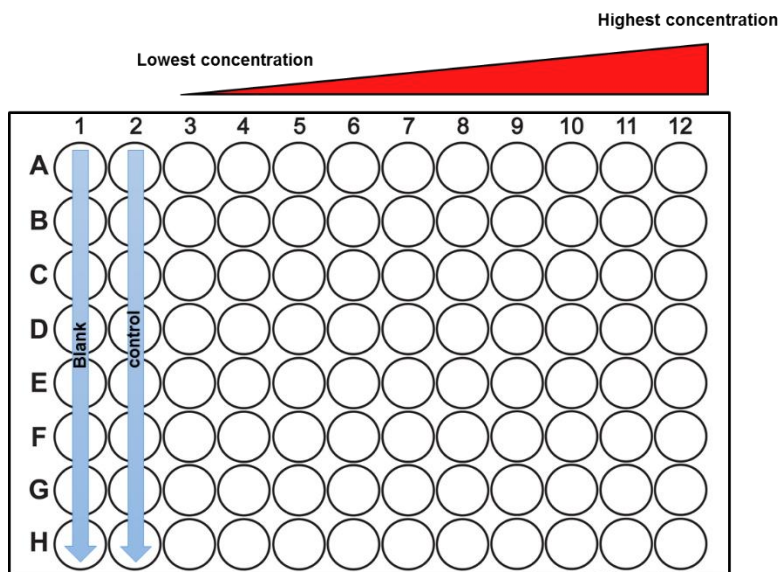


Figure 2.3 Schematic of the plate layout used to assess chemosensitivity. Lane 1 rows (A-H) treated as blank containing media only; lane 2 (rows A to H) represents controls; lanes 3 to 12 (rows A to H) represent treated lanes with each lane (rows A to H) being a single drug concentration (ie 8 replicates per drug concentration were used).

2.6.3 Chemosensitivity studies using short-term drug exposures.

The response of HT29, BE, HCT116 p53^{+/+} and HCT116 p53^{-/-} cells following short term exposures to DCA was measured using a slightly modified assay to the one described above. Setting up the plates and the pre-drug exposure incubation period was identical to the procedures above but following the addition of drugs, timed exposure periods were used. These were 1, 2, 4, 6, 8, 12 and 24 hours. After drug treatment, medium was removed and cells were washed twice with PBS before the addition of complete culture medium (200µl/well). Cells were then incubated at 37°C for up to a maximum of 96 hours prior to the addition of MTT and assessment of cell survival as described above.

2.7 Cell assays

2.7.1 Quantification of cell number and viability

In addition to chemosensitivity assays, several cell-based mode of action assays were performed. Effects on cell number and viability of different drug treatments were analysed using an NC3000 image cytometer (Chemometec) and a predefined 'ViaCount' assay (Chemometec) following the manufacturer's recommended protocol. In brief, this assay uses to determine cell viability of suspension cell samples. Via1 cassettes contain two different dyes; acridine orange stain (stains viable cells) and DAPI stain (stains non-viable cells).

2.7.2 Induction of Apoptosis

Loss of mitochondrial membrane potential was assayed as an indicator of early apoptosis induction in cancer cells in response to drug dose (Saelens et al., 2004, Elmore, 2007). This assay uses the mitochondrial membrane potential stain JC1 with levels of red and green JC1 quantified using the NC3000 image cytometer (Chemometec). Cells were grown in complete DMEM medium at 5×10^5 cells/flask in T25 flasks and incubated for 24 hours. Cells then were exposed to DCA at 75mM along with the untreated control and the cells were treated for different incubation time periods (24, 36, 48, 60 and 72 hours); (single -dose was used relevant to the influence of DCA cytotoxicity on cancer cell at different time). Post treatment with DCA, cells were harvested at each time point and washed with PBS. Cells were detached with 1x trypsin EDTA, and the suspension of cells was centrifuged at 1,200rpm for 3min. Cell pellets were re-suspended in 3 ml of PBS. Cells were

counted using Via1-Cassettes (Chemometec) and 1×10^6 cells were stained with 12.5 μ l of JC-1 reagent (5, 5, 6, 6-tetrachloro-1, 1, 3, 3-tetraethylbenzimidazolocarbo-cyanine iodide) and Solution 8 containing 1 μ g/ml DAPI in PBS according to manufacturer's instructions (Chemometec). 10 μ l of JC-1 stained cells were loaded into a slide chamber (NC-slide A8) and analysed using the NC3000 image cytometer.

2.8 Western blotting

2.8.1 Sample preparation

On the day prior to treatment with DCA, cells were inoculated into T25 flasks at a seeding density of 2.75×10^5 and immediately placed either in hypoxic (0.1% oxygen) or aerobic conditions. Following 24 hour incubation at 37°C to allow cells to adhere, cells were treated with DCA at concentrations ranging from 0 - 20mM and these were incubated at 37°C, 5% CO₂ humidity for 72 hours. Cell were harvested by removing medium from the flasks, washing three times with 5ml of PBS prior to the addition of trypsin-EDTA (1ml). The cells were then incubated at 37°C for 5 min, transferred to a centrifuge tube and centrifuged (1000 rpm, 3min room temperature). The supernatant was then removed and the cell pellet was then washed twice with cold PBS. After the final wash with PBS, the supernatant was removed and the pellet re-suspended in protein lysate buffer (RIPA buffer and a 1:100 dilution of protease cocktail inhibitor). The lysate from each tube was transferred to a 1.5ml Eppendorf tube and incubated on ice for 10 min prior to sonication using a probe sonicator (Sonics & Materials Inc) for 1 minute. Finally, cell lysates were aliquoted into new Eppendorf tubes and stored at -20°C.

2.8.2 Measuring protein concentration (BCA assay)

Total protein concentration in cell lysates was determined by using a commercially available protein assay (BCA, Pierce). A provided stock solution of BSA (2mg/ml) was diluted to give a range of concentrations of BSA standards to generate a standard curve. In a 96-well plate, 10 μ l of distilled water was introduced into 4 wells (serving as the blanks), then the standards and samples were pipetted as quadruplets according to the pipetting scheme shown in figure 2.4. 200 μ L of BCA reagent (made up of 50 parts of reagent A with 1 part of reagent B) per well was added. After an incubation period (30 min), the plate was measured in the Tecan F50 plate reader at 562nm.

Standards series				Cell lysate of unknown protein concentration							
0mg/ml BSA	0.4mg/ml BSA	1mg/ml BSA	2mg/ml BSA	10µl lysate	10µl lysate	10µl lysate	10µl lysate	10µl lysate	10µl lysate	10µl lysate	10µl lysate
0mg/ml BSA	0.4mg/ml BSA	1mg/ml BSA	2mg/ml BSA	10µl lysate	10µl lysate	10µl lysate	10µl lysate	10µl lysate	10µl lysate	10µl lysate	10µl lysate
0mg/ml BSA	0.4mg/ml BSA	1mg/ml BSA	2mg/ml BSA	10µl lysate	10µl lysate	10µl lysate	10µl lysate	10µl lysate	10µl lysate	10µl lysate	10µl lysate
0mg/ml BSA	0.4mg/ml BSA	1mg/ml BSA	2mg/ml BSA	10µl lysate	10µl lysate	10µl lysate	10µl lysate	10µl lysate	10µl lysate	10µl lysate	10µl lysate
0.2mg/ml BSA	0.8mg/ml BSA	1.4mg/ml BSA									
0.2mg/ml BSA	0.8mg/ml BSA	1.4mg/ml BSA									
0.2mg/ml BSA	0.8mg/ml BSA	1.4mg/ml BSA									
0.2mg/ml BSA	0.8mg/ml BSA	1.4mg/ml BSA									

Figure 2.4 Typical layout of the plate for conducting the Pierce BCA protein assay. The plate contains the blanks, BSA calibration curve and cell lysates.

2.8.3 SDS-PAGE electrophoresis

Following protein concentration determination, the samples (20 µg) were mixed with 4x Laemmli's SDS loading buffer and denatured at 95°C for 5min. Proteins were resolved using self-casted gels (15% SDS polyacrylamide resolving gel, with a 4% stacking gel) in a Mini-PROTEAN® Electrophoresis cell (Biorad). Protein molecular weight markers (8µl) were loaded in the first well, after which the samples (20µl) were loaded onto the gel. The electrophoresis was started with a constant voltage of 70 volts for an hour followed by electrophoresis at 120 volts for another hour.

2.8.4 Electrophoretic transfer of proteins

After electrophoresis was complete, proteins were transferred to nitrocellulose membrane using the Mini Trans-Blot® Electrophoresis Transfer cell (Biorad) in 1 x transfer buffer (10x transfer buffer (Tris base and glycine), methanol, ultrapure water and 10% SDS). All membrane and filter paper was pre-soaked in 1x transfer buffer for 30min. The 'sandwich' chamber was assembled from cathode to anode as follows and illustrated in figure 2.5; blotting pad, 2x filter papers, the gel, a nitrocellulose membrane, 2x filter papers and blotting pad. All were clamped tightly together into the Biorad sure lock apparatus, which was positioned in the tank and submerged in transfer buffer. The proteins were transferred to the membrane at a constant voltage of 45 V overnight at room temperature.

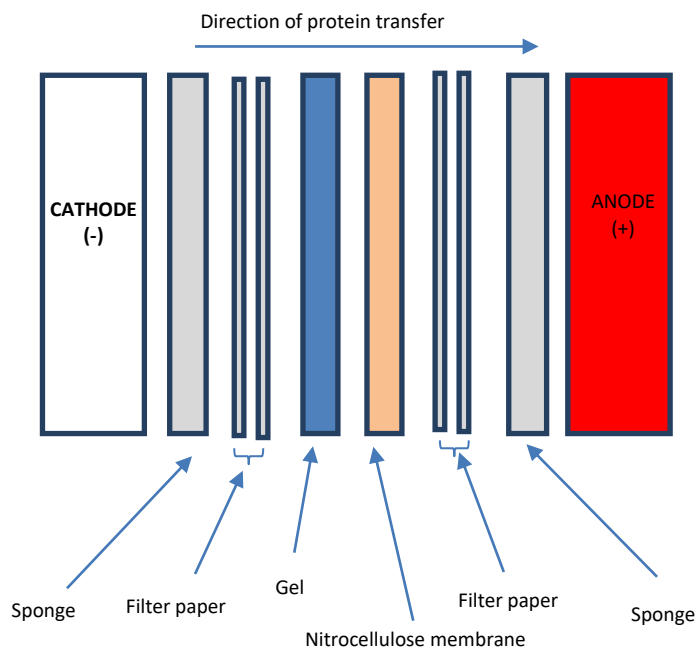


Figure 2.5 Electro-blotting sandwich used during western blot.

2.8.5 Blocking and immune-detection

Once transferred to nitrocellulose paper, the membrane was then blocked in blocking buffer (5 % powdered milk dissolved in TBS-T(1x Tris buffer saline and 0.1% Tween20)) at room temperature on rocking platform at 70rpm for 1 hour to minimize non-specific background staining by primary and secondary antibodies. Membranes were incubated overnight with the appropriate primary antibody at 4°C (see table 2.2 for details of all antibodies used) using an antibody dilution recommended by the manufacturer. After washing 3X with TBS-T buffer (TBS with 0.05% (v/v) tween20) or PBS-T for 5min, the membranes were incubated with appropriate secondary antibody solutions diluted at 1:10000 in blocking buffer for 1 hour at room temperature (table 2.2). The membranes were then washed 3 times with TBST or PBS-T as recommended. The membranes were visualized using an Odyssey infra-red imaging system (LI-COR) according to the manufacturer's instruction.

Table 2 2. List of primary and secondary antibodies.

Target	Species of primary antibody	Molecular weight	Dilution	Company	Catalogue number
PDK-1	Rabbit	47kDa	1:1000	Cell Signalling technology	mAb3820
PDK-2	Mouse	46kDa	1:1000	Proteintech	15647-1-AP
PDH	Mouse	43kDa	1:1000	Abcam	Ab110330
PDH-P	Rabbit	43kDa	1:1000	Abcam	Ab92696
HIF1 α	Mouse	120kDa	1:1000	BD transduction laboratories	610959
B-actin	Mouse	44kDa	1:50000	Millipore	MAB1501
PMM2	Mouse	23kDa	1:1000	Abnova	H00005373-A01
MPI	Rabbit	47kDa	1:2000	GeneTex	GTX114556

Secondary antibodies table:

Species	Isotype	Dilution	Company	Catalogue number
Rabbit	IgG	1:10000	Rockland	611-145-122
Mouse	IgG	1:10000	Life Technologies	A21057

Chapter 3. Evaluation of metabolic inhibitors as hypoxia selective agents

3.1 Introduction

According to the Warburg hypothesis, many malignant cells generate their energy via glycolysis, even in the presence of oxygen instead of using much more efficient oxidative phosphorylation. Cancer cells relying on glycolysis has been classified as a feature of the tumour microenvironment and would be expected for those cancer cells in hypoxic regions where oxygen is less available. This metabolic change in the cancer cells, whilst inefficient in generating ATP, not only gives them a proliferative advantage because of the provision of substrates for synthesis of lipids or nucleotides, but also may provide resistance to apoptosis. This chapter investigates the effect of glycolytic inhibitors and the PDK inhibitor DCA on hypoxic cancer cells and whether by potentially shifting the energy metabolism of tumour cells towards oxidative phosphorylation this could inhibit their growth and/or promote their cell death. In addition, several novel Akt inhibitors are evaluated for selective activity against hypoxic cancer cells. Akt pathway was described in more detail in chapter 1.

3.2 Additional methods

3.2.1 High Performance Liquid Chromatography (HPLC)

The stability of DCA was assayed using HPLC with a UV detector. DCA (9.73 mg) was dissolved in 2 ml of ultrapure water at room temperature. DCA solutions of known concentration were used to create a calibration curve at concentrations ranging from 1mM to 15.6mM. The DCA stability in culture medium at 37°C was examined over a 24 hour period. At various time points, the medium was collected into separate Eppendorf tubes and mixed with an equal volume of acetonitrile (1:1). Precipitated proteins were pelleted by centrifugation at 16,000 rpm for 5 min, the supernatant collected and then filtered through a 0.45µm membrane filter. Separations of the supernatant post acetonitrile precipitation were performed using a Beckman System Gold HPLC 166 pump, which used isocratic mobile phase (A) 0.005M tetrabutylammonium sulfate in HPLC water and (B) methanol onto a Kinetex Reversed Phase 5µm C18, 250 x 4.6 mm Column. DCA peaks were detected at a wavelength of 220 nm using a HPLC flow rate of one mL/min.

3.3 Results

3.3.1 Validation of the MTT assay

Before starting MTT chemosensitivity testing, the relationship between cell number and absorbance was determined using HT-29, BE and HCT116 p53^{+/+} cells to confirm the validity of this assay for cytotoxicity screening. The results of these initial experiments are presented in figure 3.1. The results demonstrate that a linear relationship between cell number plated and absorbance exists for all three cell lines. Furthermore, there are inherent differences in the ability of cells to convert MTT to formazan with HCT116 p53^{+/+} cells appearing more proficient than BE cells. The results demonstrate that the absorbance is proportional to viable cell number and is therefore a valid assay to measure cellular response to therapeutic agents.

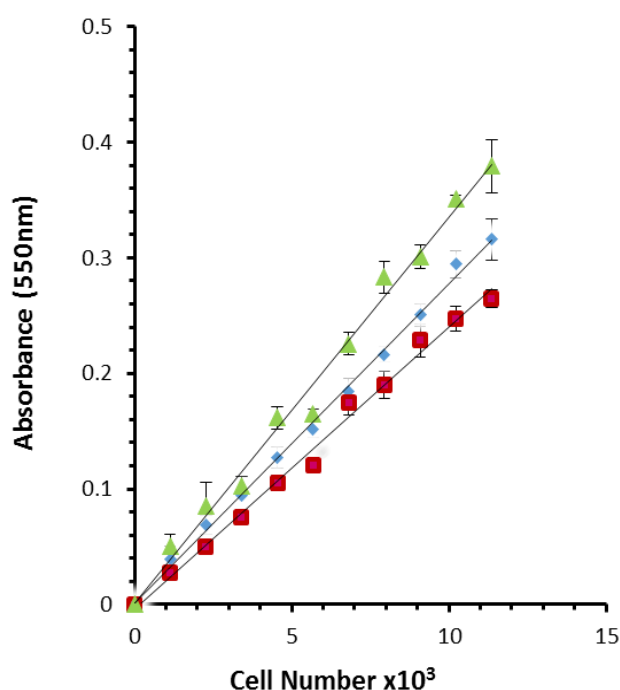


Figure 3.1 Relationship between cell number and absorbance in the MTT assay. Three cell lines are presented here; HCT116 p53^{+/+} (▲), HT-29 (●) and BE (■). Each value represents the mean \pm standard deviation for eight replicates.

3.3.2 Determine the different of cancer cells grown under aerobic and hypoxic condition.

The response of cells following continuous exposure to hypoxia (0.1% oxygen) and aerobic conditions is presented in figure 3.2. The result demonstrate that all cell lines do not grow as well under hypoxic conditions compared to aerobic conditions. In comparison to aerobic conditions, continuous exposure to hypoxic conditions resulted in growth inhibition ranging from 65% (HCT116 p53^{+/+}) to 15% (HCT116 p53^{-/-}).

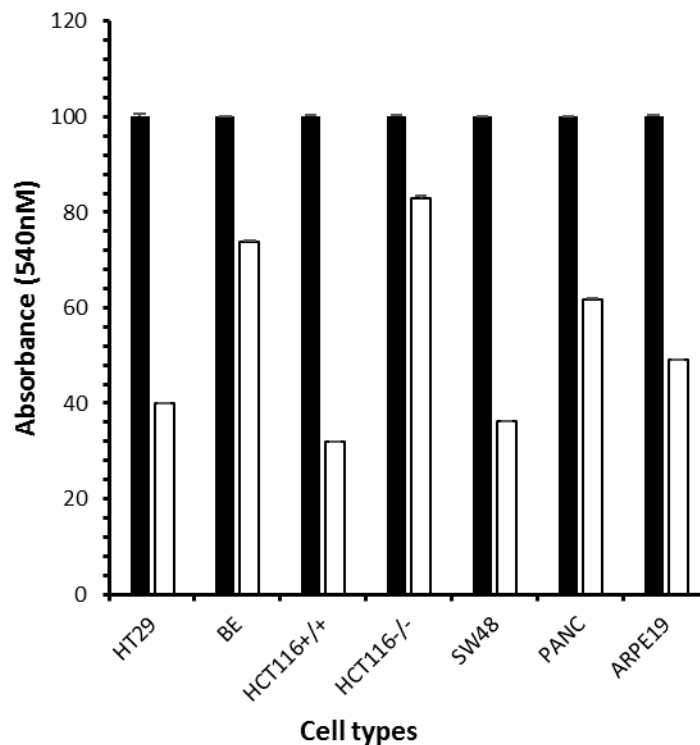


Figure 3.2 Percentage of cell survival of untreated cancer cell line under aerobic and hypoxic condition. Each value represents the mean \pm standard deviation for three replicates. Black bar represents normoxic cells; white bar represents hypoxic cells.

3.3.3 Response of HCT116 p53^{+/+} cells to tirapazamine under aerobic and hypoxic conditions.

The response of HCT116 p53^{+/+} cells to tirapazamine was assessed following a 96hr treatment period under normoxic and hypoxic conditions. Tirapazamine was used as a positive control to ensure experimental conditions were suitable for the evaluation of glycolytic inhibitors. Figure 3.3 presents dose response curves for treated cells under aerobic (blue) and hypoxic (red) conditions. Tirapazamine was significantly more cytotoxic against cell under hypoxic conditions compared to normoxic conditions. For normoxic conditions, IC₅₀ values against cancer cells were 11.85 ± 0.63 μM whereas under hypoxic conditions IC₅₀ values were 1.23 ± 0.39 μM.

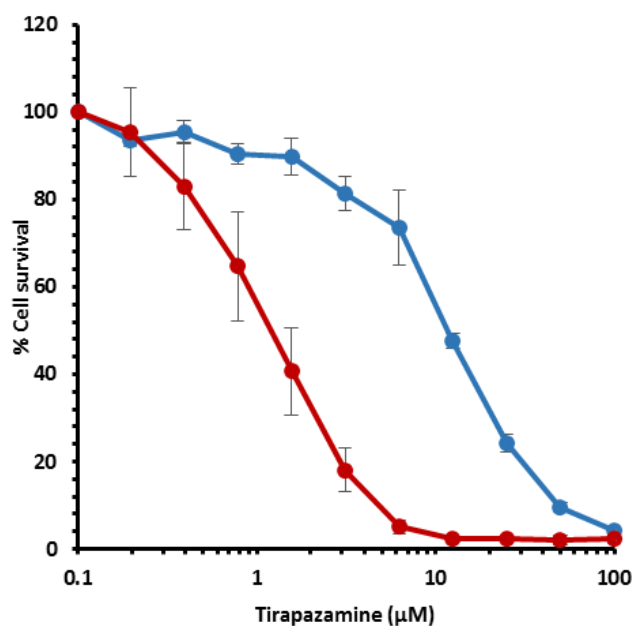


Figure 3.3 Response of HCT116 p53^{+/+} following a continuous 96-hour exposure to tirapazamine under aerobic (blue) and hypoxic (red) conditions. Each value represents the mean ± standard deviation for three independent experiments.

3.3.4 Response of a panel of cell lines to DCA under aerobic and hypoxic conditions

The response of a panel of cancer cell lines and non-cancer cells to the PDK inhibitor DCA was assessed by using the MTT assay after a 96hr treatment period under normoxic and hypoxic conditions. Six colorectal cancer cell lines (HCT116 p53^{+/+}, HCT116 p53^{-/-}, HT29, BE, LS123 and SW48), one pancreatic cancer cell line (PANC 10.05) and one non-cancer cell line ARPE-19 were investigated. Figure 3.4 and Figure 3.5 represent cytotoxicity dose responses of treated cells under aerobic (blue) and hypoxic (red) conditions. DCA was significantly more cytotoxic against some of the tested cell cancer lines under hypoxic conditions compared to normoxic conditions. For normoxic conditions, IC₅₀ values against cancer cells ranged from ~19.5 - 45.2 mM whereas under hypoxic conditions IC₅₀ values ranged from ~7.15 - 33.8 mM.

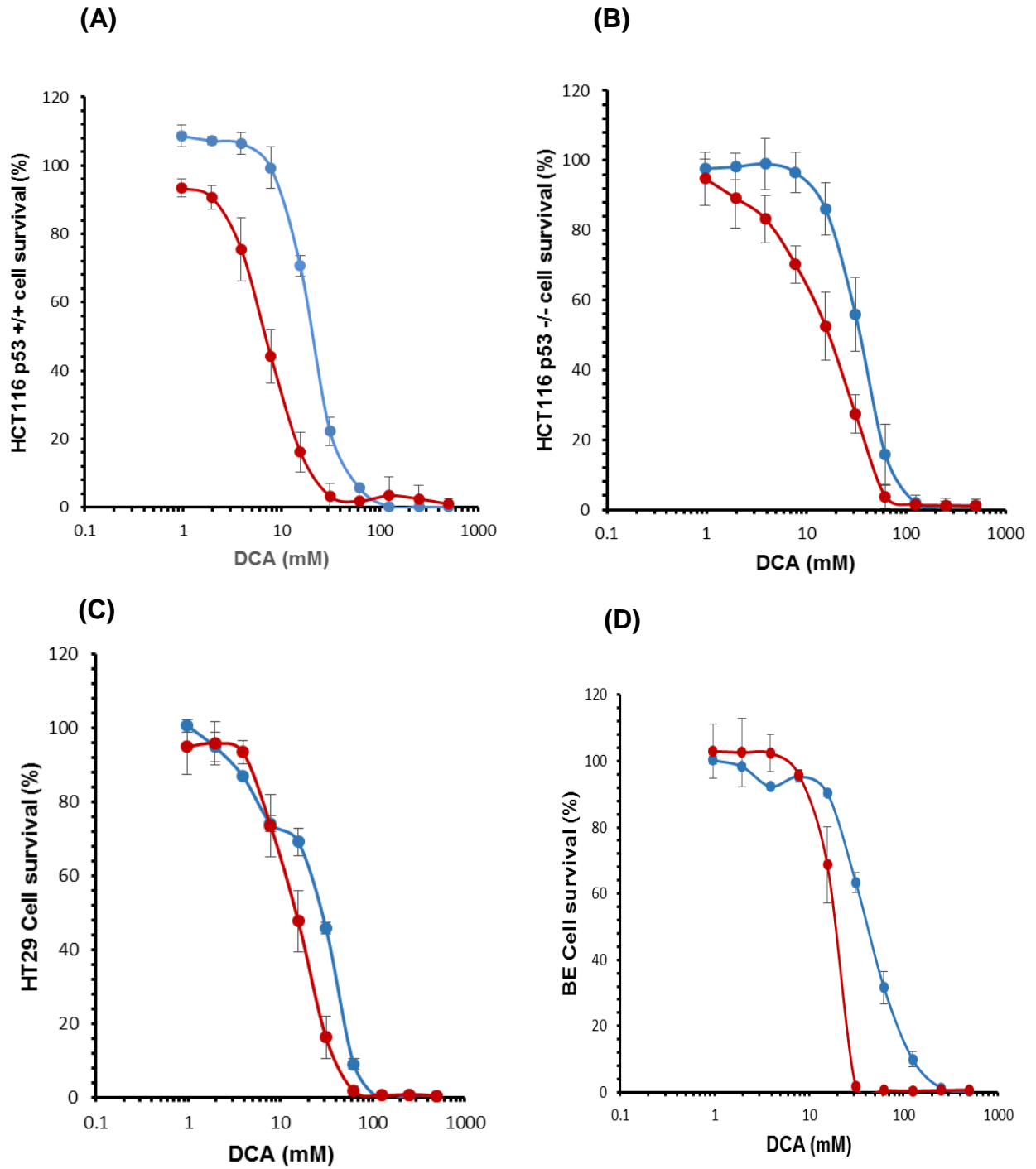


Figure 3.4 Response of HCT116 p53^{+/+} (A), HCT116 p53^{-/-} (B), HT-29 (C) and BE (D) following a continuous 96 hour exposure to DCA under aerobic (blue) and hypoxic (red) conditions. Each value represents the mean \pm standard deviation for three independent experiments.

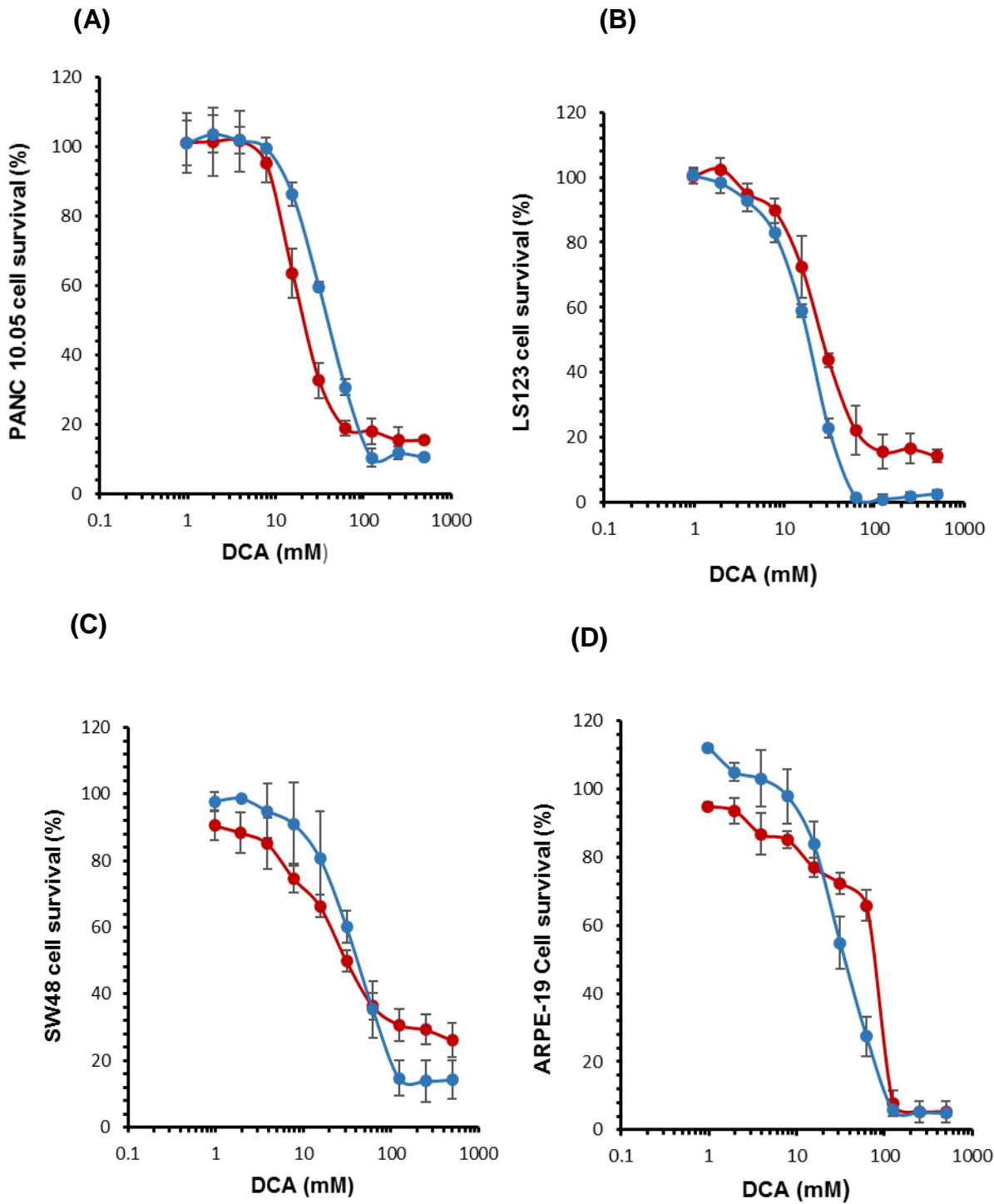


Figure 3.5 Response of PANC 10.05 (A), LS123 (B), SW48 (C) and ARPE-19 (D) following a continuous 96-hour exposure to DCA under aerobic (blue) and hypoxic (red) conditions. Each value represents the mean \pm standard deviation for three independent experiments.

3.3.5 Hypoxia cytotoxicity ratios (HCR) and selectivity ratios (SR) based upon the 96-hour continuous DCA exposure data set.

A summary of the IC₅₀ data obtained for each cell line under hypoxic and normoxic conditions is presented in figure 3.6. Further analysis of the cytotoxicity data obtained included calculation of hypoxia cytotoxicity ratios and selectivity ratios (Table 3.1). Hypoxic cytotoxicity ratio is defined the ratio of IC₅₀ values under normoxia divided by IC₅₀ values under hypoxia; a ratio greater than one means enhanced sensitivity under hypoxia a ratio of one means equipotent drug activity under aerobic and hypoxic conditions, and a ratio less than one means resistance under hypoxia; results are shown in table 3.1. DCA was active and appeared more sensitive to hypoxic HCT116 p53^{+/+}, HCT116 p53^{-/-}, HT29, BE and Panc10.05 cancer cells with varied HCRs of 3.11, 1.43, 1.85, 1.84 and 1.86 respectively. Under aerobic conditions, DCA was only substantially more active against the LS123 cancer cell than the ARPE19 non-cancer cells. However, as shown in Figure 3.6 and Table 3.1, DCA was more cytotoxic against all the cancer cell lines than the non-cancer cells under hypoxia.

Cell line	IC ₅₀ (Hypoxia) (mM)	IC ₅₀ (Aerobic) (mM)	HCR	SR
HCT116 p53 ^{-/-}	20.09 ± 3.42	28.91 ± 1.81	1.43	1.83
PANC 10.05	22.27 ± 3.30	41.62 ± 1.09	1.86	1.65
HT-29	15.29 ± 2.53	28.34 ± 1.33	1.85	2.40
HCT116 p53 ^{+/+}	7.15 ± 0.89	22.27 ± 0.58	3.11	5.15
SW48	33.76 ± 3.84	45.23 ± 2.22	1.39	1.09
BE	18.78 ± 2.40	34.66 ± 4.66	1.84	1.96
LS123	27.40 ± 1.72	19.53 ± 0.94	0.71	1.34
ARPE-19	79.46 ± 4.53	36.84 ± 7.52	0.46	N/A

Table 3.1 Response of a panel of cancer and non-cancer (ARPE19) cells following continuous exposure to DCA under aerobic and hypoxic (0.1% oxygen) conditions.

The HCR denotes hypoxic cytotoxicity ratio and this is defined as the IC₅₀ in aerobic conditions divided by the IC₅₀ under hypoxia. SR denotes the selectivity index which here represents the IC₅₀ of ARPE19 cells in aerobic conditions divided by the IC₅₀ for DCA under hypoxic conditions.

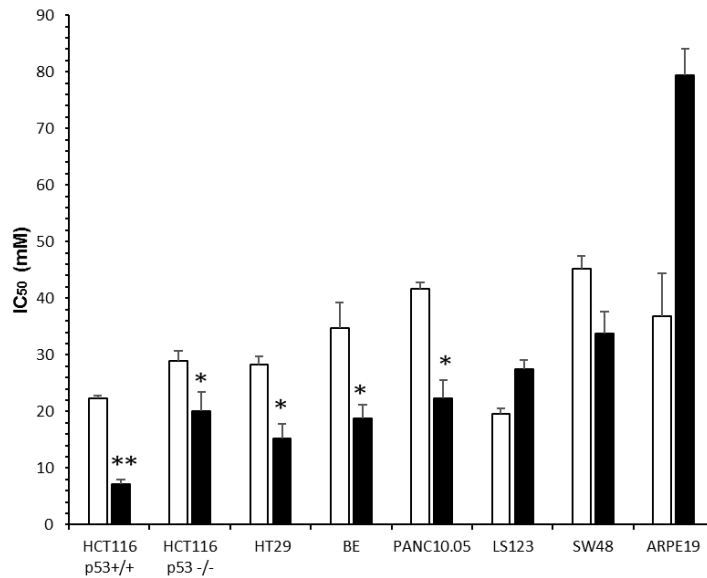


Figure 3.6 Graphical representation of the response of cells to DCA. Each value represents the mean \pm standard deviation for three independent experiments. DCA reduced cell growth of HCT116 p53^{+/+} (** $P < 0.01$), as well as reduce cell growth of HCT116, HT29, BE and PANC10.05 (* $P < 0.05$) under hypoxic condition compare to aerobic condition. Black bar represents hypoxic cells; white bar represents normoxic cells.

3.3.6 Response of colorectal cancer cells following short time exposure to DCA (1hour) under hypoxic and aerobic conditions.

The effect of DCA on HCT116 p53^{+/+}, HCT116 p53^{-/-}, HT-29 and BE cells following one-hour exposure is presented in figure 3.7. The response to DCA was varied between cell lines, but it was generally greater under hypoxic than the normoxic conditions. IC₅₀ values under hypoxic conditions ranged from 173.9mM to 224.6mM whereas IC₅₀ values under normoxic conditions ranged from 230.4 to >500mM. Given differences observed in the response to DCA between isogenic p53^{+/+} and p53^{-/-} HCT116 cells, this suggested that p53 status could influence response which might also account for some variability between some of different cancer cell lines.

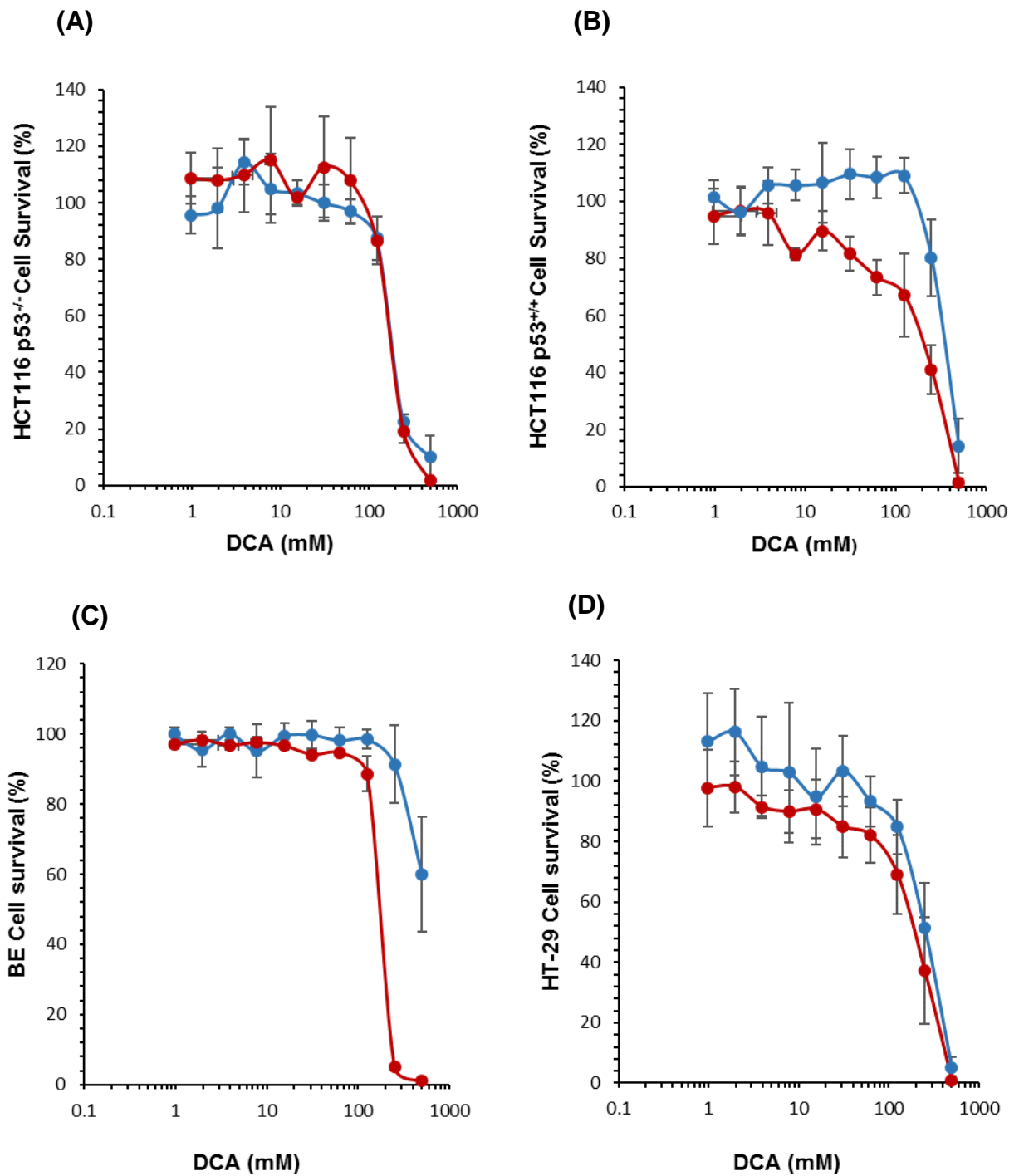


Figure 3.7 Response of HCT116 p53^{-/-} (A), HCT116 p53^{+/+} (B), BE (C) and HT-29 (D) following a one-hour exposure to DCA under aerobic (blue) and hypoxic (red) conditions. Each value represents the mean \pm standard deviation for three independent experiments.

	IC₅₀ Aerobic	IC₅₀ Hypoxic	HCR
HT-29	297.6 ± 22.2	173.9 ± 24.6	1.71
BE	>500	182.7 ± 4.83	>2.73
HCT116 p53^{+/+}	359.5 ± 14.7	224.6 ± 25.3	1.60
HCT116 p53^{-/-}	230.4 ± 4.1	195.7 ± 18.2	1.17

Table 3.2 Response of cell lines following a one-hour exposure to DCA under aerobic and hypoxic conditions. Each value represents the mean IC₅₀ (mM) ± standard deviation for three independent experiments. HCR denotes hypoxic cytotoxicity ratio.

3.3.7 Influence of duration of drug exposure on the response of cells to DCA

To investigate time dependent effects on the response of cells to DCA further experiments were conducted. The experiment compared the response of two colorectal cancer cell lines that have different p53 states HCT116 p53^{+/+} (p53 wild-type) and HT29 (p53 mutated) using the MTT assay. Cells were treated with different concentrations of DCA between 0.976 and 500mM under 21% oxygen conditions (normoxia) incubated for different times (1hr, 2hr, 4hr, 6hr, 12hr, 24hr). It was found that DCA reduced cell viability in both cell lines (figure 3.8). There were minor difference in dose response between the two cell lines following DCA treatment at each time point but generally the pattern was similar. In both cases IC₅₀ values decreased as the duration of drug exposure increases but analysis of concentration x time (C x T) parameters indicates a time dependent difference (Figure 3.8 E and F). Usually cell kill is proportional to the product of C x T but in this case, C x T parameters required to kill 50% of cells increased with time suggesting that DCA could be unstable in culture medium when incubated for long periods of time.

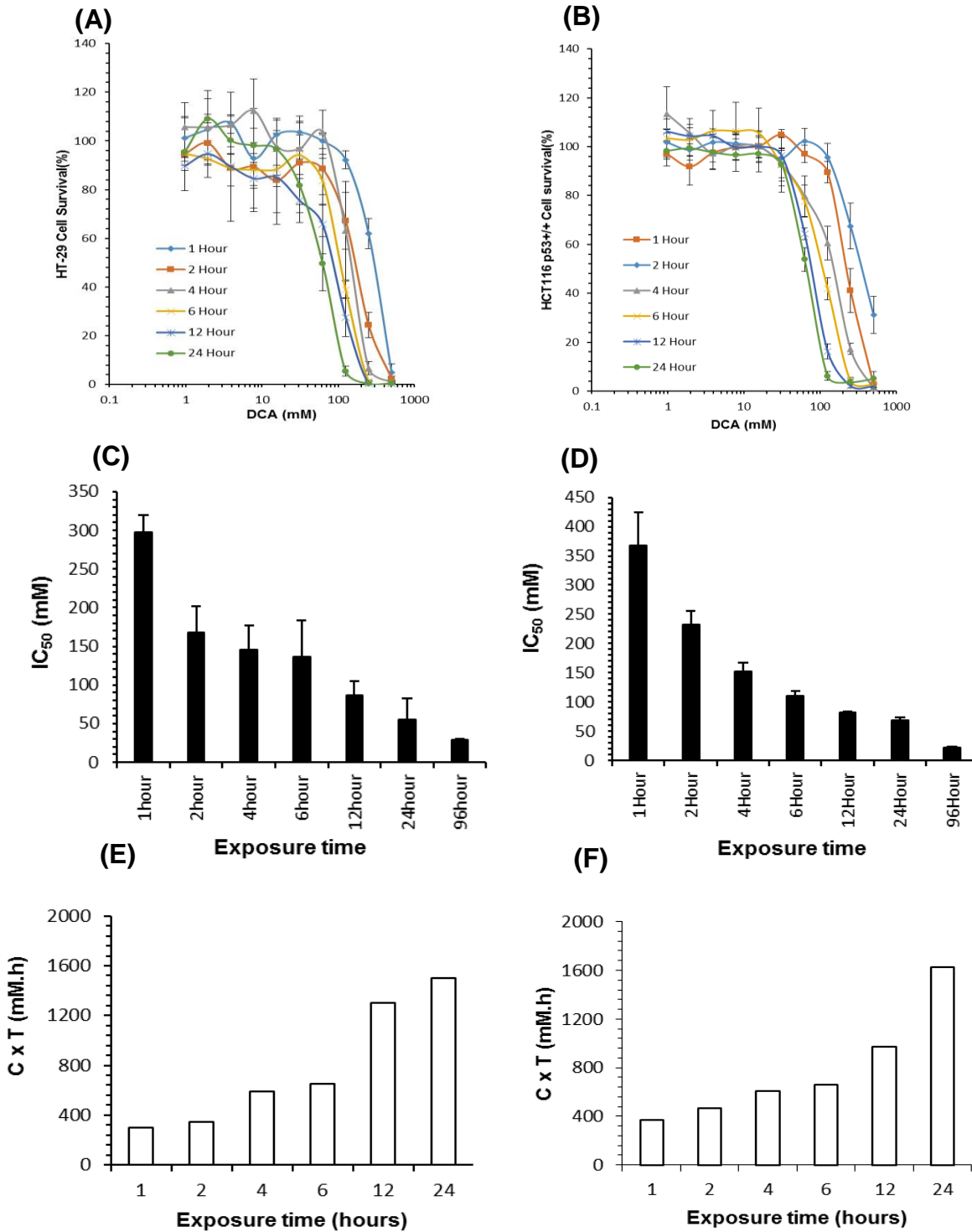


Figure 3.8 Influence of drug exposure time on the response of HT29 (left-hand panels) and CT116 p53^{+/+} (right-hand panels) to DCA. Panels A and B present dose-response curves and panels C and D present the corresponding IC_{50} values (mean \pm standard deviation for n = 3). Panels E and F represent C x T relationships for both cell lines as a function of exposure time.

3.3.8 Determination of DCA stability by using HPLC analysis

The main objective of this experiment was to test the stability of DCA in cell culture medium at 37°C and 5% CO₂ over time. For DCA measurements, standards of DCA solutions were prepared in cell culture medium (RPMI1460) with final concentrations ranging from 0.9765mM to 31.25mM. The results are presented in figure 3.9 with calibration curves and representative chromatograms presented in figure 3.10.

In this case, no degradation of DCA dissolved in cell culture medium could be observed by HPLC measurement over a 24 hour period (figure 3.9). Quantitation using the DCA calibration curve was based on the peak area ratio. This was performed by using different concentrations (two-fold dilutions) of DCA dissolved in water and in RPMI 1640 medium, extraction using acetonitrile precipitation and analysis by HPLC analysis. Using this methodology, a peak of DCA was detected with retention at 10.600 min (figure 3.10). The chromatogram in figure 3.10 shows that separation of DCA that was achieved.

The conclusion from this data is that there was no significant loss of DCA from culture media over a 24hour period at 37°C.

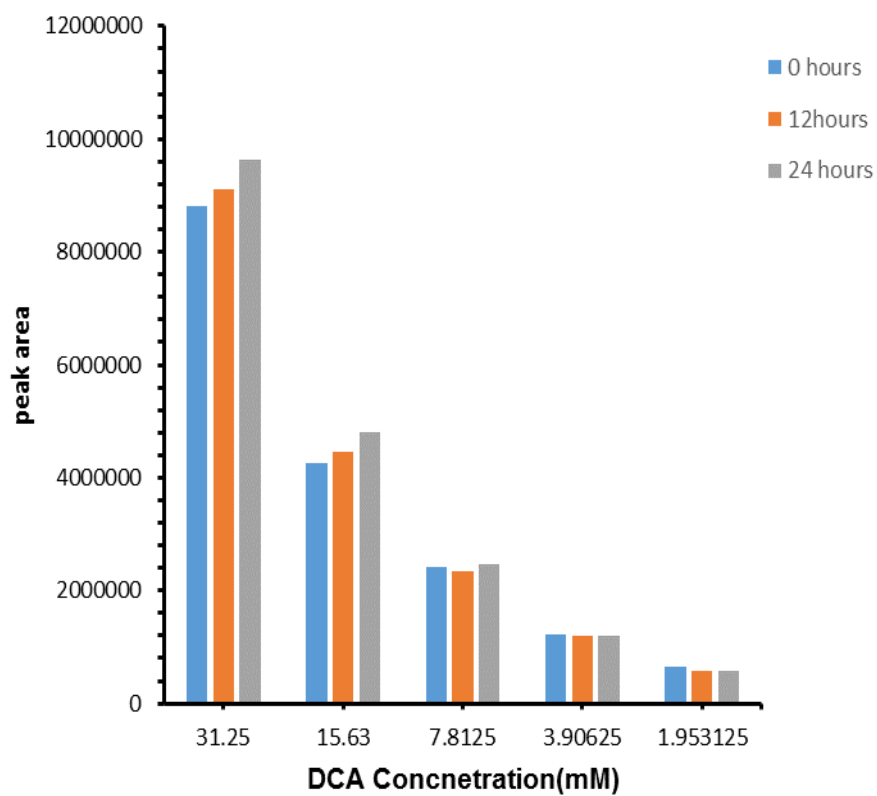


Figure 3.9 Standard calibration curve to measure stability of DCA in medium at 37°C, 5% CO₂ and humid conditions over a 24 hour period.

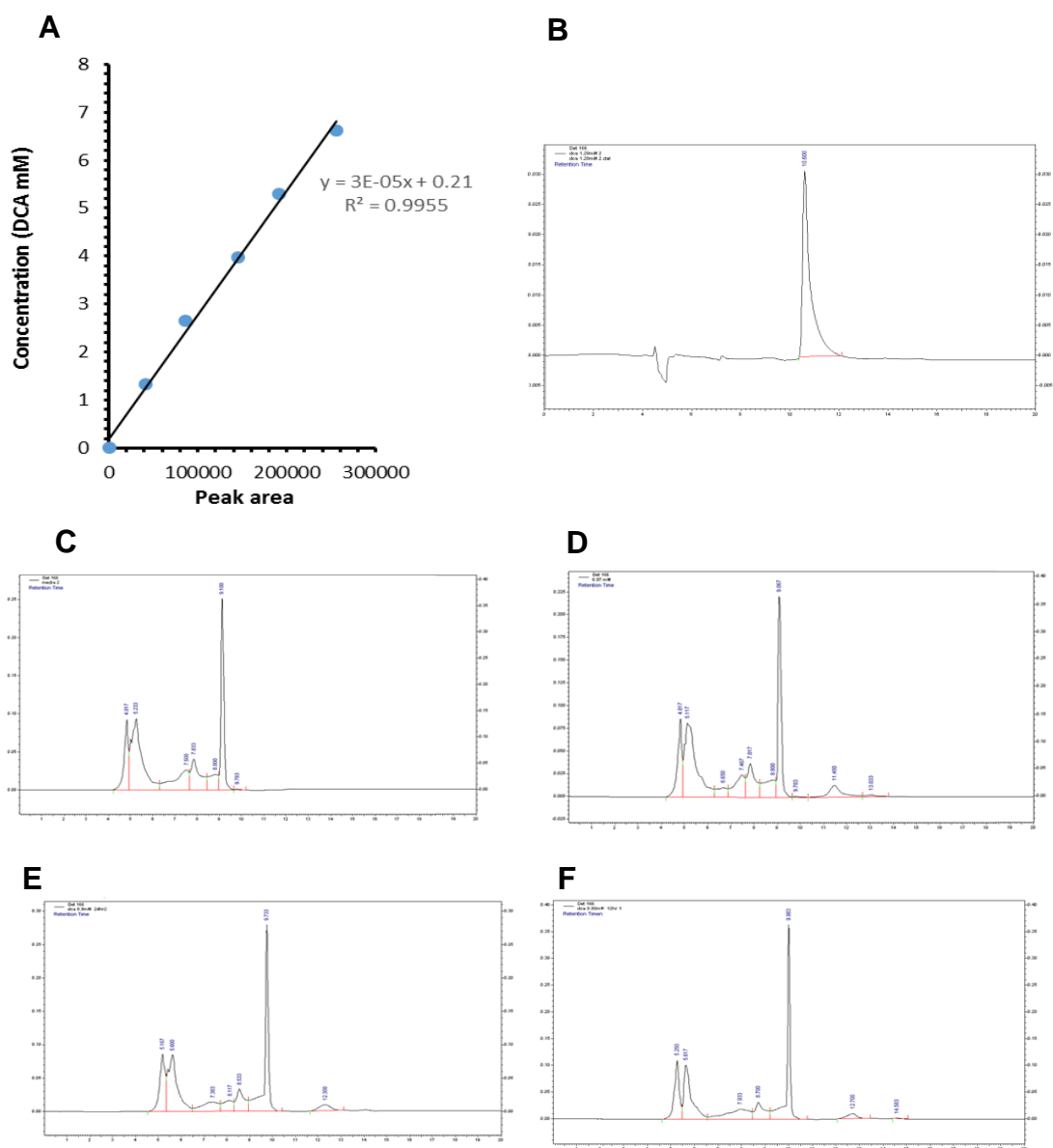


Figure 3.10 Calibration curve and representative chromatograms for the analysis of DCA. Panel A is a calibration curve using DCA dissolved in deionised water and panel B is a representative chromatogram of one of these standards. A clear peak at 10.487 min is visible. Panels C to F represent chromatograms for media only (C) and DCA extracted from media at t=0 (D), t = 12 hours (E) and t = 24 hours (F). In all the cell culture media experiments, the retention time for DCA increased to 11.2 min.

3.3.9 Influence of different growth media on the response of HCT116 cells to DCA

Figure 3.11 shows the influence of different cell culture media on the response of cells to DCA under hypoxic and normoxic conditions. HCT116 p53^{+/+} and HCT116 p53^{-/-} cells were cultured in complete DMEM and RPMI1640 media for 96 hours following a 1h exposure to DCA in these respective media. HCT116 p53^{+/+} cells that were cultured in DMEM and RPMI1640 media showed no significant difference in the response under aerobic conditions (IC₅₀ 359.5 ± 14.7 mM and 367.7 ± 57.1 mM respectively) In contrast under hypoxic conditions, HCT116 p53^{+/+} were more sensitive to DCA in RPMI1640 medium compared to DMEM with IC₅₀ values of 180.7 ± 17.4 mM and 224.6 ± 25.3 Mm, respectively.

The response of HCT116 p53^{-/-} cells differed, with cells showing increased cytotoxic response to DCA in RPMI1640 medium compared to DMEM medium under aerobic conditions (IC₅₀ values 196.3 ± 5.1mM and 230.4 ± 4.1 mM respectively) but not under hypoxic conditions (IC₅₀ values 192.4 ± 7.2 mM and 195.7 ± 18.2 mM respectively; Table 3.3). It was shown that HCT116 p53^{+/+} cells are less sensitive to DCA in DMEM and RPMI1460 media under aerobic conditions compared to HCT116 p53^{-/-} (P-value <0.01) whereas under hypoxic conditions both cell showed similar response to DCA in DMEM and RPMI1460 media represented in figure 3.12.

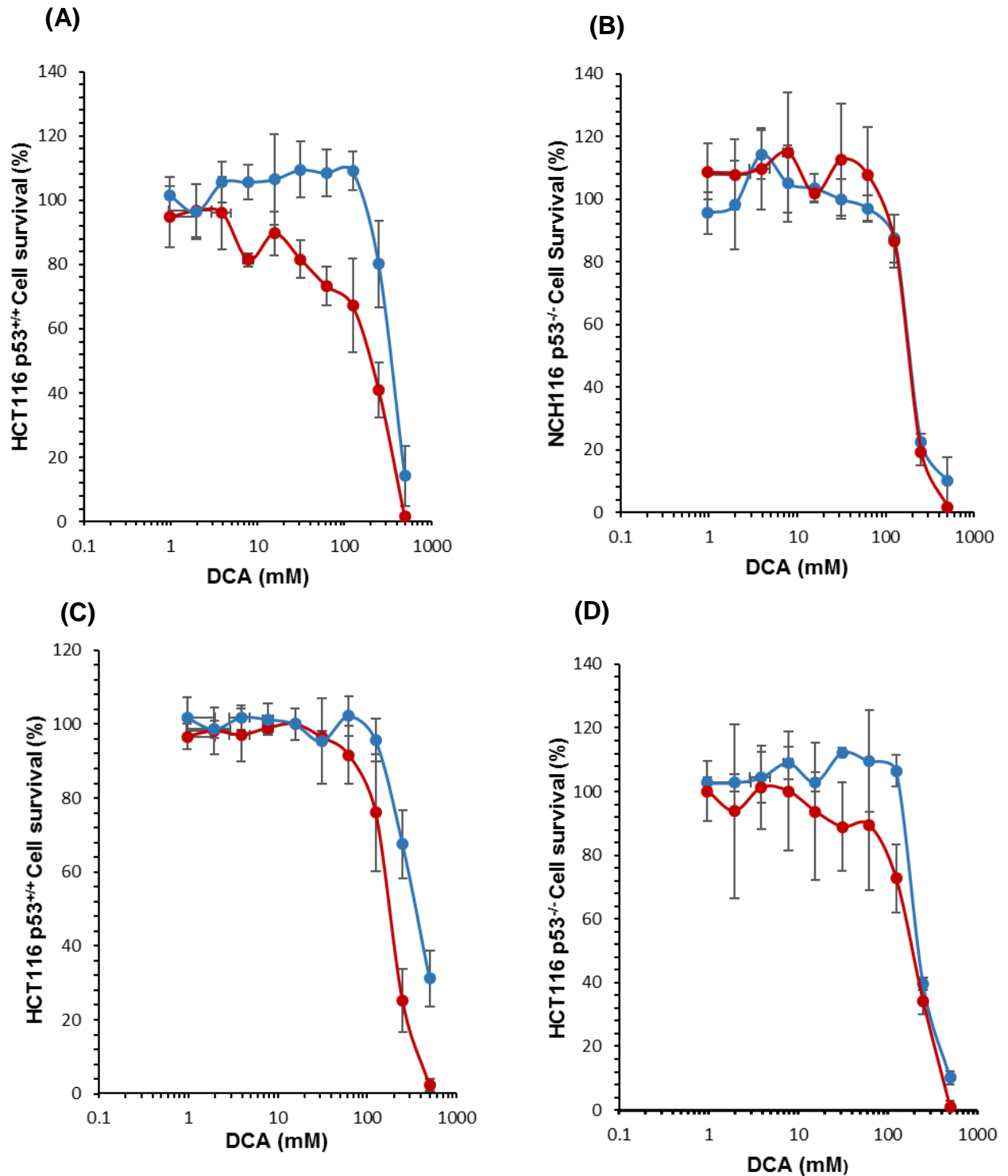


Figure3. 2 Response of HCT116 p53^{+/+} and HCT116 p53^{-/-} to DCA (1-hour exposure) in DMEM (panels A and B) and RPMI1640 (panel C and D) media. These experiments were conducted under both aerobic (blue) and hypoxic (red conditions) and each value represents the mean \pm standard deviation for three independent experiments.

Cell line	IC ₅₀ Aerobic (DMEM)	IC ₅₀ Aerobic (RPMI 1640)	IC ₅₀ Hypoxic (DMEM)	IC ₅₀ Hypoxic (RPMI 1640)
HCT116 p53 ^{+/+}	359.5 ± 14.7	367.7 ± 57.1	224.6 ± 25.3	180.7 ± 17.4
HCT116 p53 ^{-/-}	230.4 ± 4.1	196.3 ± 5.1	195.7 ± 18.2	192.4 ± 7.2

Table 3.3 Response of HCT116 cells to DCA (1-hour exposure) under aerobic and hypoxic conditions in DMEM and RPMI 1640 culture media. Values presented are the mean IC₅₀ values (mM) ± standard deviation for three independent experiments.

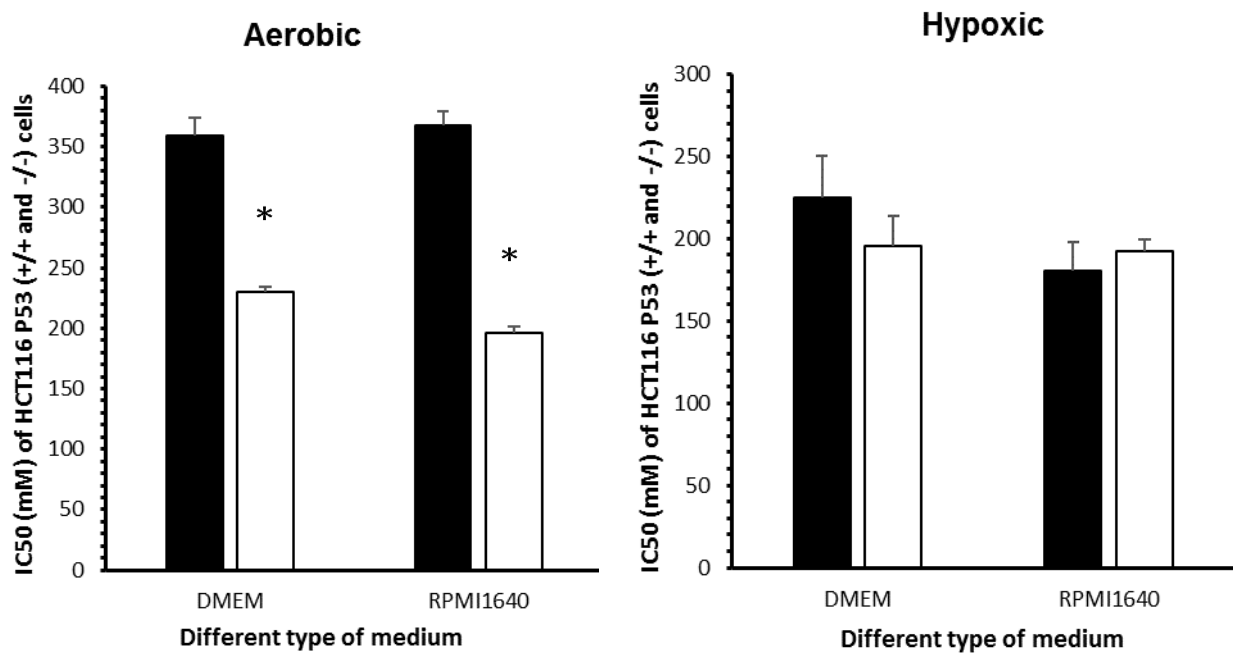


Figure 3.12 IC₅₀ values of HCT116 cells to DCA (1-hour exposure) under aerobic (left-hand panels) and hypoxic (right-hand panels) conditions in DMEM and RPMI 1640 culture media (mean ± standard deviation for n = 3), black bar represents HCT116 p53^{+/+} cells; white bar represents HCT116 p53^{-/-} cells. *P<0.01 (student's t-test).

3.3.10 Dose response of colorectal cancer cells to different glycolytic inhibitors under hypoxic and normoxic conditions.

The effect of inhibitors of the glycolytic enzymes hexokinase II and LDH-A on cancer cell survival under normoxic and hypoxic conditions was also assessed. Four colorectal cancer cell lines (BE, HT29, HCT116 p53^{+/+} and HCT116 p53^{-/-}) were investigated; two hexokinase II inhibitors, 2-Deoxy-D-glucose (2DG) and 3-Bromopyruvic acid (3BP) were compared under hypoxic and normoxic conditions. 2DG had similar cytotoxic effects under both conditions. For normoxic conditions IC50 values ranged between 1.09 and 1.65 mM whereas for hypoxic conditions the IC50 values ranged between 0.99 mM and 2.43 mM.(summarised in table 3.4). In contrast, 3BP showed different effects between cells under normoxic compared to hypoxic conditions. 3BP was consistently less active towards the cancer cells grown under hypoxic conditions(figure 3.13, 3.16 and table 3.4). Hypoxia cytotoxicity ratios ranged from 0.34-0.67 consistent with reduced activity towards hypoxic cells. All four cell lines had similar responses to gossypol and sodium oxamate. Both of these LDH-A inhibitors were consistently less active against all 4 cancer cell lines under hypoxic conditions compared to activity under aerobic conditions (Figure 3.13, 3.16 and summarised in table 3.4). It was also apparent that the BE cell line was more resistant in general to several of the inhibitors under both conditions; this was particularly so for 3BP (Table 3.4). Hexokinase and lactate dehydrogenase inhibitors have shown less effective in hypoxia conditions to colorectal cancer cells compared to aerobic conditions with average HCR 0.51-1.04 as represented in figure 3.17.

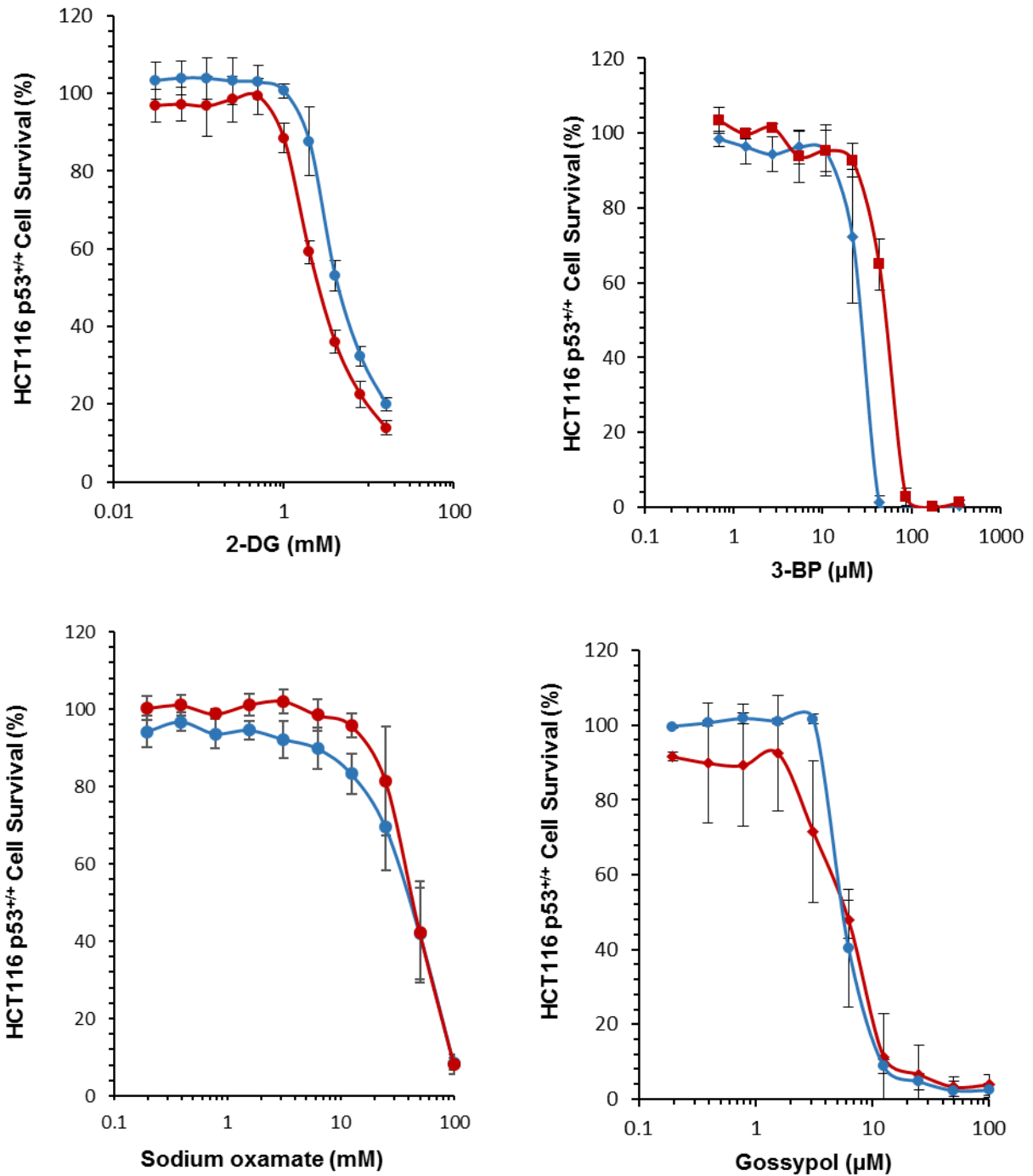


Figure 3.3 Response of HCT116 p53^{+/+} cells to 2-deoxy-glucose (2-DG), 3-bromopyruvate (3-BP), sodium oxamate and gossypol under aerobic (blue) and hypoxic (red) conditions. The duration of drug exposure was 96 hours, and each value represents the mean ± standard deviation for three independent experiments.

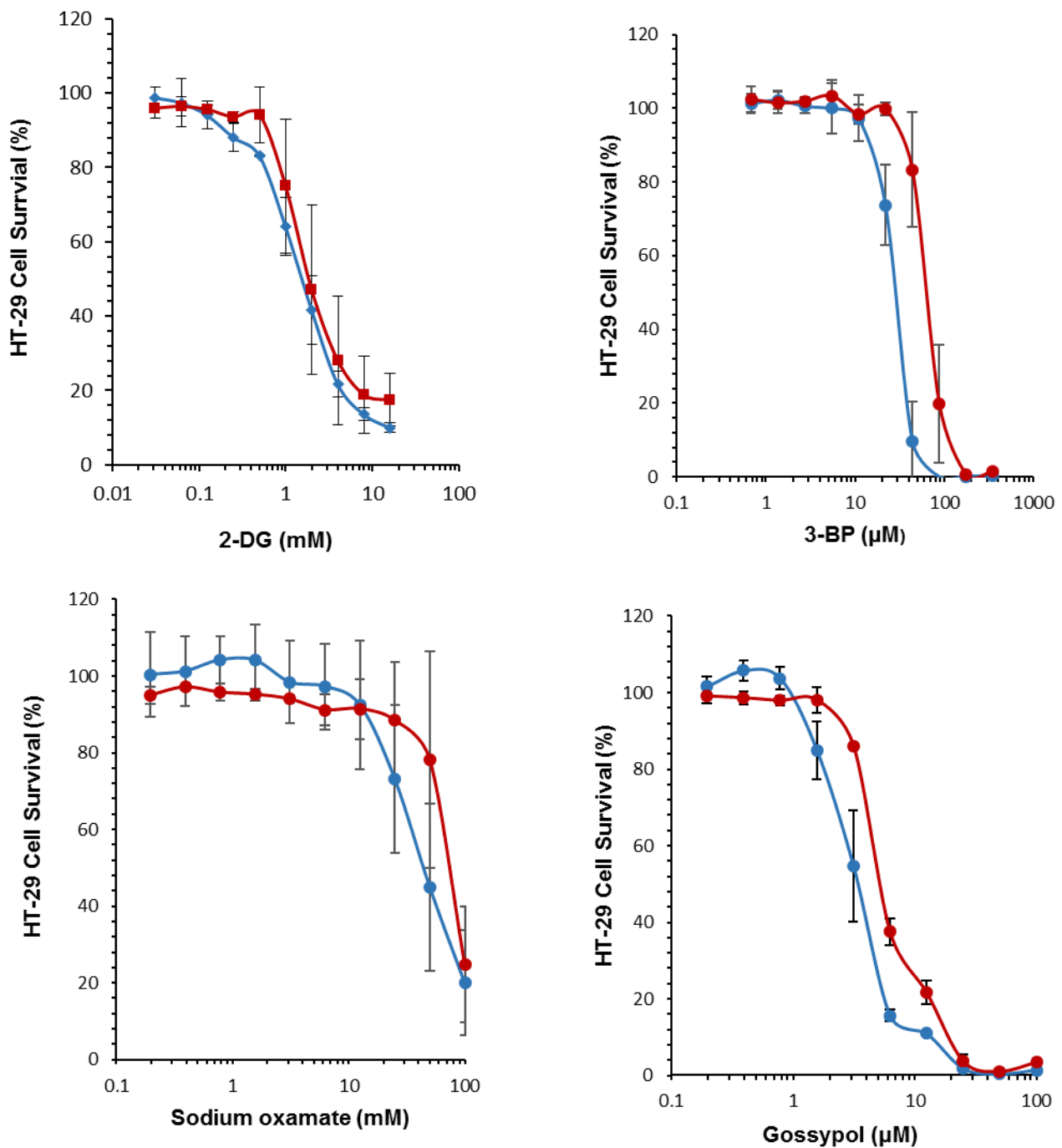


Figure 3.4 Response of HT-29 cells to 2-deoxy-glucose (2-DG), 3-bromopyruvate (3-BP), sodium oxamate and gossypol under aerobic (blue) and hypoxic (red) conditions. The duration of drug exposure was 96 hours, and each value represents the mean \pm standard deviation for three independent experiments.

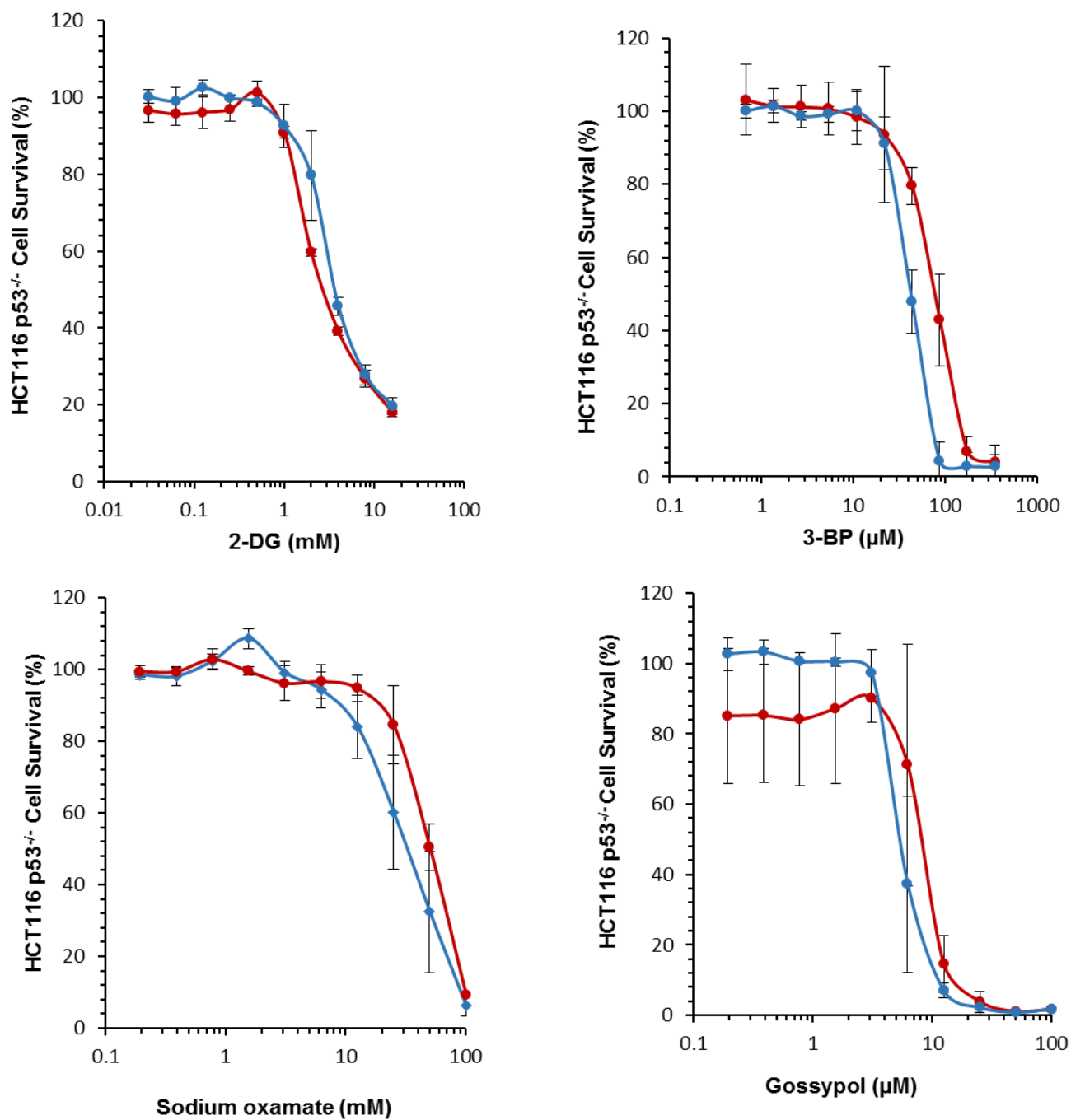


Figure 3.5 Response of HCT116 p53^{-/-} cells to 2-deoxy-glucose (2-DG), 3-bromopyruvate (3-BP), sodium oxamate and gossypol under aerobic (blue) and hypoxic (red) conditions. The duration of drug exposure was 96 hours and each value represents the mean ± standard deviation for three independent experiments.

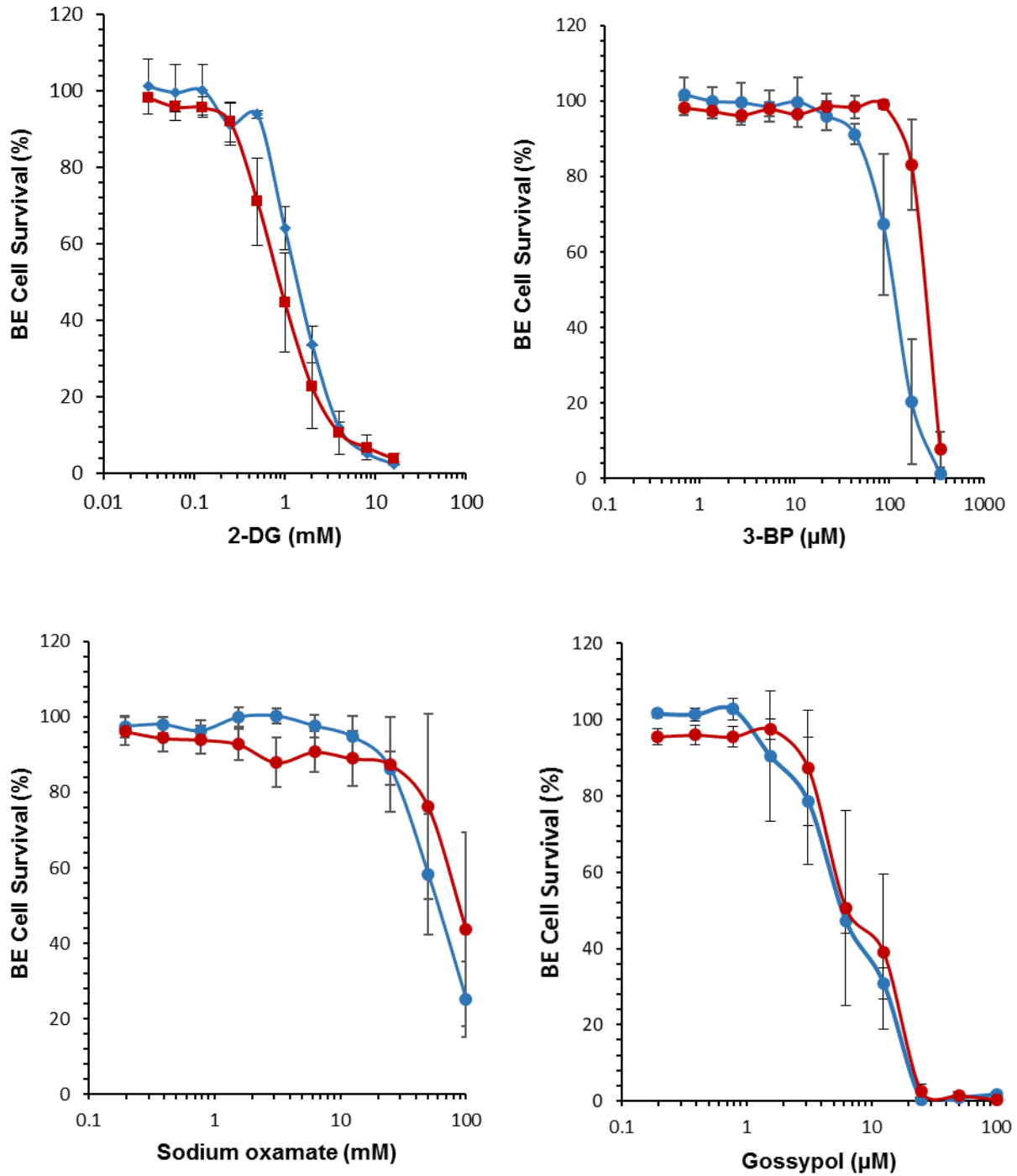
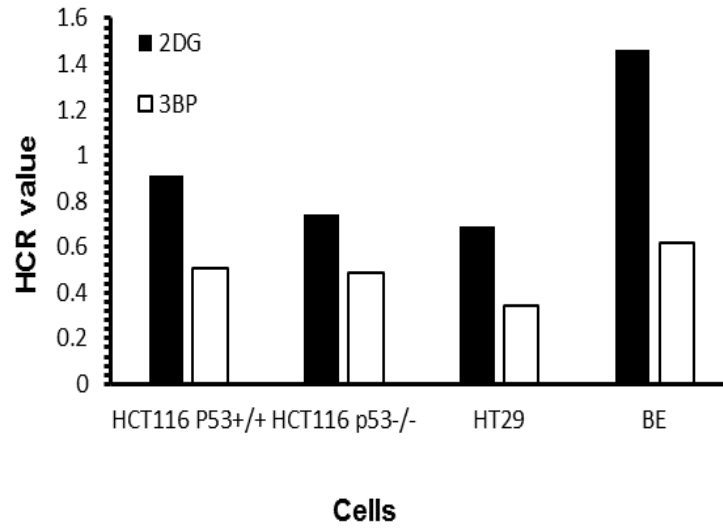


Figure 3.6 Response of BE cells to 2-deoxy-glucose (2-DG), 3-bromopyruvate (3-BP), sodium oxamate and gossypol under aerobic (blue) and hypoxic (red) conditions. The duration of drug exposure was 96 hours, and each value represents the mean \pm standard deviation for three independent experiments.

		IC₅₀ ± standard deviation (n = 3)			
Inhibitor		HT-29	BE	HCT116 p53^{+/+}	HCT116 p53^{-/-}
2-DG (mM)	Aerobic	1.65 ± 0.38	1.45 ± 0.17	1.26 ± 0.29	1.09 ± 0.21
	Hypoxic	2.43 ± 2.53	0.99 ± 0.36	1.38 ± 0.43	1.46 ± 0.39
	HCR	0.69	1.46	0.91	0.74
3-BP (μM)	Aerobic	29.9 ± 3.6	134.1 ± 18.7	27.8 ± 4.6	27.5 ± 4.8
	Hypoxic	66.5 ± 11.4	212.9 ± 57.6	54.2 ± 15.5	55.5 ± 13.1
	HCR	0.34	0.62	0.51	0.49
Gossypol (μM)	Aerobic	3.28 ± 1.22	5.68 ± 0.76	2.15 ± 0.61	2.07 ± 0.59
	Hypoxic	5.12 ± 0.63	13.3 ± 0.4	4.09 ± 1.07	4.98 ± 2.10
	HCR	0.64	0.42	0.52	0.41
Sodium Oxamate (mM)	Aerobic	49.8 ± 20.8	62.2 ± 17.6	49.2 ± 16.1	52.7 ± 17.0
	Hypoxic	71.8 ± 22.6	79.4 ± 39.3	60.4 ± 13.2	60.1 ± 18.2
	HCR	0.69	0.78	0.81	0.87

Table 3.4 Response of a panel of cells lines to glycolytic inhibitors under aerobic and hypoxic conditions (continuous 96-hour drug exposure). Each value represents the mean IC₅₀ ± standard deviation for three independent experiments. HCR denote the hypoxic cytotoxicity ratio define as the IC₅₀ under aerobic conditions divided by the IC₅₀ under hypoxic (0.1% oxygen) conditions.

(A)



(B)

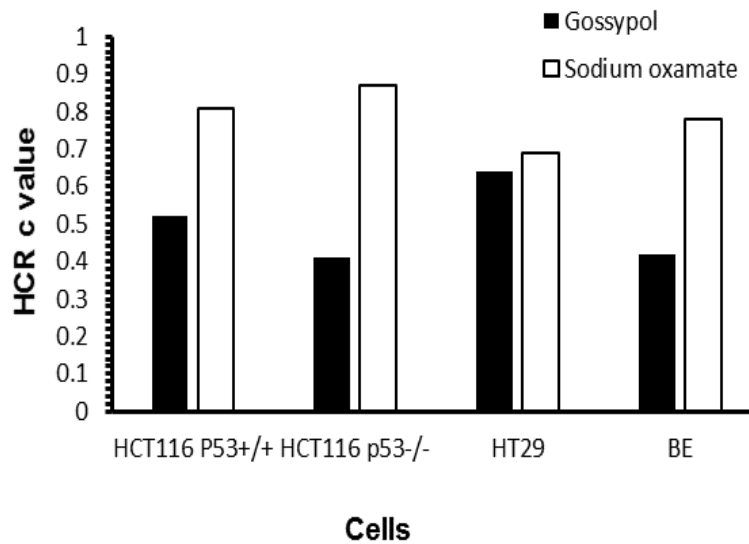


Figure 3.17 Summary of Hypoxia Cytotoxicity Ratios (HCRs) for tested glycolytic inhibitors.

Panel A Hexokinase inhibitors and panel B lactate dehydrogenase inhibitors HCR value > 1 indicate selectivity for hypoxic cells whereas HCR values < 1 indicate resistance under hypoxia.

Figure 3.18 summarises the differences in response obtained under hypoxia and normoxia for each of different metabolic inhibitors tested. The key question being addressed in this chapter was whether any of these metabolic inhibitors might serve as hypoxia selective agents. As can be seen from this figure, unexpectedly, with the exception of DCA, none of the other inhibitors showed preferential activity against hypoxic cancer cells.

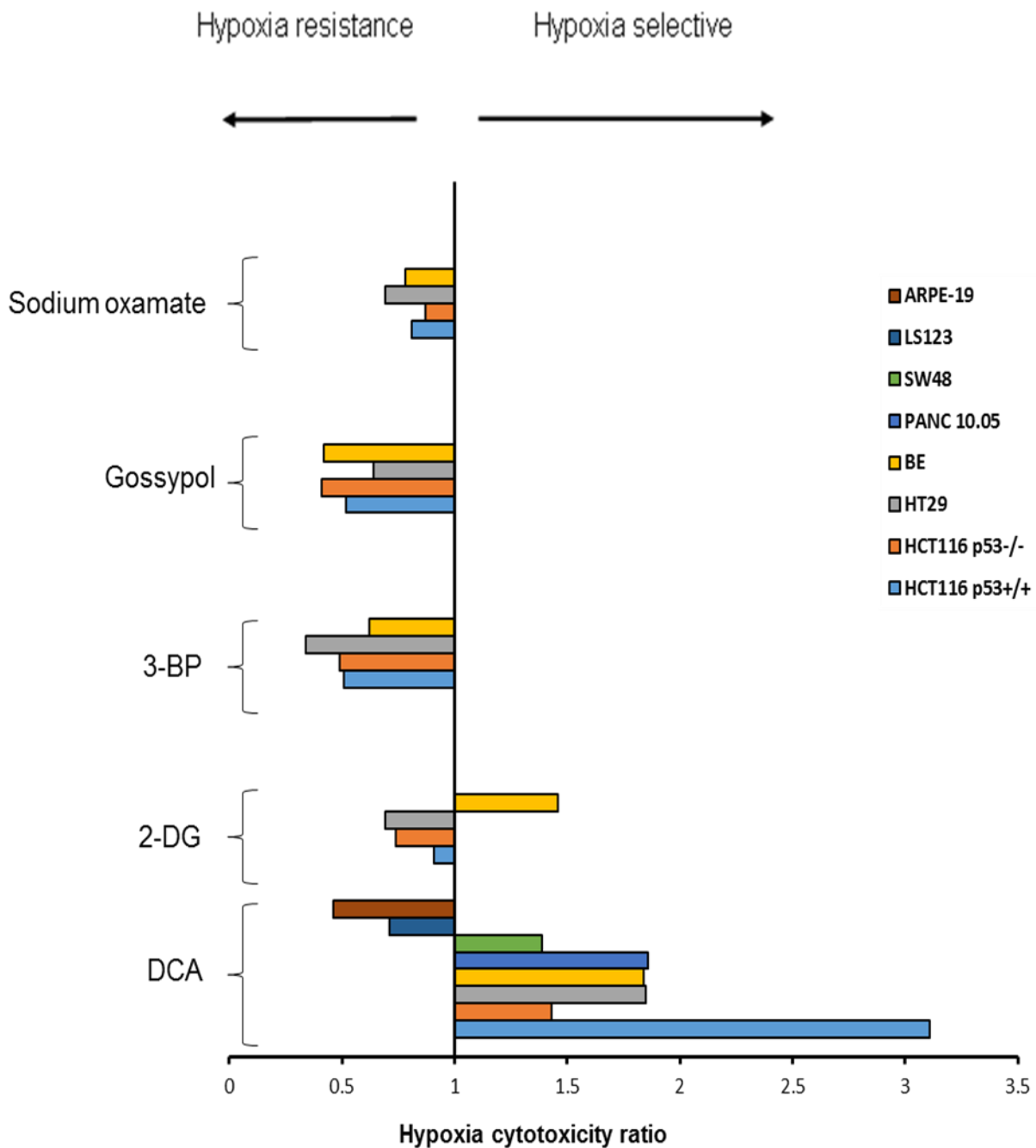
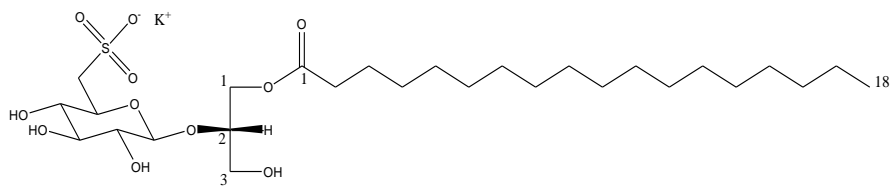


Figure 3.7 Summary of all the HCR data generated using a panel of glycolytic inhibitors and cell lines. The Y-axis is set at a HCR of 1 on the X-axis, and this represents equal activity against aerobic and hypoxic cells. HCR value > 1 indicate selectivity for hypoxic cells whereas HCR values < 1 indicate resistance under hypoxia. As the HCR values are calculated from the mean IC₅₀ values, there are no error bars on this graph.

3.3.11 Dose response of ovarian cancer cells to AKT inhibitors under hypoxic and normoxic conditions.

The response of IGROV cells, a human ovarian cancer cell line provided by Dr. Paola Perego (National Cancer Institute / Italy) to novel Akt inhibitors PP-1, PP-2 and PP-3 was investigated (figure 3.19). IGROV cells were selected in order to align with previous studies performed by Dr. Perego. The effects of these compounds on IGROV cells under both normoxic and hypoxic conditions were determined. Dose response curves are presented in figure 3.20. The cells did not respond to PP-3 with IC_{50} values greater than $30\mu M$ under both aerobic and hypoxic conditions. Whilst no IC_{50} values were obtained with PP-1, there was evidence of activity with survival values close to 50% at the highest concentration tested. There was no evidence of differential PP-1 activity between aerobic and hypoxic conditions. The most active compound was PP-2 with IC_{50} values under hypoxic and aerobic conditions of 23.38 ± 3.25 and 21.57 ± 2.73 respectively. The difference between the two groups was not however statistically significant ($P > 0.1$).

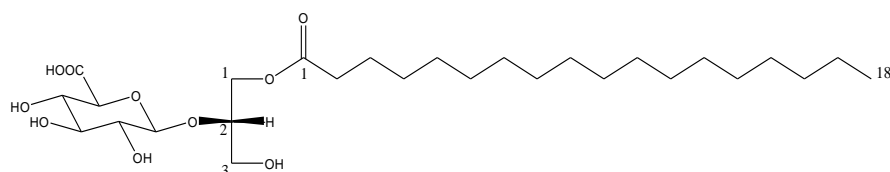
COMPOUND : PP-1



$C_{27}H_{51}KO_{11}S$
Mol. Wt.: 622,85

Soluble in DMSO
Purity = 95% by NMR
amount : about 2,0 mg

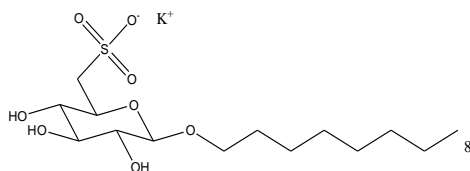
COMPOUND : PP-2



$C_{27}H_{50}O_{10}$
Mol. Wt.: 534,68

Soluble in DMSO
Purity >95% by NMR
amount : about 2,5 mg

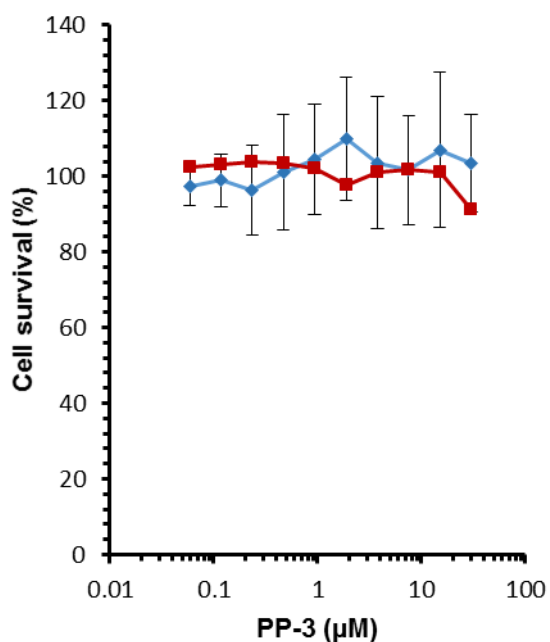
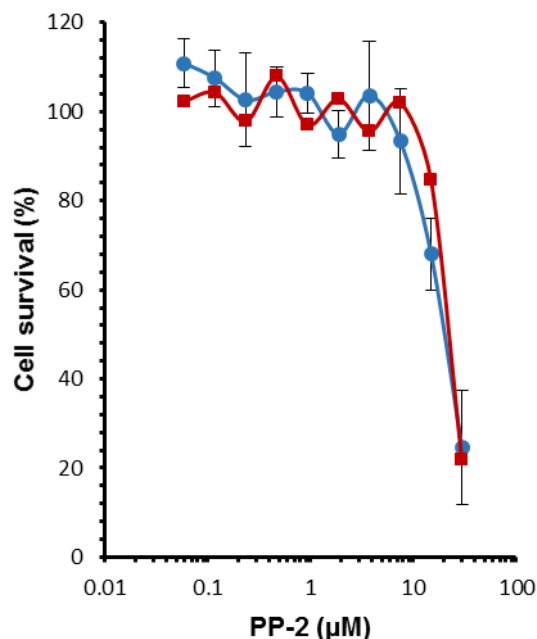
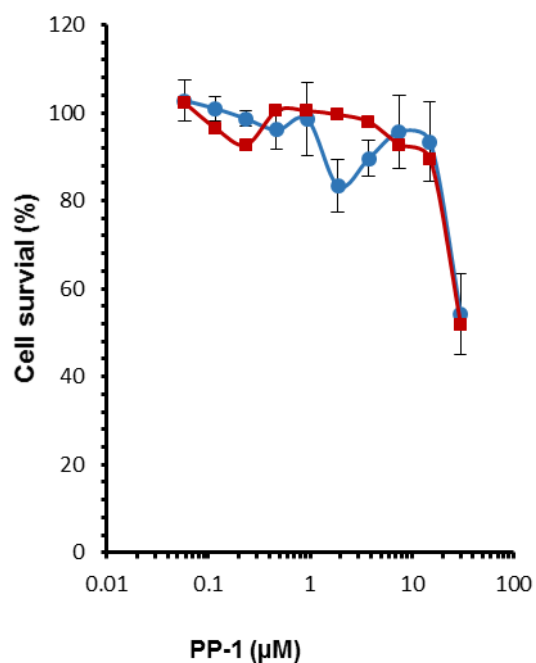
COMPOUND : PP-3



$C_{14}H_{27}KO_8S$
Mol. Wt.: 394,52

Soluble in DMSO
Purity >95% by NMR
amount : about 2,9 mg

Figure 3.19 Chemical structure and molecular weight of PP-1, PP-2 and PP-3 compounds.



Drug	IC ₅₀ (μM) Aerobic	IC ₅₀ (μM) Hypoxic
PP-1	> 30	>30
PP-2	23.4 ± 2.6	21.6 ± 2.2
PP-3	>30	>30

Figure3. 20 Response of IGROV cells to PP-1 to PP-3 under aerobic (blue) and hypoxic (red) conditions. Dose-response curves are presented in the three graphs, and each value represents the mean ± standard deviation for three independent experiments. The inset table represents IC₅₀ values for all experimental conditions. IC₅₀ values >30 indicate that an IC₅₀ was not reached at the highest concentration of drug tested (30 μM).

3.3.12 Western blot analysis of cellular PDH phosphorylation levels in response to DCA treatment

Of the metabolic inhibitors investigated in this chapter, the PDK inhibitor DCA was the only inhibitor that showed any preferential activity towards hypoxic cells (Figure 3.18) and was therefore selected for further evaluation. DCA was presumed to have its cytotoxic effects via inhibition of PDKs. As discussed in section 1.12 PDKs phosphorylate and inactivate pyruvate dehydrogenase (PDH), thus it was predicted that DCA might cause a decrease in levels of phosphorylated PDH. This in turn would be expected to promote entry of pyruvate into the TCA cycle/OXPHOS rather than its reduction by LDH-A to lactate. Effects of DCA on PDH phosphorylation and PDK expression levels were therefore analysed by immunoblotting following SDS PAGE of total cell lysates.

3.3.12.1 Bradford assay calibration curve

For these analyses, correlating with IC₅₀ values for 96h exposure obtained by chemosensitivity testing, HCT116 p53^{+/+} and HCT116 p53^{-/-} cells were exposed to a range of DCA concentrations (0mM, 5mM, 10mM and 20mM) for 72 hours in the defined environment (aerobic or hypoxic conditions). Following treatment, the expression levels of PDK1, PDK2, PDH-P and PDH protein were measured by western blot analysis of HCT116 p53^{+/+} and HCT116 p53^{-/-} cells. In each case, 30µg of protein from prepared cell lysates (see Methods) were applied to each lane of a SDS-polyacrylamide gel. Protein concentrations of cell lysates were determined using the Bradford assay; an example of a calibration curve generated using BSA

standards to determine the concentration of prepared lysates is shown in Figure 3.21.

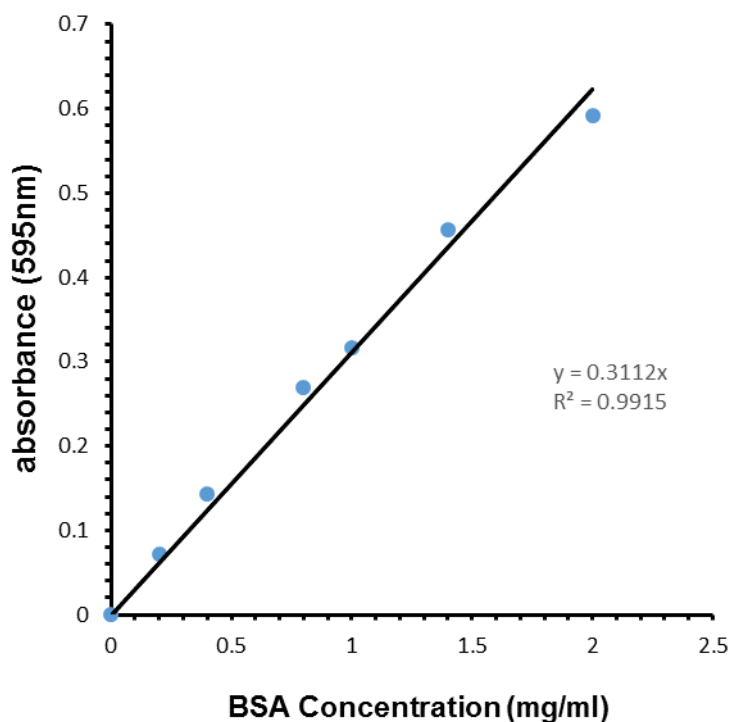


Figure 3.21 Bradford calibration curve that was used to determine the concentration of cell lysates.

3.3.12.2 Immunoblots

Immunoblotting results are presented in Figure 3.22, 3.23 and 3.24. The results show that the level of PDH expression does not significantly change with DCA treatment across the different doses tested although there is some variation between normoxic and hypoxic samples. PDH total expression serves as a comparative control in assessing PDH phosphorylation levels, Importantly, DCA induced a decrease in PDH phosphorylation relative to total PDH levels in both HCT116 p53^{+/+} and HCT116 p53^{-/-} cells under normoxic conditions. In hypoxic conditions and in the

absence of any DCA treatment, PDH phosphorylation levels were notably higher than under aerobic conditions suggesting increased inactivation of the PDH complex, potentially by PDK-1. In the HCT116 p53^{+/+} cells, DCA also caused a dose-dependent reduction in PDH phosphorylation levels consistent with PDK inhibition by DCA. However, in the HCT116 p53^{-/-} cells, DCA treatment at the doses tested did not reduce PDH phosphorylation levels (figure 3.22 and 3.23). This could potentially be due to alterations in expression or activity of PDKs or PDH phosphatases as a compensatory response to DCA. In addition, the blots indicate that levels of PDK2 expression were particularly hard to detect in both cell lines under all conditions due to interfering non specific bands. With additional time available, this study would have included measuring the enzyme activity of PDK1 and other PDK isoforms alongside protein expression studies.

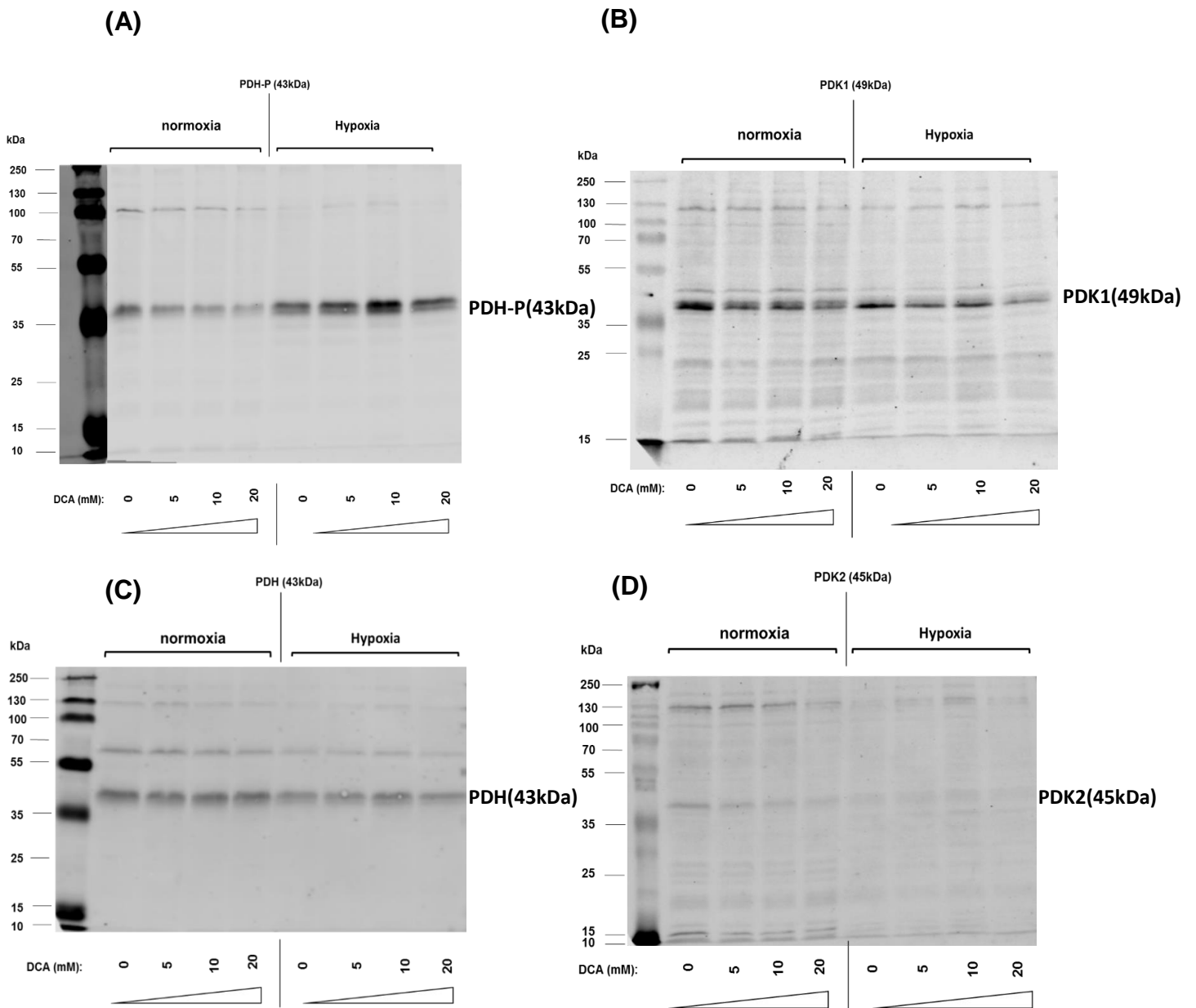


Figure 3.22 Western blot analysis of HCT116 p53^{+/+} cells treated with different dose of DCA under hypoxic and aerobic conditions for 72 hours. An exposure time of 72 hours was chosen as extending the time point beyond this time point would induce significant cell kill and a reduction of protein available for analysis. (A) Western blot analysis of PDH-P expression. (B) Western blot measure expression of PDK1. (C) Western blot measure expression of PDH. (D) Western blot measure expression of PDK2.

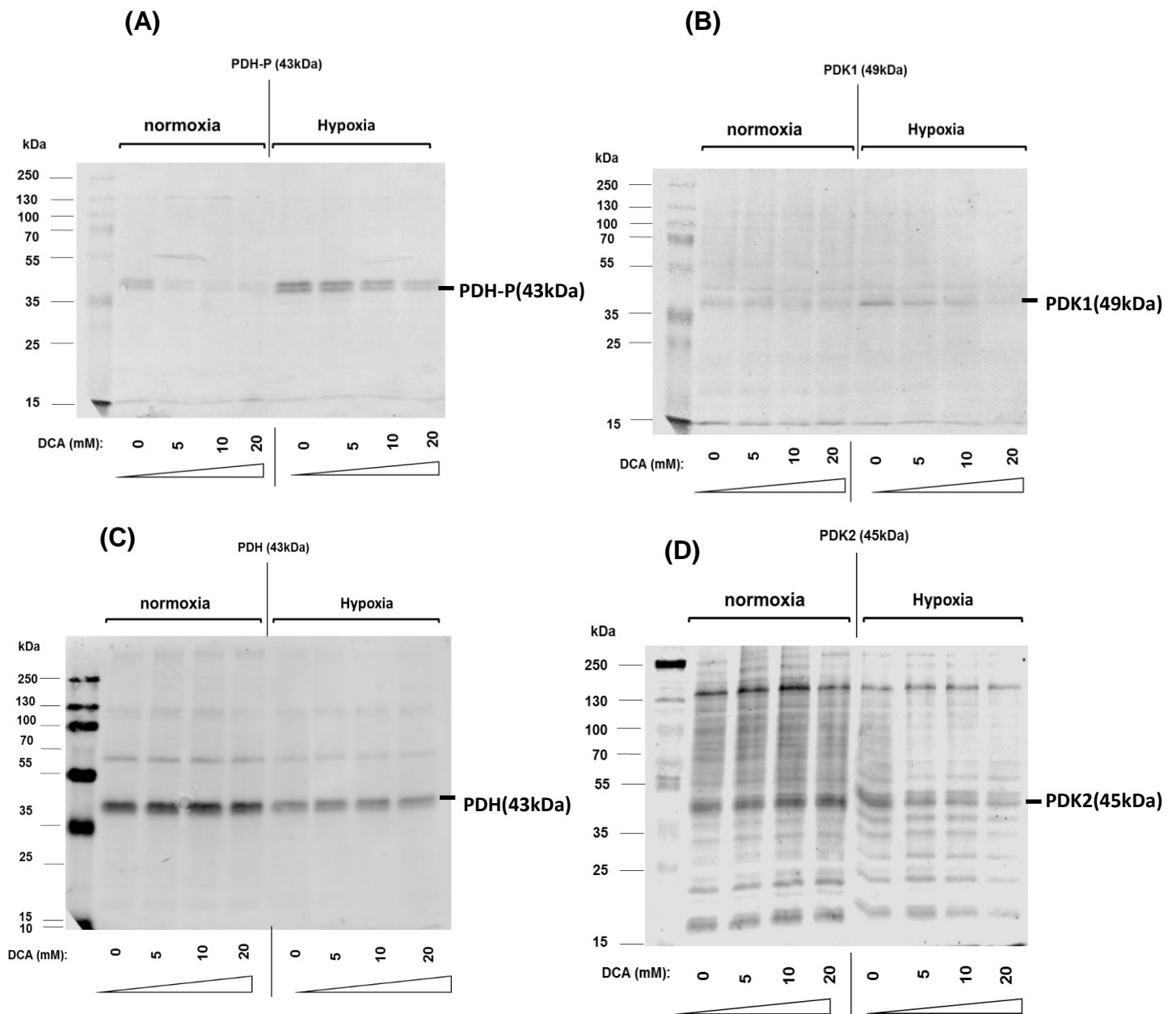


Figure 3. 23 Western blot analysis of HCT116 p53^{-/-} cells treated with a different dose of DCA under hypoxic and aerobic conditions for 72 hours. An exposure time of 72 hours was chosen as extending the time point beyond this time point would induce significant cell kill and a reduction of protein available for analysis (A) Western blot analysis of PDH-P expression. (B) Western blot measure expression of PDK1 (C) Western blot analysis of PDH protein expression (D) Western blot measure expression of PDK2.

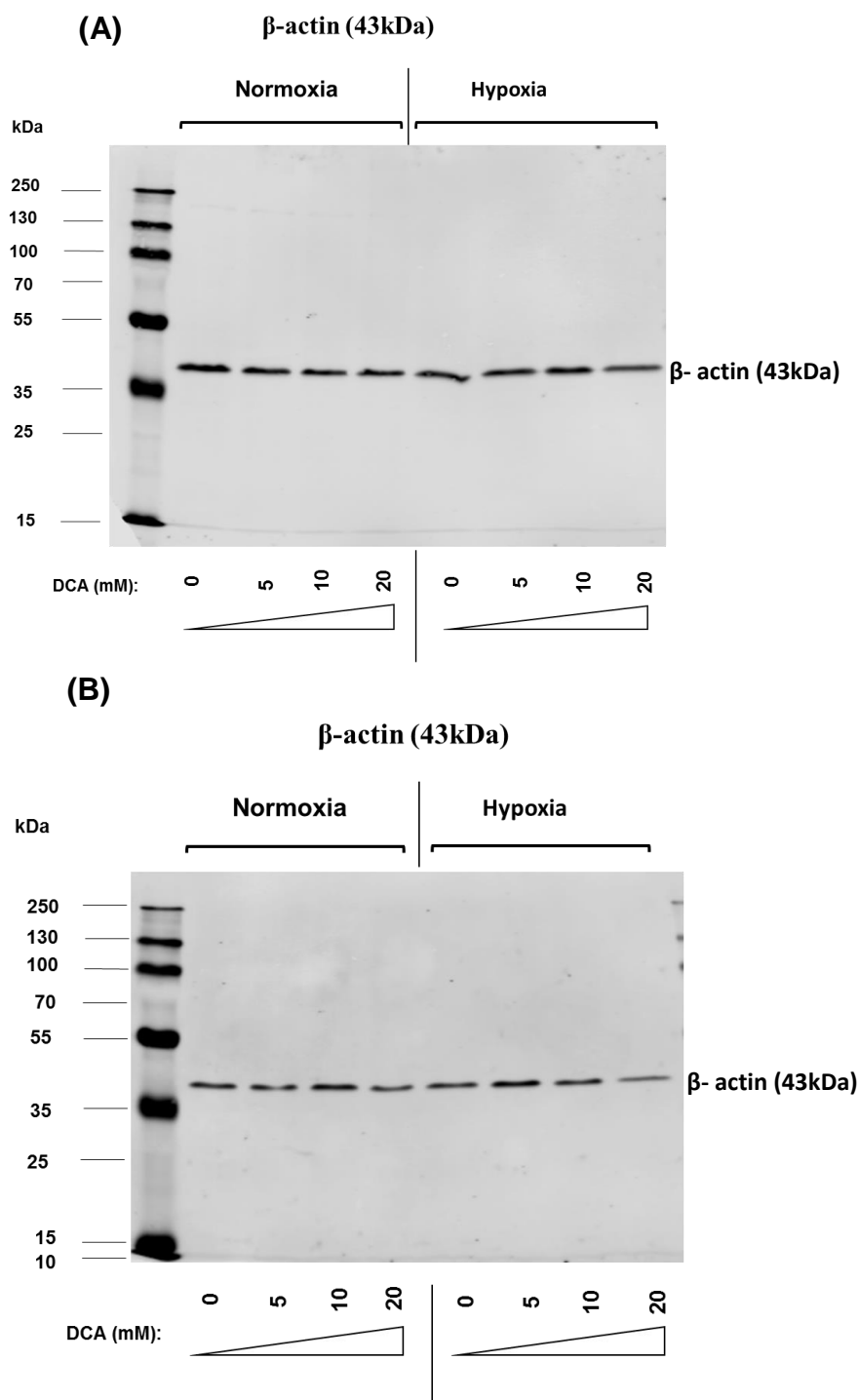


Figure 3.24 Western blot analysis of β -actin of treated cells with a different dose of DCA under hypoxic and aerobic conditions for 72 hours. Panel (A) represents HCT116 p53^{+/+} cells and panel (B) represents HCT116 p53^{-/-} cells.

3.3.13 Measurement of cell viability and mitochondrial membrane potential of cells treated with DCA under hypoxic and aerobic conditions.

To investigate further the chemosensitivity of cell lines to DCA, quantification of effects on cell viability and total cell number and on loss of mitochondrial membrane potential as an early marker of apoptosis were carried out. These assays were performed on HCT116 p53^{+/+} and HT29 cells with varying concentrations of DCA under hypoxic and normoxic conditions. Loss of mitochondrial membrane potential was assessed using J-aggregate-forming cation JC-1 and analysis of JC1 red/green fluorescence by image cytometry. DCA was shown to induce mitochondrial membrane depolarisation with increased loss of mitochondrial membrane potential observed in both the HCT116 and HT29 cells under hypoxic conditions using a dose of 62.5mM DCA. (Figure 3.25. & 3.26 for HCT116 p53^{+/+}; Figure 3.28 and 3.29 for HT29). DCA also caused a decrease in total cell numbers and percentage of cell viability in both HCT116 p53^{+/+} and HT29 cells (figure 3.27 and figure 3.30 respectively).

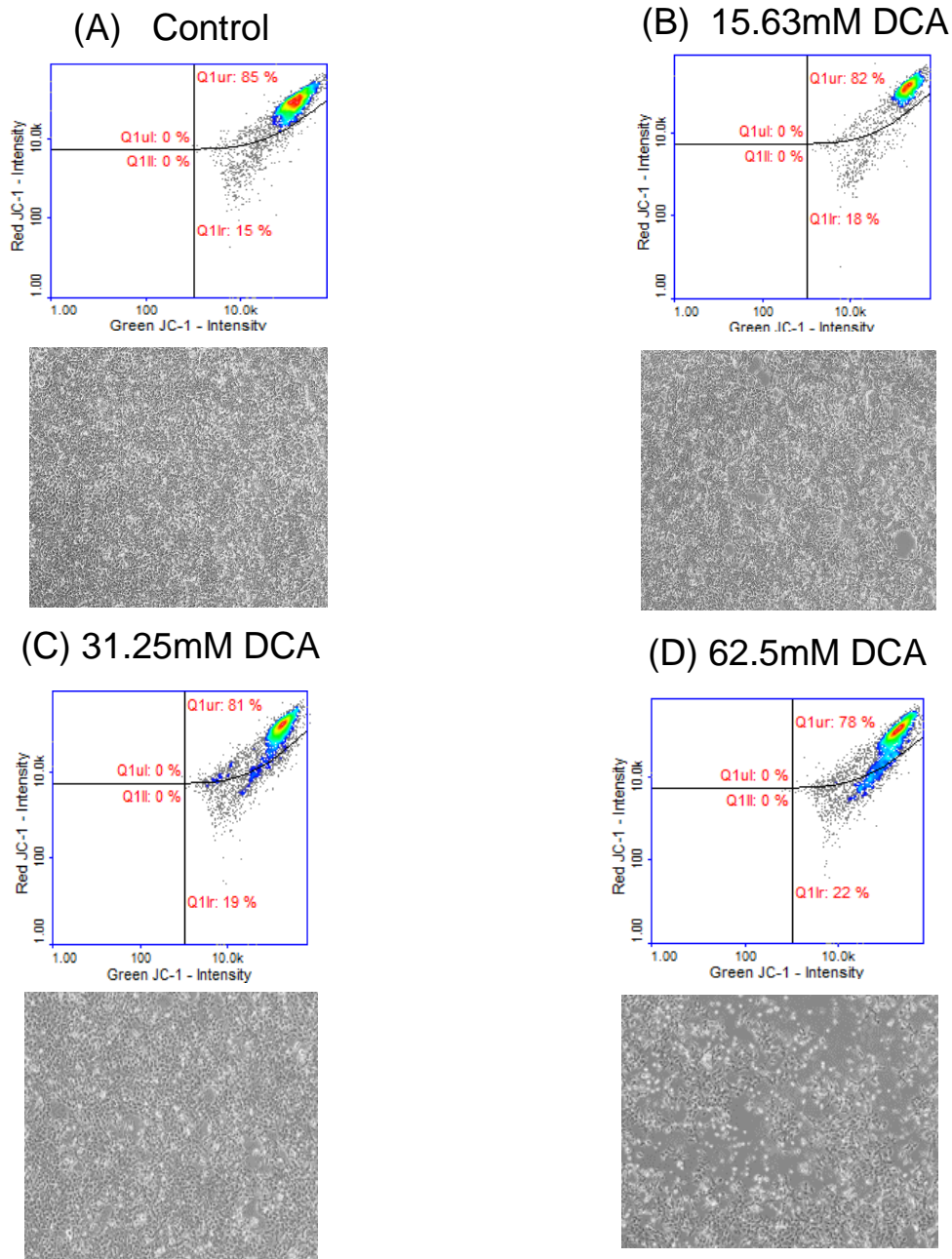
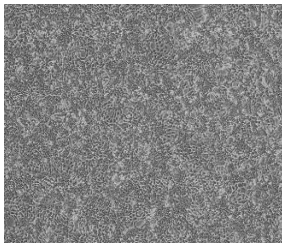
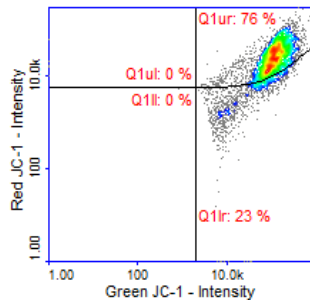
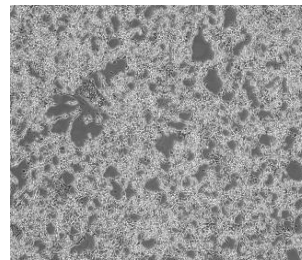
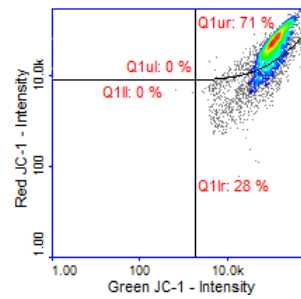


Figure 3.25 Mitochondrial potential membrane of HCT116 p53^{+/+} cells treated with a range of DCA concentrations under aerobic conditions for 72 hours. Panel A untreated cells (control), panel B cells treated with 15.63mM of DCA. Panel C cells treated with 31.255 mM of DCA and Panel D cells treated with 62.5 mM of DCA. Cells in the lower right quadrant represent cells with depolarised mitochondria as indicated by a decrease in the red/green fluorescent intensity ratio

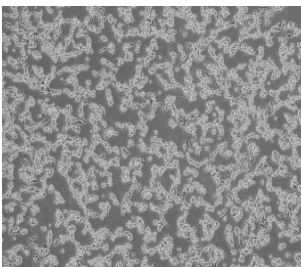
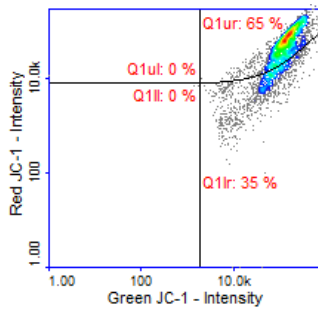
(A) Control



(B) 15.63mM DCA



(C) 31.25mM DCA



(D) 62.5mM DCA

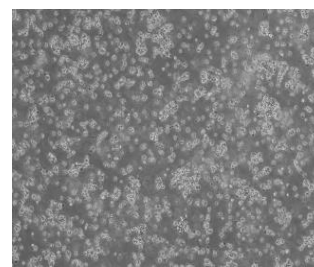
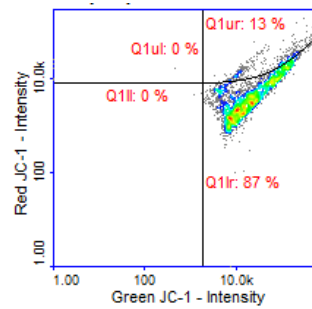


Figure 3.8 Mitochondrial potential membrane of HCT116 p53^{+/+} cells treated with a range of DCA concentrations under hypoxic conditions for 72hours. Panel A untreated cells (control), panel B cells treated with 15.63Mm of DCA. Panel C cells treated with 31.255mM of DCA and Panel D cells treated with 62.5 mM of DCA. Cells in the lower right quadrant represent cells with depolarised mitochondria as indicated by a decrease in the red/green fluorescent intensity ratio.

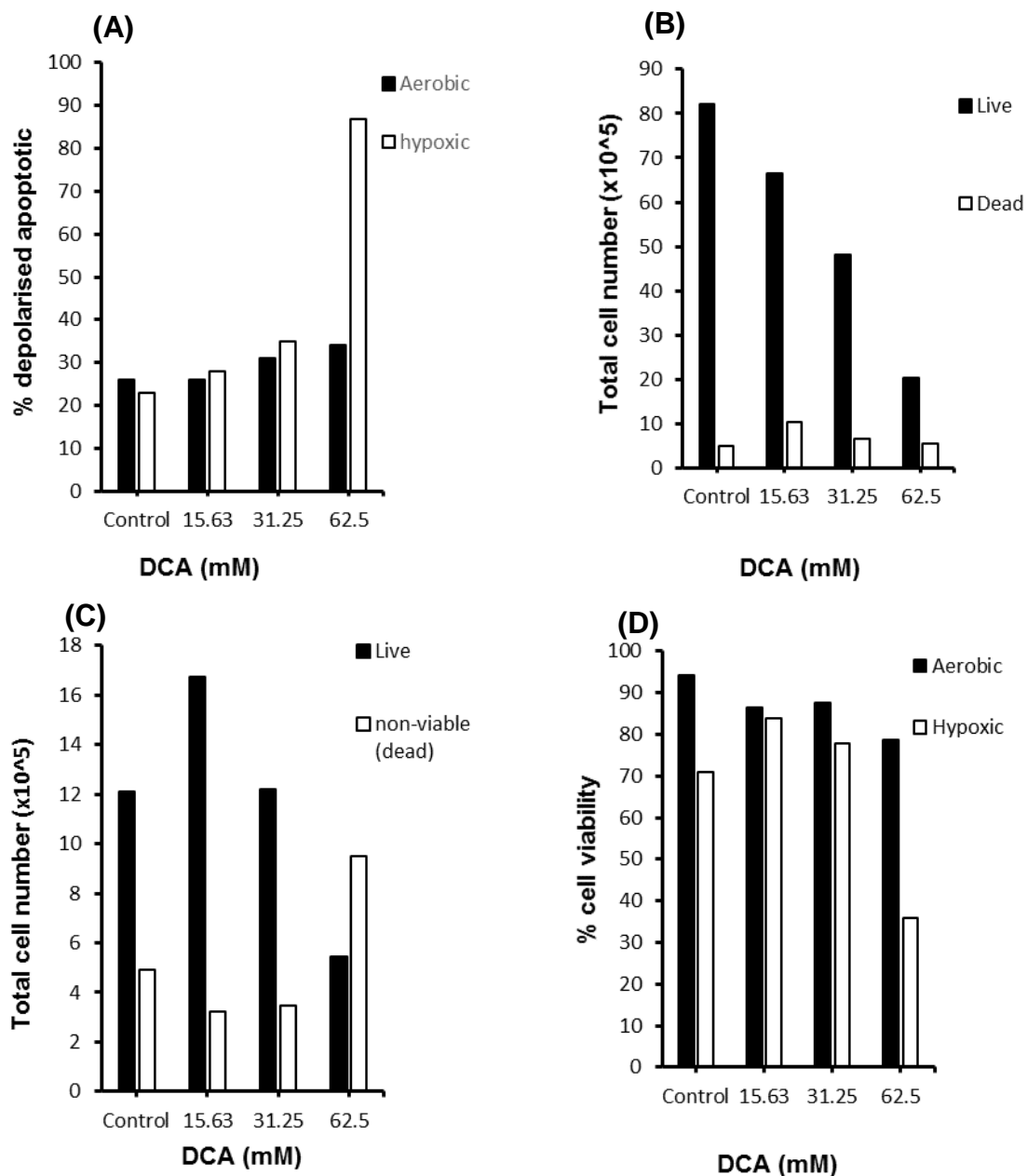
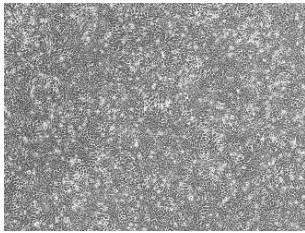
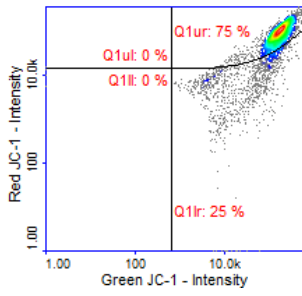
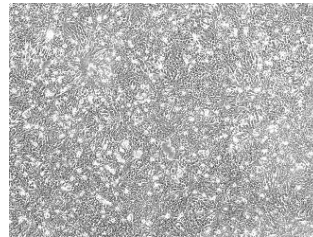
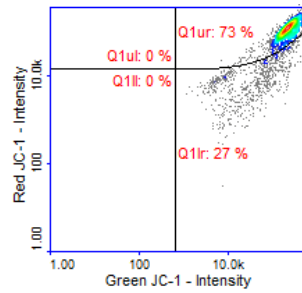


Figure 3.9 Summary of the effects of DCA on mitochondrial potential membrane, cell number and cell viability of HCT116 p53^{+/+} cells treated under aerobic and hypoxic conditions for 72hours. Panel A: Percentage of apoptotic cells under aerobic and hypoxic conditions as determined by measurement of loss of mitochondrial membrane potential, panel B: The total number of live and dead cells following 72h DCA treatment under aerobic conditions; , and Panel C The total number of live and dead cells following 72h DCA treatment under hypoxic conditions panel D: Percentage cell viability (number of live cells/total number of cells) following DCA exposure under normoxic and hypoxic conditions

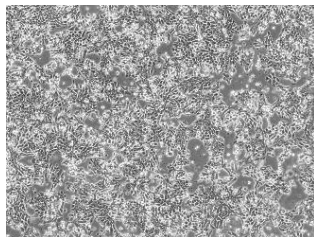
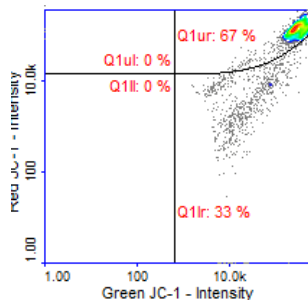
(A) Control



(B) 15.63mM DCA



(C) 31.25mM DCA



(D) 62.5mM DCA

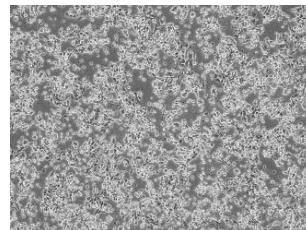
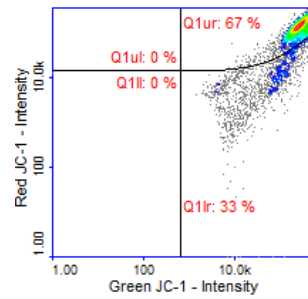


Figure 3.10 Mitochondrial potential membrane of HT29 cells treated with a range of DCA concentrations under aerobic conditions for 72 hours. Panel A is untreated cells (control), panel B cells treated with 15.63mM of DCA. Panel C cells treated with 31.25mM of DCA and Panel D cells treated with 62.5mM of DCA.

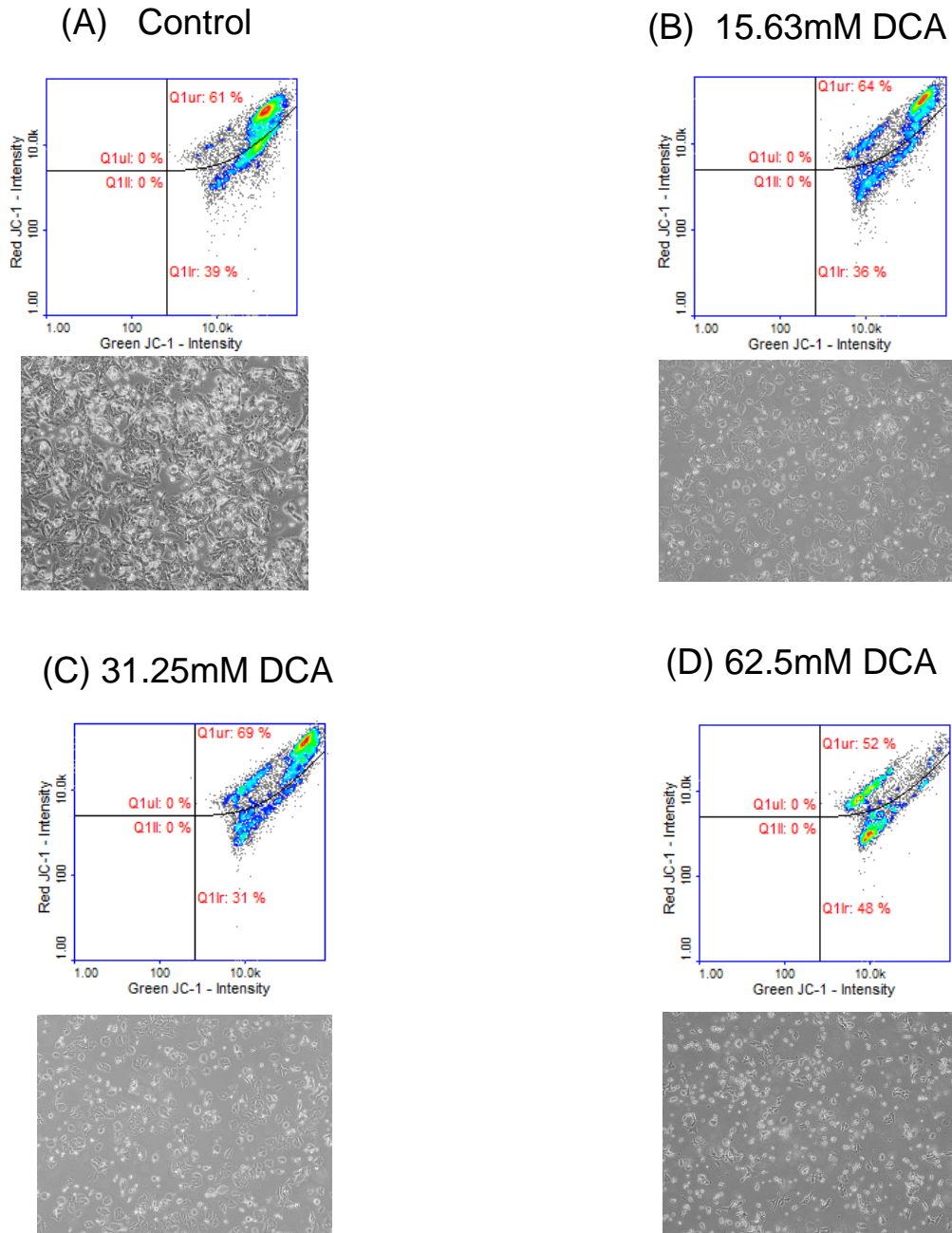


Figure 3.11 Mitochondrial potential membrane of HT29 cells treated with a range of DCA concentrations under hypoxic conditions for 72 hours. Panel A is untreated cells (control), panel B cells treated with 15.63mM of DCA. Panel C cells treated with 31.25mM of DCA and Panel D cells treated with 62.5mM of DCA.

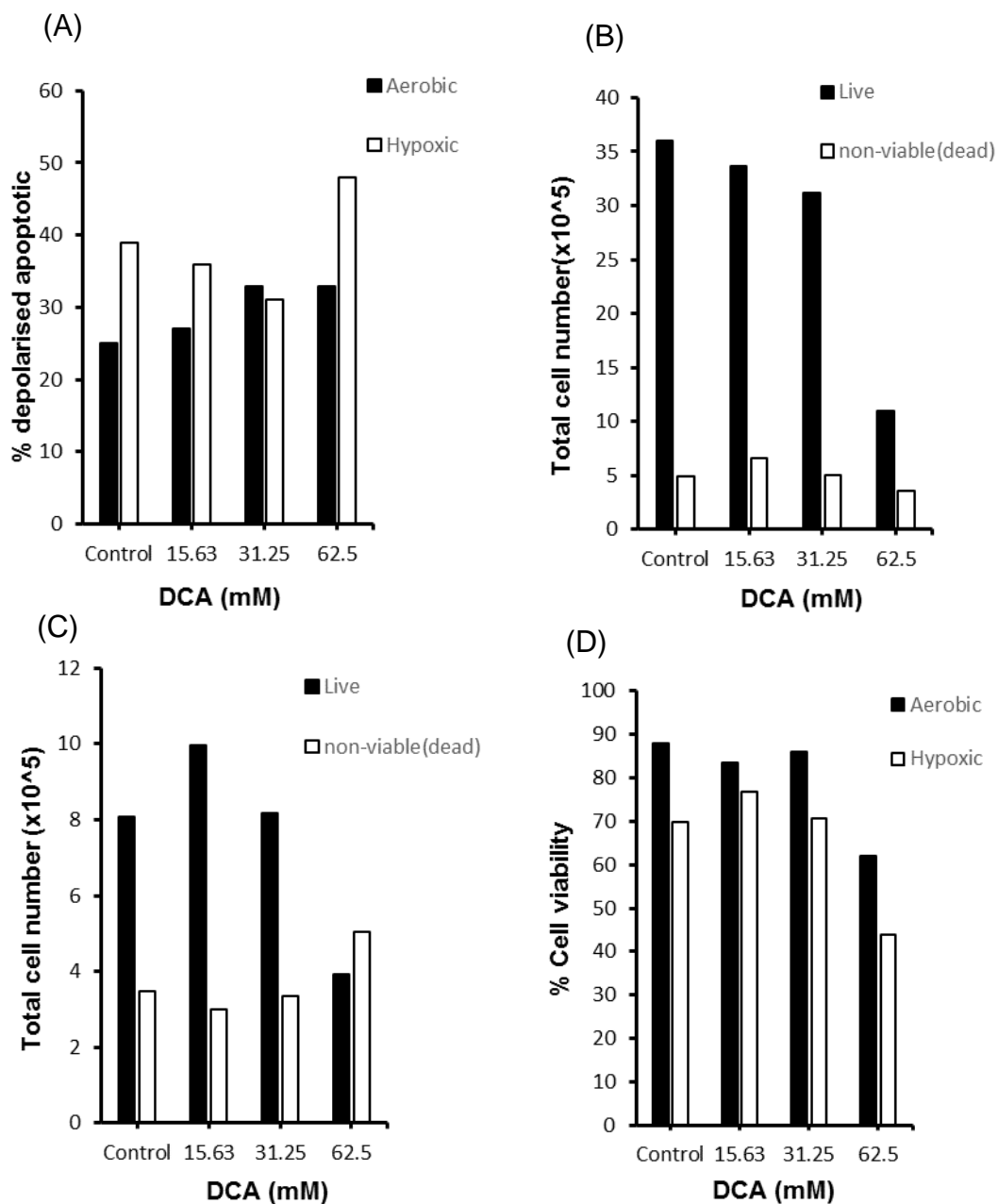
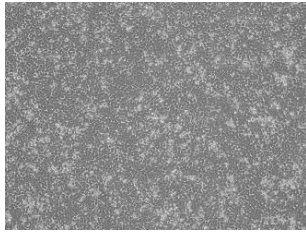
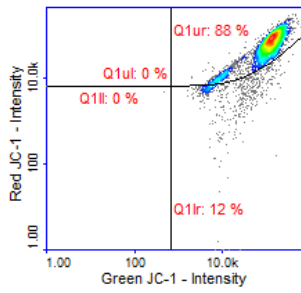


Figure3. 30 Summary of the effects of DCA on the mitochondrial potential membrane, cell number and cell viability of HT29 cells treated under aerobic and hypoxic conditions for 72hours. Panel A apoptosis levels under aerobic and hypoxic conditions as determined by loss of mitochondrial membrane potential, panel B total of live and dead cells under hypoxic conditions, panel C is total of live vs dead cells under aerobic condition, and Panel D percentage cell viability under aerobic and hypoxic conditions in response to DCA treatment.

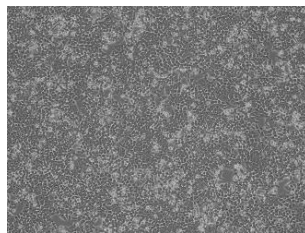
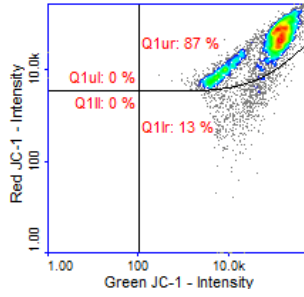
3.3.14 Comparison of the effects of different DCA treatment durations on mitochondrial potential membrane and cell viability of HCT116 cells under normoxic conditions

HCT116 p53^{+/+} (wild-type) cells were treated with 75mM DCA under 21% oxygen conditions (normoxia) for different times (24hr, 36hr, 48hr, 60hr, 72hr). DCA caused an increase in mitochondrial membrane depolarisation in a time-dependent manner suggesting induction of early apoptosis with time (Figure 3.31 and 3.32). Consistent with cells being in the early stages of apoptosis, effects on cell viability were much less pronounced with a small decrease observed over time (Figure 3.33).

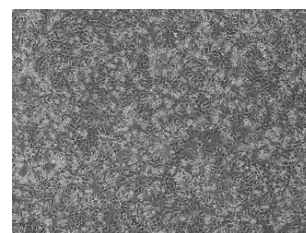
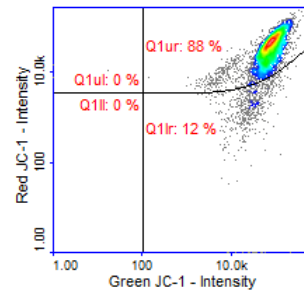
(A.1) Control (24hr)



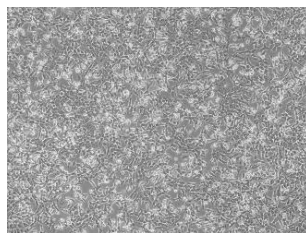
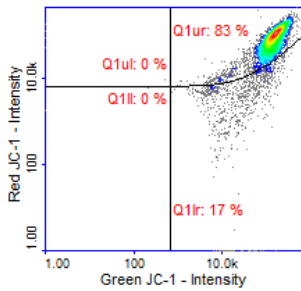
(B.1) Control (36hr)



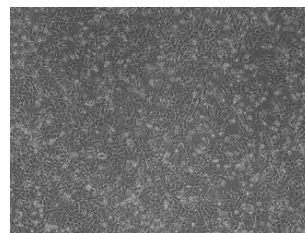
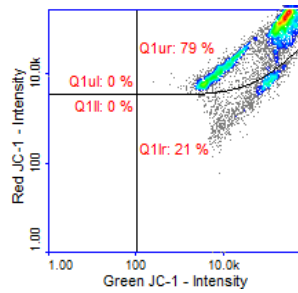
(C.1) Control (48hr)



(A.2) 75mM DCA (24hr)



(B.2) 75mM DCA (36hr)



(C.2) 75mM DCA (48hr)

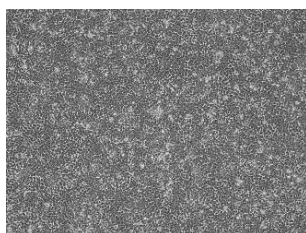
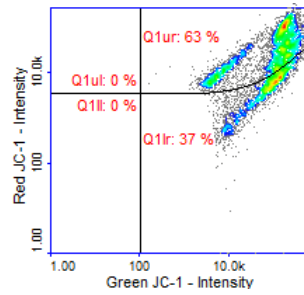
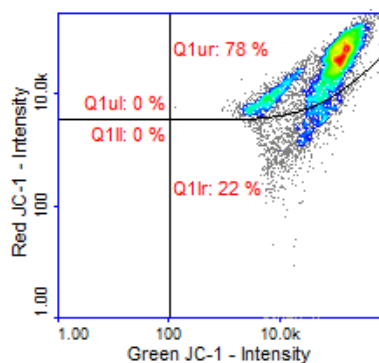


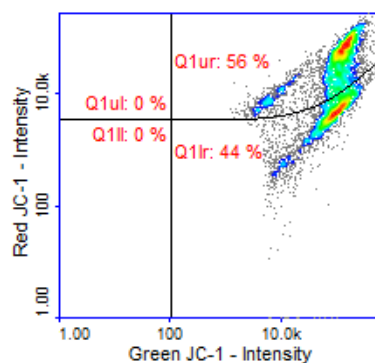
Figure 3.31 Mitochondrial membrane potential of HCT116 p53^{+/+} cells exposed 75mM DCA for different time periods under aerobic conditions. Panel A.1 And A.2 is 24 hours dose exposure. Panel B.1 and B.2 cells treated for 36 hours. Panel C.1 control and C.2 cells treated for 48hours.

...

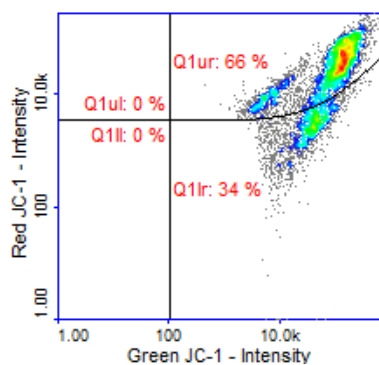
(A.1) Control (60hr)



(B.1) 75mM DCA (60hr)



(A.2) Control (72hr)



(B.2) 75mM DCA (72hr)

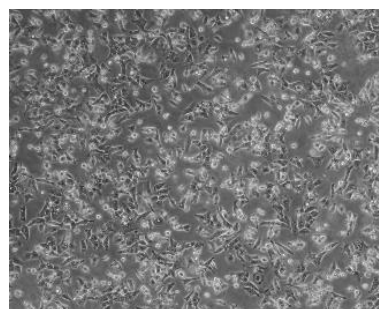
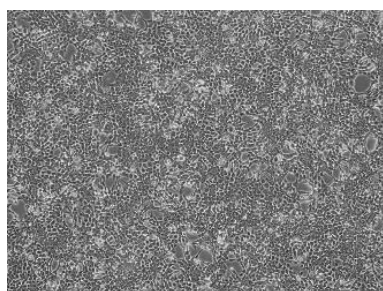
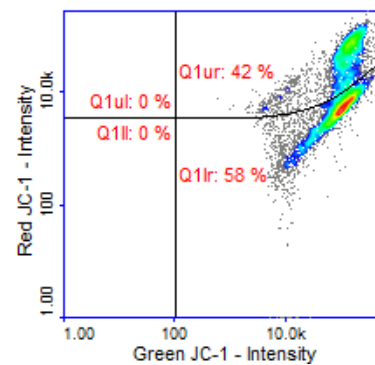
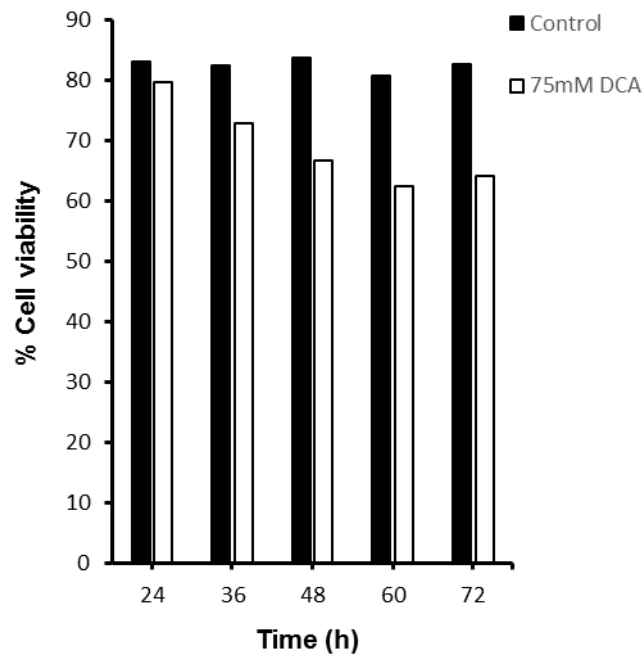


Figure 3.32 Mitochondrial membrane potential of HCTt116 p53^{+/+} cells exposed to 75mM DCA for different time periods under aerobic conditions. Panel A.1 And A.2 is 60 hours dose exposure. Panel B.1 and B.2 cells treated for 72hours.

(A)



(B)

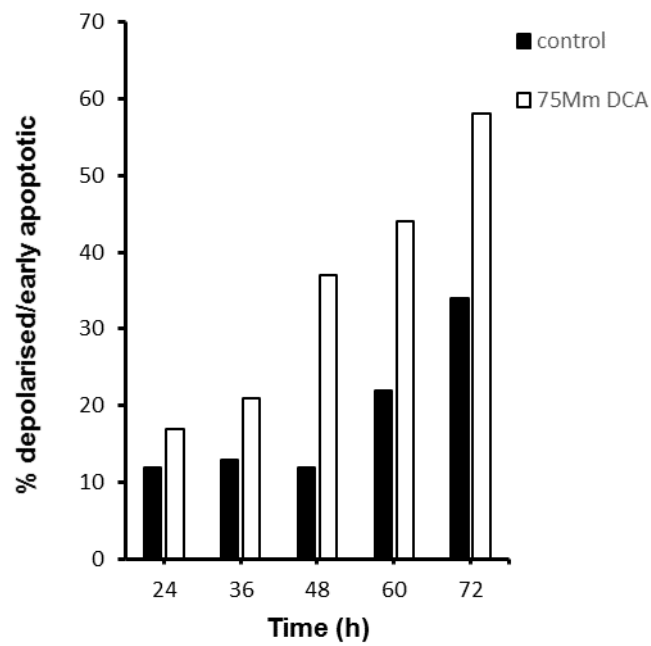


Figure 3.33 Mitochondrial membrane potential and viability of HCT116 p53^{+/+} cells exposed to 75mM DCA for different time points under aerobic conditions. Panel A is presenting the percentage of cell viability. Panel B percentage of live cells for treated VS untreated at each time point.

3.4 Discussion

Many independent studies highlight the important metabolic alterations of cancer cells and this is now recognised as an emerging hallmark of cancer (Hanahan and Weinberg 2011). This biological understanding provides novel opportunities for therapeutic intervention, particularly in the hypoxic fraction of tumours where the glycolytic phenotype may be even more prominent than in aerobic cells. This study focused on the comparative response of the cancer cells to glycolytic inhibitors (hexokinase and lactate dehydrogenase inhibitors) and the PDK inhibitor DCA under hypoxic and normoxic conditions. Whilst our results with tirapazamine demonstrate that our experimental conditions are suitable for evaluating hypoxia targeted drugs, the results obtained using 2DG or 3BP (hexokinase inhibitors), DCA (pyruvate dehydrogenase kinase inhibitor), gossypol and sodium oxamate (LDH inhibitors) show limited effects on hypoxic cells and in many cases, hypoxic cells proved more resistant to treatment than aerobic cells. The potential reasons for each of the key sets of results obtained are discussed below.

First, the results obtained for DCA did show a degree of hypoxia selectivity although the magnitude of the HCR was much lower (HCR ranged from 3.11 to 0.71, table 3.1) than that obtained for tirapazamine (HCR = 9.63, figure 3.3). Furthermore, HCR values varied depending on the cell line with only LS123 cancer cells had an HCR value below 1 (HCR=0.71, table 3.1). These modest effects are consistent with other studies showing little or no potentiation under hypoxia (0.5% oxygen) in MCF7 and MDA-MB-231 breast cancer cell lines (Xintaropoulou et al 2015). Other studies have demonstrated is less effective against hypoxic HeLa cells and may in fact promote

the survival of an aggressive hypoxic cell population (Anderson et al, 2009). Similarly, Shahrzad et al (2010) demonstrated that SW480 and CaCo-2 cells were less sensitive to DCA under hypoxic compared to normoxic conditions and concluded that DCA may in fact be cytoprotective to some colorectal cancer cell lines under hypoxic conditions (0.1% oxygen). The results presented in this thesis together with evidence in the literature suggests that DCA may demonstrate modest hypoxia selectivity in some cell lines but in others, little or no hypoxia selectivity occurs and in some cases, a protective effect against hypoxic cancer cells was observed.

Mechanistically, DCA is known to inhibit the enzyme pyruvate dehydrogenase kinase (PDK) which plays a key role in regulating the pyruvate dehydrogenase (PDH) complex thereby controlling the entry of pyruvate into the Kerbs cycle (Michelakis et al, 2008, Bonnet et al, 2007). PDK phosphorylates the PDH complex at specific serine residues resulting in inhibition of enzyme activity (Rardin et al 2009). Using antibodies to the PDH E1 α (phospho S293), immunoblot studies showed modest inhibition of PDH phosphorylation under normoxic conditions following the treatment of HCT116p53^{+/+} and HCT116p53^{-/-} cells with DCA for 72 hours (figures 3.22A and 3.23A respectively). Under hypoxic conditions, PDH-P expression was elevated in control cultures which would be consistent with a HIF1 mediated induction of PDK1. Whilst a very modest induction of PDK1 levels occurred in HCT116p53^{-/-} cells (figure 3.23B), no noticeable change in expression occurred in HCT116p53^{+/+} cells (figures 3.22B). It should be noted however that the results of the immunoblot studies are preliminary and need to be repeated before any firm conclusions can be reached. Nevertheless, there was evidence in both cell lines that DCA reduces PDH-P levels

under hypoxic conditions although the effect is modest and is not qualitatively different from the results of studies in oxygenated conditions. As DCA has been shown to alter mitochondrial membrane potential and induce apoptosis (Michelakis et al, 2009, Bonnet et al, 2007), further mechanistic studies were conducted to determine the effects of DCA on mitochondrial membrane depolarisation under aerobic and hypoxic conditions (figures 3.27A, 3.30A and 3.33A). The results demonstrate that DCA does induce mitochondrial membrane depolarisation which is consistent with previously published studies (Bonnet et al, 2007). Under hypoxic conditions, the extent of membrane depolarisation was similar to aerobic conditions except at a dose of 62.5 mM where greater depolarisation occurred. This concentration of DCA is high however and at therapeutically relevant concentrations (IC_{50} values range from 7.15 to 33.76 mM, table 3.1), no major differences in mitochondrial membrane potential exist between hypoxic and aerobic cells. These results are preliminary in nature and further replicates are required to confirm these findings.

In summary, DCA has shown some modest hypoxia selectivity in a panel of cancer cell lines but the magnitude of this effect is small and cell line dependent. Mechanistically, these preliminary studies demonstrate that DCA reduces PDH-P levels and alters mitochondrial membrane potential but the effects are similar under both aerobic and hypoxic conditions (at therapeutically relevant DCA concentrations). In conjunction with the evidence in the literature, the enhanced effects of DCA on the hypoxic cell population are minimal at best.

Turning to the other glycolytic inhibitors used in this study, hexokinase inhibitors (2-deoxyglucose and 3-bromopyruvate) were generally less active against hypoxic cells compared to aerobic cells (table 3.4). The only exception to this was in the case of the BE cell line where a modest HCR of 1.46 was obtained. These results are consistent with other studies demonstrating that hypoxic cells were significantly less sensitive to 3-bromopyruvate than aerobic cells (Xintaropoulou et al 2015) but conflict with others demonstrating that osteosarcoma 143b cells were hypersensitive to 2-deoxyglucose under hypoxic conditions (Maher et al 2004). The results obtained with 2-deoxyglucose were however consistent with other studies demonstrating that hypoxia protects glioblastoma cells from the apoptotic effects of 2-deoxyglucose (Pistollato et al, 2010). With regards to inhibitors of LDH, both gossypol and sodium oxamate were significantly less active against hypoxic cells compared to aerobic cells with HCR values ranging from 0.41 to 0.87 (table 3.4). These results are consistent with similar studies conducted using oxamate in MCF7 and MDA-MB-231 cells where hypoxic cells (0.5% oxygen) were significantly less responsive than aerobic cells (Xintaropoulou et al 2015). In this same study, similar results were obtained with another LDH inhibitor (NHI1). Limited studies have been published on the response of hypoxic cells to gossypol but the results of this study clearly demonstrate that gossypol is less active against hypoxic compared to aerobic cells. Other inhibitors of LDH-A have however been shown to have significant hypoxia selectivity in vitro. In contrast to the results from Xintaropoulou et al (2015), NHI1 was significantly more active against hypoxic LPC006 pancreatic cancer cells (Maftouh et al, 2013). Similarly, quinoline-3-sulfonamide compounds were shown to

be selectively toxic to hypoxic cells, the magnitude of the effect being greater in cell lines that expressed low levels of LDH-B (Billiard et al, 2013).

In summary therefore, the glycolytic inhibitors used in this study did not exhibit selectivity towards hypoxic cells and in just about all cases, they were less active. Evidence in the literature however suggest that targeting LDH-A can generate hypoxia selective effects in certain cell lines. The reasons for the discrepancies between the results of this study and evidence in the literature are not clear but could be cell line or inhibitor specific. Gossypol and sodium oxamate for example are not specific inhibitors of LDH-A and may have multiple mechanisms of action whereas other inhibitors with greater selectivity for LDH-A may elicit hypoxia selective effects in vitro. It is of interest to note however that the magnitude of any hypoxia selectivity effects induced by glycolytic inhibitors and DCA is typically small and this raises intriguing questions; are hypoxic cells really glucose dependent and can hypoxic cells use alternative sources of carbon as metabolic fuels? These questions will be addressed in the next chapter of this thesis.

Chapter 4

Investigation into alternative carbon sources as metabolic fuels to support cancer cell growth under hypoxic conditions.

4.1 Introduction

Cancer cells have very high energy and biosynthetic needs that are required to support their rapid cell growth and proliferation. To provide sufficient energy and biosynthetic precursors for synthesis of cellular macromolecules, cancer cells commonly reprogram their metabolism towards glycolysis. This phenomenon contributes to high glucose import (via glucose transporters) into the cells and high glucose consumption (via upregulation of glycolytic enzymes) to generate ATP (Fadaka et al., 2017). However, glucose deprivation and lactic acidosis are a common feature in hypoxic cells that arise in areas of the tumour microenvironment further away from blood vessels which therefore do not receive sufficient oxygen or glucose. In the context of the tumour microenvironment, a metabolic symbiotic model has been proposed by Sonveaux and colleagues where 'metabolic coupling' between 'oxidative' tumour cells near to blood vessels and hypoxic cancer cells occurs. In this model, the hypoxic cells metabolise glucose to lactate which is then exported and used as an fuel by 'oxidative' tumour cells near blood vessels reducing their consumption of glucose. These metabolic interactions are similar to the "reverse Warburg effect" concept developed by Lisanti et al (Fu et al., 2017) where normal cells are 'told' by tumour cells to produce lactate which is then used as a fuel by the cancer cell. As described in Chapter 1, another important carbon source for

cancer cells is glutamine action (Reitzer et al., 1979). Whilst use of glucose and glutamine as carbon sources by cancer cells is well established, potential differences in dependency between normoxic and hypoxic cells and the use of alternative carbon sources to support cancer cell survival have yet to be extensively studied. In case of insufficient of glucose, in which the energy is produced by glycolysis. Data show that tumour cells possible can use for example mannose and survive under severe condition up to concentration limit 2.5mM. Mannose plays an important role in the metabolism of many cancer cells, it is mainly essential for glycoprotein biosynthesis (glycosylation). In this way, mannose promotes the proliferation of cancer cells. This is particularly relevant for hypoxic cells and may highlight novel therapeutic strategies for their targeting.

4.2 Materials and Methods

4.2.1 Cell culture

Investigation of the effects of glucose deprivation on cell survival under aerobic and hypoxic conditions was conducted using the MTT assay and verified using the SRB assay. The panel of cell lines used included HCT116 p53^{-/-}, HCT116 p53^{+/+}, HT29, BE and DLD1 cells, all of which were derived from colorectal tumours. Normal cell culture media for these cells were as follows: HCT116 p53^{-/-} and HCT116 p53^{+/+} cells were cultured in DMEM media containing 20mM glucose supplemented with 10% FBS, 2mM L-glutamine and 1mM of sodium pyruvate. HT29, BE and DLD1 were cultured with RPMI1640 media containing 20mM glucose supplemented with 10% FBS, 2mM L-glutamine and 1mM of sodium pyruvate. In addition to the colorectal

cancers, the pancreatic cancer cell line (PSN1) cell was also used and this was cultured in RPMI1460 media supplemented with 10% FBS and 2mM L-glutamine and 1mM of sodium pyruvate. The non-cancer cell line ARPE 19 cell was cultured in DMEM/ F12 media supplemented with 10% FBS and 2mM L-glutamine. Cells were maintained under standard cell culture conditions in a humidified atmosphere containing 5% CO₂ and 37C.

4.2.2 Influence of glucose deprivation on cell growth

Influence of glucose deprivation on cell survival was evaluated using a range of glucose concentrations and under different oxygen tensions. Cells were seeded in 96 well plates at 2×10^3 cells per well and following an overnight incubation in normal glucose rich media and aerobic conditions (to allow cells to adhere and recover from trypsinisation), cells were transferred to the hypoxystation and the media replaced with glucose deprived culture medium that had been allowed to equilibrate overnight at 0.1% oxygen. Initially, HCT116 p53^{+/+} and HCT116 p53^{-/-} cells were exposed to glucose free media (DMEM without glucose), supplemented with 10% FBS, L-glutamine (2mM) and sodium pyruvate (1mM) for 96 hours in a humidified atmosphere containing 0.1% oxygen. Following 96 hours, cell viability was determined using the MTT assay. To determine the effect of different glucose concentrations on cell survival, glucose (Sigma-Aldrich, G8270) was added to culture medium to give a concentrations ranging from 0.625mM to 20mM. These experiments were carried out at 0.1%, 1% and 5% oxygen in the hypoxia chamber as well as under standard atmospheric conditions.

4.2.3 The recovery of cells following glucose deprivation under aerobic and hypoxic conditions

To determine whether cells are able to recover following a period of glucose deprivation, glucose rich media was added to cultures following a 96 hour incubation in glucose deprived media. Following the addition of glucose rich media, cells were cultured for a further 48 hours and cell survival determined using the MTT assay as described previously. The same cell line panel was employed as in section 4.2.2 and experiments were conducted under atmospheric and hypoxic (0.1% oxygen) conditions.

4.2.4 Validation of the results obtained using the MTT assay using the sulforhodamine B (SRB) assay.

Because the MTT assay measures mitochondrial function that could be influenced significantly by changes in glucose concentration and oxygen tension, the SRB assay was used to confirm whether or not the results generated by the MTT assay are valid. The SRB assay is a colorimetric test based on the determination of the amount of cellular protein content as an indicator of viable cell number. Sulforhodamine B is an anionic dye that binds to cellular proteins. Fixed cells are SRB-stained which is then solubilized by a basic solution (10mM Tris) in order to be measured optically. Thus, the optical density is a measure of total protein concentration and this is proportional to the number of living cells.

Cells were cultured into 96 well plates at 2000 cells per well, after 24 hours media was replaced with test medium (contains variable concentration of glucose ranging

from 0mM to 20mM). Cells were incubated at aerobic and hypoxic conditions for 96 hours. Cells were fixed with 10% (w/v) TCA buffer (100µl was added per well). Plates were incubated at 4C° for 1 hour following which fixed cells were washed 4 times with deionised water in order to remove the fixing buffer. Plates were dried for up to 2 days on the bench. Fixed cells were then stained with 0.057% (w/v) of sulforhodamine B (SRB) (dissolved in 1% (v/v) acetic acid) for 30 minutes at room temperature. After this, stained cells were washed 4 times with 1% acetic acid in order to remove unbound stain. Protein dye was solubilized with 10mM Tris-base (200 µl was added per each well). The optical density was measured by using a Tecan f500 plate reader at 590nm.

4.2.5 Analysis of alternative carbon sources to glucose

Tumour cells were exposed to glucose deprived media supplemented with a series of alternative carbon sources. These included the most common monosaccharides fructose (F3510), D-galactose (G5388) and D-mannose (M6020) and the disaccharide sucrose (S8501). In addition, sodium lactate (L7022) was included as this is known to be exported from cells undergoing aerobic glycolysis and it is likely to be at high concentrations in poorly perfused regions of tumours. In addition, lactate is able to fuel mitochondrial respiration through its conversion to pyruvate by LDH-B. All sugars were obtained from Sigma-Aldrich and the information in parenthesis represent the catalogue numbers. Cells were exposed to supplemented media for 96 hours in aerobic and hypoxic conditions and cell survival was determined using the MTT assay as described above. In addition, images of cells following treatment were captured using the EVOS cell imaging system (Thermo

Fisher Scientific).

4.2.6 Western blot analysis of mannose 6 phosphate isomerase and mannose monophosphate.

HCT116 p53^{-/-} and HCT116 p53^{+/+} cells were cultured in T25 flasks at 2.75x10⁵ cells/flask with high glucose media under aerobic and hypoxic condition. After 24 hours, high glucose media was replaced with free glucose media enriched with 10mM mannose (control cells contained high glucose media only). Cells were incubated for 96 hours under aerobic and hypoxic (0.1% oxygen) following that they were lysed in RIPA buffer for 10 minutes on ice. The lysed cells were sonicated and stored at -20C. Protein concentrations were determined using the BCA assay (described earlier in section 3.3.10) and samples (30µg) were separated on 15% SDS-PAGE gel and proteins transferred to nitrocellulose membrane as described elsewhere (see section 2.8.4). Membranes was blocked with 5% TBS-T milk buffer and probed with primary antibody for mannose-6 phosphate isomerase (P6MI), phosphomannomutase 2 (PMM2) and β-Actin overnight at 4 ° C. The appropriate secondary antibody recognizes the protein of interest and this was incubated with the blot for 1 hour at room temperature. The membrane was visualized using the LICOR fluorescent imaging. Details of all antibodies used are presented in section 2.8.5 of this thesis.

4.2.7 Influence of glutamine on the survival of cells under aerobic and hypoxic conditions.

In addition to evaluating the effect of various sugars on the survival of cells under

hypoxia, the effect of glucose deprivation with and without glutamine was determined under both aerobic and hypoxic conditions. The experimental design is similar to that described above and specific experimental conditions are described in the legends to relevant figures in the results section.

4.2.8 The effect of 2DG and 968 on the survival of cells under aerobic and hypoxic conditions.

Based on the results obtained in the previous experiment, glutamine can be used as a fuel to promote the survival of cells in glucose deprived conditions under aerobic conditions. This suggests that the use of a glycolytic inhibitor (such as 2DG) in combination with a glutaminase inhibitor (such as 968) could work together to eradicate aerobic cells under glucose rich conditions. The studies described below were designed to determine the effects of 2DG and 968 on aerobic cells in glucose rich medium prior to using them in combination (due to time constraints however, combination studies were not performed). The effects of 2DG on cell survival under hypoxic and aerobic conditions has been described in the previous chapter (figure 3.12 to 3.16) but in order to obtain a direct comparison on the same batch of cells, the 2DG experiments were repeated and done at the same time as the 968 experiments. In addition to studies being conducted under aerobic conditions, parallel studies under hypoxic conditions were performed as a comparison.

Cell survival of HCT116 p53^{+/+} and HCT116 p53^{-/-} cells following continuous exposure to 2DG (glycolytic inhibitor) and 968 (glutaminase inhibitor; TOCRIS; 311795-38-7) was determined using the MTT assay. Cells were seeded into 96-well

flat bottom plates at a final concentration of 2000 cells per well in appropriate culture medium. For studies conducted under normoxia, plates were incubated under standard conditions of 37 °C in humidified air with 5% CO₂. For hypoxic conditions, plates were incubated in a H35 HypOxystation (Don Whitley Scientific, Shipley, UK) which provides a stable atmosphere of humidified gases consisting of 5% CO₂, 0.1% oxygen with the remainder made up with nitrogen. The chamber is also heated to maintain a temperature of 37°C. In both cases, cells were seeded into 96well plates and incubated under normoxic or hypoxic conditions for 24 hours prior to drug exposure.

Following 24-hours incubation, medium was removed from each well and replaced with high glucose medium and glucose free medium contained various concentrations of inhibitor. Details of the inhibitors used and their preparation is presented in table 2.1. Plates were set up for each compound as described in chapter two (section 2.6.2). Plates were incubated at 37°C for 96 hours before cell survival was assessed using the MTT assay. As described in chapter two, 20µl of 5mg/ml MTT solution was added to each well and allowed to incubate for 4hours in the incubator at 5% CO₂ and 37°C. The cells were processed as described above and cell survival was determined by dividing the true absorbance of the treated wells by the true absorbance of the controls (expressed as a percentage). Cell survival was plotted against drug concentration to generate a dose response curve and the IC₅₀ (concentration required to kill 50% of cells) was determined for each cell line and treatment. Due to time constraints, combination studies were not performed but these will be conducted in future studies.

4.2.9 Measuring glucose level in cell culture medium

Glucose levels were measured in high glucose medium (supplemented with 10% FBS, 1mM, 2mM l-glutamine) and Free glucose medium (supplemented with 10% FBS, 1mM, 2mM l-glutamine) using the Roflotion chamber (Roche). A 32 μ L sample of medium was loaded onto the magnetic strip and immediately measured by Roflotion chamber according to the manufacturer's instructions (Roche).

4.3 Results

4.3.1 Influence of glucose deprivation on cell growth under aerobic and hypoxic conditions.

The effect of glucose deprivation on the survival of a panel of cancer cell lines under aerobic and hypoxic conditions are presented in figure 4.1 to 4.6. For all six cell lines, glucose deprivation was generally well tolerated for cells grown under aerobic conditions. For many of the cell lines (HCT116 p53^{+/+} and p53^{-/-}, HT29, DLD1) depletion of glucose to levels 0.625mM only modestly reduced cell survival. For these cell lines, even in the complete absence of glucose, survival levels remained high (for example for HCT116 p53^{+/+} and DLD1, survival >75%). The most significant drop in survival under aerobic conditions occurred in HT-29 (figure 4.3) and BE (figure 4.4) cells where cell survival fell to ~40% compared to the control in the absence of glucose in the media.

Under hypoxic conditions, the absence of glucose markedly reduced cell survival in

all cell lines. This was associated with notable morphological changes in the appearance of cells under phase contrast microscopy. The most significant effects were observed in the HCT116 p53^{+/+} cell line (figure 4.1) with cell survival values typically ~10% of that of controls. For HCT116 p53^{-/-}, HT29, BE and PSN1 cell lines, survival under hypoxia in the absence of glucose was ~15-20%. The use of media with of different concentrations of glucose revealed dose dependent effects of glucose deprivation on cell survival under hypoxia with effects of specific concentrations being cell line dependent. In the case of HCT116 p53^{+/+} and HCT116 p53^{-/-} cells, glucose concentrations above 9mM were required to maintain cell survival under hypoxia with a pronounced drop in survival observed at 9mM (figures 4.1 and 4.2) whereas survival of BE cells appeared unaffected by a reduction in glucose concentrations to 5mM. (figure 4.4). Although there is some variability between the six cell lines in response to low glucose conditions, consistently the cancer cells appeared much more dependent on glucose for cell survival under hypoxic culture conditions than in normoxia.

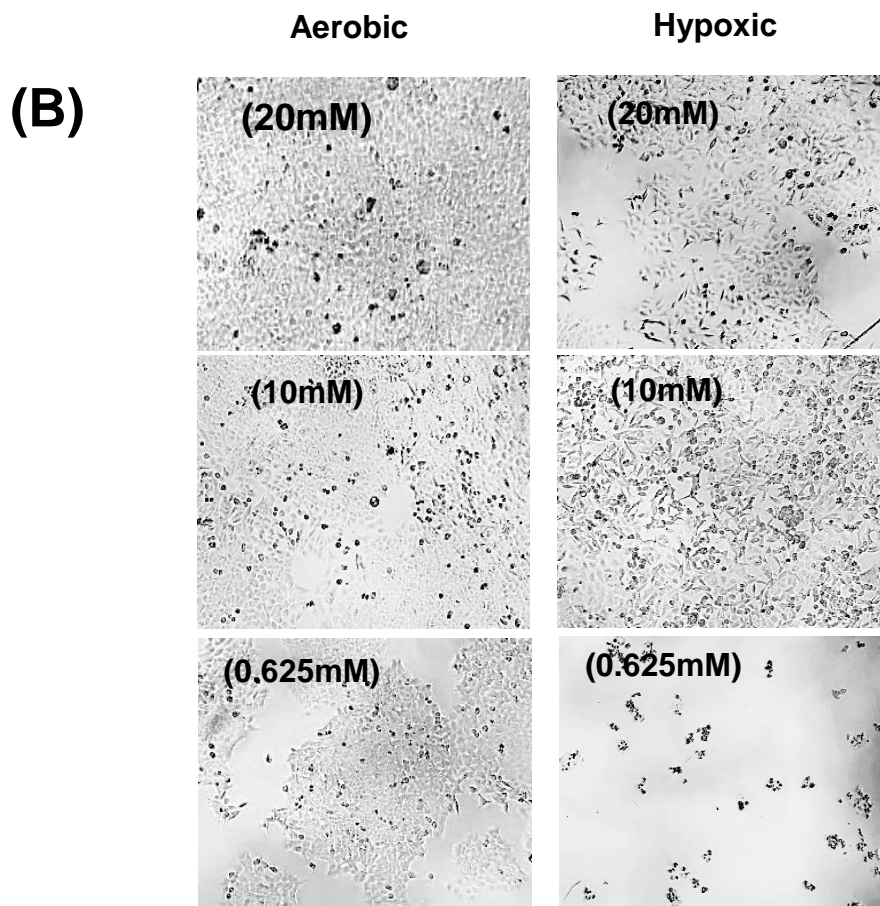
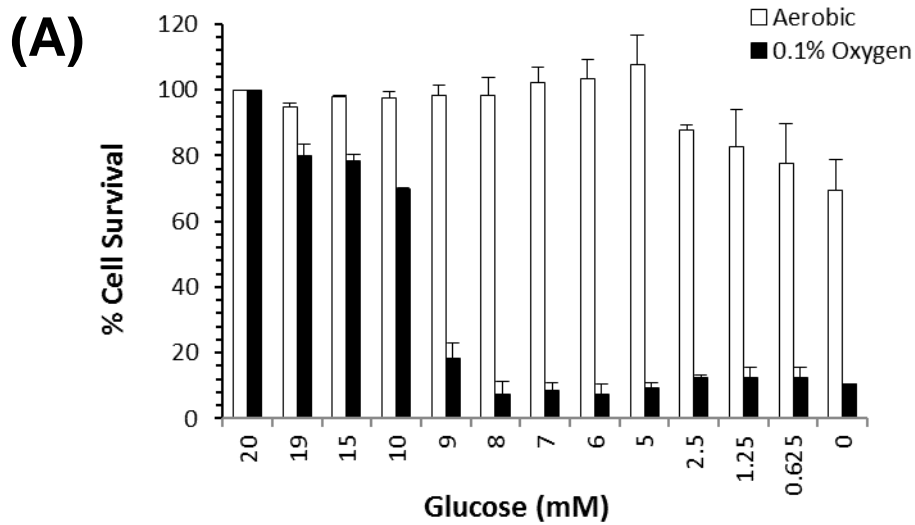
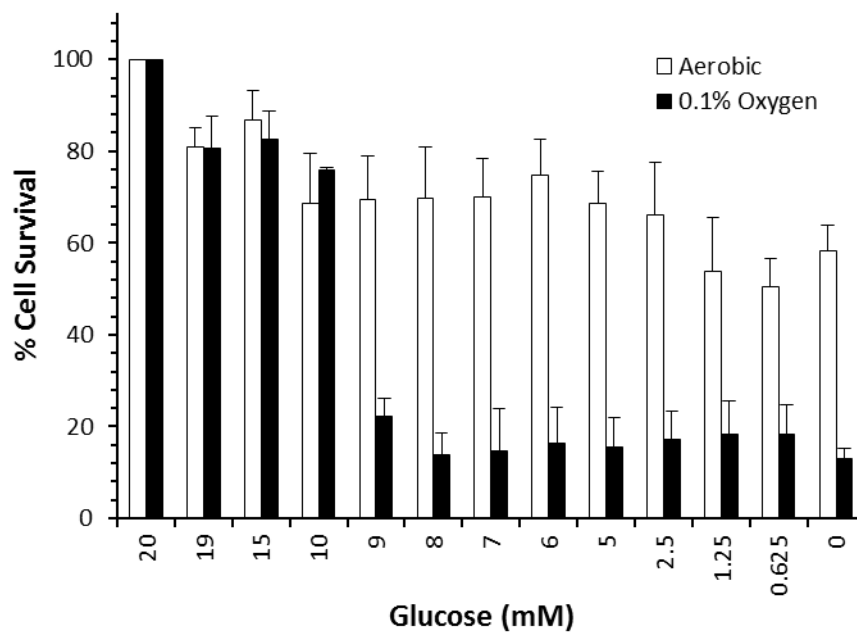


Figure 4.1 Influence of glucose concentration on the survival of HCT116 p53^{+/+} cells. Panel A represents the survival of cells under different glucose concentrations under aerobic and hypoxic conditions and panel B presents representative images of cells under aerobic and hypoxic conditions (the values in parenthesis represent the concentration of glucose in the culture medium).

(A)



(B)

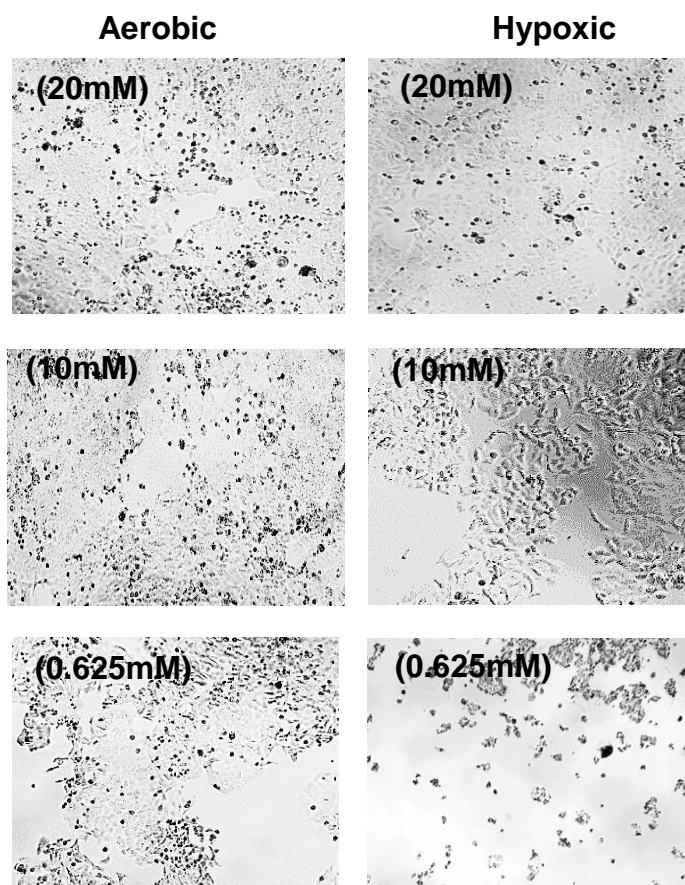


Figure 4.2 Influence of glucose concentration on the survival of HCT116 p53^{-/-} cells. Panel A represents the survival of cells under different fructose concentrations under aerobic and hypoxic conditions and panel B presents representative images of cells under aerobic and hypoxic conditions (the values in parenthesis represent the concentration of fructose in the culture medium).

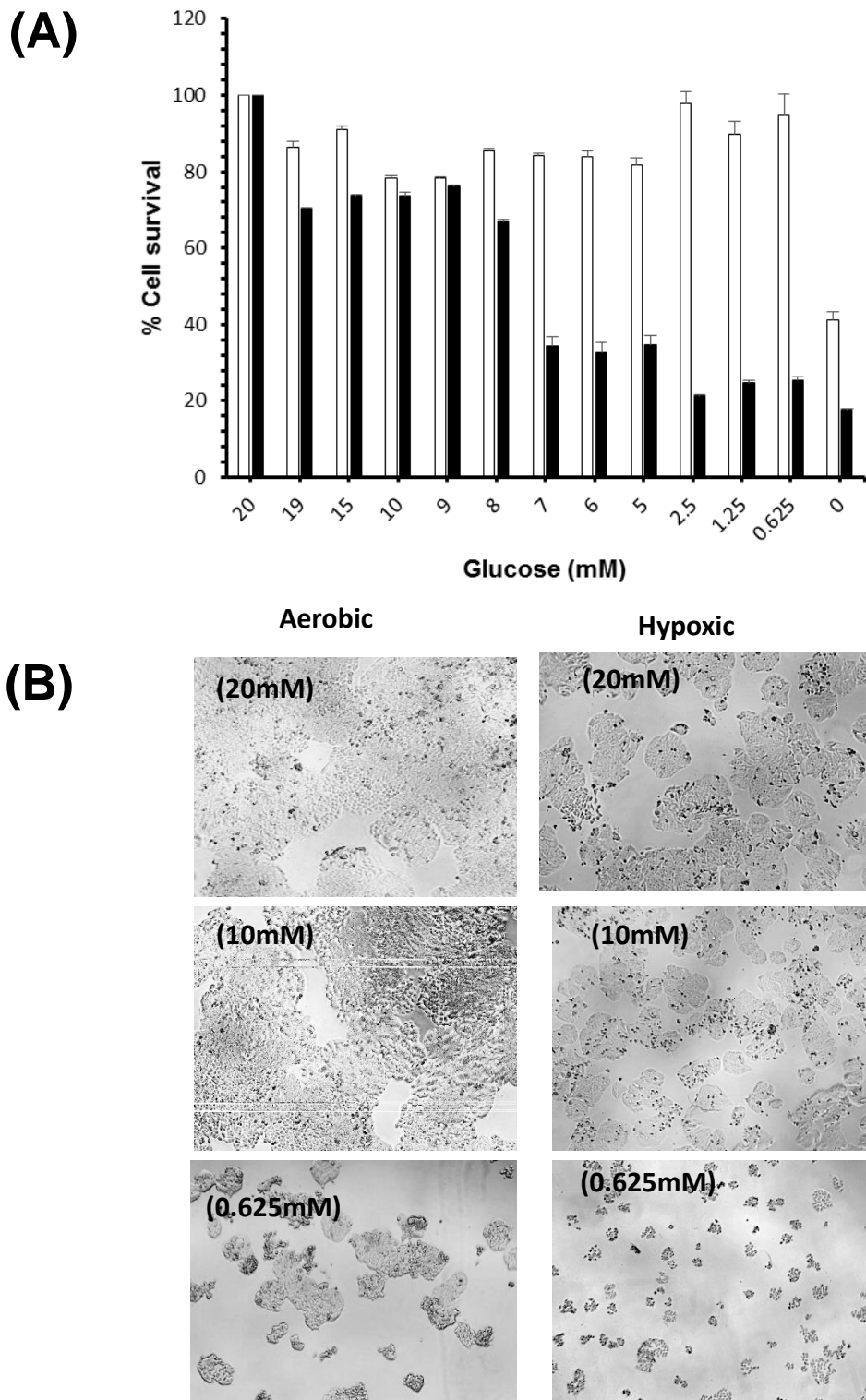
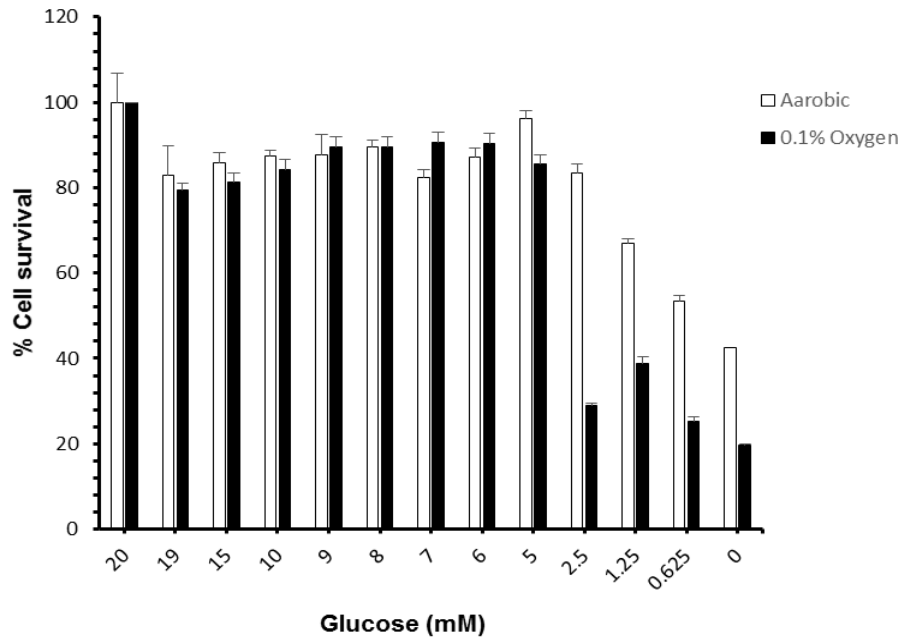


Figure 4.3 Influence of glucose concentration on the survival of HT29 cells. Panel A represents the survival of cells under different glucose concentrations under aerobic and hypoxic conditions and panel B presents representative images of cells under aerobic and hypoxic conditions (the values in parenthesis represent the concentration of glucose in the culture medium).

(A)



(B)

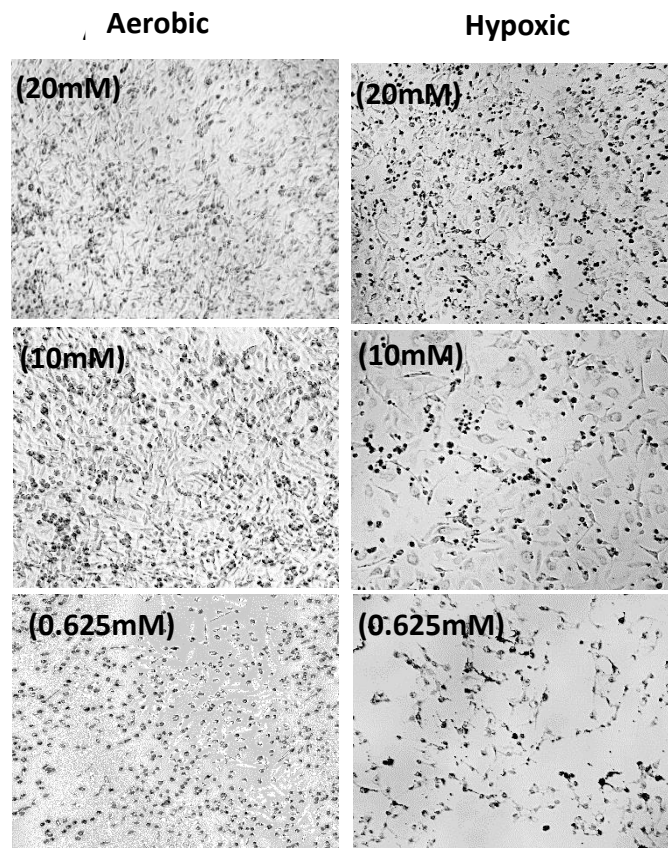


Figure 4.4 Influence of glucose concentration on the survival of BE cells. Panel A represents the survival of cells under different glucose concentrations under aerobic and hypoxic conditions and panel B presents representative images of cells under aerobic and hypoxic conditions (the values in parenthesis represent the concentration of glucose in the culture medium).

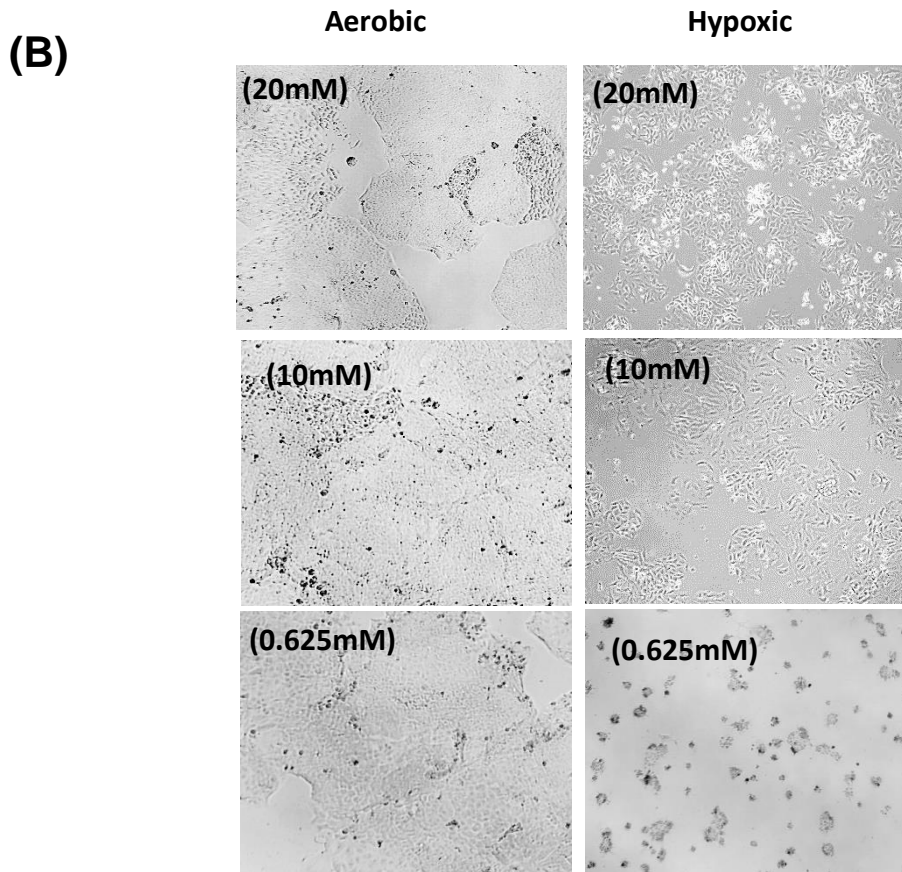
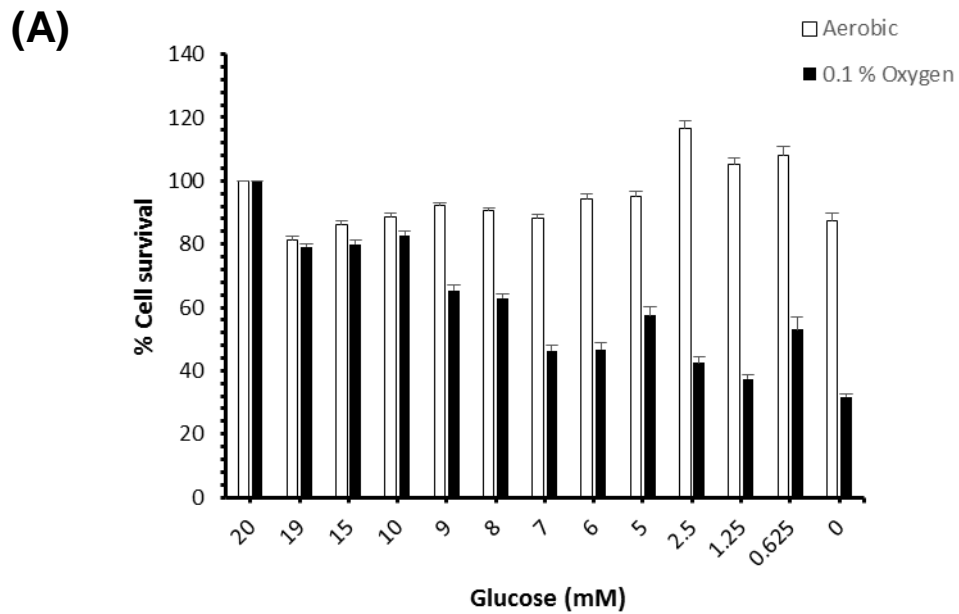
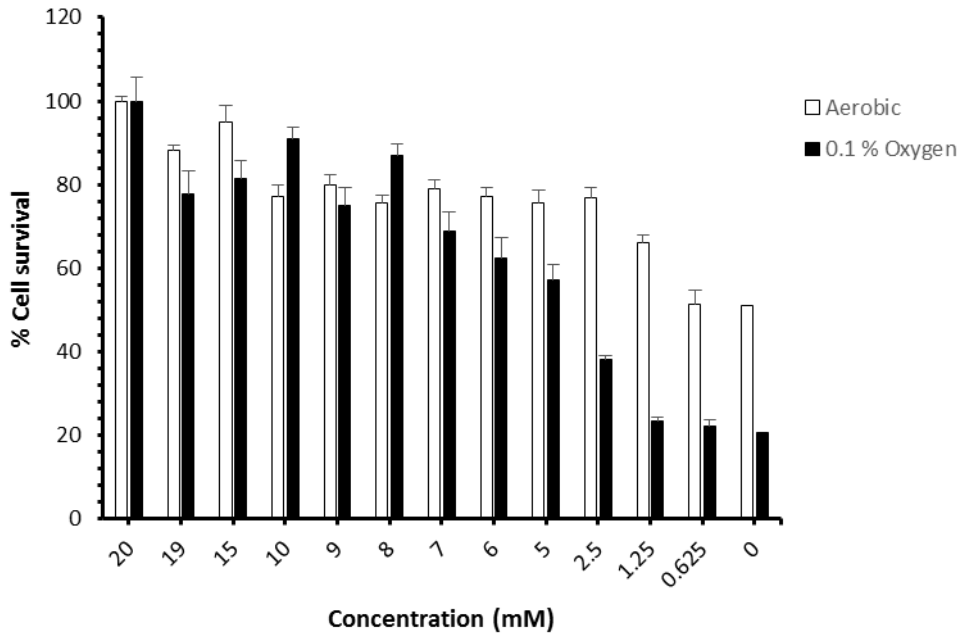


Figure 4.4 Influence of glucose concentration on the survival of DLD1 cells. Panel A represents the survival of cells under different glucose concentrations under aerobic and hypoxic conditions and panel B presents representative images of cells under aerobic and hypoxic conditions (the values in parenthesis represent the concentration of glucose in the culture medium).

(A)



(B)

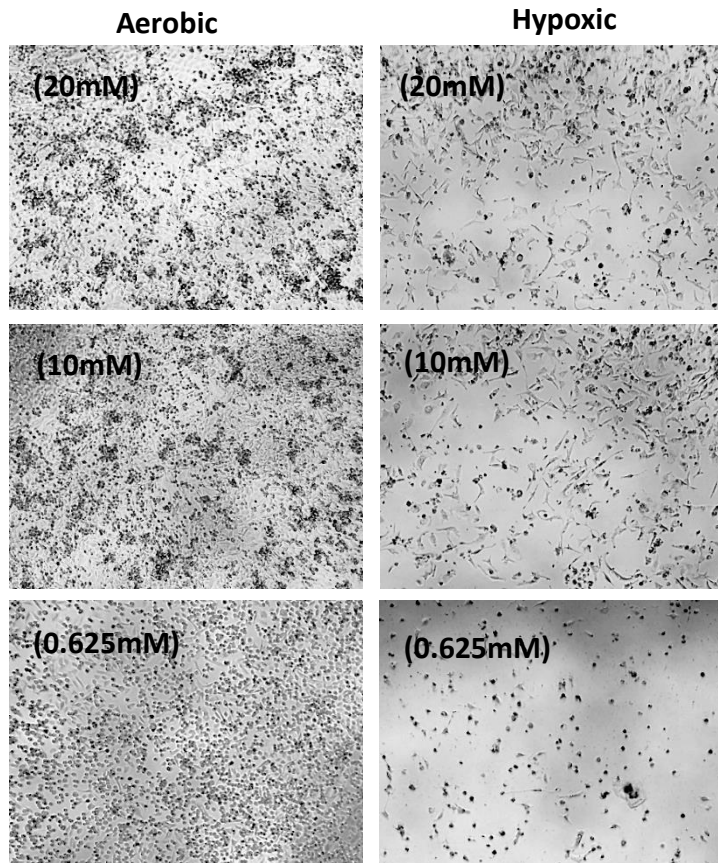


Figure 4.5 Influence of glucose concentration on the survival of PSN-1 cells. Panel A represents the survival of cells under different glucose concentrations under aerobic and hypoxic conditions and panel B presents representative images of cells under aerobic and hypoxic conditions (the values in parenthesis represent the concentration of glucose in the culture medium).

4.3.2 Validation of results using the SRB assay

The results of studies conducted using the SRB endpoint assay instead of the MTT assay for HT29 cells are presented in figure 4.7. These results demonstrate a similar trend to the MTT assay in that cell survival is reduced significantly in glucose deprived media under hypoxic conditions. Direct comparison with the MTT assay results presented in figure 4.3 above show that under hypoxic conditions in the presence of 0.625mM glucose, cell survival values were similar in the SRB assay (30.65%) compared to the MTT assay (25.38%). Similarly in aerobic conditions and 0.625mM glucose cell survival in the SRB assay was 93.64% and in the MTT assay, it was 94.71%. Based upon these findings, the MTT assay is generating data that is similar to the SRB assay.

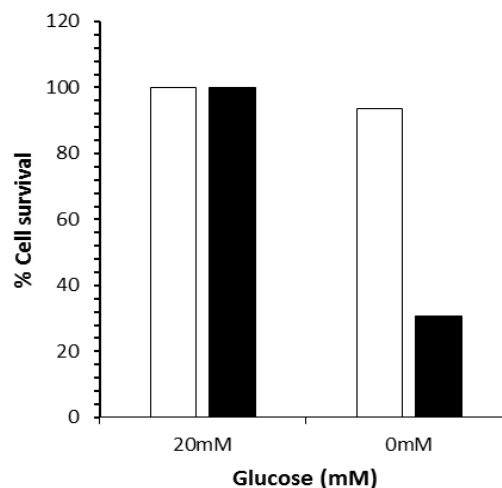


Figure4. 6 Influence of glucose concentration on cell survival using the SRB assay. The data represents the survival of HT29 cells after 96 hours of glucose deprivation media (0.625mM glucose) under aerobic (open bars) and hypoxic conditions (solid bars) using the SRB assay. The controls used medium containing 20mM glucose under both aerobic and hypoxic conditions. The values represent the mean of two experiments and as such, no error bars are presented.

4.3.3 Recovery of cell survival following glucose deprivation for 96 hours.

The results presented above demonstrate that glucose is required for cells to survive under hypoxic conditions but cell survival did not go below 10% suggesting that some cells were able to tolerate no glucose in the culture media in 0.1% oxygen conditions. To address the question of whether these surviving cells might be able to fully recover and commence proliferation when provided with glucose, glucose-rich media (20mM glucose) was added to cells following 96 hours of glucose deprivation. Cell survival was measured 48 hours after the addition of glucose-rich medium, and the results (white colour) are presented in comparison with glucose deprivation results (black colour) in figure 4.8.

In the case of HCT116 p53^{+/+} cells, the addition of glucose rich media following 96 hours of glucose deprivation had no effect on cell survival for cells incubated in 5mM glucose or less in the deprivation phase of the experiment (figure 4.8A). Whilst concentrations of glucose of 6 to 9mM significantly reduced the survival of cells under hypoxia, the addition of glucose rich media after the glucose deprivation period resulted in a significant increase in cell survival. Similar results were obtained for the HCT116 p53^{-/-} cells although recovery was apparent only for cells exposed to 7mM or more during the deprivation phase of the experiment (figure 4.8B).

These results show that cells exposed for 4 days to glucose levels below 5 or 6mM under hypoxic conditions (0.1% oxygen) did not fully recover when glucose levels returned to normal. Above 5 to 6mM glucose however, HCT116 cells were able to fully recover.

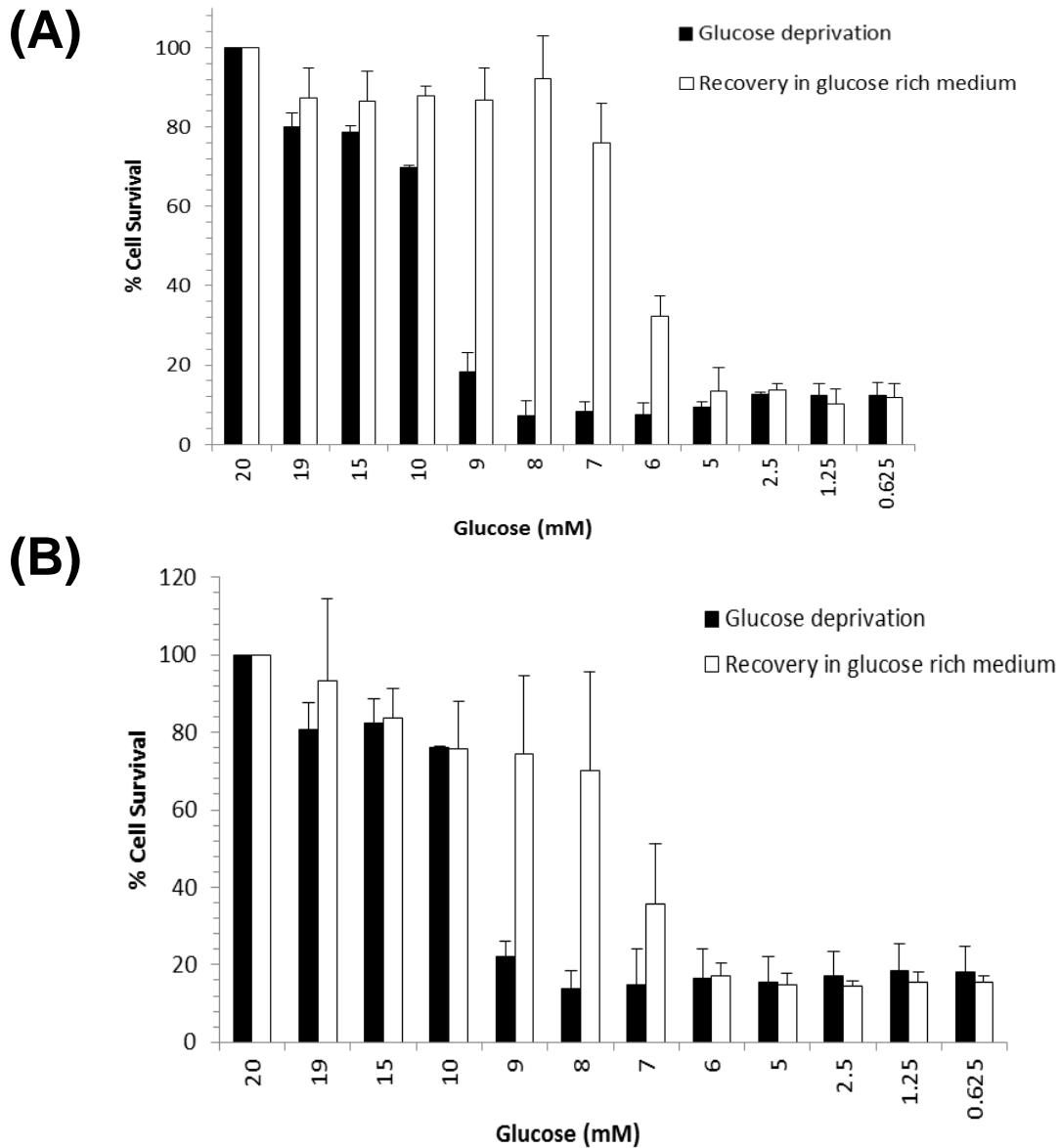


Figure 4.7 Recovery of cells following glucose deprivation under hypoxic conditions. Panels A and B represents the recovery of HCT116 p53^{+/+} and HCT116 p53^{-/-} cells respectively following 96 hours of glucose deprivation. The values on the X-axis represent the concentrations of glucose used during the deprivation phase of the experiment and in all cases, glucose rich medium (20mM) was added at the end of the deprivation period. Cell survival was measured 48 hours later using the MTT assay. Please note that the results for glucose derived conditions are a repeat of the data presented in figures 4.1 and 4.2 and they are included here for the purpose of providing a direct comparison with the recovery experiments.

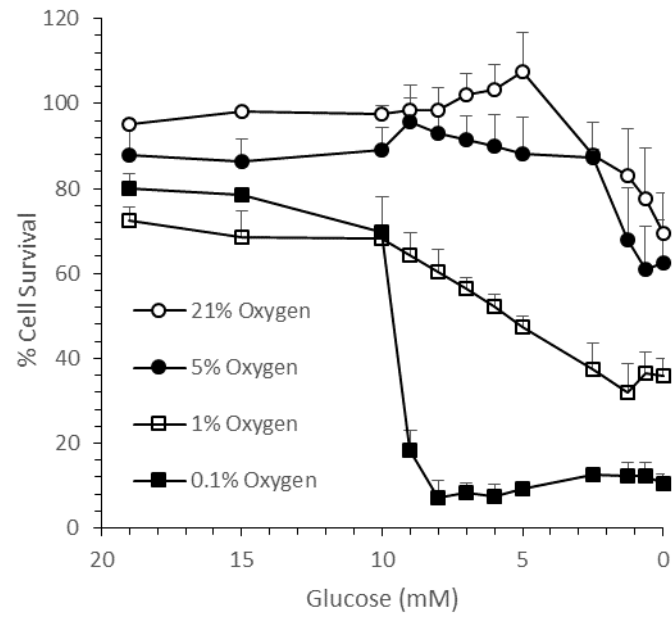
4.3.4 Influence of oxygen tension and glucose concentration on the survival of cells.

The results presented above were conducted at 0.1% oxygen. To determine the effect of glucose deprivation on cells at different oxygen concentrations, similar studies were conducted over a range of oxygen tensions. The results of these studies are presented in figures 4.9 and 4.10

In the case of both HCT116 p53^{+/+} and HCT116 p53^{-/-} cells, the effect of glucose deprivation is similar at 21% and 5% oxygen with effects on survival generally observed at very low levels of glucose. Even when glucose is absent, cell survival is typically above 60% of controls. The effects of glucose deprivation increased as oxygen tension is reduced with significant effects observed at 1% oxygen and these effects increase further as oxygen tension is reduced to 0.1%. The results are comparable in both cell lines.

The results demonstrate that (i) the combination of low glucose and low oxygen tension have significant effects on cell survival and (ii) the magnitude of the effect on cell survival reduces as both oxygen tension and glucose concentration increase.

(A)



(B)

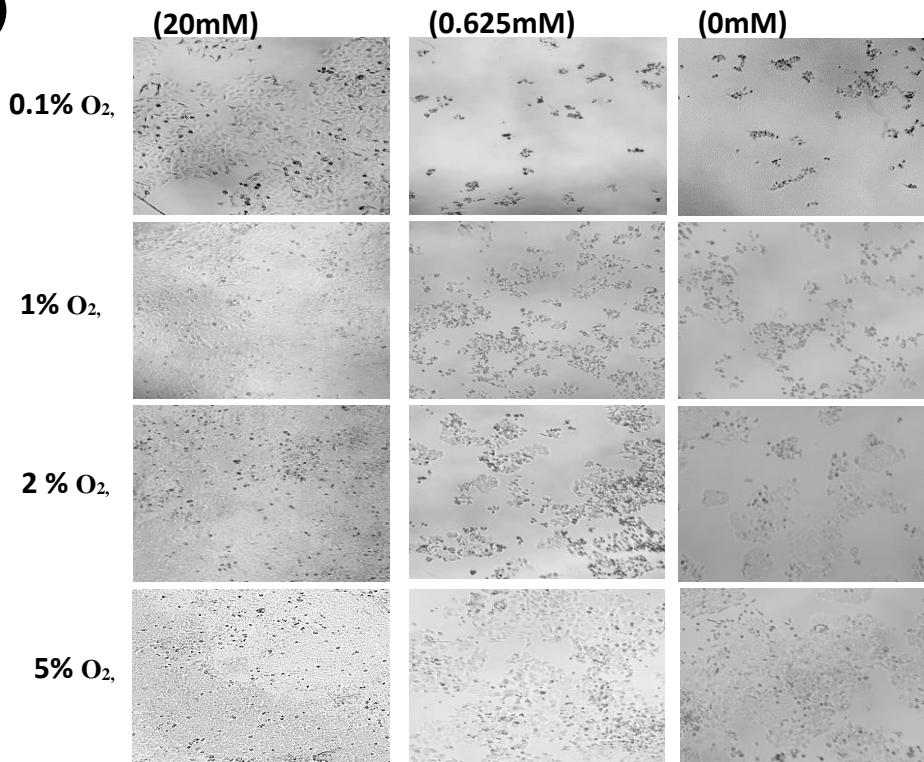


Figure 4.8 Influence of oxygen tension and glucose concentration on HCT116p53^{+/+} cell survival. Panel A represents the survival of cells under different glucose concentrations and different oxygen tensions. Panel B presents representative images of cells exposed to different glucose concentrations (in parenthesis) and oxygen tension. Errors bars are present standard deviation for actual readings from triplicates.

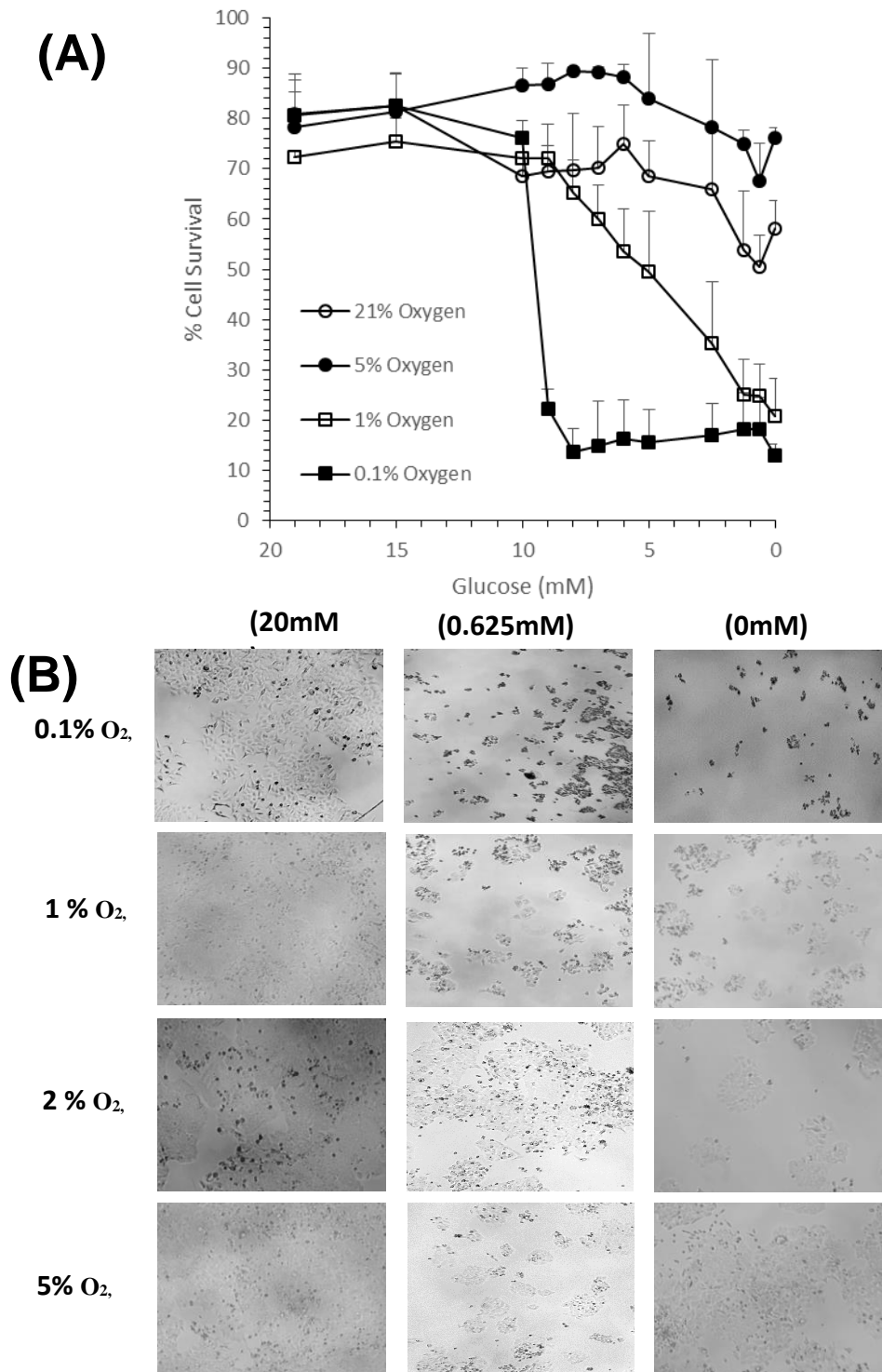


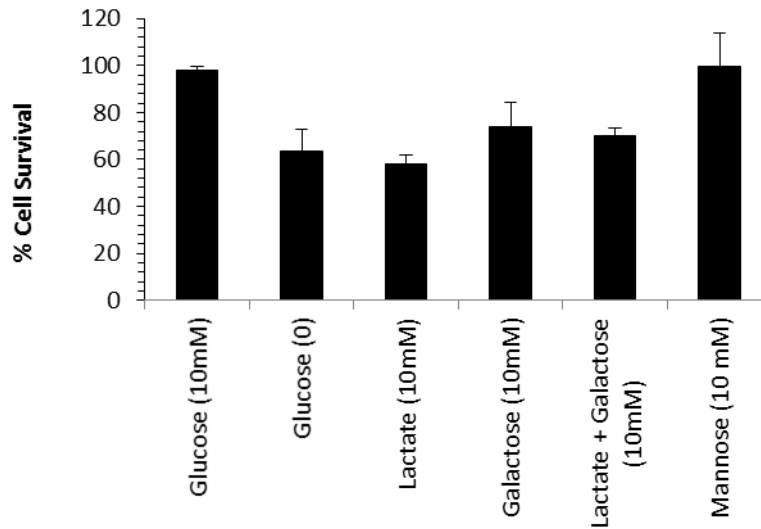
Figure 4.9 Influence of oxygen tension and glucose concentration on HCT116p53^{-/-} cell survival. Panel A represents the survival of cells under different glucose concentrations and different oxygen tensions. Panel B presents representative images of cells exposed to different glucose concentrations (in parenthesis) and oxygen tension, errors bars are present standard deviation for actual readings from triplicates.

4.3.5 Influence of different sugars on cell growth *in vitro* under aerobic and hypoxic conditions.

The previous studies have demonstrated that under hypoxic conditions, cells are dependent upon glucose for survival. These conditions provide an experimental opportunity to determine whether or not other carbon sources can be utilised to maintain cell survival under hypoxic conditions. For comparative purposes, similar studies were performed under aerobic conditions and these are presented in figures 4.11 (HCT116 p53^{+/+} cells) and figure 4.13 (HCT116 p53^{-/-} cells). Under normoxia, addition of lactate failed to increase survival above that of glucose-deprived cells. Galactose marginally increased survival in HCT116 p53^{+/+} cells. Mannose increased survival levels of ~60% in glucose-deprived HCT116 p53^{+/+} and HCT116 p53^{-/-} cells to survival levels in cells cultured in glucose-rich media.

Under hypoxic conditions only mannose was able to support the growth of cells in the absence of glucose. In both HCT116 p53^{+/+} and HCT116 p53^{-/-} cells, mannose (10 mM) was able to completely reverse the effects of glucose deprivation (figures 4.12 and 4.14). These results suggest that mannose could be a fuel that can be used alongside or instead of glucose to support the growth and survival of cells under hypoxia (0.1% oxygen).

(A)



(B)

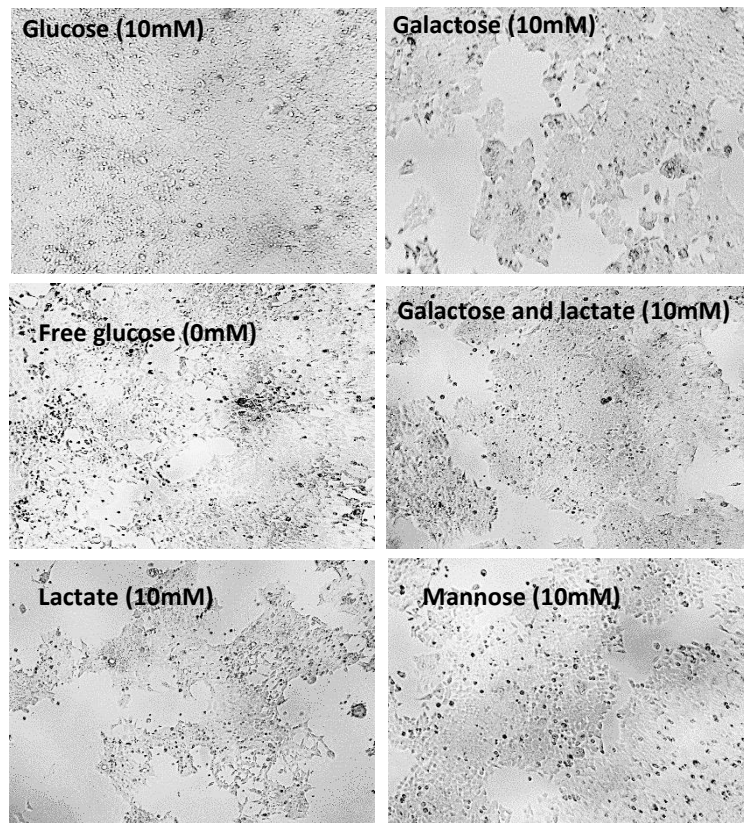
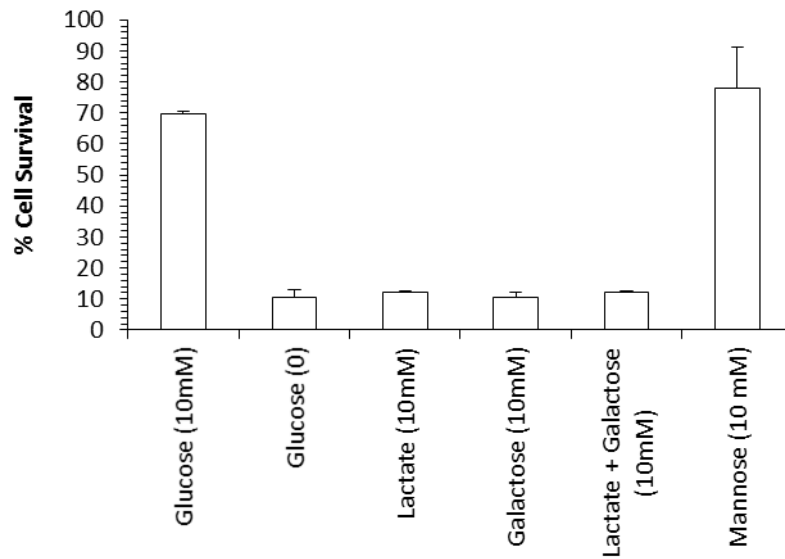


Figure 4.10 Effect of replacing glucose with various sugars on the survival of HCT116^{+/+} cells under aerobic conditions. Panel A represents the survival of cells grown with culture media without glucose but with different sources of carbon (mannose, lactate, galactose, and the combination of galactose with lactate) at (10mM) under aerobic conditions. Panel B presents representative images of treated cells under aerobic conditions (the values in parenthesis represent the concentration of sugar in the culture medium). The controls are media supplemented with glucose at 10 mM and glucose free media.

(A)



(B)

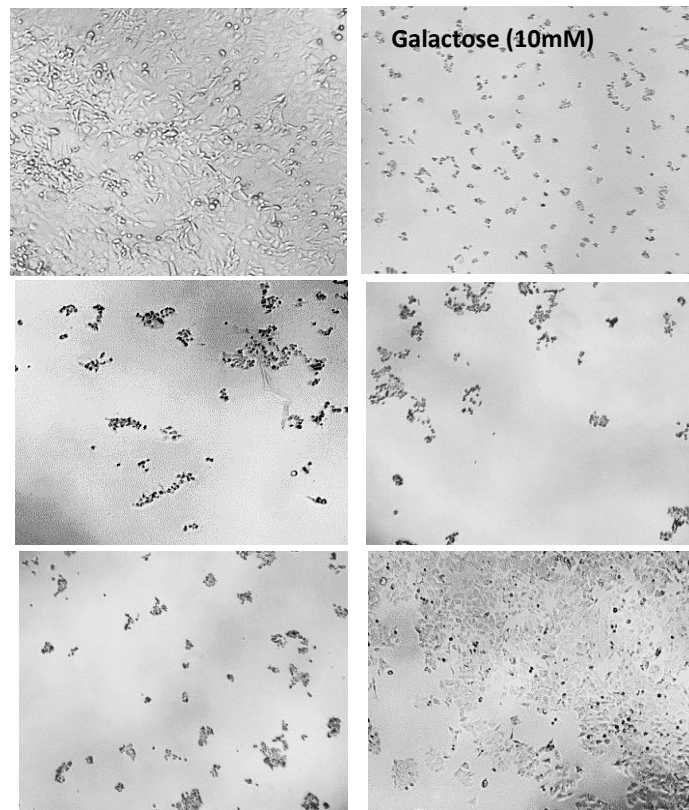
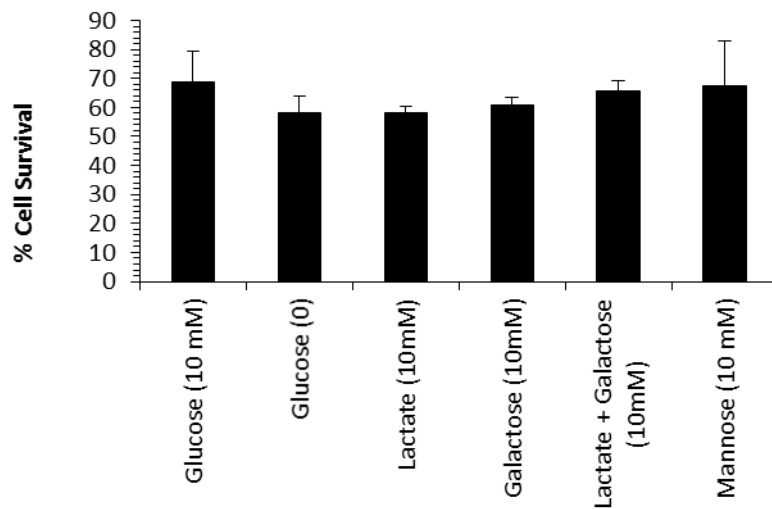


Figure 4.11 Effect of replacing glucose with various sugars on the survival of HCT116 ^{+/+} cells under hypoxic conditions. Panel A represents the survival of cells grown with culture media without glucose but with different sources of carbon (mannose, lactate, galactose, and the combination of galactose with lactate) at (10mM) under hypoxic conditions. Panel B presents representative images of treated cells under hypoxic conditions (the values in parenthesis represent the concentration of sugar in the culture medium). The controls are media supplemented with glucose at 10 mM and glucose free media.

(A)



(B)

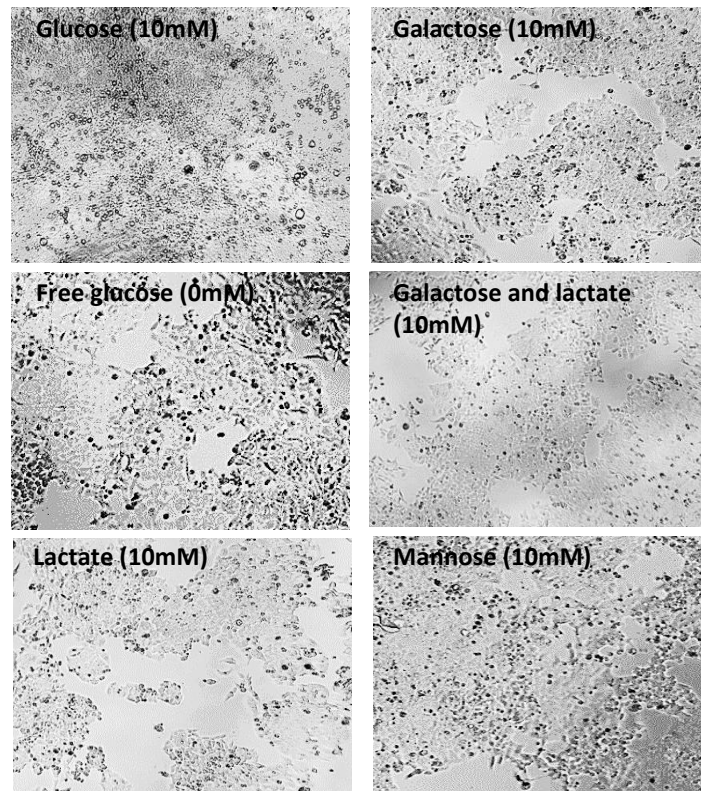
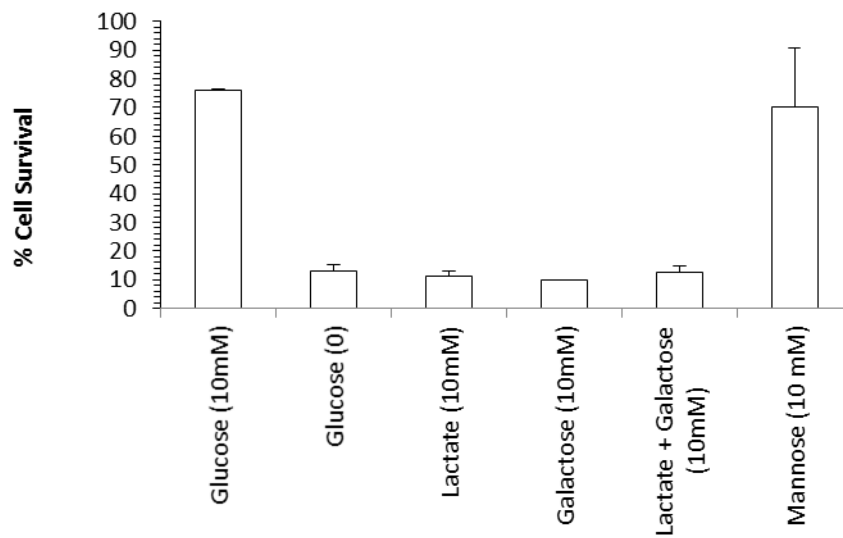


Figure 4.12 Effect of replacing glucose with various sugars on the survival of HCT116^{-/-} cells under aerobic conditions. Panel A represents the survival of cells grown with culture media without glucose but with different sources of carbon (mannose, lactate, galactose, and the combination of galactose with lactate) at (10mM) under aerobic conditions. Panel B presents representative images of treated cells under aerobic conditions (the values in parenthesis represent the concentration of sugar in the culture medium). The controls are media supplemented with glucose at 10mM and glucose free media.

(A)



(B)

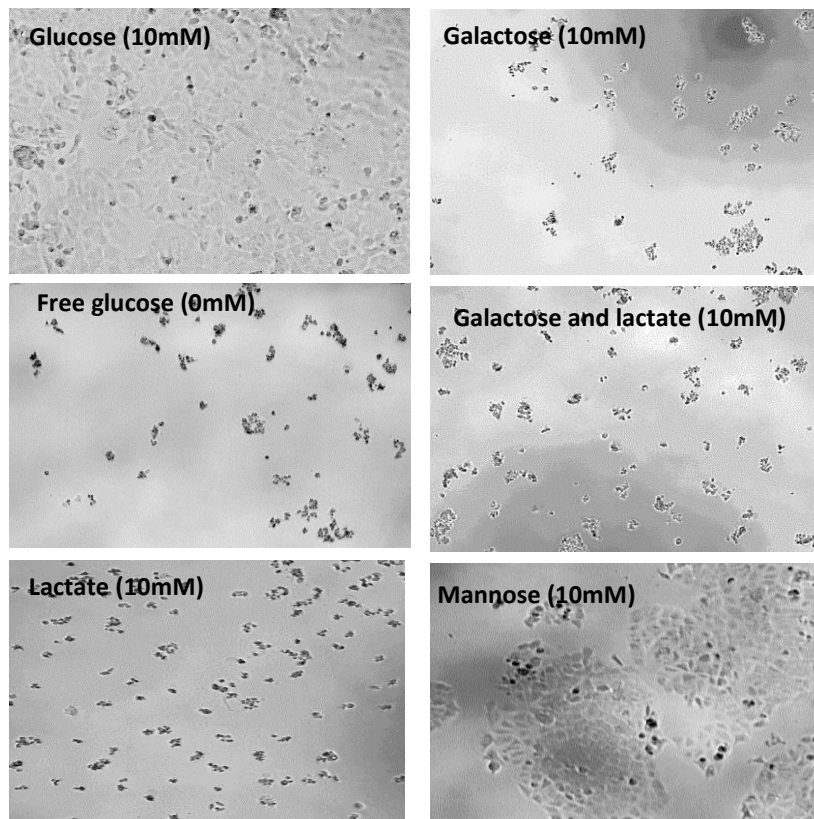


Figure 4.13 Effect of replacing glucose with various sugars on the survival of HCT116^{-/-} cells under hypoxic conditions. Panel A represents the survival of cells grown with culture media without glucose but with different sources of carbon (mannose, lactate, galactose, and the combination of galactose with lactate) at (10mM) under hypoxic conditions. Panel B presents representative images of treated cells under hypoxic conditions (the values in parenthesis represent the concentration of sugar in the culture medium). The controls are media supplemented with glucose at 10mM and glucose free media.

4.3.6 Comparison between the ability of glucose and mannose to support the growth of cells under hypoxic conditions.

As described above, mannose can support the growth of cells under hypoxic conditions when glucose is absent. This series of experiments compares the relative efficiency of glucose or mannose to support growth under hypoxic conditions and the results are presented in figures 4.15 to 4.17.

In the case of HCT116 p53^{+/+} and HCT116 p53^{-/-} (figure 4.15), mannose was clearly superior to glucose in supporting the growth of cells under hypoxic conditions when compared at equimolar concentrations. Comparatively greater cell survival was observed in the presence of mannose at just almost all concentrations of mannose or glucose used, down to 1.25mM mannose in HCT116 p53^{+/+} cells (figure 4.15A) but differences were only seen down to 5mM mannose in the HCT116 p53^{-/-} cells (figure 4.15B) suggesting a p53 related effect.

In contrast to the HCT116 cell lines, the abilities of mannose or glucose to promote cell survival under hypoxia was similar in HT29, BE and PSN1 (figures 4.16A, 4.16B and 4.17B respectively). There was some evidence that mannose was superior to glucose in the case of DLD1 cells (figure 4.17A) but the magnitude of the effect was reduced compared to the HCT116 cell lines.

These results demonstrate that mannose may be a more effective fuel than glucose under hypoxic conditions but this effect is cell line dependent and not a universal feature of many cell lines.

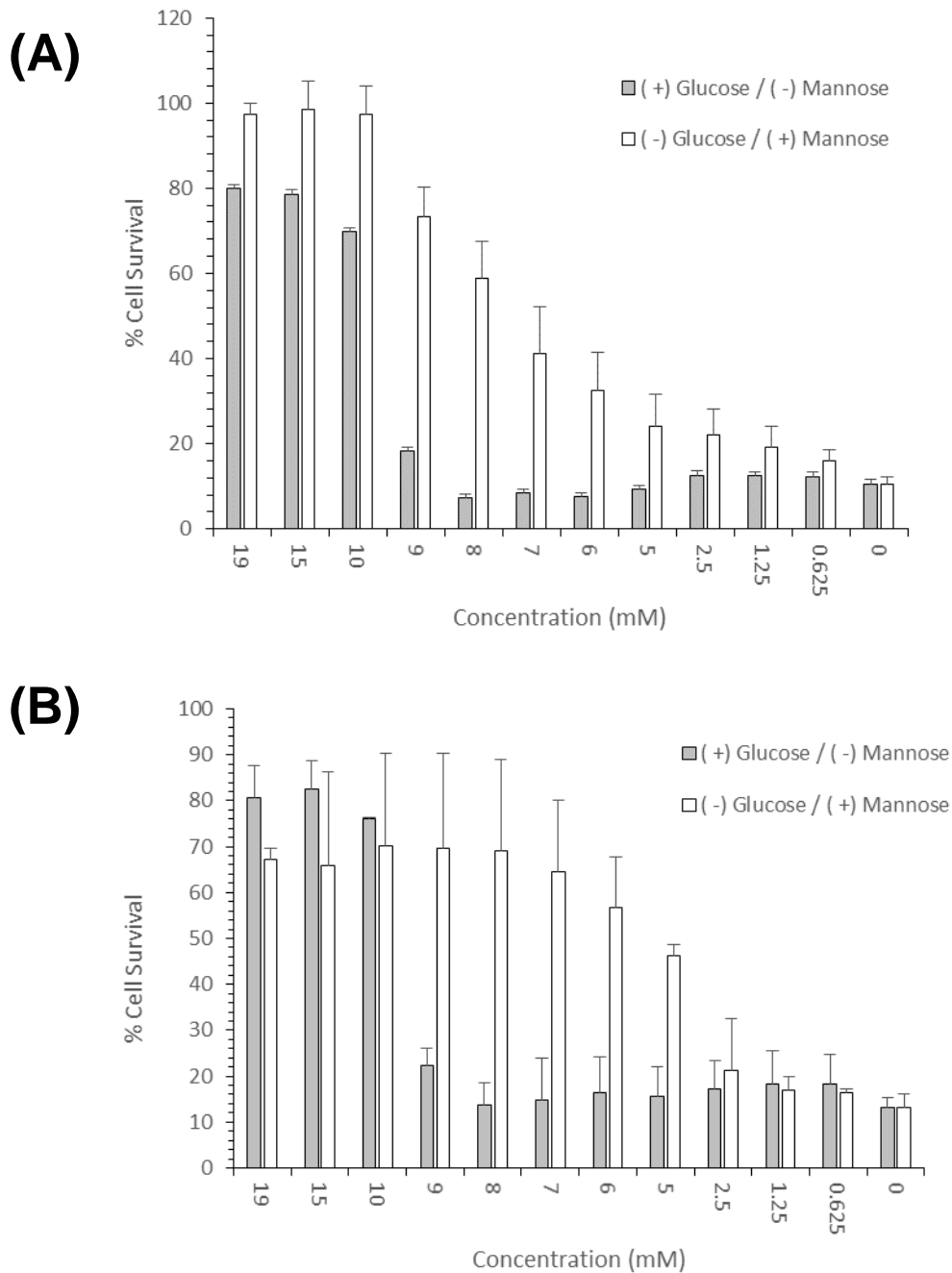


Figure 4.14 Influence of glucose or mannose on the survival of cells under hypoxia (0.1% oxygen). Panel A represents the survival of HCT116 p53^{+/+} cells following 96 hours with glucose and mannose supplemented media (variable concentrations) and Panel B representing survival of HCT116 p53^{-/-} cells following 96 hours with glucose and mannose supplemented media (variable concentrations).

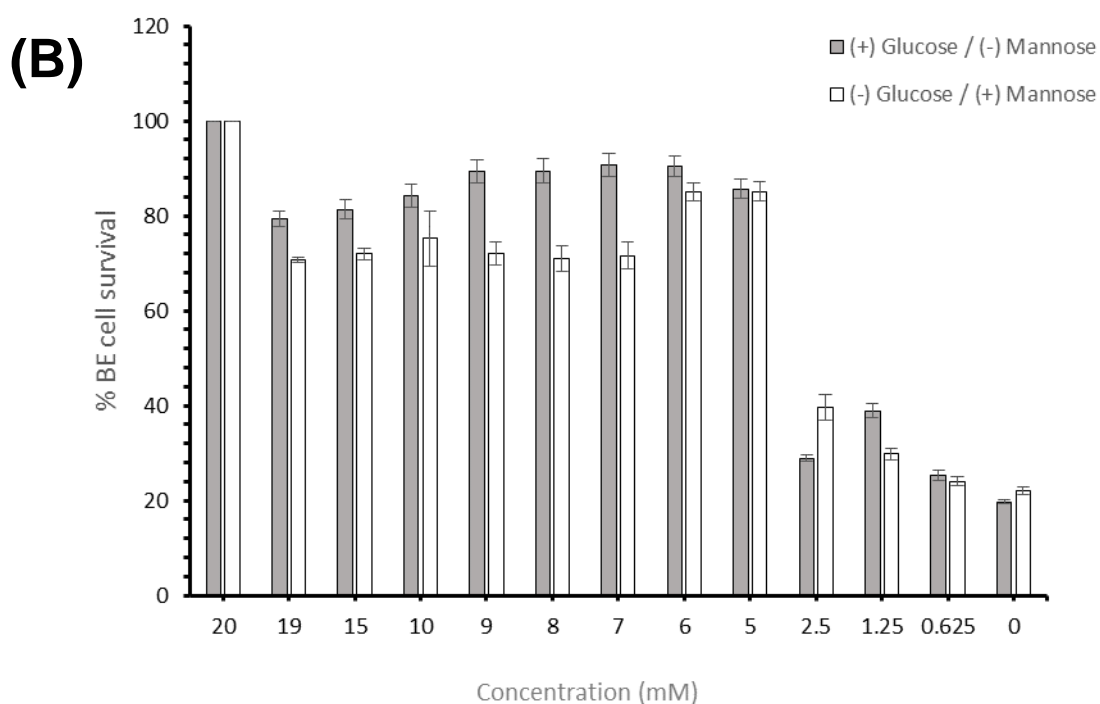
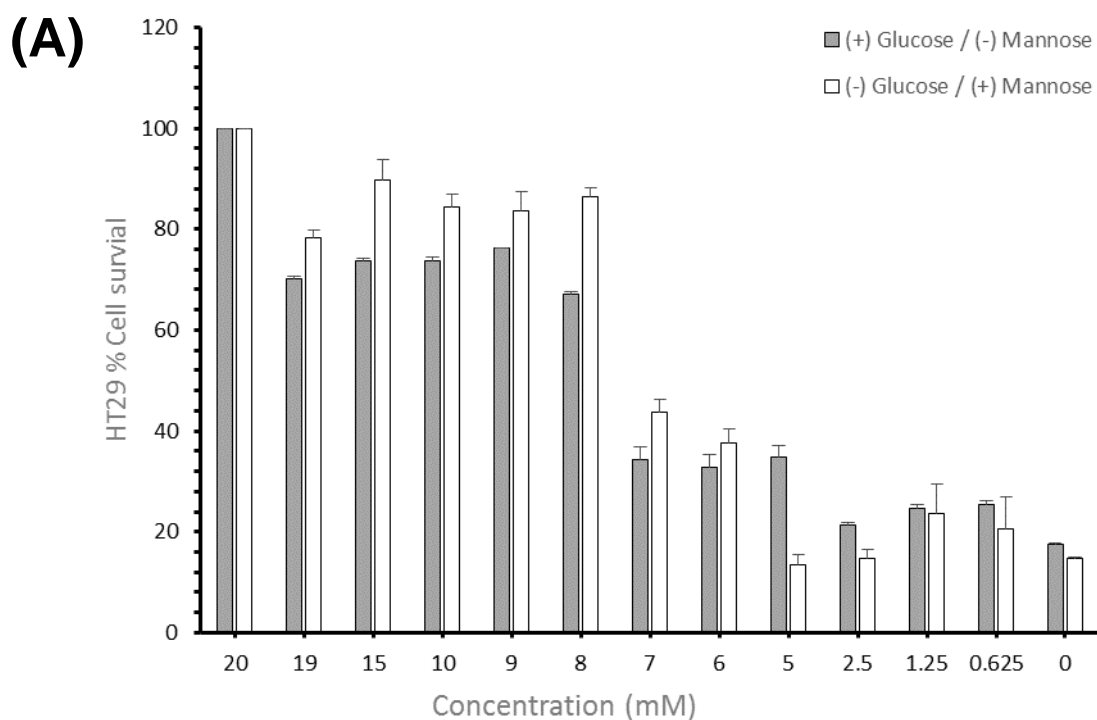


Figure 4.15 Influence of glucose or mannose on the survival of cells under hypoxia (0.1% oxygen). Panel A represents the survival of HT29 cells following 96 hours with glucose and mannose supplemented media (variable concentrations) and Panel B representing survival of BE cells following 96 hours with glucose and mannose supplemented media (variable concentrations).

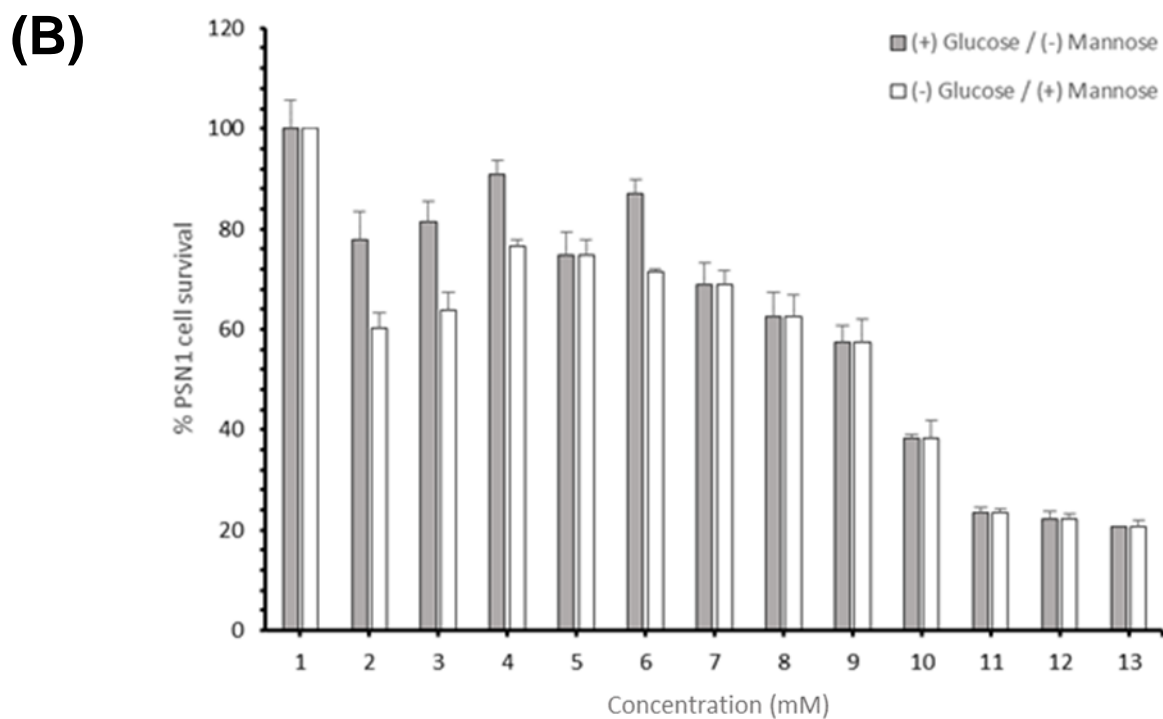
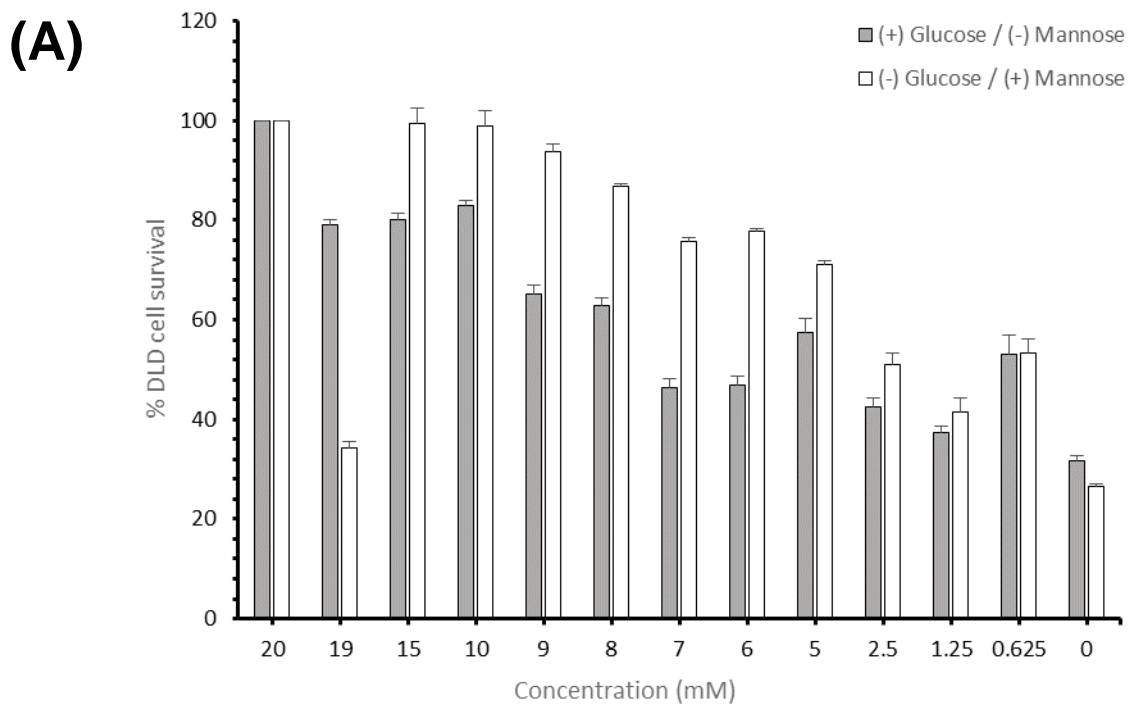
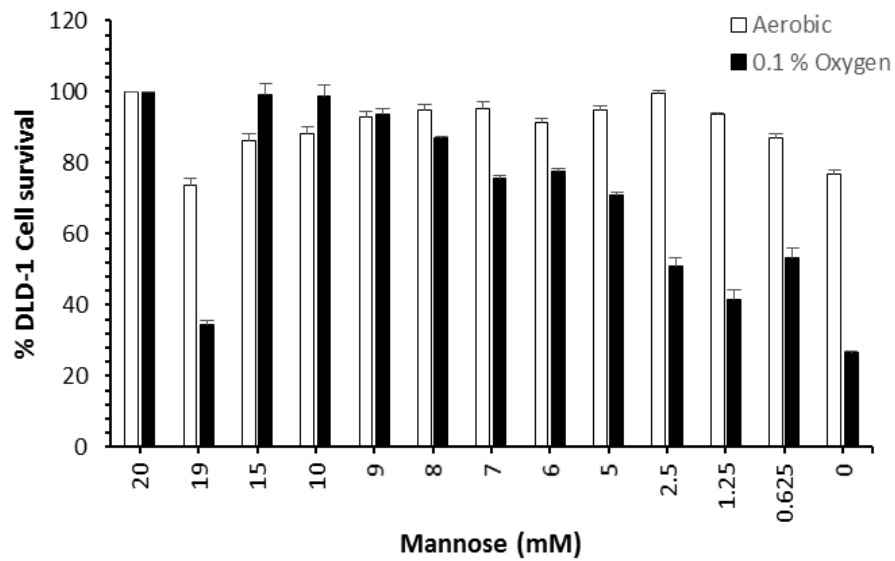


Figure 4.16 Influence of glucose or mannose on the survival of cells under hypoxia (0.1% oxygen). Panel A represents the survival of DLD-1 cells following 96 hours with glucose and mannose supplemented media (variable concentrations) and Panel B representing survival of PSN1 cells following 96 hours with glucose and mannose supplemented media (variable concentrations).

4.3.7 Influence of mannose to support the growth of DLD1 and PSN1 cells under hypoxic conditions.

In a set of experiments that are similar in design to those described in figures 4.5 and 4.6, the influence of mannose on the survival of DLD1 and PSN1 cells is presented in figure 4.18. The results presented in figure 4.18 are consistent with other cell lines in that mannose is being used as a fuel to support the growth and survival of DLD-1 and PSN-1 cells under hypoxia.

(A)



(B)

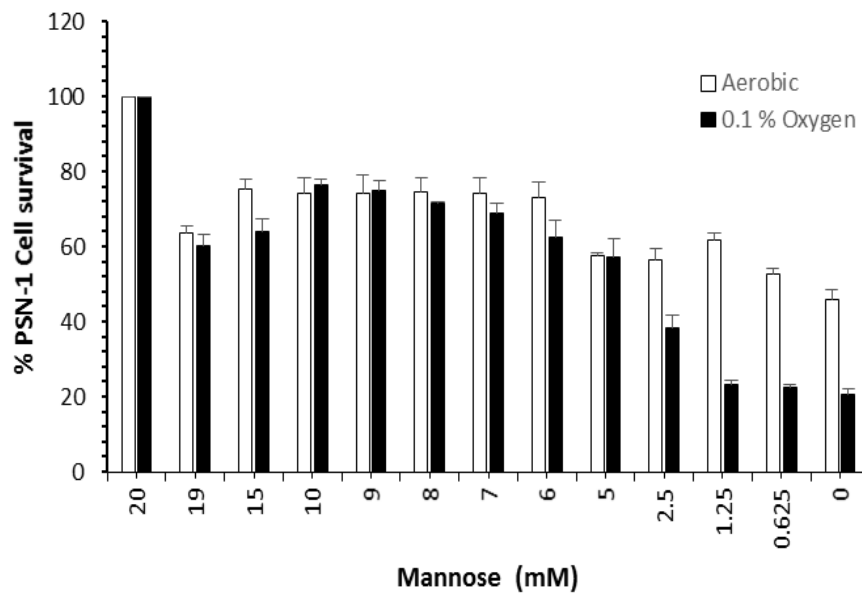


Figure 4.17 Influence of mannose concentration on the survival of DLD1 cells. Panels A and B represents the survival of DLD1 and PSN-1 cells respectively over a range of mannose concentrations (glucose free medium) under aerobic and hypoxic conditions.

4.3.8 Influence of fructose and sucrose on the survival of HCT116 p53^{+/+} and HCT116 p53^{-/-} cells under aerobic and hypoxic conditions.

An additional series of experiments were conducted to broaden the spectrum of sugars evaluated to include sucrose and fructose as these sugars are commonly available in the diet. The objective of these experiments to determine whether or not they can serve as fuels to support the growth of cells under hypoxic conditions. The design of these experiments involved supplementation of glucose deprived medium with either sucrose or fructose (over a range of concentrations) followed by measurement of cell survival using the MTT assay 96 hours later. The results are presented in figure 4.19 to 4.22. The results show that in contrast to mannose, neither fructose nor sucrose are able to fully substitute for the absence of glucose in sustaining cancer cell survival.

For both HCT116 p53^{+/+} and HCT116 p53^{-/-} cells; fructose at high concentrations (15mM and 19mM) was shown to increase cell survival under aerobic conditions. Under hypoxic conditions, lower doses of fructose (10mM) had some beneficial effect but even at the highest concentration tested (19mM), survival was only ~40-60% of that in glucose-rich media. Levels were restored to ~40% survival in HCT116 HCT116 p53^{-/-} cells suggesting possible p53-dependent differences in the ability of fructose to support survival under hypoxic conditions Addition of sucrose across the concentration range tested (0.625-19mM) failed to improve survival of glucose-deprived cells (Fig. 4.21, 4.22) either under normoxic or hypoxic conditions. This suggests that sucrose is unable to substitute for glucose as an alternative fuel in either conditions.

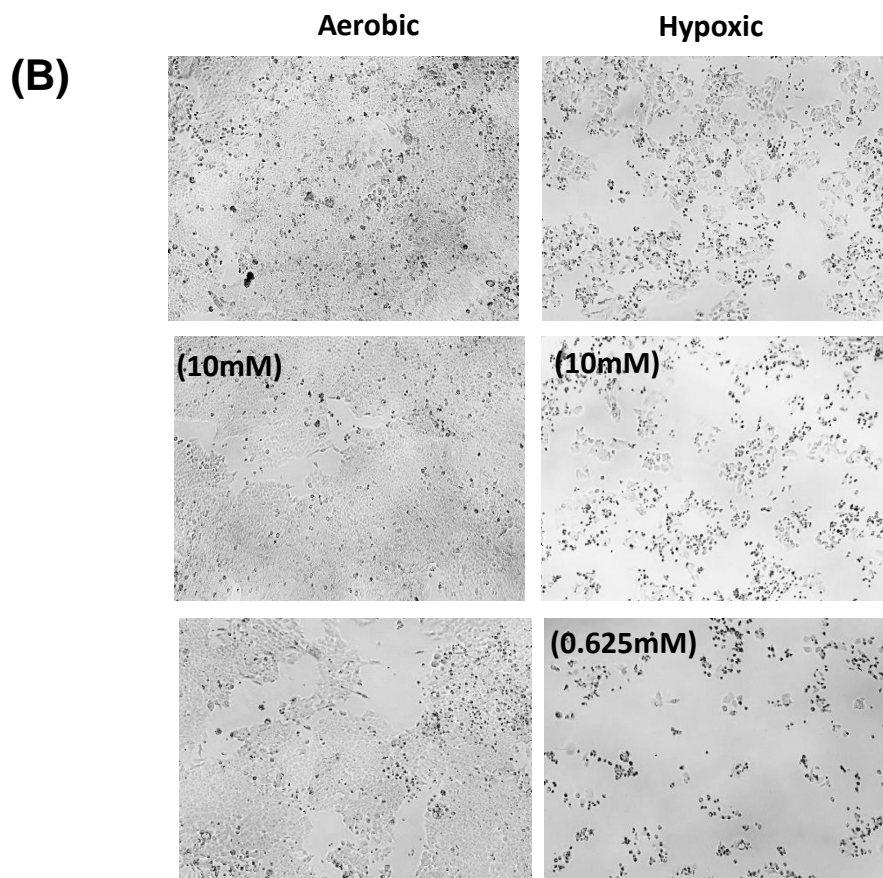
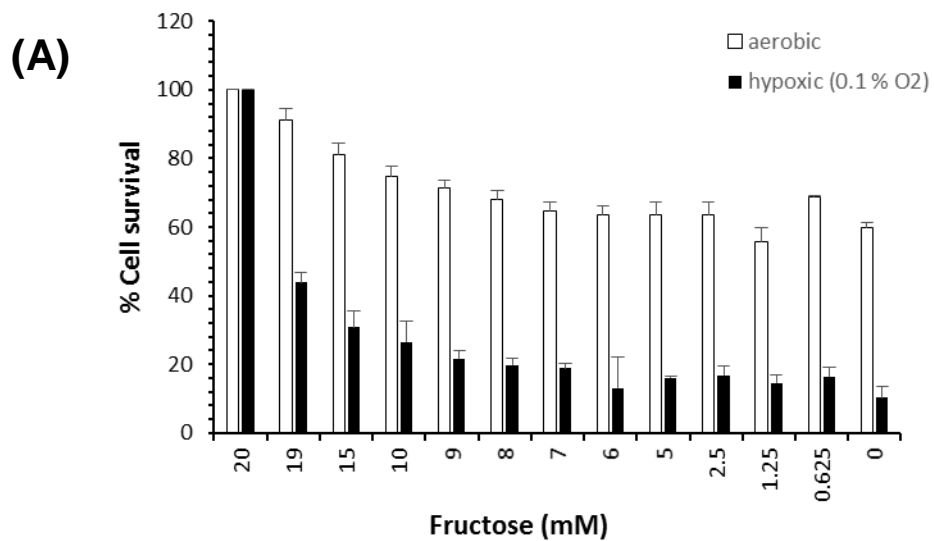


Figure 4.18 Influence of fructose concentration on the survival of HCT116 p53^{+/+} cells. Panel A represents the survival of cells under different fructose concentrations under aerobic and hypoxic conditions and panel B presents representative images of cells under aerobic and hypoxic conditions (the values in parenthesis represent the concentration of fructose in the culture medium). Cell survival is expressed as a % relative to levels in the presence of 20mM glucose.

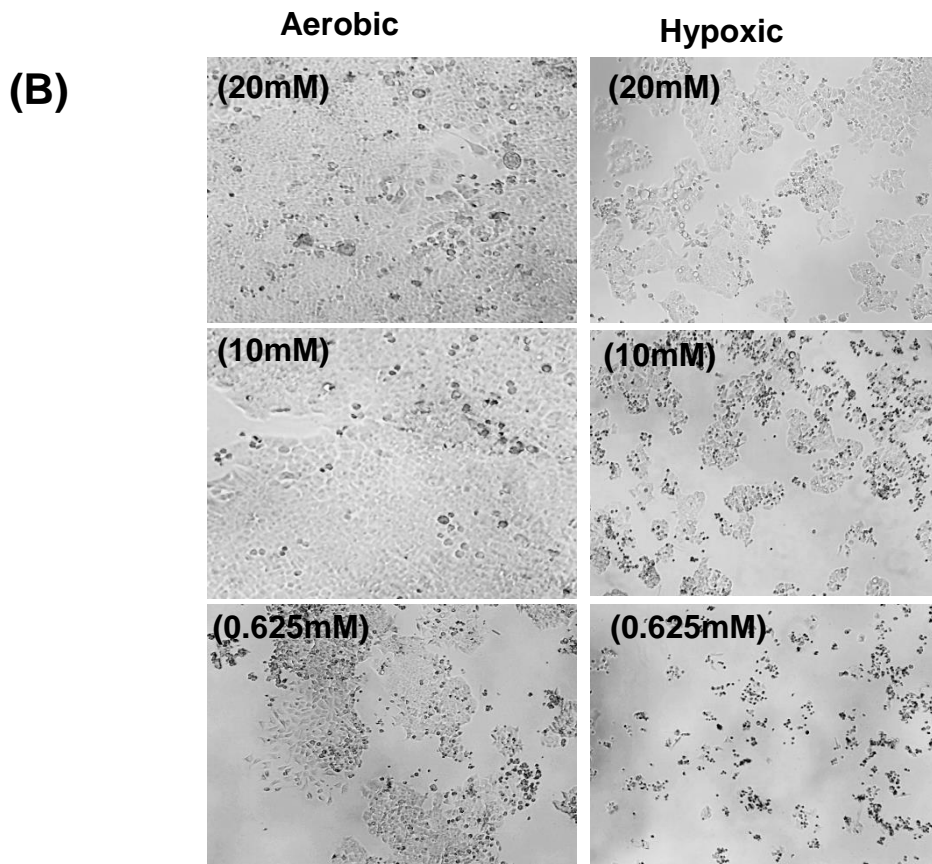
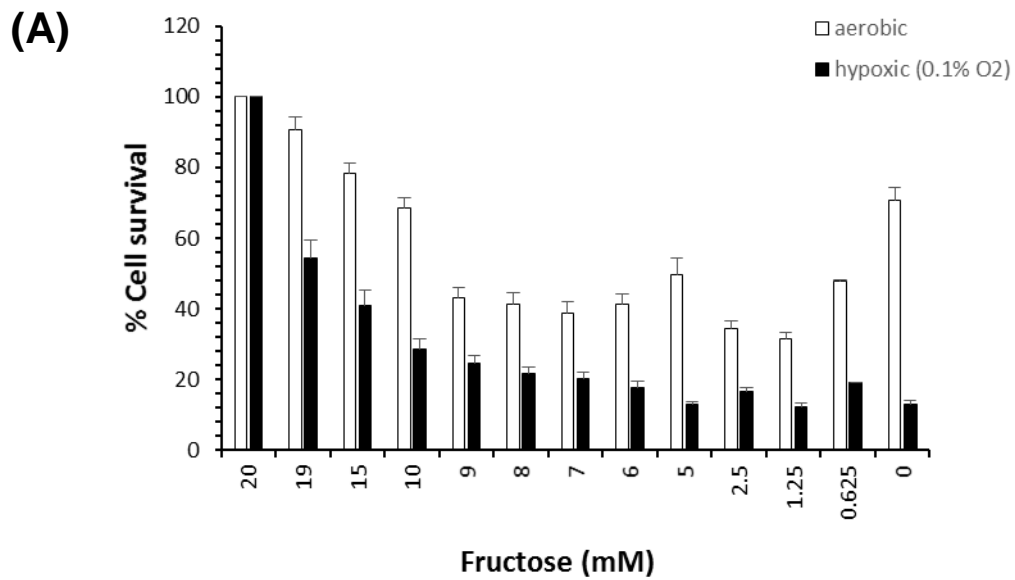


Figure 4.19 Influence of fructose concentration on the survival of HCT116 p53^{-/-} cells. Panel A represents the survival of cells under different fructose concentrations under aerobic and hypoxic conditions and panel B presents representative images of cells under aerobic and hypoxic conditions (the values in parenthesis represent the concentration of fructose in the culture medium).

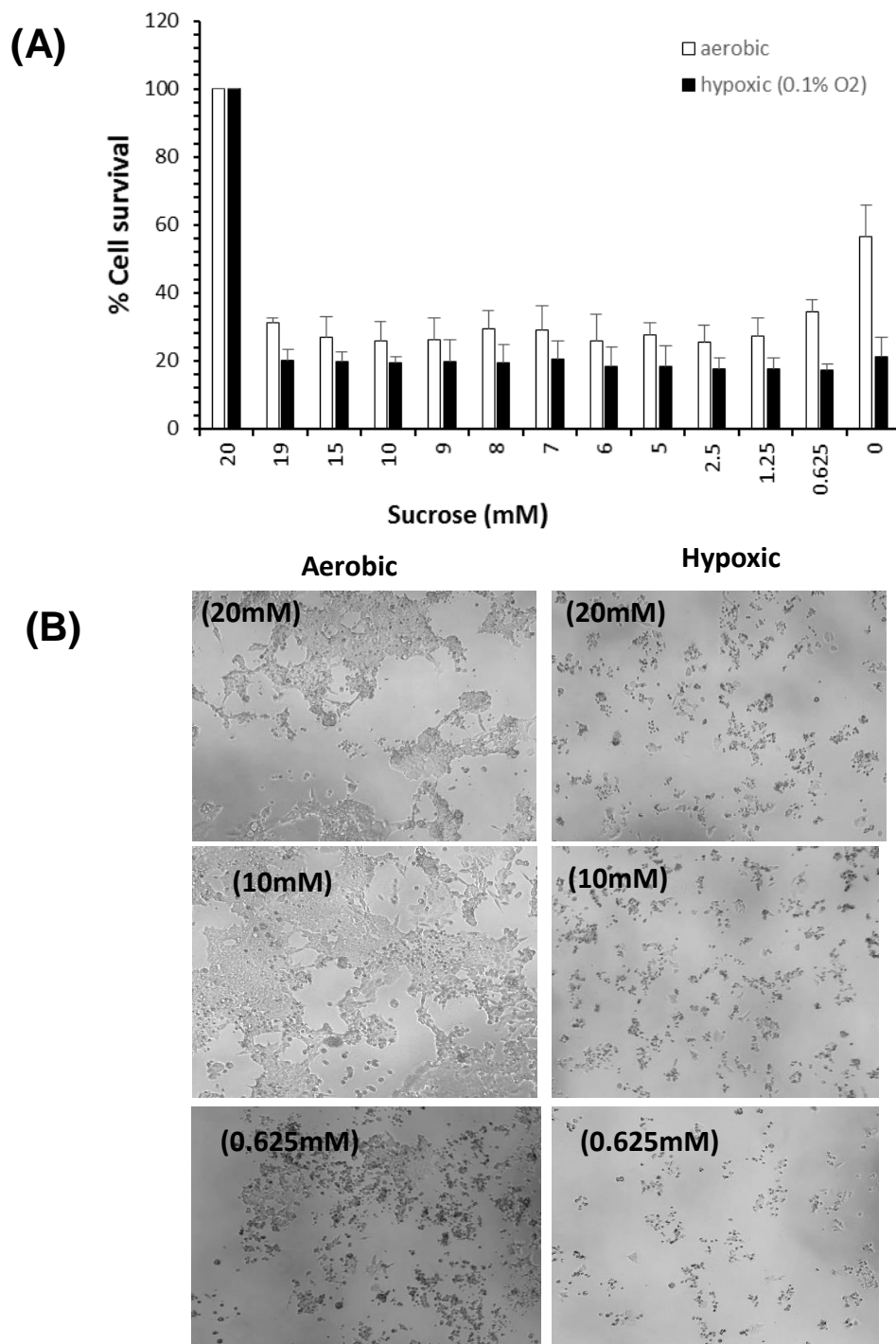


Figure 4.20 Influence of sucrose concentration on the survival of HCT116 p53^{+/+} cells. Panel A represents the survival of cells under different sucrose concentrations under aerobic and hypoxic conditions and panel B presents representative images of cells under aerobic and hypoxic conditions (the values in parenthesis represent the concentration of sucrose in the culture medium).

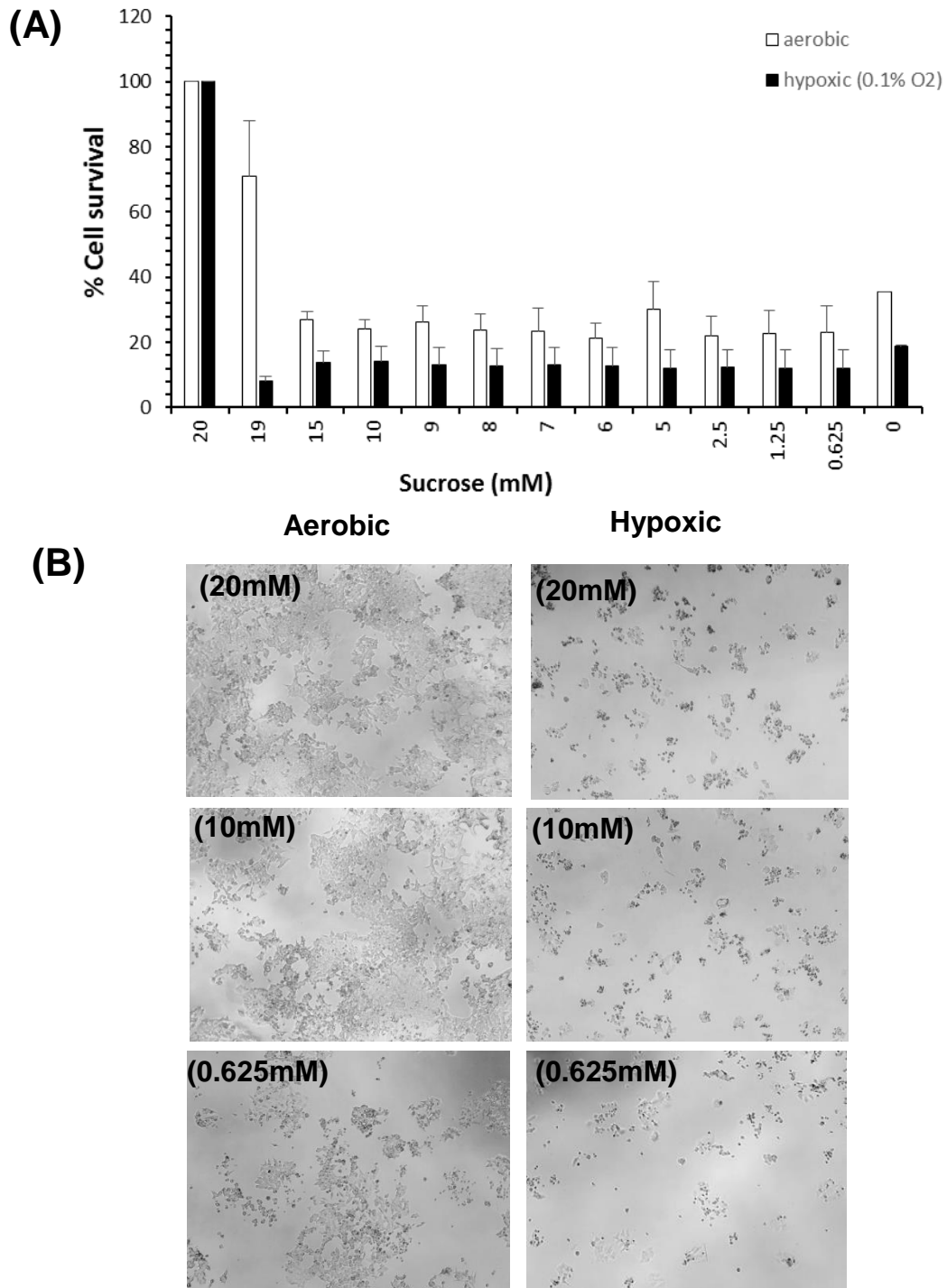


Figure 4.21 Influence of sucrose concentration on the survival of HCT116 p53^{-/-} cells. Panel A represents the survival of cells under different sucrose concentrations under aerobic and hypoxic conditions and panel B presents representative images of cells under aerobic and hypoxic conditions (the values in parenthesis represent the concentration of sucrose in the culture medium).

4.3.9 Influence of L-glutamine and glucose deprivation on cell survival under aerobic and hypoxic conditions

To examine dependency of cells on glutamine under normoxia and hypoxia and effects of both glucose and glutamine deprivation on cell viability under aerobic and hypoxic conditions, media was prepared with or without glucose (20mM) and/or glutamine (2mM). Cells were cultured in these media for 96 hours following which, cell survival was determined using the MTT assay. The results are presented in figure 4.23.

Under aerobic conditions (open bars, figure 4.23), cells are able to survive in either the absence of glucose or in the absence of L-glutamine. In the absence of both glucose and L-glutamine however, cell survival was significantly reduced to ~10-20% of that of cells in media containing both glucose and glutamine. Overall, these results suggest that when glucose levels are low, aerobic cells can switch to L-glutamine metabolism. Furthermore, it suggests that strategies designed to target both glucose and L-glutamine metabolism may produce synergistic effects *in vitro* under aerobic conditions. Under hypoxic conditions (solid bars, figure 4.23), however, the presence of glutamine failed to improve survival of cells cultured in the absence of glucose. This suggests that cells are unable to use L-glutamine as an alternative fuel to support cell survival under hypoxia when glucose levels are low.

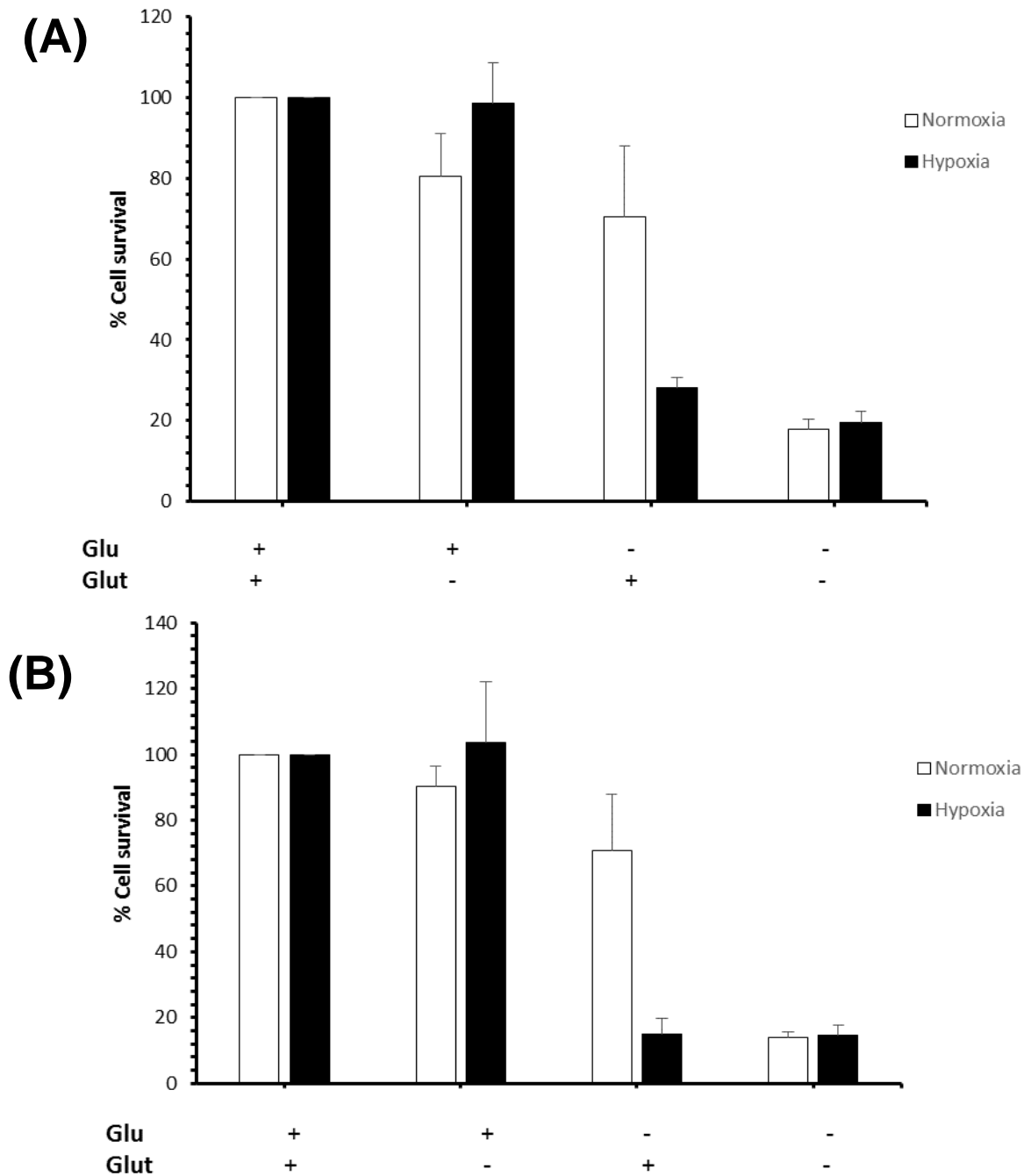


Figure 4.22 Influence of glucose and L-glutamine concentration on cell survival. Panel A represent the survival of HCT116 p53^{+/+} cells after 96 hours with 20 mM glucose (Glu +), without (Glu -) glucose, with 2mM L-glutamine (+ Glut) or without glutamine (- Glut). Panel B represent the same set of experimental conditions using the HCT116 p53^{-/-} cell line.

4.3.10 Influence of glucose and glutamine on cell sensitivity to the glutaminase inhibitor 968.

The results presented in figure 4.24 demonstrate that the glutaminase inhibitor compound 968 is significantly more cytotoxic in the absence of glucose compared to glucose rich conditions. This was observed in both the HCT116 p53^{+/+} and HCT116 p53^{-/-} cells. The results suggest that in the presence of glucose, these cells can better tolerate inhibition of glutamine metabolism which is consistent with the results of Fig. 4.23 and effects of glutamine deprivation. It was also noted that the HCT116 p53^{-/-} cells were more sensitive to glutaminase inhibitor indicating p53-dependent effects.

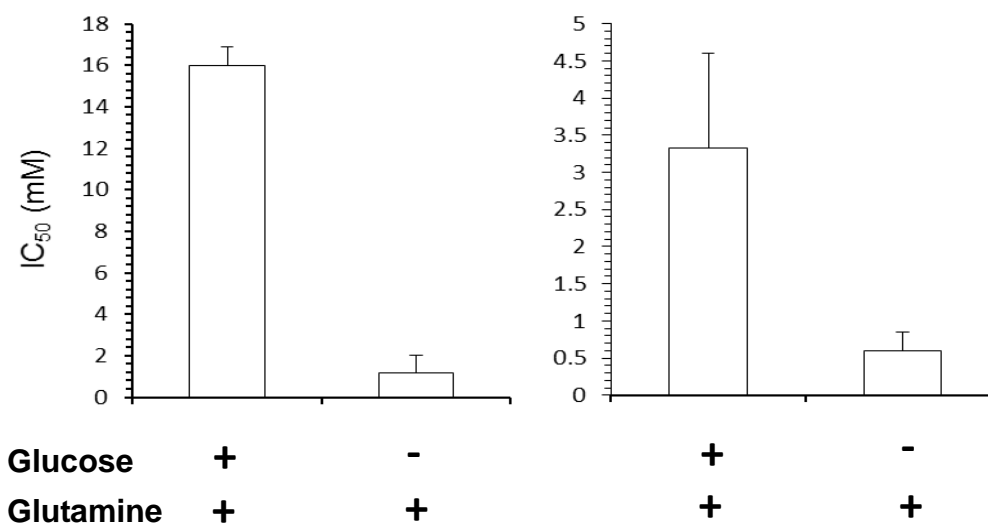


Figure 4.23 Response of HCT116 p53^{+/+} (left hand panel) and HCT116 p53^{-/-} (right hand panel) cells to glutaminase inhibitor 968 under aerobic conditions in the presence and absence of glucose. The results represent the mean \pm standard deviation for three independent experiments. Drug exposures were continuous 96 hour exposures and cell survival was determined using the MTT assay.

Cytotoxicity response of HCT116 p53^{+/+} and HCT116 p53^{-/-} cell lines to 968 in high glucose medium following 96 hours exposure under aerobic and hypoxic conditions is represented in figure 4.25 and figure 4.26. In aerobic conditions results showed that cells are not very sensitive to 968 (with IC₅₀ >30μM). In hypoxic conditions HCT116 p53^{+/+} and HCT116 p53^{-/-} cell lines were very sensitive to 968 with IC₅₀ values of 4.97 ± 1.65 μM and 8.6 ± 1.16 μM respectively (Fig. 4.26). In addition, the cytotoxicity response of HCT116 p53^{+/+} and HCT116 p53^{-/-} cell lines to 968 in glucose free medium following 96 hours exposure under aerobic conditions is shown in figure 4.25C and 4.25D. Cells were very sensitive to 968 with IC₅₀ values of 1.19 ± 0.84 μM and 0.60 ± 0.25 μM respectively.

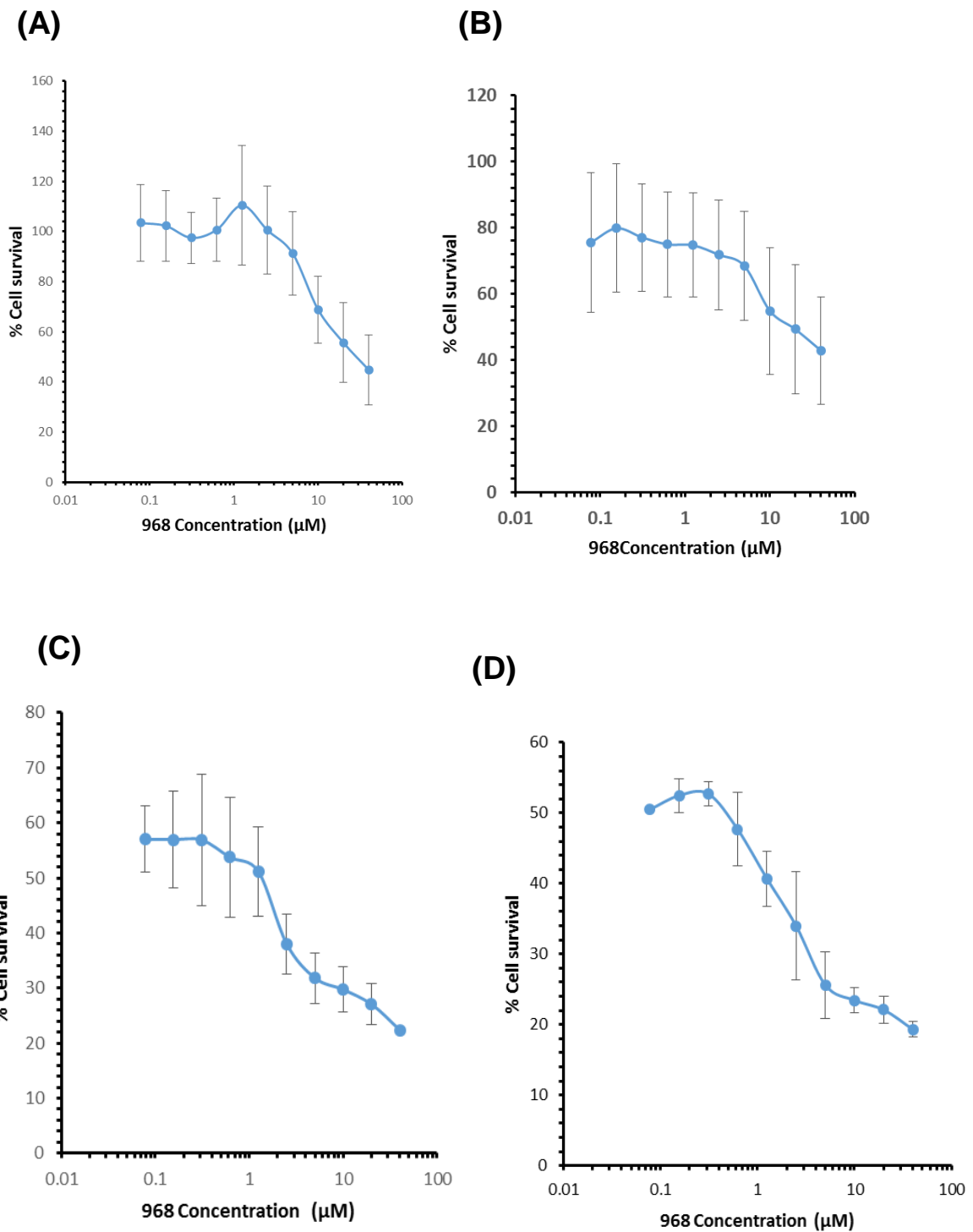
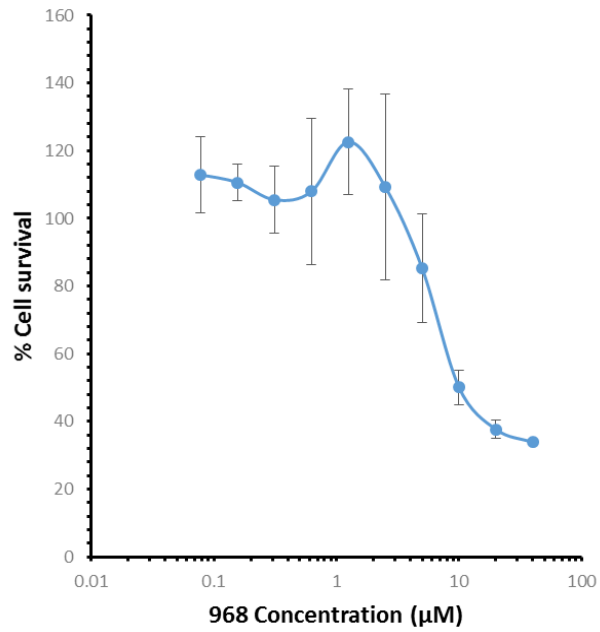


Figure 4.24 Response of HCT116 p53^{+/+} and HCT116 p53^{-/-} to 968 (96-hours exposure) in high glucose DMEM (panels A and B) and free glucose DMEM (panel C and D) media. These experiments were conducted under both aerobic and hypoxic condition and each value represents the mean ± standard deviation for three independent experiments.

(A)



(B)

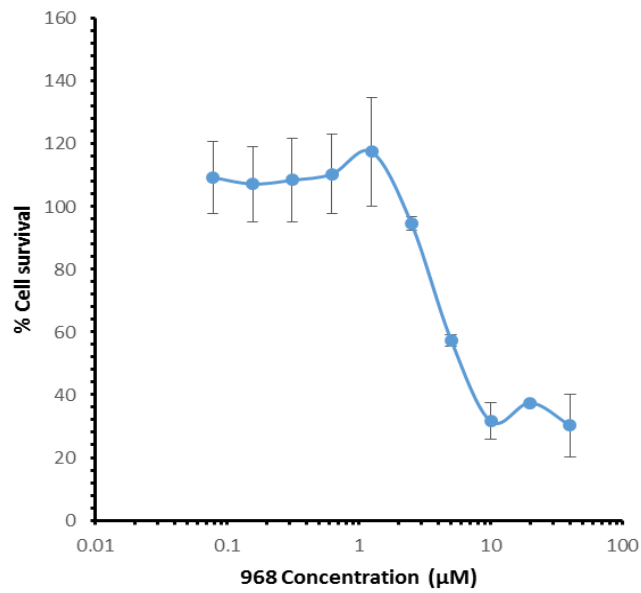


Figure 4.25 Response to 968 in high glucose DMEM (panels A HCT116 p53^{+/+} and panel B HCT116 p53^{-/-} following 96-hours exposure under hypoxic condition. These experiments were conducted under both aerobic and hypoxic conditions and each value represents the mean \pm standard deviation for three independent experiments.

4.3.11 The influence of glucose deprivation on cell viability and the cell cycle of HCT116p53^{+/+} and HCT116p53^{-/-} cells cultured under hypoxic conditions.

Cell viability and cell cycle

High glucose and glucose free medium was tested for effects of glucose deprivation for 96h on the cell cycle of HCT116 p53^{+/+} and HCT116 p53^{-/-} cells under hypoxic conditions alongside assessment of effects on cell viability (figure 4.27A and figure 4.28 B and C). For HCT116 p53^{-/-} cells (Figure 4.27B and Figure 4.29B and C), culture in glucose free medium caused an increase in sub G1 levels to ~50% of the total cell population consistent with effects observed on cell survival by chemosensitivity testing. Concomitant with this, the % of G1 phase cells decreased from ~50% to ~20%. For HCT116 p53^{+/+} cells (Figure 4.27A), culture in glucose free medium caused an increase in sub G1 to ~60% of the total cell population and a concomitant decrease in G1 phase and S-phase populations.

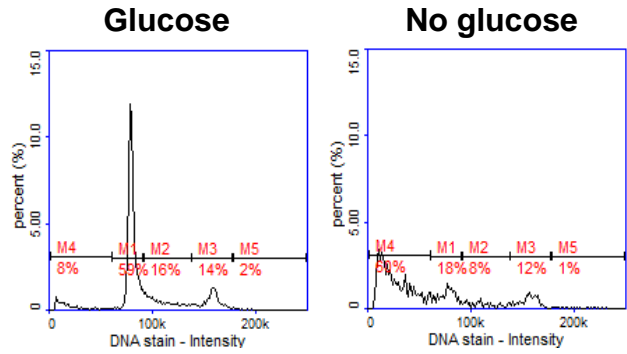
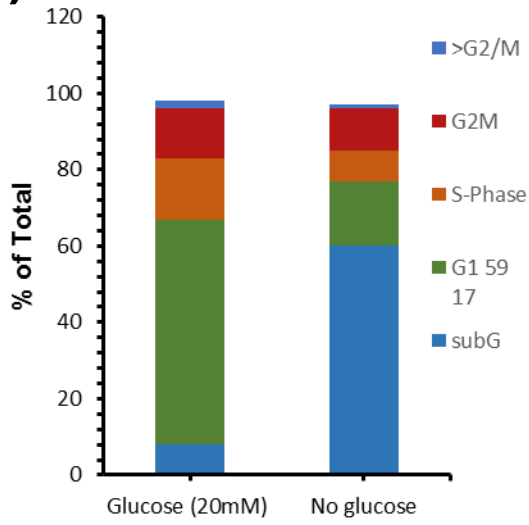
The effects of glucose deprivation on mitochondrial membrane potential, cell viability and total cell numbers are presented in figures 4.27 and 4.28. Incubation in glucose-free medium (96hour) was shown to decrease cell viability in HCT116 p53^{+/+} and HCT116 p53^{-/-} cells by 53% and 36% respectively. In addition, the mitochondrial membrane potential was measured as an indicator of early apoptosis and the results demonstrate that glucose deprivation under hypoxic conditions induces extensive membrane depolarisation. These results are consistent with the decrease in cell number and cell viability described above (figures 4.27 and 4.28).

4.3.12 Assessment of glucose-free complete media for trace levels of glucose

Glucose levels in cell culture media were measured by the Reflotron glucose assay.

Glucose levels in high glucose medium were 19.5mM. In purchased glucose free medium supplemented with FBS (10%), l-glutamine (2 mM) and sodium pyruvate (1 mM), basal glucose was detected at a concentration of 0.555 mM.

(A)



(B)

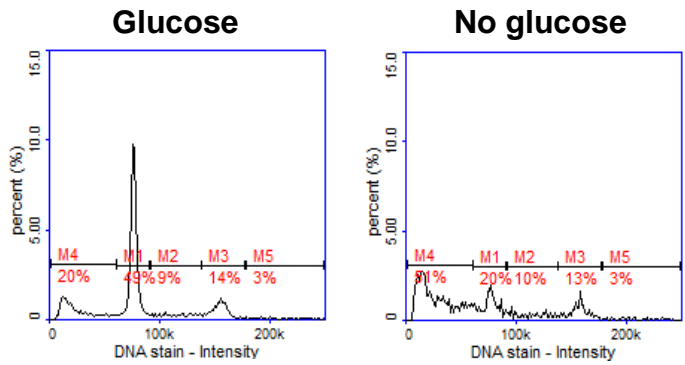
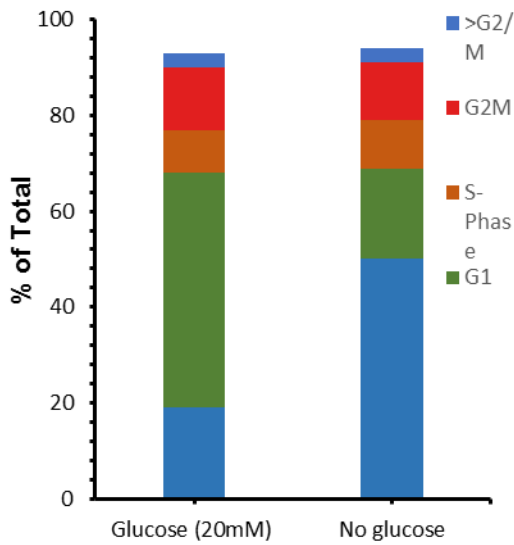
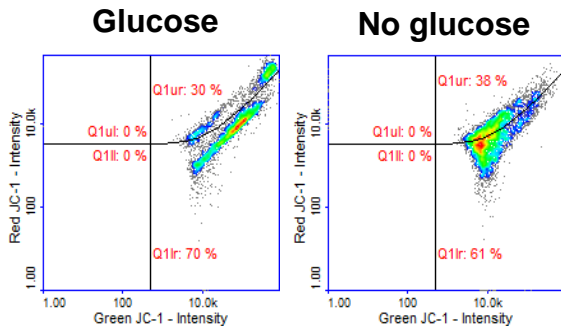
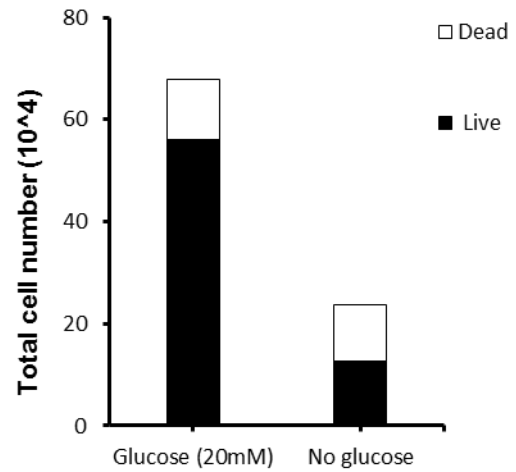


Figure 4.26 Cell Cycle analysis. Panel A HCT116 p53^{+/+} cells grown in 20mM glucose or free glucose medium for 96 hours under hypoxic conditions, Panel B HCT116 p53^{-/-} cells grown in 20mM glucose or free glucose medium for 96 hours under hypoxic conditions.

(A)



(B)



(C)

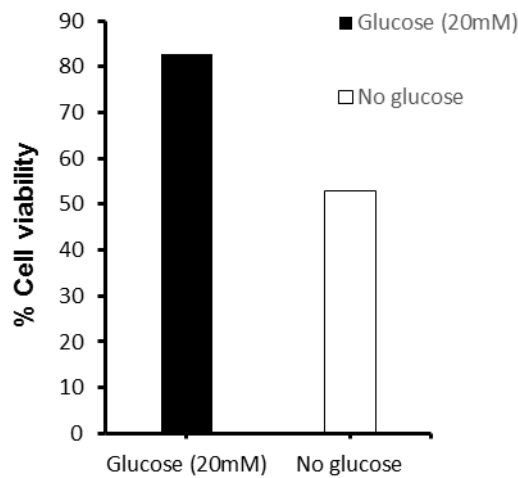


Figure 4.27 Cell viability, and determination of loss of mitochondrial membrane potential of HCT116 p53^{+/+} cells following 96 hours culture in high glucose or free glucose medium under hypoxic conditions. Panel A Quantification of mitochondrial membrane depolarisation using JC-1 stain. Panel B total number of dead and live cells and panel C percentage of cell viability under hypoxic condition.

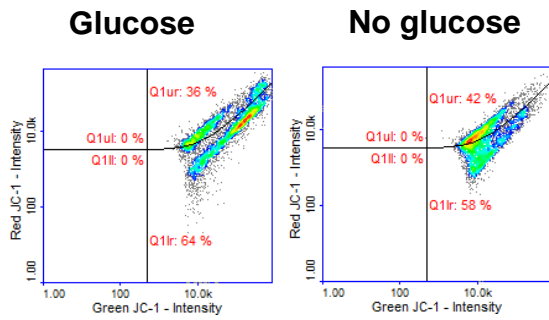
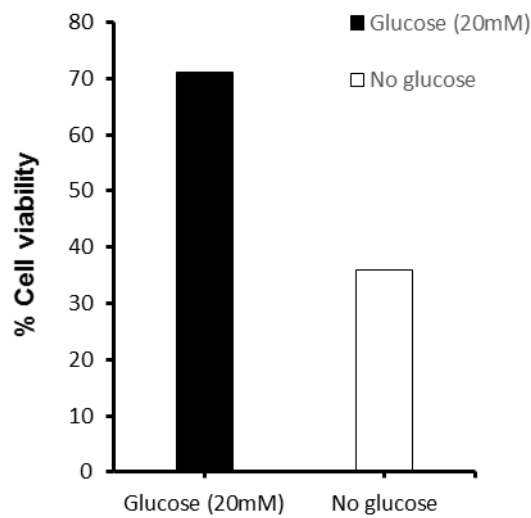
(A)**(B)****(C)**

Figure 4.28 Cell viability, and determination of loss of mitochondrial membrane potential of HCT116 p53^{-/-} cells following 96 hours culture in high glucose or free glucose medium under hypoxic conditions. Panel A Quantification of mitochondrial membrane depolarisation using JC-1 stain. Panel B total number of dead and live cells and panel C percentage of cell viability under hypoxic condition.

4.3.13 Assessment of MPI and PMM2 expression following growth of cells in mannose or glucose-containing medium under aerobic and hypoxic conditions.

Western blot analysis was performed to measure the expression of two key enzymes (MPI and PMM) involved in mannose metabolism which regulate whether or not mannose enters glycolysis or glycosylation pathways. The results are presented in figures 4.30 and 4.31. For MPI a band of 47kDa was expected. A band was observed around this size, however, lots of other non-specific bands were observed and without validation it is unclear whether the band at the correct size is actually MPI. Similarly, for the PMM2 (Figure 5.30 B), detection of a specific band at the correct size proven difficult with lots of non-specific bands observed. Attempts were made to reduce background by testing blocking the membrane with two different blocking buffers, 5% TBST-milk buffer (Figure 4.31 B) or LI-COR TBST buffer (Figure 31A and Figure 30). Further work has been done in terms of detection of MPI and PMM2 protein expression by using ECL technique. Using ECL detection, much clearer bands were obtained on the Western blot as illustrated in figure 4.32. The results must be regarded as preliminary (n=1) but they do demonstrate that levels of MPI and PMM2 change under different experimental conditions (eg. normoxia versus hypoxia and glucose vs mannose). Further studies are required to determine whether the ratio of MPI to PMM2 reproducibly changes under the indicated experimental conditions, however, the results demonstrate that ECL detection methods are superior to LI-COR detection for these antibodies.

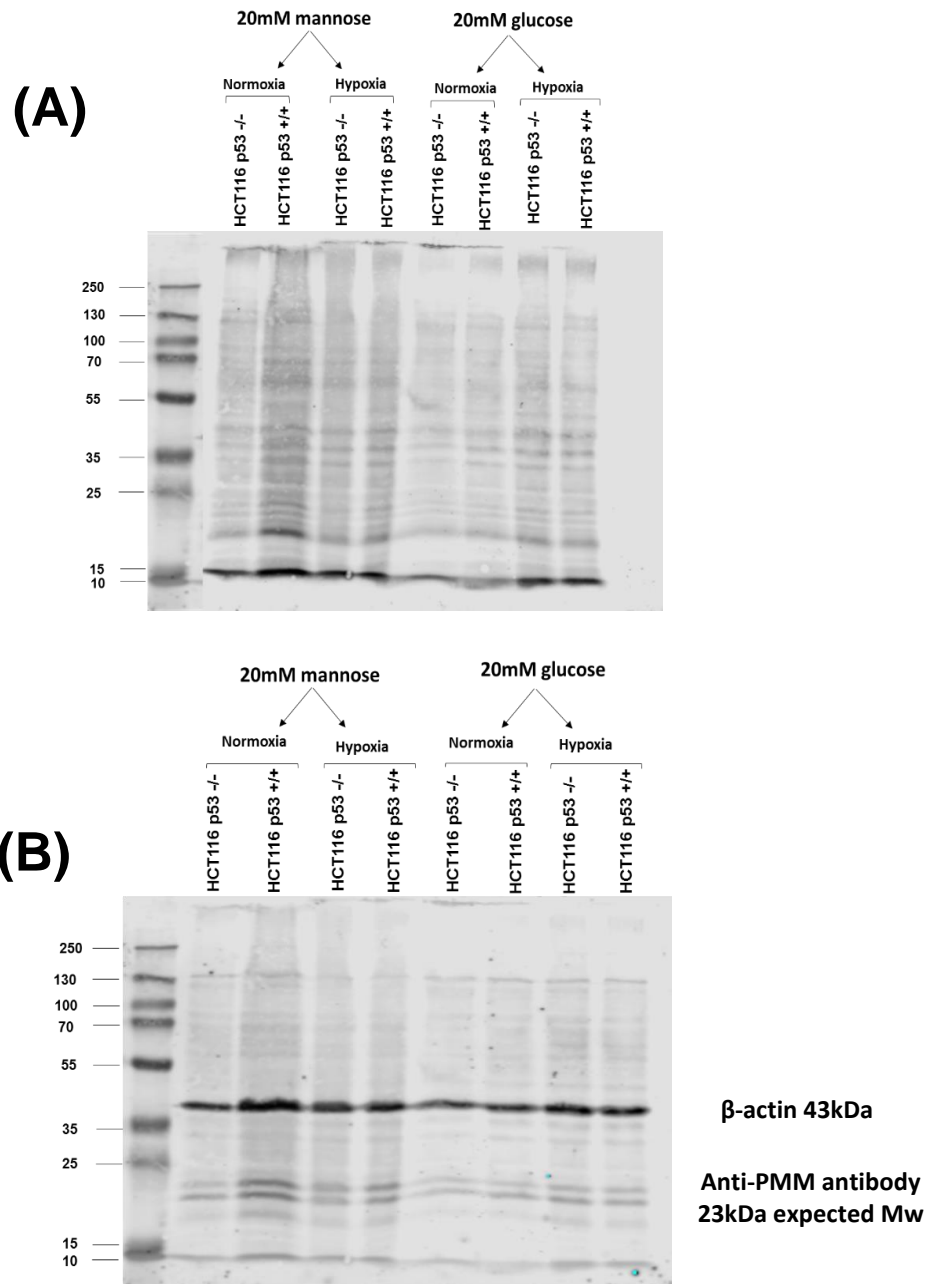


Figure 4.29 Western blot analysis of MPI in HCT116 p53^{-/-} and HCT116 p53^{+/+} cells grown in mannose media and glucose media (20Mm) under aerobic and hypoxic conditions for 96hours using LI-COR system.

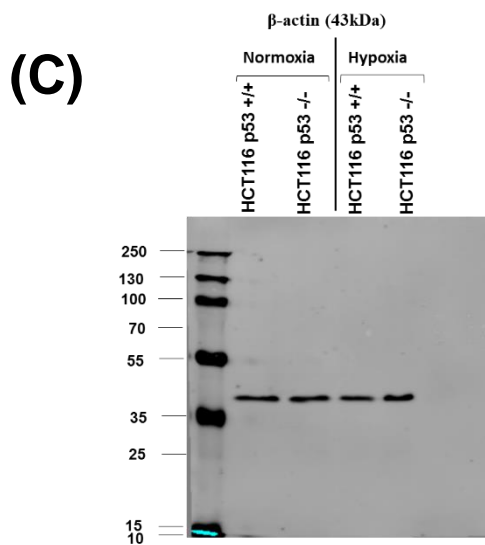
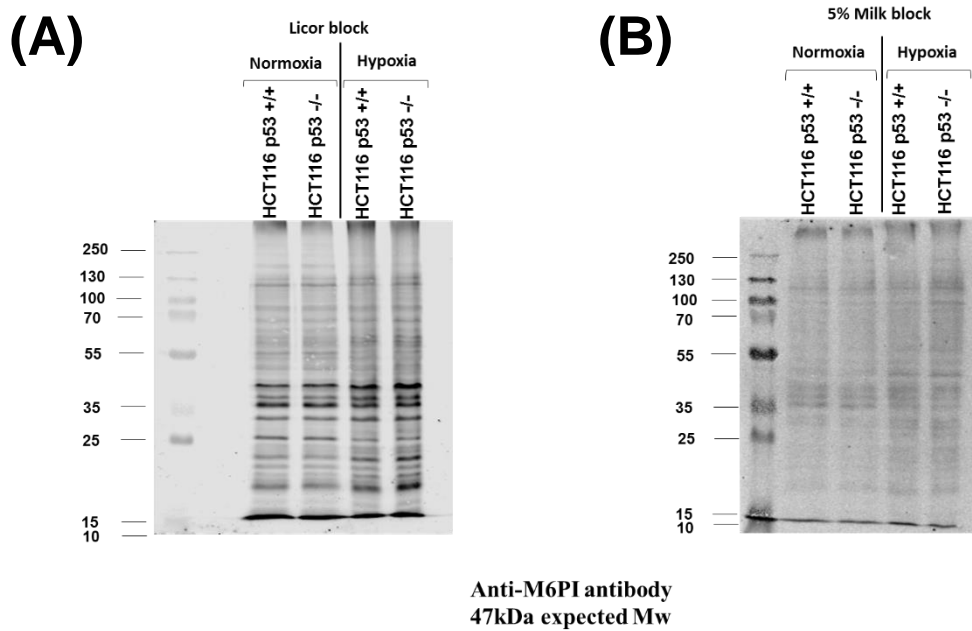


Figure 4.30 Western blot analysis of MPI in HCT116 p53^{-/-} and HCT116 p53^{+/+} cells was grown up with mannose media (20Mm) under hypoxic and aerobic condition for 96hours using LI-COR system.

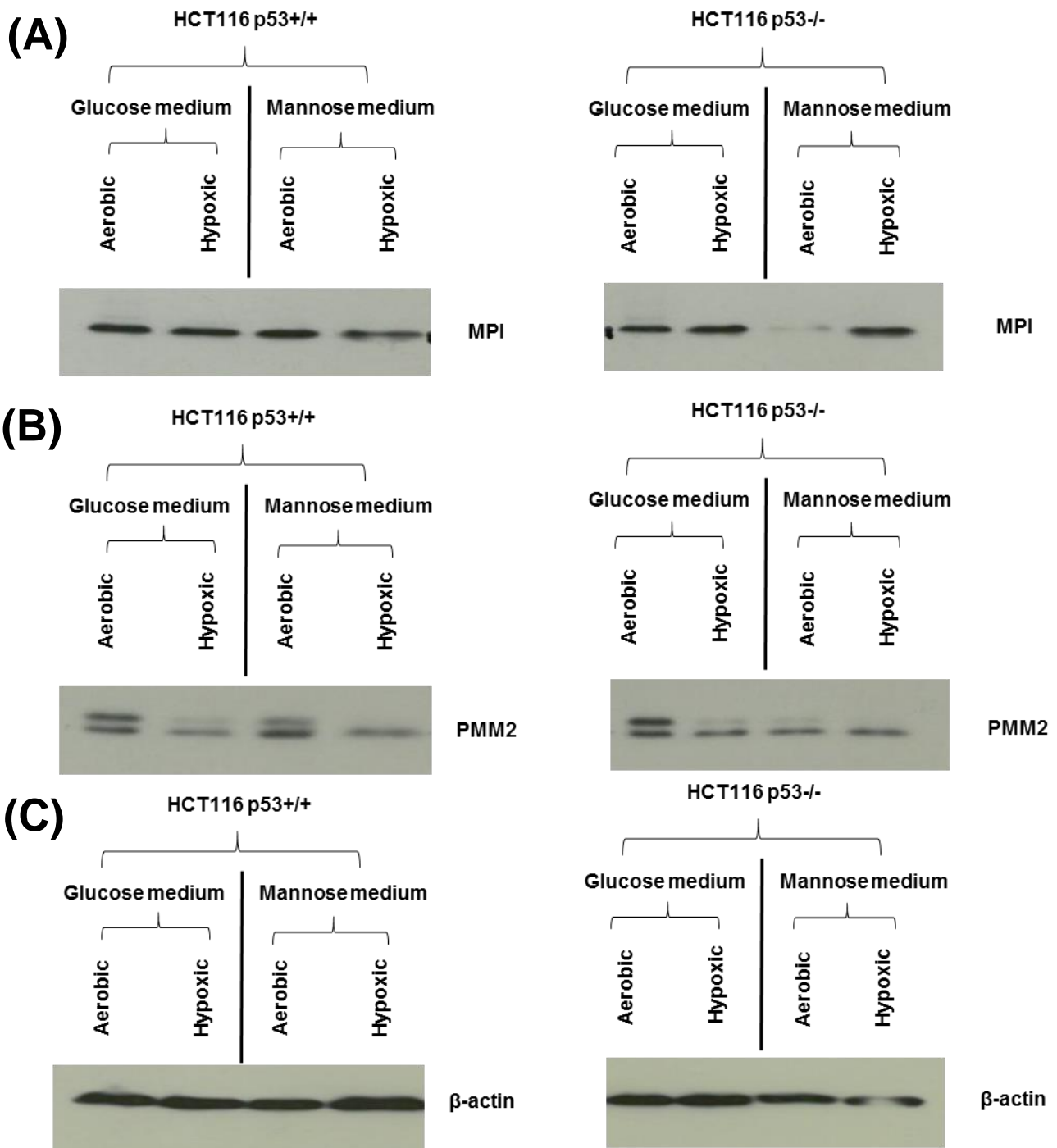


Figure 4.32 Western blot analysis of MPI (Panel A), PMM2 (Panel B) and β -actin (Panel C) in HCT116 p53^{-/-} and HCT116 p53^{+/+} cells grown in mannose or glucose media (20mM) under a hypoxic and aerobic condition for 96 hours; detection using ECL technique.

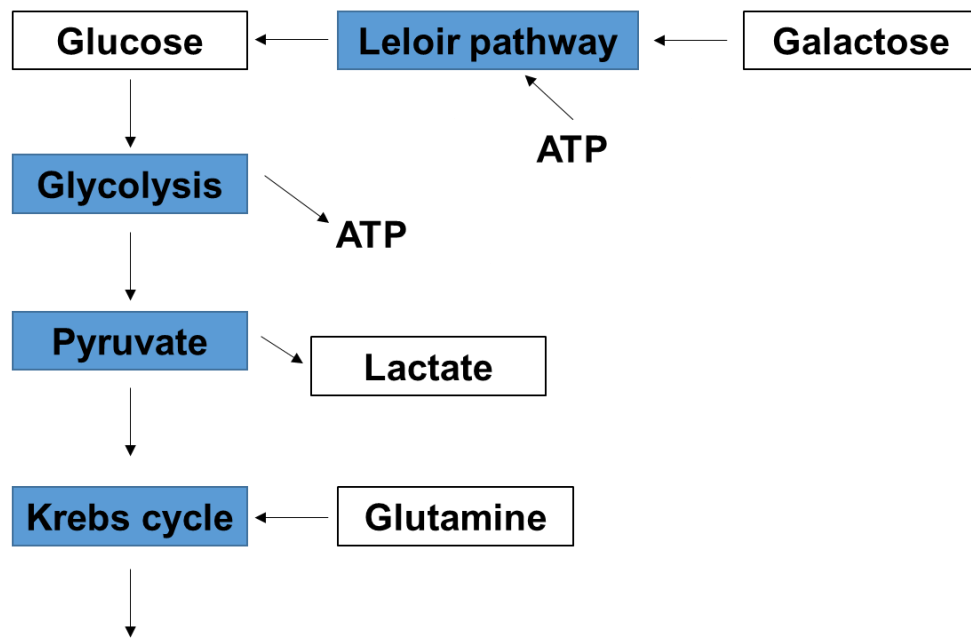
4.4 Discussion

This chapter assesses the influence of glucose deprivation on cancer cell lines under hypoxic and normoxic conditions and the ability of other carbon sources to substitute. There are a number of important and novel findings from this work. One key observation was the different dependency of normoxic and hypoxic cancer cells to glucose. For all six cancer cell lines tested, glucose deprivation had little effect on cell survival for cells grown under normoxic conditions. In contrast, hypoxic cancer cells showed a clear dependency on glucose for survival identifying a potential hypoxia-selective vulnerability that might be exploitable. A low proportion of the hypoxic cell population appeared to survive, however, recovery experiments indicated that these cells were unable to fully recover and proliferate. More in-depth analyses revealed that absence of glucose in the culture media under hypoxic conditions substantially increased the proportion of cells in subG1 and reduction in cell numbers and loss of cell viability was also evident by independent assays. This was supported by some studies that reported that glucose deprivation has shown apoptosis in colon carcinoma, which showed the cells are a glucose dependent (Caro-Maldonado et al., 2010). The data presented here suggests that cell death of tumour cells induced by glucose deprivation is influenced by oxygen tension. This was also confirmed in a study by Palorini, in which it was demonstrated that transformed cells in medium with low glucose concentration (1 mM) proliferated more slowly than in medium with high glucose content (25 mM) (Palorini et al., 2013) but importantly, they also demonstrated that this effect was more pronounced in oxygen deprived conditions. This is broadly supported by another study which shows

that glucose deprivation can induce apoptosis of cancer cells (Wise-Faberowski et al., 2001).

The lack of much effect of glucose deprivation under normoxic conditions led us to hypothesise that cells under normoxia may utilise glutamine as a source of carbon to generate energy and support cell growth. To test this hypothesis, glutamine deprivation and glutamine inhibition experiments (using a glutaminase inhibitor) were performed which showed that glutamine was necessary to support survival under normoxic conditions in the absence of glucose. In contrast, glutamine was unable to sustain hypoxic cells deprived of glucose. These results suggest that therapeutic strategies targeting glucose metabolism may be effective against hypoxic cells whereas for aerobic cancer cells dual targeting of both glucose and glutamine metabolism would be necessary.

Experiments were also performed to investigate whether other sugars could be effectively used by hypoxic cells in place of glucose to support growth and survival. Sucrose, galactose, fructose, mannose and also lactate as the end product of aerobic glycolysis were tested. Lactate, the disaccharide sucrose and the monosaccharide fructose were all unable to support survival of hypoxic cells in the absence of glucose. Kamel and his group have reported that the monosaccharide galactose can be converted to glucose through the Leloir pathway, but that this process also requires energy (figure 4.32) (Kamel et al., 2014). Galactose was able to modestly increase survival of aerobic cancer cells but had no beneficial effect on hypoxic cell survival in the absence of glucose which relate to this requiring ATP to fuel conversion of galactose to glucose. (figure 4.12 and figure 4.14).



ATP and reduced electron carriers

Figure 4.31 Summary of key metabolic pathways and how galactose and glucose interlink through the Leloir pathway (Kamel et al., 2014).

In contrast to the other sugars tested, interestingly the results showed that mannose is able to fully support the survival of hypoxic cancer cells in the absence of glucose. Normally however, mannose is understood to be metabolised by cells primarily to support glycosylation of proteins rather than as a fuel source. Protein glycosylation is an important post-translational modification of proteins which is the covalent addition of mannose and other sugar moieties to proteins. Importantly, alterations in glycosylation are commonly observed in many cancers and increased glycosylation of cell surface proteins has been linked with increased cancer cell motility and invasive potential. However, mannose can be converted to fructose 6 phosphate by the enzyme MPI providing an entry point for it to be used as a glycolytic fuel. (Alton

et al., 1998). Figure 4.33 summarises these different pathways of mannose metabolism, mannose first being converted to mannose 6 phosphate (M6P) by hexokinase. M6P may then either be metabolised to mannose 1 phosphate (glycosylation pathway, catalysed by PMM2) or into glycolysis by conversion to F6P through the action of MPI. Preliminary investigations were performed to assess expression levels of these two key enzymes regulating mannose metabolism, PMM2 and MPI, however, reliable detection by immunoblotting proved difficult. Nevertheless, the findings are very important and it is possible that in the context of the tumour microenvironment, in hypoxic cells mannose is diverted towards glycolysis. Based on the results presented here this may be very important for hypoxic cancer cell survival in glucose deprived conditions and is significant in the context of identifying new therapeutic approaches to target hypoxic cancer cells and also perhaps reducing their metastatic potential (Hakomori, 1989) .

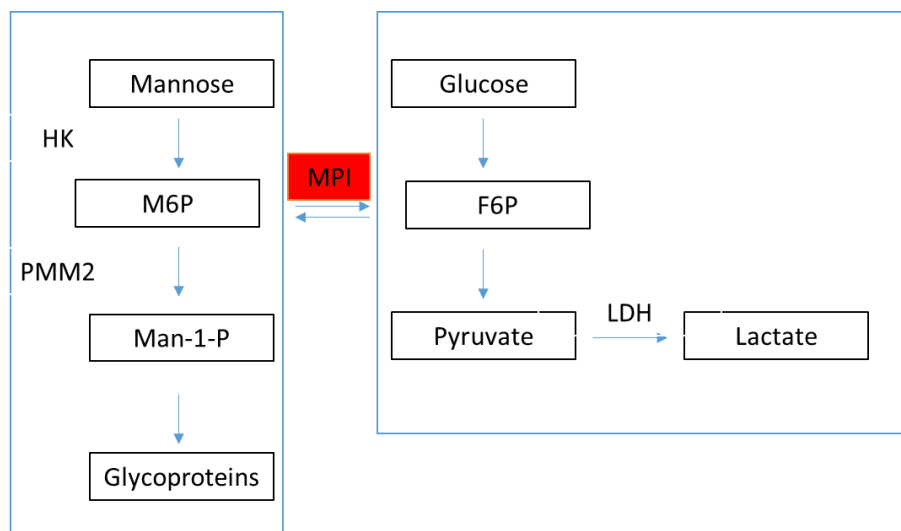


Figure 4.32 Schematic summarising mannose metabolism and regulation of mannose utilisation for glycosylation or as a fuel for glycolysis by the respective activities of PMM2 and MPI.

Chapter 5

Inhibition of glycolytic enzymes by silver complexes.

5.1 Introduction

The results presented in chapters 3 and 4 demonstrate that whilst cancer cells require glucose to survive under hypoxic conditions, current glycolytic inhibitors (eg. Sodium oxamate and Gossypol) do not significantly kill cancer cells under hypoxia. As these inhibitors can have non-specific effects on cells and work via similar mechanisms of action, other inhibitors of the glycolytic pathway may be more effective. The purpose of this chapter is to explore the effects of novel organometallic complex on glycolytic enzymes based upon previous studies in this laboratory demonstrating that they inhibit glycolysis.

In a recent study by Allison et al (2017), a silver N-heterocyclic carbene (NHC) complex called Ag8 was shown to inhibit glycolysis in cell lines. The inhibition of glycolysis was determined by measurement of glycolytic rate using a XF96 metabolic analyser (seahorse Biosciences) in collaboration with colleagues at the University of Manchester and these studies demonstrated that Ag8 selectively reduced glycolysis and glycolytic reserve in a dose and time dependent manner in A2780 and OVCAR3 cancer cells compared to non-cancer ARPE-19 cells. Whilst the ability of Ag8 to inhibit glycolysis is clear, it is not known where in the glycolytic pathway that the pharmacological inhibition occurs. Metal NHC complexes are of interest as potential inhibitors of glycolytic enzymes including lactate dehydrogenase (Rubbiani et al., 2010). The major aim of this chapter was to determine whether or not Ag8 and other silver-based complexes inhibit lactate dehydrogenase and other glycolytic enzymes

(hexokinase) in cell-free and cell-based assays.

5.2 Materials and Methods

5.2.1 Compounds

A series of silver complexes were obtained from Dr Charlotte Willans (University of Leeds), details of which are presented in figure 5.1. The chemical synthesis of these compounds has been described elsewhere together with initial preclinical evaluation against a panel of cell lines *in vitro* (Allison et al., 2017).

5.2.2 Inhibition of purified Rabbit muscle LDH.

Purified L-lactate dehydrogenase from rabbit muscle was obtained from Sigma Aldrich (Poole, Dorset UK; L5132). All compounds were dissolved in DMSO at 100mM, aliquoted and stored at -20C until required. LDH-A activity was determined by measuring the oxidation of NADH at 340nm as described in detail elsewhere (Song and Mechref). Briefly, each reaction consisted of NADH (100 μ M), Sodium Pyruvate (600 μ M), purified LDH (0.35 μ g), solvent control (0.1% DMSO) or test compound (100 μ M) in a total volume of 1ml Tris-HCl buffer (200mM, pH7.3). The reaction was started by the addition of NADH and the rate of change of absorbance ($\Delta A/\text{min}$) was determined at 340nm using a Cary 60 UV-Vis spectrophotometer over a 1 min period. Specific enzyme activity was determined using a molar extinction coefficient for NADH of $6.22 \text{ mM}^{-1}\text{cm}^{-1}$. Each reaction was performed in triplicate and percentage inhibition was calculated as $1 - (\text{specific activity of treated LDH} / \text{specific activity of control LDH}) \times 100$.

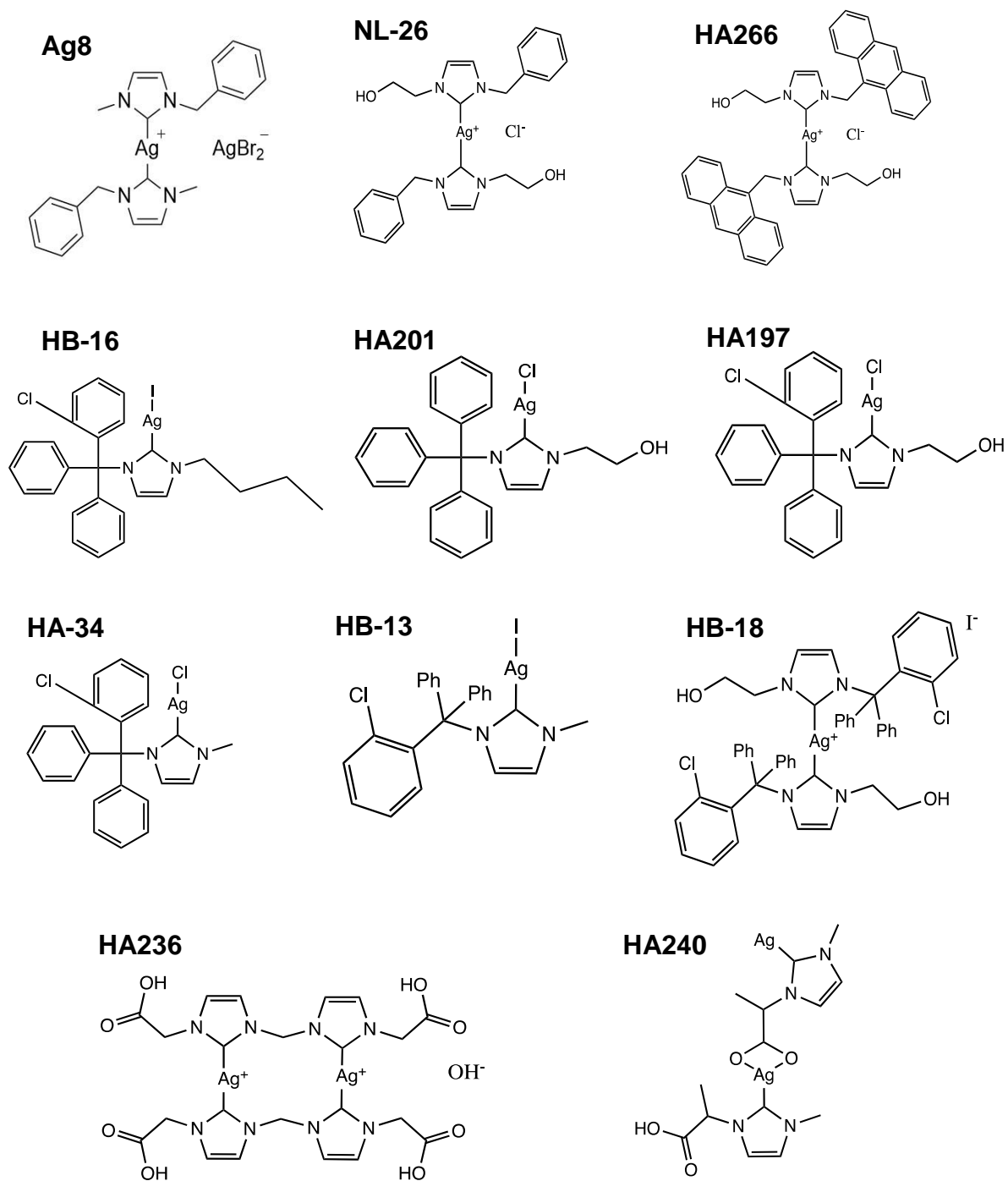


Figure 5.1 Chemical structures of silver complexes evaluated as inhibitors of glycolytic enzymes.

5.2.3 Analysis of LDH-A and LDH-B activity in a panel of cell lines.

Analysis of LDH activity was determined in a panel of cell lines consisting of: HCT116 p53^{+/+}, HCT116 p53^{-/-}, HT-29, DLD1, PSN10.05, BE and ARPE-19. Cells at approximately 80% confluence were harvested by trypsinisation, washed twice in PBS before being re-suspended in Tris-HCl (0.2M, pH7.3). Cells were sonicated (Sonics and Material Vibro-cell VCX130 set at 50% amplitude for 3 x 30s bursts on ice) and cell lysates were used immediately for enzyme assays

For LDH-A assays, each reaction contained 0.132 mM NADH, 0.6 mM Sodium Pyruvate and cell lysate (10µl) in a final reaction volume of 1 ml Tris-HCl (0.2M, pH7.3). The oxidation of NADH was determined over a 1 min reaction period at 340nm using a Cary 60 UV-Vis spectrophotometer (Agilent Technologies).

For LDH-B assays, each reaction contained 60mM sodium lactate, 0.132 mM sodium lactate and cell lysate (50 µl) in a final volume of 1 ml Tris-HCl (0.2M, pH7.3). The reduction of NAD was determined over a 1 min reaction period at 340nm using a Cary 60 UV-Vis spectrophotometer as above.

In both cases, background rates of reaction were determined by omitting sodium pyruvate (for LDH-A) or sodium lactate (for LDH-B) from the reaction. Background rates were subtracted from full reaction rates to obtain true $\Delta A/\text{min}$ values. Protein concentration was determined using the Pierce BCA assay (described below) and specific activity ($\mu\text{mol}/\text{min}/\text{mg}$) was determined using the equation:

$$\text{Specific activity} = \Delta A/\text{min} / (\epsilon \times P)$$

Where $\Delta A/\text{min}$ is the rate of change of absorbance at 340nm, ϵ = molar extinction

coefficient for NADH ($6.220 \text{ mM}^{-1}\text{cm}^{-1}$) and P = total amount of protein in the cuvette.

5.2.4 Determination of protein concentration using the Pierce BCA assay

Protein concentrations in cell lysates were determined using the Pierce BCA assay (Thermo Fisher Scientific) according to manufacturer's instructions. Briefly, cell lysates or BSA standards (2 mg/ml to 0.2 mg/ml) were added to a 96-well flat-bottomed plate (10 μ l per well, 4 wells per sample/standard). To this, 200 μ l of BCA reagent (1:50 mix of reagent B to reagent A) was added and following mixing, the plate was incubated at 37C for 30 min prior to reading the absorbance at 540nm in a Magnellan Tecan F50 spectrophotometer. A calibration curve was generated and the concentration of protein in unknown samples determined by reference to the calibration curve. If the absorbance of the samples exceeded the absorbance in the highest BSA standard used, the sample was diluted so that absorbance values within the calibration curve were obtained.

5.2.5 Western blot analysis of LDH-A and LDH-B protein expression in a panel of cell lines.

Cells at approximately 80% confluence were harvested by trypsinisation, washed twice in PBS before the addition of RIPA buffer (965 μ l RIPA buffer plus 10 μ l phosphatase inhibitor and 25 μ l protease inhibitor). Cells were lysed on ice for 10 min following which they were sonicated for 3 x 30s at 50% amplitude as described above. The cell lysates were then stored at -20C until required.

Samples 30 μ g were loaded onto SDS-PAGE gels (4% stacking and 15% separating gels) in Laemmli buffer and separated at 120V for approximately one hour (or until

the bromophenol blue dye had reached the bottom of the gel). The apparatus used was the mini-PROTEAN II electrophoresis system (Biorad).

Following separation, proteins were transferred to nitrocellulose using the mini-transblot apparatus (Biorad). Briefly, the separating gel was soaked in transfer buffer (200ml 10X transfer buffer [30g Tris base and 144g glycine in 1L dH₂O], 400ml methanol, 20ml 10% ultrapure SDS and dH₂O to a final volume of 2L) together with nitrocellulose paper, blotting paper and absorbent pads for 10min. The transfer 'sandwich' was constructed according to manufacturer's instructions and run at 35mA for 2 hours.

Following transfer, the nitrocellulose paper was washed in TBS-T (TBS plus 0.1% Tween 20). The membrane was then blocked overnight with TBS-T plus 5% Marvel. Following blocking, LDH antibody (rabbit monoclonal antibody, ab134187) was added at 1:1000 dilution to TBS-T and 5% Marvel and the nitrocellulose membrane incubated overnight in the fridge under constant agitation. The blot was washed 3 x in TBS-T for 5 min each wash before the secondary antibody was added (anti-rabbit-HRP conjugated antibody from Dako). Following a one-hour incubation at room temperature, the blot was washed 3 x in TBS-T before chemiluminescent detection was performed using ECL (Amersham). Separate blots were also probed for β -actin using a primary rabbit monoclonal antibody from Chemicon International (MAB1510). The procedures were identical to above with the exception that the primary antibody was used at a concentration of 1:40,000.

5.2.6 Inhibition of LDH-A and LDH-B in cell lysates.

Ag8 was dissolved in DMSO at 10mM and diluted to generate a range of drug concentrations ranging from 0.085mM to 10mM. Reaction conditions were as described above (5.2.3) and to each reaction 1µl of Ag8 was added prior to the addition of NAD(H). The final DMSO concentration therefore was 0.1% v/v in all cases including the control. Specific enzyme activities were calculated as describe above and each reaction was repeated in triplicate (per experiment) and a total of three independent experiments were performed.

5.2.7 Release of lactate from cell cultures.

The release of lactate from HCT116 p53^{+/+} and HCT116 p53^{-/-} cells was determined enzymatically based upon the conversion of lactate to pyruvate by lactate dehydrogenase. Cells were placed in either T25 or T75 flasks and grown to various levels of confluence to determine the best conditions to measure lactate release. In all cases, culture media was removed at various times following the addition of fresh culture medium and this was centrifuged at 13,000 rpm for 30s to remove any cells that may have been in suspension. Each reaction consisted of 0.5 ml of culture media and 0.5ml of a hydrazine buffer (60.5g Tris base, 2.92g EDTA and 6.5g hydrazine dissolved in 500ml of dH₂O and pH adjusted to 9.8) containing L-Lactate dehydrogenase and NAD. The reaction was monitored at 340nm over a one min reaction time and the rate of change of absorbance determined using a Cary 60 UV-Vis spectrophotometer. A calibration curve was generated using culture media supplemented with L-lactate (0.195 to 100mM).

To determine whether Ag8 inhibited the release of lactate from cells, cells were treated with Ag8 at 5 μ M and 10 μ M and lactate release was monitored at various time points up to a maximum of 24hours. The concentration of lactate in the media was determined using the calibration curve and each experiment was performed in triplicate.

5.2.8 Analysis of the effect of Ag8 on NAD(H) and NAD/NADH ratios.

Analysis of NAD(H) in cells was conducted using the assay described by Allison et al (2014). Briefly, HCT116 p53^{+/+} and HCT116 p53^{-/-} cells were seeded into T75 flasks at 1.5 x 10⁶ cells per flask and incubated at 37°C for 4 days prior to treatment with Ag8. Cells were treated with Ag8 (various concentrations as defined in the results section) and cells were harvested at various time points by first washing the monolayer twice with PBS followed by the addition of 1 ml of extraction buffer (20mM Sodium Bicarbonate, 100mM Sodium Carbonate, 10mM Nicotinamide and 0.05% Triton-X-100). The extraction buffer was swirled around the flask until all cells had lysed and a 'jelly like' lysate had formed. The lysate was transferred to Universal tubes and sonicated on ice as described previously (see section 5.2.3).

The lysate was separated into two vials, one of which was heated at 60°C for 30min to degrade NAD. The other vial was kept on ice. Each 1ml reaction consisted of 0.830ml Cycling buffer (100mM Tris HCL (pH.8.0), 5mM EDTA and 0.5mM MTT), 10 μ l Alcohol Dehydrogenase (20mg/ml), 10 μ l PES (200mM) and 50 μ l of sample or standard (NAD or NADH). The reaction started by adding 100 μ l of 6M ethanol to the cuvette and the absorbance was read at 570nm for 30 seconds using a Cary UV-Vis spectrophotometer. The assay was repeated three times for each sample or

standard.

A calibration curve using either NAD or NADH (100 μ M to 0.78 μ M) was generated using the procedure above. Using this calibration curve, the unheated sample provides the total NAD(H) in the sample and the heated sample directly measures the concentration of NADH in the sample. The difference between the two is the concentration of NAD. The values for NAD(H), NAD and NADH were normalized relative to protein concentration which was determined using the Pierce BCA assay as described above (see section 5.2.4).

5.2.9 Inhibition of hexokinase by silver complexes

The ability of silver complexes to inhibit yeast (*Saccharomyces cerevisiae*) hexokinase was determined using a coupled reaction as described below:



Each reaction consisted of NADP (14mM), ATP (19mM), G6PDH (Glucose 6 phosphate dehydrogenase, 125 units), d-glucose (555mM) and purified hexokinase (4 units) in a total volume of 1ml triethanolamine buffer (50mM, pH 7.6). The reaction was started by the addition of hexokinase and the formation of NADPH was

monitored at 340nm over a period of 1 min. All silver compounds were dissolved in DMSO at 100mM and the final concentration of each compound in the reaction was 100µM.

5.3 Results

5.3.1 Inhibition of purified rabbit lactate dehydrogenase.

The ability of silver complexes and cisplatin to inhibit purified rabbit lactate dehydrogenase is presented in figure 5.2. Cisplatin was used in order to compare the activity of novel silver complexes with an established anti-cancer drug that is approved for use in humans but which is not reported to inhibit LDH. At a concentration of 100 µM, HB13, HA236, HA201 and cisplatin had minimal effects on the activity of rabbit LDH. In contrast, HA266, NL26 and Ag8 completely inhibited rabbit LDH in this cell free assay. The other compounds also inhibited rabbit LDH but inhibition was partial, particularly in the case of HB 34, HB18 and HA197.

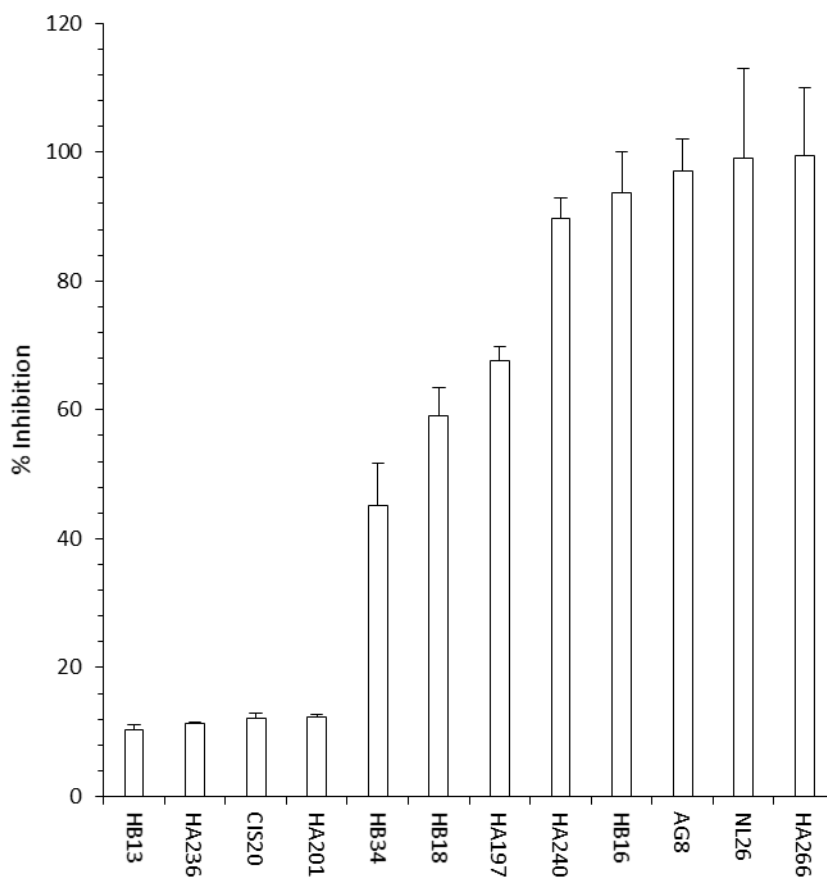


Figure 5.2 Inhibition of purified rabbit muscle lactate dehydrogenase by a series of silver complexes and cisplatin (CIS20). The concentration of each compound in this initial test was 100 μ M and each value represents the mean \pm standard deviation for three independent experiments.

5.3.2 Specific activity of LDH-A and LDH-B in a panel of cell lines

The specific activity of LDH-A and LDH-B in a panel of cell lines is presented in figure 5.3. In all cases, the activity of LDH-A was significantly higher than LDH-B. Whilst LDH-B activity was highest in the non-cancer ARPE-19 cell line, LDH-A activity was surprisingly high in this cell line.

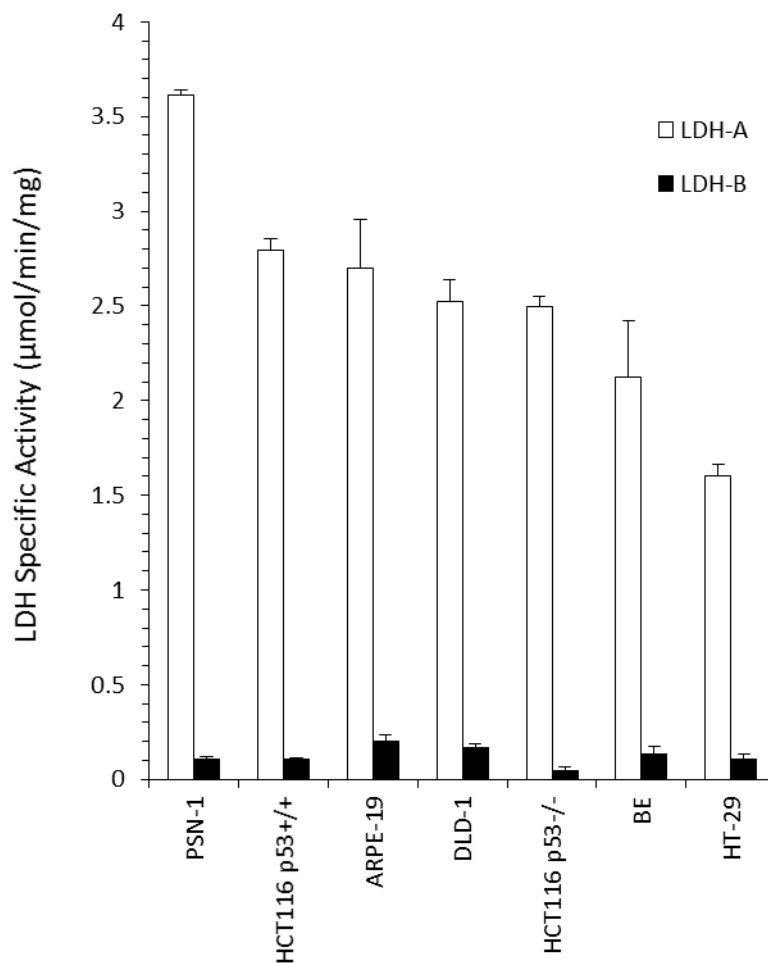


Figure 5.3 Specific activities of LDH-A and LDH-B in a panel of cell lines. Each value represents the mean \pm standard deviation for three independent experiments.

5.3.3 Protein expression of LDH-A and LDH-B in a panel of cell lines

The results of western blot analysis of LDHA and LDH-B in a panel of cell lines is presented in figure 5.4. These results are preliminary and only one run of the experiments was possible due to time constraints. Nevertheless, the results demonstrate that both LDH-A and LDH-B were detectable in HCT116 p53^{+/+},

HCT116 p53^{-/-}, HT-29, DLD-1, BE and ARPE-19 cells. No LDH-B was visible in PSN10.05 cells. LDH-A levels varied across the panel of cells however there were more marked variations in LDH-B intensity with strong bands present in HCT116 and DLD1 cells and low levels in BE and PSN10.05 cells. Protein loading as indicated by β -actin staining was equivalent for all cell lines.

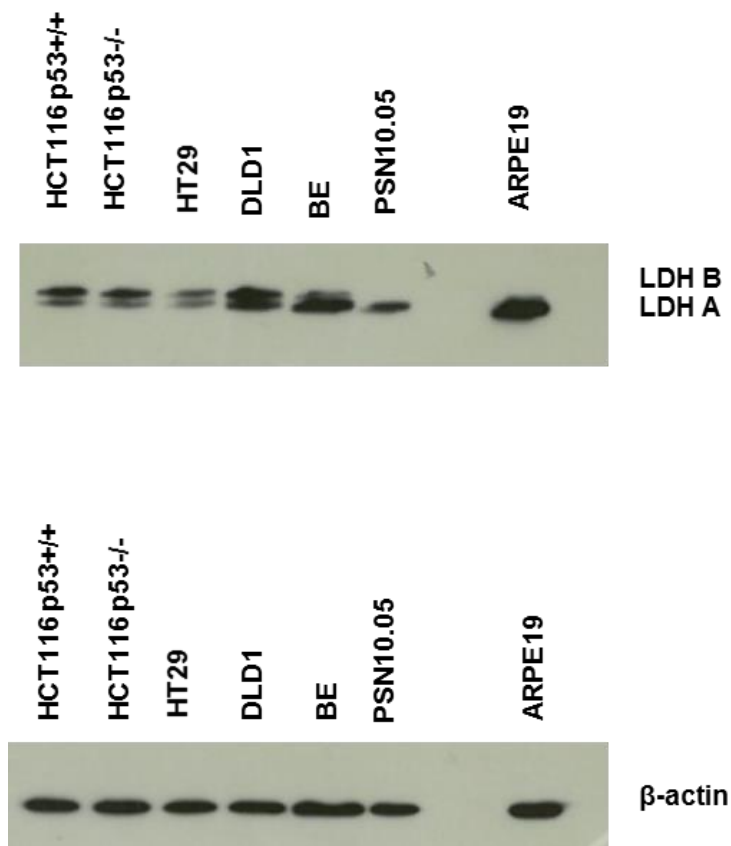


Figure 5.4 Preliminary western blot analysis of LDH-A and LDH-B in a panel of cell lines (n=1).

5.3.4 Inhibition of LDHA and LDH-B in cell lysates.

The ability of Ag8 to inhibit human LDH derived from BE cell lysates is presented in figure 5.5. Whilst Ag8 does partially inhibit LDH-B at 10 μ M, Ag8 preferentially inhibits LDH-A with significant inhibition at 5 μ M compared to no inhibition of LDH-B at the same dose. Ag8 is therefore a selective inhibitor of LDH-A compared to LDH-B with IC50 values of 1.82 μ M and >10 μ M respectively.

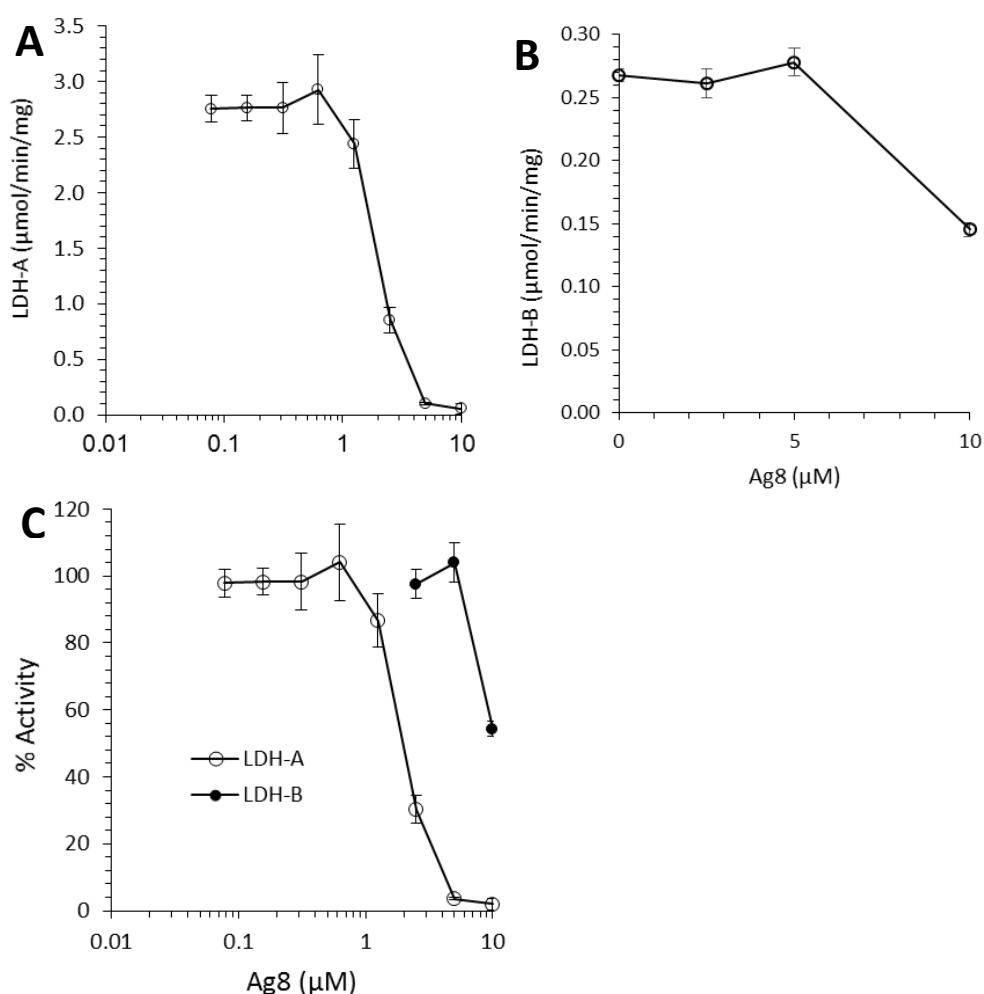


Figure 5.5 Inhibition of LDH-A (A) and LDH-B (B) and percentage activity remaining (C) in cell lysates from BE cells treated with Ag8. Each value represents the mean \pm standard deviation from three independent experiments.

5.3.5 Release of lactate from cells in culture.

The calibration curve using media spiked with various concentrations of sodium lactate is presented in figure 5.6. The results demonstrate that the regression analysis does not go through zero and at higher concentrations of lactate, the data points for a distinct curve. Regression analysis is not suitable for this data and concentrations of lactate were read manually off the calibration curve

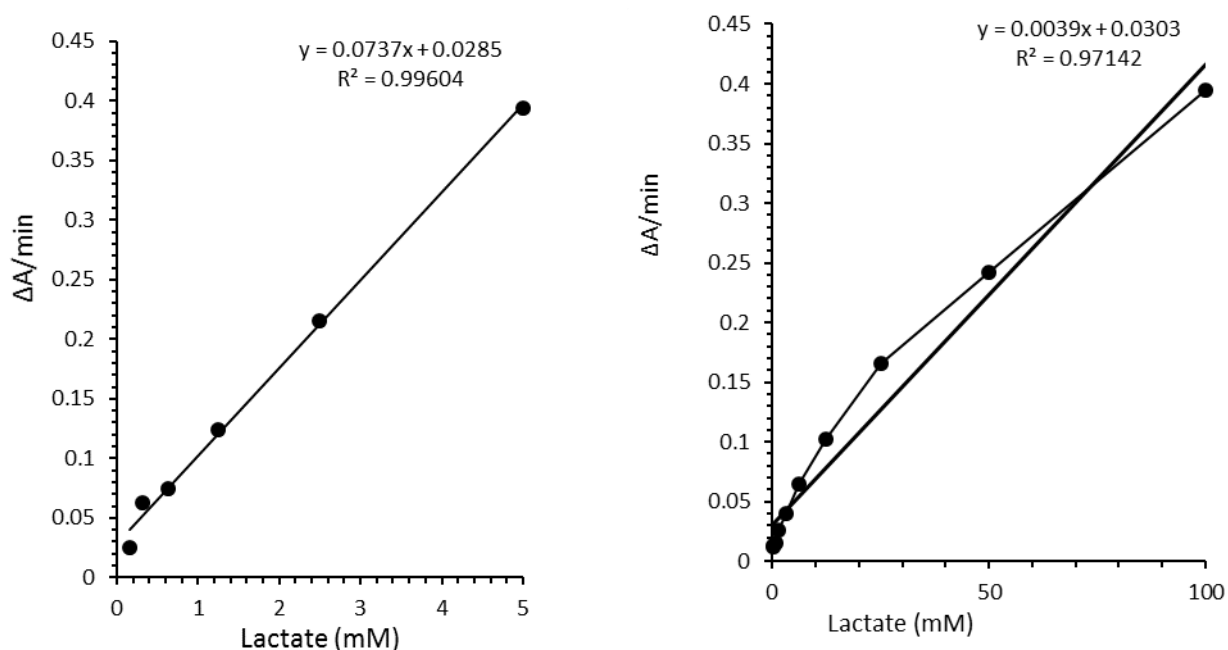


Figure 5.6 Lactate calibration curves using a narrow and broad range of lactate concentrations (left and right hand panels respectively). The straight lines represent the result of linear regression analysis and the equations demonstrate that the line of best fit does not go through zero in both cases.

Using these calibration curves, the number of cells required to detect lactate release in cell culture media was determined over a 24 hour period (figure 5.7). An initial seeding density of 1×10^5 cells per T25 flask did not result in significant levels of lactate in culture media 24 hours after starting the experiment. Lactate release was detectable using 1×10^6 cells per T25 flask and this improved further if cells were left until approximately 80% confluent (figure 5.7, left hand panel). In this case, the rate of lactate release was similar across all time points ranging from 0.54mM/h to 0.39mM/h at the 2 hour and 8 hour time points respectively (figure 5.7, right hand panel).

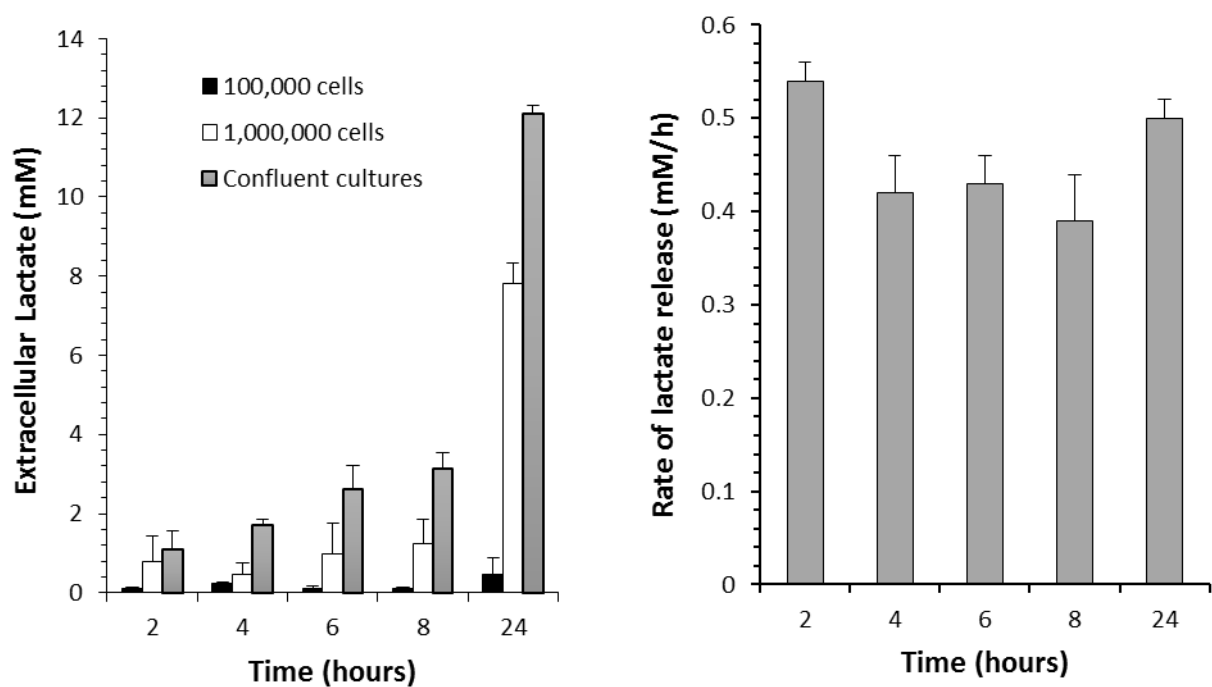


Figure 5.7 Release of lactate from HCT116 p53^{-/-} cells. In the left hand panel, the levels of lactate released from cells over a 24 hour period was determined at three different cell culture states. These were, 24 hours after seeding T25 flasks with 1×10^5 cells or 1×10^6 cells and 5 days after seeding 1×10^6 cells to get cultures that are approximately 80% confluent. The right hand panel presents the rate of release of lactate at the various time points specified using cultures that are at 80% confluence. Each value represents the mean \pm standard deviation for three experiments.

The effect of Ag8 on the release of lactate from HCT116 cells is presented in figure 5.8. Extracellular lactate was undetectable in the cell culture media up to 6 hours in both cell lines (HCT116 p53^{+/+}, HCT116 p53^{-/-}). Extracellular lactate was detected at 8 and 24 hours (figure 5.8). In HCT116 p53^{-/-} cells, Ag8 induces a dose dependent reduction in extracellular lactate at 8 hour and 24 hour time points (*P<0.01). In contrast, in the HCT116 p53^{+/+} cells no effect of Ag8 was observed at 8 hours whilst at 24h a decrease in extracellular lactate was observed at 5 and 10uM Ag8 but this was not statistically significant.

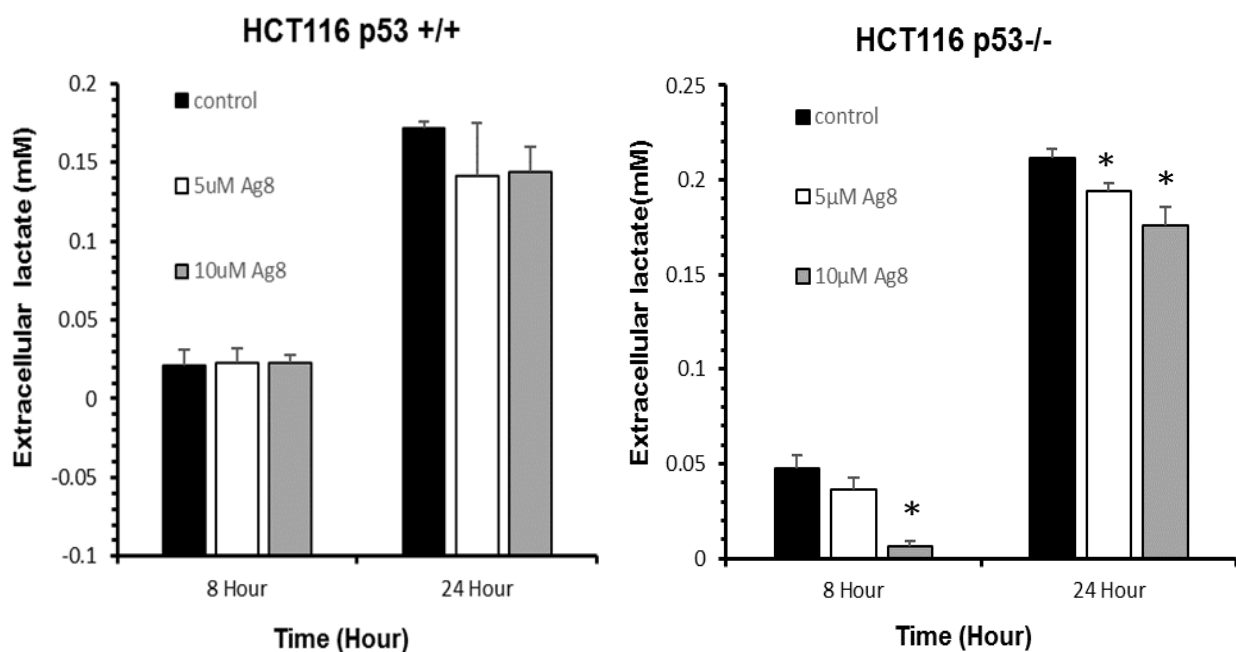


Figure 5.8 The effect of Ag8 on extracellular levels of lactate in HCT116 p53^{-/-} and HCT116 p53^{+/+} cells. Cells were at 80% confluence before treatment with Ag8 commenced and the time on the X-axis represents both the duration of drug exposure. The results presented are the mean of three independent experiments and the error bars represent standard deviation values. *P<0.01, unpaired student's t-test.

5.3.6 Effect of Ag8 on NAD, NADH, NAD(H) and the NAD/NADH ratio.

Calibration curves using both NAD and NADH are presented in figure 5.9. In both cases, there is a linear relationship between NAD(H) and $\Delta A/\text{min}$ with virtually identical regression analysis results.

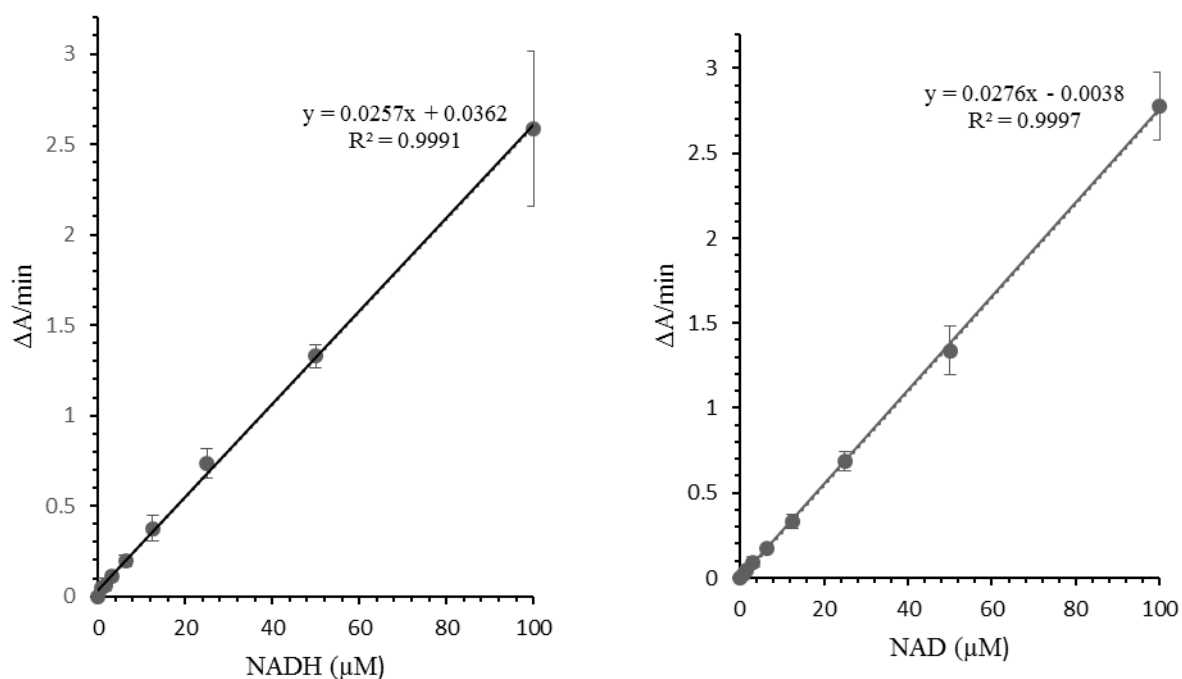


Figure 5.9 Calibration curves for NADH and NAD. Each value represents the mean \pm standard deviation for three independent experiments.

Validation of the heating step in the reaction is shown in figure 5.10 and this demonstrates that whilst NADH is stable at 60C for 30min, NAD is almost completely lost. There was some very low level activity present but compared to the non-heated samples, it was minimal.

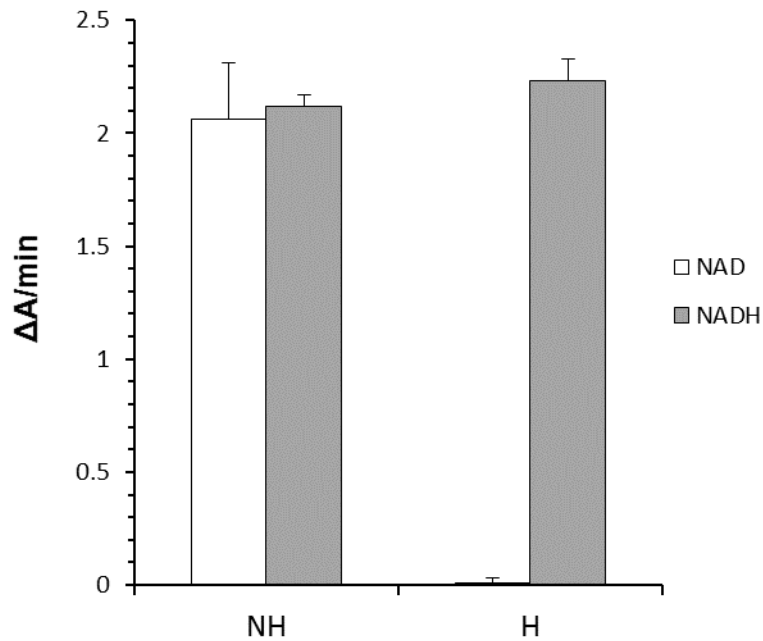


Figure 5.10 Validation of the NAD(H) assay. The concentration of NAD and NADH in these reactions was 100 μ M in both cases and both samples were either heated at 60C for 30min (H) or not heated (NH). Each value represents the mean \pm standard deviation for three independent experiments.

Prior to measuring the effect of Ag8 on NAD(H) levels, the morphological effects induced by Ag8 following a one hour exposure were determined to see if major short term effects were being observed (short term exposures to Ag8 had not been performed previously). The results are presented in figure 5.11 and these clearly demonstrate that Ag8 is inducing significant morphological damage to both HCT116 p53^{+/+} and HCT116 p53^{-/-} cells following a one-hour exposure to Ag8 (50 μ M). As the concentration of Ag8 decreases, morphological effects become less visible and at or below 20 μ M, there are no major effects visible under the microscope. A concentration of 20 μ M was chosen to evaluate the effects of Ag8 on NAD(H) levels

in cells. These concentration was selected based on effect of Ag8 at 5μM and 10μM, on lactate released up to 24 hours time exposure.

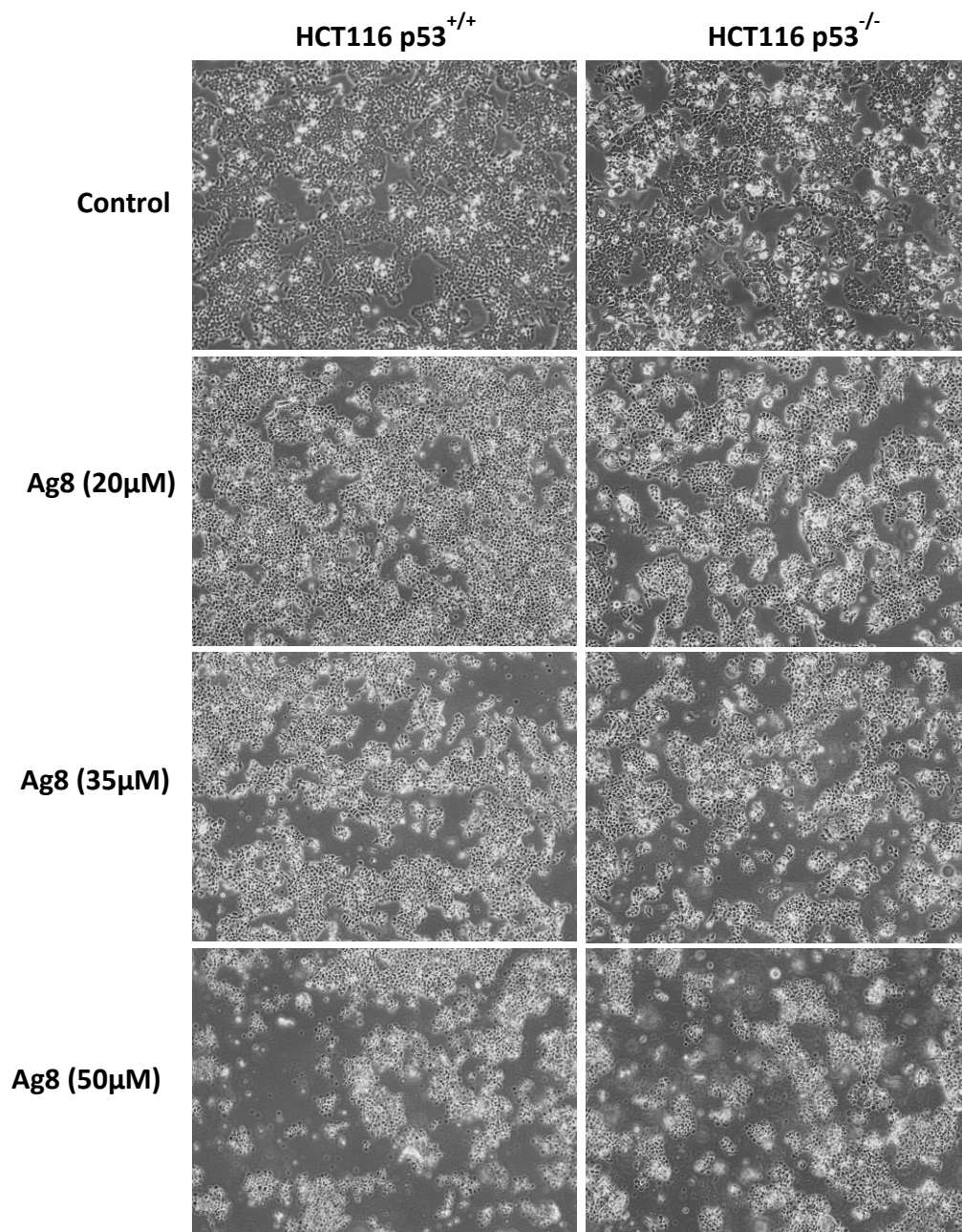


Figure 5.11 Morphological effects of different doses Ag8 following short time exposure. Cells were exposed to Ag8 for one hour before image capture using the EVOS light microscope.

Treatment of HCT116 p53^{-/-} cells with Ag8 (20µM) had significant effects on redox levels within the cell as illustrated in figure 5.12. Whilst the levels of total NAD(H) did not significantly change during the 45min drug exposure period, there was a significant and rapid rise in NAD levels with a corresponding drop in NADH. Effects were observed within 5 min of drug treatment and it peaked at 10 min before dropping back to a steady state between 15 and 45 min. The levels in this steady state phase were much higher (in the case of NAD) or lower (in the case of NADH) than control (t = 0) levels. The effect on the NAD/NADH ratio was significant with a significant increase in NAD/NADH ratios occurring within 10 min of Ag8 treatment.

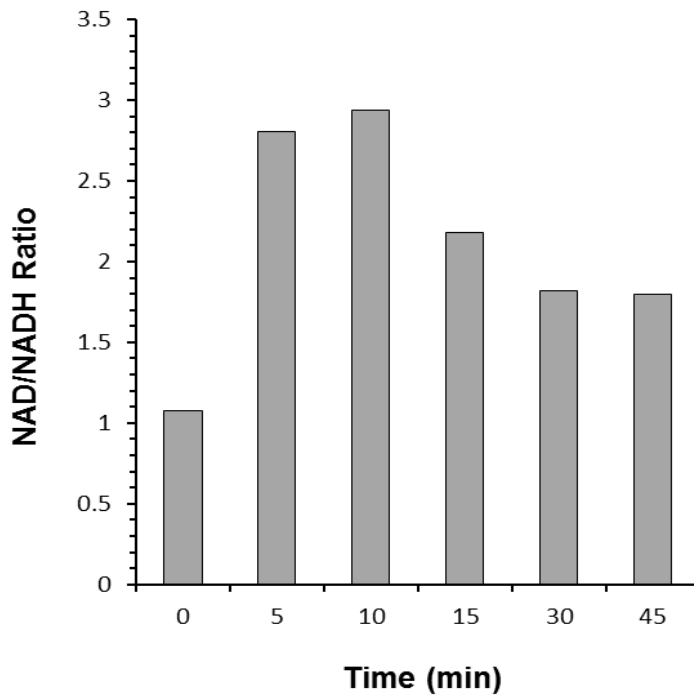
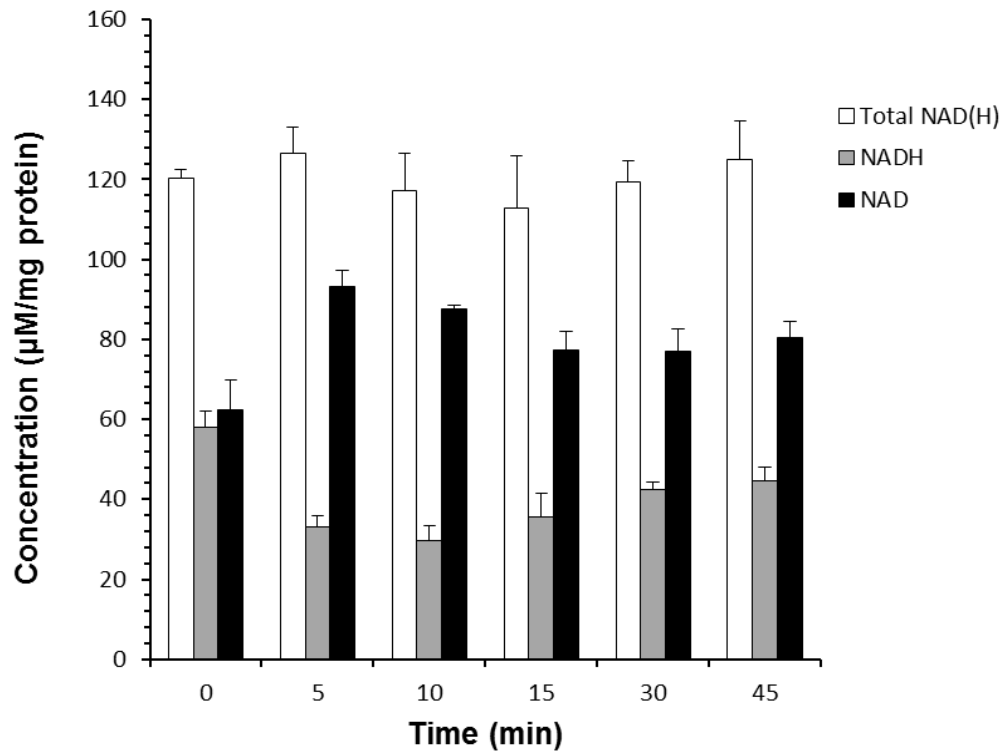


Figure 5.11 The effect of Ag8 on the levels of NAD and NADH in HCT116 p53^{-/-} cells. The upper graph presents the levels of NAD, NADH and NAD(H) and each value represents the mean \pm standard deviation for 3 independent experiments.

5.3.7 Inhibition of hexokinase by silver complexes

The ability of a series of silver complexes to inhibit purified yeast hexokinase is presented in figure 5.13. Whilst cisplatin does not inhibit hexokinase, several silver complexes did. These include 100 μ M of HB16, HA201, HA266 and Ag8 where hexokinase activity was almost completely inhibited. The other compounds in the series were partial inhibitors of hexokinase under the experimental conditions used

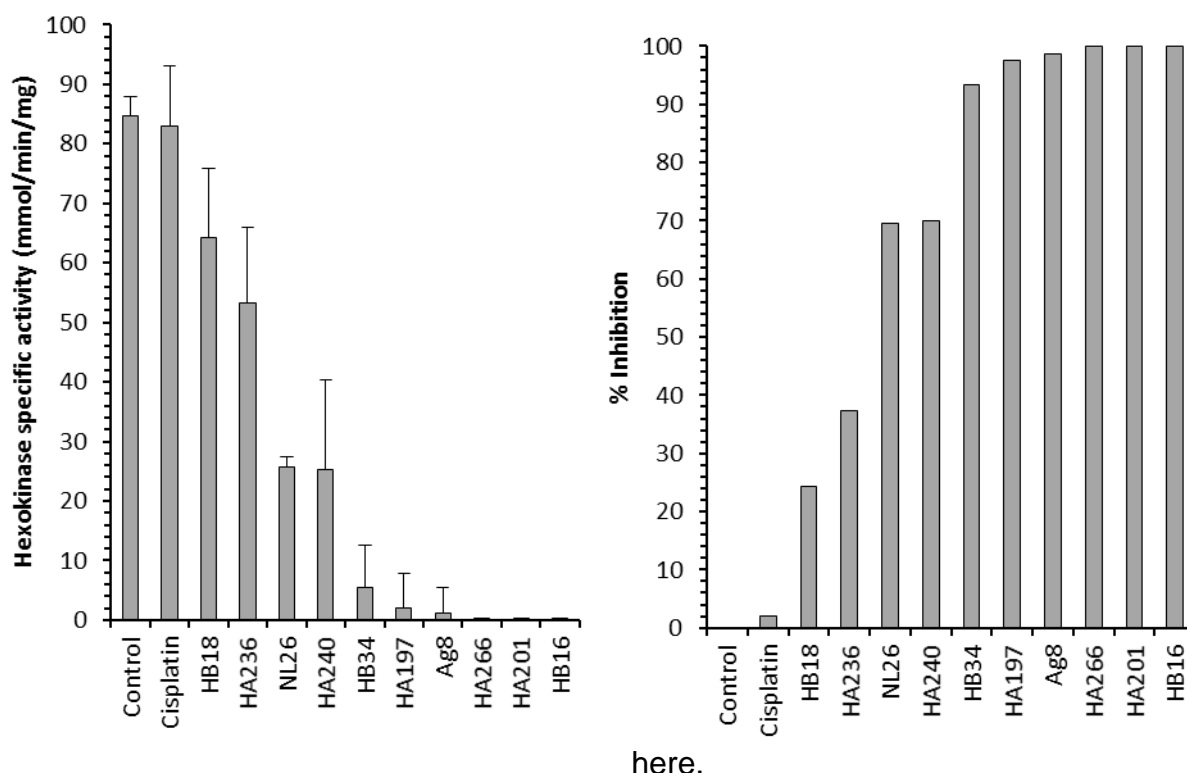


Figure 5.12 Inhibition of yeast hexokinase by silver complexes. The left hand panel presents the specific enzyme activities and the right hand panel presents the % inhibition based upon the specific activity of test compounds relative to the control. The data in the left hand panel represents the mean \pm standard deviation for three experiments.

5.4 Discussion

Recent collaborative research with the University of Manchester has identified the silver N-heterocyclic carbene complex Ag8 as a potent and selective inhibitor of glycolysis in cancer cells (Allison et al., 2017). However, the cellular target or targets of Ag8 that result in this inhibition of glycolysis have yet to be identified. This chapter investigates the ability of Ag8 to inhibit key glycolytic enzymes LDH-A and hexokinase (HK), as well as LDH-B which promotes the reverse enzymatic reaction (conversion of lactate to pyruvate) to that of LDH-A. In addition, ten novel silver organometallic complexes were analysed alongside Ag8 for possible effects as well as cisplatin as a control.

In a cell-free assay of LDH-A activity, Ag8 as well as many of the other silver complexes at the single tested concentration of 100 μ M strongly inhibited LDH-A, whereas cisplatin and four of the series of novel silver complexes had very little effect (<10% inhibition). This prompted our investigation of LDH-A and LDH-B expression and activity in a range of cancer cell lines and the ability of Ag8 to inhibit LDH-A and LDH-B in cell lysates. Preliminary expression data is presented and needs repeating, however, LDH-A activity was readily detectable in all cell lines tested (Fig. 5.3). In BE colorectal cancer cell lysates, Ag8 inhibited LDH-A at low micromolar concentrations with an IC₅₀ of 1.8 μ M compared to >10 μ M for inhibition of LDH-B. This is significant as many of the existing LDH inhibitors lack good selectivity towards one isoform or the other and this work identifies Ag8 as a selective inhibitor of LDH-A. This also provides a mechanistic explanation for the reported inhibition of glycolysis by Ag8.

LDH-A inhibition has previously been reported to reduce extracellular lactate levels and alter intracellular NAD(H) redox balance (Allison et al., 2014). This is consistent with LDH-A enzyme catalysing the NADH-dependent reduction of pyruvate to lactate. The effects of Ag8 on lactate and NAD(H) levels were therefore also investigated. 5 μ M concentrations of Ag8 consistently reduced extracellular lactate levels in both HCT116 p53^{-/-} and p53^{+/+} cancer cells with sampling times ranging from 2h up to 24h. Effects on NAD(H) were also investigated, in this case, in response to an acute (up to 45min) treatment with 20 μ M Ag8. Whilst total cellular levels of NAD(H) did not change over this duration, NAD levels rapidly increased within 5 minutes. It is unclear whether this relates to LDH-A inhibition, however, or other effects on cellular metabolic flux and this warrants future experimental investigation. Indeed, Ag8 was also found to potently inhibit hexokinase in a cell-free assay, however, this has yet to be investigated using cell lysates. It is also noteworthy that across the panel of novel silver complexes screened here, whilst some of the complexes inhibited both LDH-A and HK in cell-free assays, selective inhibition of either LDH-A or HK was also observed for several complexes. For example, whilst Ag8 inhibited both LDH-A and HK, the related complex HA201 had little effect on LDH-A activity but strongly inhibited HK. Given the dependency of hypoxic cancer cells on glucose for their survival as presented in chapter 4, this is an interesting series of compounds for further studies as potential hypoxia targeting agents.

Chapter 6

General Discussion

The metabolic reprogramming of cancers to favour aerobic glycolysis over oxidative phosphorylation and the emerging evidence that oncogenic events drive this process is of considerable interest as a target for therapeutic intervention (Yeung et al., 2008, DeBerardinis et al., 2008a). Whilst considerable attention has focused on the Warburg effect under aerobic conditions, there is another level of complexity that has received comparatively less attention and that is the metabolic phenotype under hypoxic conditions (Devic, 2016). The problem of hypoxia remains a significant challenge for drug discovery and strategies such as hypoxia activated prodrugs have not generated effective anti-cancer drugs so far (Phillips, 2016). New approaches to target hypoxic cells are required and the primary objective of this thesis was to determine whether or not targeting cancer cell metabolism under hypoxia results in preferential cell kill under these conditions.

In the first of the major chapters in this thesis, the ability of a range of metabolic enzyme inhibitors to preferentially kill hypoxic cells was evaluated. The inhibitors used include 2-deoxyglucose (2-DG) which is phosphorylated by the enzyme hexokinase and accumulates in the cell leading to inhibition of hexokinase (Zhang et al., 2006). 2-DG also causes ATP deficiency and cell death, especially in cells with mitochondrial defects under hypoxic conditions (Maher et al., 2004). In this study, 2DG caused a decrease in cell viability under both aerobic and hypoxic conditions but there was no significant hypoxia selectivity in a panel of cell lines with the

exception of BE cells (table 3.4). The potency of 2-DG was low and this is consistent with other studies that reported that 2-DG might not be a potent inhibitor of tumour metabolism (Ledoux et al., 2003). In addition, there are reports in the literature showing that hypoxic cells are more resistant to 2-DG under hypoxic conditions (Maher et al., 2007). Other studies have reported that 2-DG should always be used in combination with other drugs rather than as a single agent (Bénéteau et al., 2012) and further studies should be conducted to explore this further. The results of this study demonstrate that 2-DG is not a potent compound and is less effective against hypoxic compared to aerobic cells *in vitro* with the exception of BE cells where a HCR of 1.46 was obtained.

Another inhibitor used was 3-bromopyruvate (3-BP) which is also a hexokinase inhibitor. All tumour cell lines responded to 3-BP under both aerobic and hypoxic conditions but without showing any hypoxic selectivity (table 3.4). In fact, cells under hypoxia were less sensitive to 3-BP than under aerobic conditions with HCR values of 0.34 to 0.62. Ko et al. were reported that 3-BP inhibits mitochondrial respiration and hexokinase at low concentrations *in vitro* (Ko et al., 2001). The doses used in this study are consistent with these values and inhibition of hexokinase should have occurred. No enzyme inhibition studies were conducted however because the HCR values were low in the initial screen.

Similarly, sodium oxamate did not show any significant selectivity for hypoxic cells *in vitro*. Indeed, cells were more resistant under hypoxia than aerobic conditions with HCR values ranging from 0.87 to 0.69 (table 3.4). Sodium oxamate is an inhibitor of lactate dehydrogenase (LDH) but it is not specific for LDH-A and has other

mechanisms of action (Moreno-Sánchez et al., 2017). Other studies have demonstrated that LDH-A specific inhibitors have hypoxia selectivity (Granchi et al., 2011) and behave synergistically with other anticancer drugs (Maftouh et al., 2014). The lack of hypoxia selectivity observed in this study using sodium oxamate may reflect the fact that it is not a good inhibitor of LDH-A.

To conclude this section of the thesis, this study has demonstrated that the use of established glycolytic inhibitors did not demonstrate hypoxia selectivity *in vitro* and in the majority of cases, resistance under hypoxia was observed. The hypoxia activated prodrug tirapazamine did produce good HCR values confirming that the experimental conditions used were suitable. These results raise questions as to whether or not glycolysis under hypoxic conditions is important for cell survival but the fact that other glycolytic inhibitors have shown hypoxia selectivity *in vitro* (Granchi et al., 2011) suggests that targeting glycolysis under hypoxia is a potential strategy for hypoxia selectivity.

In addition to glycolytic inhibitors, this study also focused on the inhibition of pyruvate kinase 1 (PK1) using dichloroacetate (DCA). DCA is an inhibitor of PK1 leading to activation of the pyruvate dehydrogenase complex and causes a shift back to oxidative phosphorylation and induction of apoptosis (Bonnet et al., 2007, Michelakis et al., 2008, Stacpoole et al., 2008). The results of this study demonstrate that DCA is more potent under hypoxia than aerobic conditions in some cell lines but not others (table 3.1) with HCR values ranging from 2.09 to 1.11 For HCT116 p53^{+/+}, PANC 10.05, HT-29, HCT116 p53^{-/-}, SW48 and BE cells. These effects are modest compared to tirapazamine with an HCR 9.63. It is of interest that in the case of non-

cancer ARPE-19 cells, DCA was less active under hypoxic conditions than aerobic conditions. The results were significant and suggest that DCA maybe less active against hypoxic normal cells in tissues such as the bone marrow (Bonnet et al., 2007). Much more detailed research needs to be done to confirm this but the result is interesting. The mechanism underpinning these differential effects is not known. Western blot analysis does show that DCA is inhibiting PDK1 (reduced levels of p-PDH) and this is consistent with other studies in the literature (Crewe et al., 2017). Further studies are however required to explore the reasons why HCR values are different between HCT116p53^{+/+} and ARPE-19 for example.

The potency of DCA was low (mM range) but this is consistent with other studies in the literature (Bonnet et al., 2007). Also, the effectiveness of DCA is very different between different cancer cell lines and in some cases, DCA did not demonstrate a direct cytotoxic effect *in vitro* (Shahrzad et al., 2010, Zheng and Shen, 2013). The low potency of DCA may be related to the fact it is a weak inhibitor of PDK1 (McFate et al., 2008) and more effective inhibitors of PDK1 may have greater potency and increased HCR. In addition, synergy between PDK1 inhibitors and other chemotherapeutic agents have been documented in monolayer cultures (Sradhanjali et al., 2017) and further studies using three dimensional models (eg spheroids) that mimic more closely the microenvironment of tumours are required (Asghar et al., 2015).

With the exception therefore of DCA, the results of this study have demonstrated that established glycolytic inhibitors do not selectively kill hypoxic cells *in vitro* and in many cases, hypoxic cells are more resistant. These findings suggest that the

survival of cells in hypoxic conditions may not in fact depend on glucose metabolism as proposed in the rationale for this thesis. This raised the question of whether or not cells require glucose to survive under hypoxia and the studies in chapter three address this question. When glucose was removed from the media, cells survived under aerobic conditions but not under hypoxic conditions (figure 4.23). The effect of glucose deprivation was concentration dependent and at concentrations below 8mM, the suppression of growth could not be rescued when glucose was supplied after a 96 hour deprivation period (figure 4.8). These results confirm that cancer cells require glucose to survive under hypoxic conditions suggesting that hypoxic cells are glycolysis depending to generate energy required in cell growth, but this raises the intriguing question as to why hypoxic cells are not extremely sensitive to glycolytic inhibitors? It is clear that other mechanisms are able to 'get around' the block in glycolysis or that inhibition of glycolysis is incomplete and even a low level of glycolytic flux is sufficient to keep the cells alive.

The results showing that glucose deprivation reduces cell survival provided an opportunity to determine whether other sugars are important for the survival of cancer cells under hypoxia. By adding various sugars to glucose deprived media, it was possible to determine which sugars are able to promote cell survival when glucose levels are low. A somewhat surprising result was the lack of any increase in survival when lactate was added to glucose deprived media. Lactate is a potential fuel and the lack of any effect on hypoxic cells was unexpected. It has recently been shown however that glucose deprivation upregulates the lactate transporter MCT1 but this effect was observed primarily in oxygenated cells (Sonveaux et al., 2012).

Furthermore, this result is consistent with the model proposed by Sonveaux et al where lactate produced by hypoxic cells is used as a fuel to support the growth of oxygenated cells (Sonveaux et al., 2008). The most striking result obtained in these studies was with mannose which was able to completely reverse the effects of glucose deprivation. This suggests that mannose in addition to glucose are important sugars that promote the survival of cancer cells under hypoxic conditions. To the best of my knowledge, this is a novel finding and it opens up a new avenue of research.

Mannose is a simple sugar but its biochemistry and physiological function is complex (Sharma et al., 2014). Its metabolism is illustrated in figure 6.1 and following transport into the cells via GLUT transporters, it is converted to mannose-6-phosphate by hexokinase. It can then be either catabolised by conversion to fructose-6-phosphate by phosphomannose isomerase (MPI) or used to produce mannose-1-phosphate by phosphomannomutase (PMM1) which is then used in the synthesis of N-glycans (figure 6.1). The ratio of MPI to PMM1 largely determines which pathway mannose-6-phosphate goes down with higher ratios favouring entry into glycolysis. It is therefore possible that mannose could be an alternative source of energy for hypoxic cells, especially if glucose levels are low.

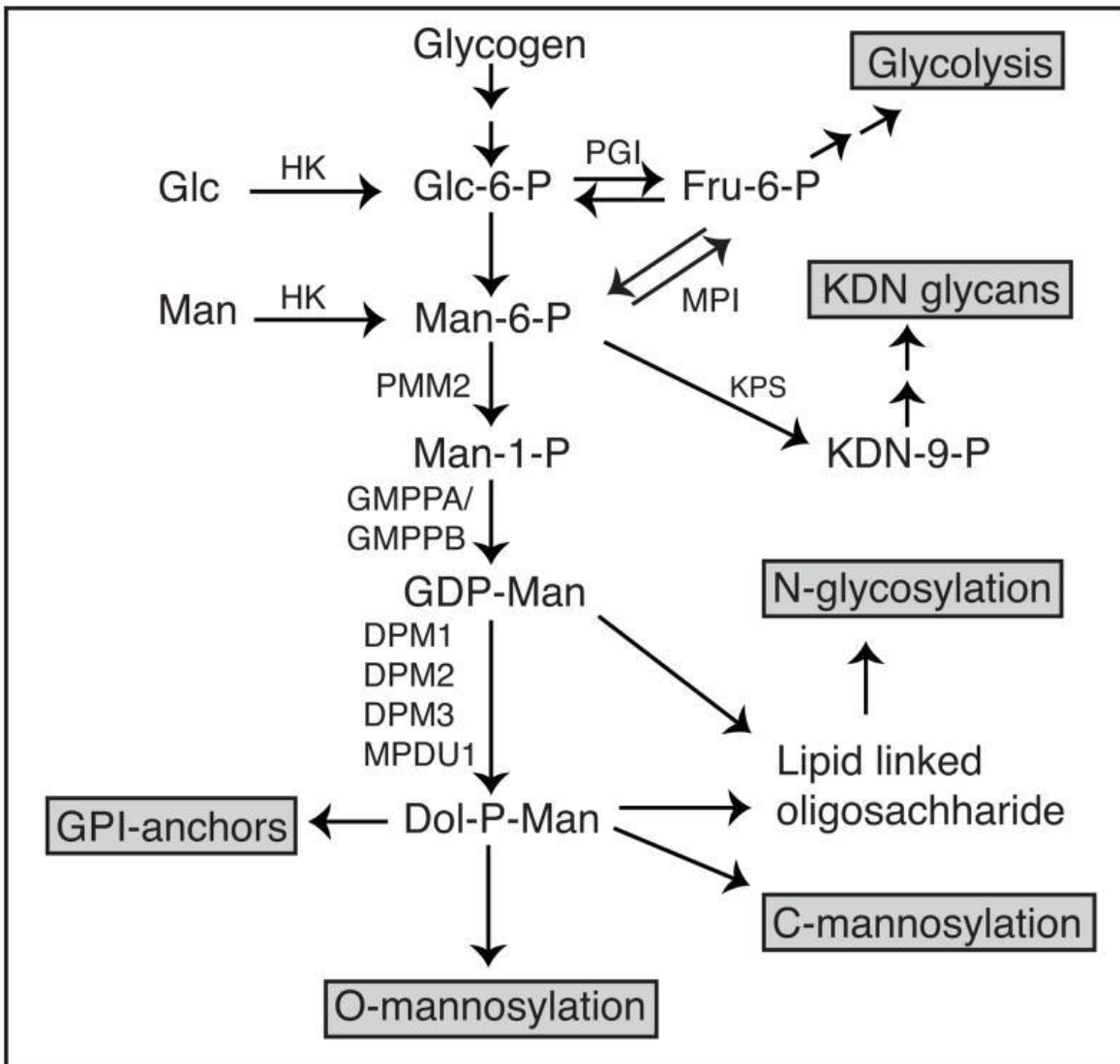


Figure 6.1 Metabolism of mannose (Sharma et al, 2014).

The levels of mannose in human plasma have been quantified and these are generally around 50 μ M(Sharma and Freeze, 2011) and this is well below the levels required to restore cell survival under conditions of glucose deprivation. Typically, concentrations of mannose above 5mM are required to increase cell survival under

hypoxic conditions. If mannose is important in promoting hypoxic cell survival, the key question that needs to be addressed is where is the mannose coming from if circulating levels of mannose are in the μM range? Mannose is the major sugar (monosaccharide) present in N-glycans which are attached to proteins to form glycoproteins that play multiple roles in cells including cell-cell interactions. More than 50% of human proteins are believed to be glycosylated and aberrant glycosylation is associated with several disease types including cancer (Song and Mechref, 2015). Altered glycosylation of proteins also plays an important role in the metastatic process (Oliveira-Ferrer et al., 2017) and hypoxia is known to regulate glycosylation reactions via HIF1 mediated reactions (Shirato et al., 2010). Furthermore, glycoproteins can be 'recycled' by degradation in the cytoplasm and lysosome resulting in the release of free mannose (Aebi et al., 2010, Chantret and Moore, 2008). Hypoxia is also known to induce autophagy (Fang et al., 2015) and autophagy has been shown to play a role in recycling glycoproteins (Huang et al., 2015) The evidence in the literature demonstrates a clear link between N-glycan biology and catabolic metabolism and it is possible that recycling of glycoproteins could provide cells with the mannose required to enter glycolytic reactions and promote survival under hypoxic conditions. The link to metastasis is also interesting, especially as hypoxia is a known 'driver' of the metastatic process (Rankin and Giaccia, 2016) To conclude this part of the thesis, mannose has been shown to promote cell survival under hypoxic conditions and further studies are required to explore the possibility that release of mannose from N-glycans occurs under hypoxia and that this can be used as a fuel to support the survival of hypoxic cancer cells.

Also within chapter 4, studies demonstrated that cells survived in the absence of glucose under aerobic conditions suggesting that alternative sources of energy were being used for catabolic purposes. Cell survival significantly decreased however when both glutamine and glucose were depleted from the media. These results are consistent with other studies in the literature (Wise et al., 2008) and suggest that targeting both glycolysis and glutaminolysis could produce synergistic effects. Subsequently, the cells were tested with 2DG (hexokinase inhibitor) and 968 (glutaminase inhibitors) using high glucose medium and glucose-free medium (in the presence of glutamine). The response of cells treated with 2DG and 968 in glucose-free medium showed that both inhibitors increase cell death. These results suggested that by targeting metabolic pathway of cancer cells in combination with HK inhibitors and glutaminase inhibitors might induce effective results for targeting cancer cells. Also, the response of cancer cells to 968 was tested under hypoxic conditions in high glucose medium for 96 hours. 968 had a significant effect on both HCT116 p53^{+/+} and HCT116 p53^{-/-} cells under hypoxic condition compare to aerobic conditions (figure. 4.25 and 4.26). Under hypoxic conditions, it has been shown that glutamine metabolism is required for the synthesis of lipids that are required to promote cell growth instead of entry into the TCA cycle (Sun and Denko, 2014). The potentiation of 968 activity under hypoxia is therefore consistent with the findings of Sun and Denko (Sun and Denko, 2014).

The final results chapter of this thesis focused on the evaluation of a series of silver complexes as inhibitors of lactate dehydrogenase (and hexokinase). This study demonstrated that several silver complexes were inhibitors of LDH but Ag8 was

explored in greater depth due to the fact that previous studies had studied its pharmacological properties in detail (Allison et al, 2017). Ag8 is a silver N-heterocyclic carbene (NHC) complex that has been shown to inhibit glycolysis in cancer cells (Allison et al 2017) but the inhibition of LDH is a novel finding for this class of compound. The kinetic nature of the inhibition of purified LDH is not known but Ag8 selectively inhibits LDH-A compared to LDH-B in cell lysates. The reduction in lactate release from cells is also consistent with the inhibition of LDH-A but it is also conceivable that inhibition of the MCT4 transporter (which exports lactate out of the cell) could also result in reduced extracellular lactate levels. Copper and zinc bipyridyls have been shown to inhibit LDH (Koiri et al., 2008) but this is the first report of a silver NHC complex selectively inhibiting LDH-A.

Inhibition of LDH-A using siRNA led to a significant decrease in the NAD/NADH ratio in cancer cells (Allison et al 2014) but in this study, there was a rapid and significant increase in NAD levels in cells treated with Ag8. Significant effects were observed within 5 min of adding Ag8 and whilst the magnitude of these changes decreased to a steady state, the levels of NAD remained higher than control levels. These results are not consistent with the inhibition of LDH-A indicating that other mechanisms are operating. Ag8 is known to inhibit several key enzymes including NAD dependent enzymes such as PARP (Allison et al 2017). It is possible therefore that inhibition of NAD dependent enzymes could cause elevated levels of NAD but this hypothesis requires further investigation. This study also demonstrated that Ag8 induces very rapid morphological changes in cells with loss of viability occurring within one hour of treatment at high concentrations (50 μ M). Similar effects were observed at 20 μ M but

the effects were less dramatic. The mechanism of cell death is not known however and further studies are required to explore this further. In conclusion, this chapter has demonstrated that Ag8 is a novel selective inhibitor of LDH-A that causes a significant reduction in the release of lactate from cells. Further studies are required to determine whether this leads to hypoxia selectivity *in vitro* but this is a promising hit compound for further studies.

In conclusion, this thesis has demonstrated that the use of glycolytic inhibitors does not result in hypoxia selective cell kill *in vitro*. DCA however does show a degree of hypoxia selectivity but the magnitude of the enhancement is lower than the HAP tirapazamine. Glucose is essential for the survival of cells under hypoxia as deprivation induces significant cell kill. Mannose provides an alternative source of 'fuel' for the survival of cells under hypoxia and further studies are required to determine whether the recycling of N-glycans occurs to release free mannose under hypoxic conditions. Finally, Ag8 is a novel inhibitor of LDH and is the first silver NHC complex to selectively inhibit LDH-A.

Chapter 7. References

- AEBI, M., BERNASCONI, R., CLERC, S. & MOLINARI, M. 2010. N-glycan structures: recognition and processing in the ER. *Trends in biochemical sciences*, 35, 74-82.
- AFT, R. L., ZHANG, F. & GIUS, D. 2002. Evaluation of 2-deoxy-D-glucose as a chemotherapeutic agent: mechanism of cell death. *British journal of cancer*, 87, 805.
- AHLUWALIA, A. & S TARNAWSKI, A. 2012. Critical role of hypoxia sensor-HIF-1 α in VEGF gene activation. Implications for angiogenesis and tissue injury healing. *Current medicinal chemistry*, 19, 90-97.
- AHN, K. J., HWANG, H. S., PARK, J. H., BANG, S. H., KANG, W. J., YUN, M. & LEE, J. D. 2009. Evaluation of the role of hexokinase type II in cellular proliferation and apoptosis using human hepatocellular carcinoma cell lines. *Journal of nuclear medicine*, 50, 1525-1532.
- ALBERTELLA, M. R., LOADMAN, P. M., JONES, P. H., PHILLIPS, R. M., RAMPLING, R., BURNET, N., ALCOCK, C., ANTHONY, A., VJATERS, E. & DUNK, C. R. 2008. Hypoxia-selective targeting by the bioreductive prodrug AQ4N in patients with solid tumors: results of a phase I study. *Clinical cancer research*, 14, 1096-1104.
- ALLISON, S. J., KNIGHT, J., GRANCHI, C., RANI, R., MINUTOLO, F., MILNER, J. & PHILLIPS, R. M. 2014. Identification of LDH-A as a therapeutic target for cancer cell killing via (i) p53/NAD (H)-dependent and (ii) p53-independent pathways. *Oncogenesis*, 3, e102.
- ALLISON, S. J., SADIQ, M., BARONOU, E., COOPER, P. A., DUNNILL, C., GEORGOPOULOS, N. T., LATIF, A., SHEPHERD, S., SHNYDER, S. D. & STRATFORD, I. J. 2017. Preclinical anti-cancer activity and multiple mechanisms of action of a cationic silver complex bearing N-heterocyclic carbene ligands. *Cancer Letters*, 403, 98-107.
- ALTMAN, B. J., STINE, Z. E. & DANG, C. V. 2016. From Krebs to clinic: glutamine metabolism to cancer therapy. *Nature Reviews Cancer*, 16, 619.
- ALTON, G., HASILIK, M., NIEHUES, R., PANNEERSELVAM, K., ETCHISON, J. R., FANA, F. & FREEZE, H. H. 1998. Direct utilization of mannose for mammalian glycoprotein biosynthesis. *Glycobiology*, 8, 285-295.
- ANASTASIOU, D. & CANTLEY, L. C. 2012. Breathless cancer cells get fat on glutamine. *Cell Res*, 22, 443-6.
- ASGHAR, W., EL ASSAL, R., SHAFIEE, H., PITTERI, S., PAULMURUGAN, R. & DEMIRCI, U. J. M. T. 2015. Engineering cancer microenvironments for in vitro 3-D tumor models. 18, 539-553.
- AUGER, K. R., SERUNIAN, L. A., SOLTOFF, S. P., LIBBY, P. & CANTLEY, L. C. 1989. PDGF-dependent tyrosine phosphorylation stimulates production of novel polyphosphoinositides in intact cells. *Cell*, 57, 167-175.
- BAILEY, K. M., WOJTKOWIAK, J. W., HASHIM, A. I. & GILLIES, R. J. 2012. Targeting the metabolic microenvironment of tumors. *Advances in*

- pharmacology. Elsevier.
- BALINT, E. & VOUSDEN, K. 2001. Activation and activities of the p53 tumour suppressor protein. *British journal of cancer*, 85, 1813.
- BARKER, H. E., PAGET, J. T., KHAN, A. A. & HARRINGTON, K. J. 2015. The tumour microenvironment after radiotherapy: mechanisms of resistance and recurrence. *Nature reviews Cancer*, 15, 409.
- BÉNÉTEAU, M., ZUNINO, B., JACQUIN, M. A., MEYNET, O., CHICHE, J., PRADELLI, L. A., MARCHETTI, S., CORNILLE, A., CARLES, M. & RICCI, J.-E. 2012. Combination of glycolysis inhibition with chemotherapy results in an antitumor immune response. *Proceedings of the National Academy of Sciences*, 109, 20071-20076.
- BENSAAD, K., TSURUTA, A., SELAK, M. A., VIDAL, M. N. C., NAKANO, K., BARTRONS, R., GOTTLIEB, E. & VOUSDEN, K. H. 2006. TIGAR, a p53-inducible regulator of glycolysis and apoptosis. *Cell*, 126, 107-120.
- BERTOUT, J. A., PATEL, S. A. & SIMON, M. C. 2008. The impact of O₂ availability on human cancer. *Nature Reviews Cancer*, 8, 967.
- BILLIARD, J., DENNISON, J. B., BRIAND, J., ANNAN, R. S., CHAI, D., COLÓN, M., DODSON, C. S., GILBERT, S. A., GRESHOCK, J., JING, J. J. C. & METABOLISM 2013. Quinoline 3-sulfonamides inhibit lactate dehydrogenase A and reverse aerobic glycolysis in cancer cells. 1, 19.
- BONNET, S., ARCHER, S. L., ALLALUNIS-TURNER, J., HAROMY, A., BEAULIEU, C., THOMPSON, R., LEE, C. T., LOPASCHUK, G. D., PUTTAGUNTA, L. & BONNET, S. 2007. A mitochondria-K⁺ channel axis is suppressed in cancer and its normalization promotes apoptosis and inhibits cancer growth. *Cancer cell*, 11, 37-51.
- BORAD, M. J., REDDY, S. G., BAHARY, N., URONIS, H. E., SIGAL, D., COHN, A. L., SCHELMAN, W. R., STEPHENSON JR, J., CHIOREAN, E. G. & ROSEN, P. J. 2015. Randomized phase II trial of gemcitabine plus TH-302 versus gemcitabine in patients with advanced pancreatic cancer. *Journal of Clinical Oncology*, 33, 1475.
- BRAHIMI-HORN, M. C., CHICHE, J. & POUYSSÉGUR, J. 2007. Hypoxia and cancer. *Journal of molecular medicine*, 85, 1301-1307.
- BRAITHWAITE, A., DEL SAL, G. & LU, X. 2006. Some p53-binding proteins that can function as arbiters of life and death. *Cell death and differentiation*, 13, 984.
- BRIZEL, D. M., DODGE, R. K., CLOUGH, R. W. & DEWHIRST, M. W. 1999. Oxygenation of head and neck cancer: changes during radiotherapy and impact on treatment outcome. *Radiotherapy and Oncology*, 53, 113-117.
- BROWN, J. 1962. Effects of 2-deoxyglucose on carbohydrate metabolism: review of the literature and studies in the rat. *Metabolism*, 11, 1098-1112.
- BROWN, J. M. & GIACCIA, A. J. 1998. The unique physiology of solid tumors: opportunities (and problems) for cancer therapy. *Cancer research*, 58, 1408-1416.
- BROWN, J. M. & WILSON, W. R. 2004. Exploiting tumour hypoxia in cancer treatment. *Nature Reviews Cancer*, 4, 437.
- BULUSU, V., TUMANOV, S., MICHALOPOULOU, E., VAN DEN BROEK, N. J., MACKAY, G., NIXON, C., DHAYADE, S., SCHUG, Z. T., VOORDE, J. V. &

- BLYTH, K. 2017. Acetate recapturing by nuclear acetyl-CoA synthetase 2 prevents loss of histone acetylation during oxygen and serum limitation. *Cell reports*, 18, 647-658.
- CARO-MALDONADO, A., TAIT, S., RAMIREZ-PEINADO, S., RICCI, J., FABREGAT, I., GREEN, D. & MUÑOZ-PINEDO, C. 2010. Glucose deprivation induces an atypical form of apoptosis mediated by caspase-8 in Bax-, Bak-deficient cells. *Cell death and differentiation*, 17, 1335.
- CAY, O., RADNELL, M., JEPSSON, B., AHREN, B. & BENGMARK, S. 1992. Inhibitory effect of 2-deoxy-D-glucose on liver tumor growth in rats. *Cancer research*, 52, 5794-5796.
- CHANTRET, I. & MOORE, S. E. 2008. Free oligosaccharide regulation during mammalian protein N-glycosylation. *Glycobiology*, 18, 210-224.
- CHEN, X., THAKKAR, H., TYAN, F., GIM, S., ROBINSON, H., LEE, C., PANDEY, S. K., NWOKORIE, C., ONWUDIWE, N. & SRIVASTAVA, R. K. 2001. Constitutively active Akt is an important regulator of TRAIL sensitivity in prostate cancer. *Oncogene*, 20, 6073.
- CHEN, Z., ZHANG, H., LU, W. & HUANG, P. 2009. Role of mitochondria-associated hexokinase II in cancer cell death induced by 3-Bromopyruvate. *Biochimica et biophysica acta*, 1787, 553.
- CIARDIELLO, F., ARNOLD, D., CASALI, P., CERVANTES, A., DOUILLARD, J.-Y., EGGERMONT, A., ENIU, A., MCGREGOR, K., PETERS, S. & PICCART, M. 2014. Delivering precision medicine in oncology today and in future—the promise and challenges of personalised cancer medicine: a position paper by the European Society for Medical Oncology (ESMO). Oxford University Press.
- CLOTTE, E. 2005. Hypoxia-inducible factor 1: regulation, involvement in carcinogenesis and target for anticancer therapy. *Bulletin du cancer*, 92, 119-127.
- CONTRACTOR, T. & HARRIS, C. R. 2012. p53 negatively regulates transcription of the pyruvate dehydrogenase kinase Pdk2. *Cancer research*, 72, 560-567.
- CREWE, C., SCHAFER, C., LEE, I., KINTER, M. & SZWEDA, L. I. 2017. Regulation of pyruvate dehydrogenase kinase 4 in the heart through degradation by the Lon protease in response to mitochondrial substrate availability. *Journal of Biological Chemistry*, 292, 305-312.
- DAVIDESCU, M., MACCHIONI, L., SCARAMOZZINO, G., MARCHETTI, M. C., MIGLIORATI, G., VITALE, R., CORCELLI, A., ROBERTI, R., CASTIGLI, E. & CORAZZI, L. 2015. The energy blockers bromopyruvate and lonidamine lead GL15 glioblastoma cells to death by different p53-dependent routes. *Scientific reports*, 5, 14343.
- DAYE, D. & WELLEN, K. E. Metabolic reprogramming in cancer: unraveling the role of glutamine in tumorigenesis. *Seminars in cell & developmental biology*, 2012. Elsevier, 362-369.
- DEBERARDINIS, R. J. & CHANDEL, N. S. 2016. Fundamentals of cancer metabolism. *Science advances*, 2, e1600200.
- DEBERARDINIS, R. J., LUM, J. J., HATZIVASSILIOU, G. & THOMPSON, C. B. 2008a. The biology of cancer: metabolic reprogramming fuels cell

- growth and proliferation. *Cell metabolism*, 7, 11-20.
- DEBERARDINIS, R. J., MANCUSO, A., DAIKHIN, E., NISSIM, I., YUDKOFF, M., WEHRLI, S. & THOMPSON, C. B. 2007. Beyond aerobic glycolysis: transformed cells can engage in glutamine metabolism that exceeds the requirement for protein and nucleotide synthesis. *Proceedings of the National Academy of Sciences*, 104, 19345-19350.
- DEBERARDINIS, R. J., SAYED, N., DITSWORTH, D. & THOMPSON, C. B. 2008b. Brick by brick: metabolism and tumor cell growth. *Current opinion in genetics & development*, 18, 54-61.
- DEICHMANN, M., BENNER, A., BOCK, M., JÄCKEL, A., UHL, K., WALDMANN, V. & NÄHER, H. 1999. S100-Beta, melanoma-inhibiting activity, and lactate dehydrogenase discriminate progressive from nonprogressive American Joint Committee on Cancer stage IV melanoma. *Journal of clinical oncology*, 17, 1891-1891.
- DENDY, P. & WARDMAN, P. 2006. Hypoxia in biology and medicine: the legacy of LH Gray. *The British journal of radiology*, 79, 545-549.
- DEPREZ, J., VERTOMMEN, D., ALESSI, D. R., HUE, L. & RIDER, M. H. 1997. Phosphorylation and activation of heart 6-phosphofructo-2-kinase by protein kinase B and other protein kinases of the insulin signaling cascades. *Journal of Biological Chemistry*, 272, 17269-17275.
- DEVIC, S. 2016. Warburg effect-a consequence or the cause of carcinogenesis? *Journal of Cancer*, 7, 817.
- DEYOUNG, M. P., HORAK, P., SOFER, A., SGROI, D. & ELLISEN, L. W. 2008. Hypoxia regulates TSC1/2-mTOR signaling and tumor suppression through REDD1-mediated 14-3-3 shuttling. *Genes & development*, 22, 239-251.
- DWARAKANATH, B. & JAIN, V. 2009. Targeting glucose metabolism with 2-deoxy-D-glucose for improving cancer therapy. *Future oncology*, 5, 581-585.
- EALLES, K., HOLLINSHEAD, K. & TENNANT, D. 2016. Hypoxia and metabolic adaptation of cancer cells. *Oncogenesis*, 5, e190.
- ELMORE, S. 2007. Apoptosis: a review of programmed cell death. *Toxicologic pathology*, 35, 495-516.
- ELSTROM, R. L., BAUER, D. E., BUZZAI, M., KARNAUSKAS, R., HARRIS, M. H., PLAS, D. R., ZHUANG, H., CINALLI, R. M., ALAVI, A. & RUDIN, C. M. 2004. Akt stimulates aerobic glycolysis in cancer cells. *Cancer research*, 64, 3892-3899.
- FADAKA, A., AJIBOYE, B., OJO, O., ADEWALE, O., OLAYIDE, I. & EMUOWHOCHERE, R. 2017. Biology of glucose metabolism in cancer cells. *Journal of Oncological Sciences*, 3, 45-51.
- FANG, Y., TAN, J. & ZHANG, Q. 2015. Signaling pathways and mechanisms of hypoxia-induced autophagy in the animal cells. *Cell biology international*, 39, 891-898.
- FRANKE, T. 2008. PI3K/Akt: getting it right matters. *Oncogene*, 27, 6473.
- FU, Y., LIU, S., YIN, S., NIU, W., XIONG, W., TAN, M., LI, G. & ZHOU, M. 2017. The reverse Warburg effect is likely to be an Achilles' heel of cancer that can be exploited for cancer therapy. *Oncotarget*, 8, 57813.

- GIACCIA, A. J. & KASTAN, M. B. 1998. The complexity of p53 modulation: emerging patterns from divergent signals. *Genes & development*, 12, 2973-2983.
- GOLDBERG, E. B., NITOWSKY, H. M. & COLOWICK, S. P. 1965. The Role of Glycolysis in the Growth of Tumor Cells IV. THE BASIS OF GLUCOSE TOXICITY IN OXAMATE-TREATED, CULTURED CELLS. *Journal of Biological Chemistry*, 240, 2791-2796.
- GOODMAN, L. & WINTROBE, M. 1946. Nitrogen mustard therapy; use of methyl-bis (beta-chloroethyl) amine hydrochloride and tris (beta-chloroethyl) amine hydrochloride for Hodgkin's disease, lymphosarcoma, leukemia and certain allied and miscellaneous disorders. *Journal of the American Medical Association*, 132, 126.
- GRANCHI, C., ROY, S., GIACOMELLI, C., MACCHIA, M., TUCCINARDI, T., MARTINELLI, A., LANZA, M., BETTI, L., GIANNACCINI, G. & LUCACCHINI, A. 2011. Discovery of N-hydroxyindole-based inhibitors of human lactate dehydrogenase isoform A (LDH-A) as starvation agents against cancer cells. *Journal of medicinal chemistry*, 54, 1599-1612.
- GRANCHI, C., FANCELLI, D., MINUTOLO, F. J. B. & LETTERS, M. C. 2014. An update on therapeutic opportunities offered by cancer glycolytic metabolism. 24, 4915-4925.
- GRAY, L. H., CONGER, A. D., EBERT, M., HORNSEY, S. & SCOTT, O. 1953. The concentration of oxygen dissolved in tissues at the time of irradiation as a factor in radiotherapy. *The British journal of radiology*, 26, 638-648.
- GRAZIA CIPOLLESCHI, M., MARZI, I., SANTINI, R., FREDDUCCI, D., CRISTINA VINCI, M., D'AMICO, M., ROVIDA, E., STIVAROU, T., TORRE, E. & DELLO SBARBA, P. 2014. Hypoxia-resistant profile implies vulnerability of cancer stem cells to physiological agents, which suggests new therapeutic targets. *Cell cycle*, 13, 268-278.
- GUISE, C. P., MOWDAY, A. M., ASHOORZADEH, A., YUAN, R., LIN, W.-H., WU, D.-H., SMAILL, J. B., PATTERSON, A. V. & DING, K. 2014. Bioreductive prodrugs as cancer therapeutics: targeting tumor hypoxia. *Chinese journal of cancer*, 33, 80.
- HAASE, V. H. 2006. Hypoxia-inducible factors in the kidney. *American Journal of Physiology-Renal Physiology*, 291, F271-F281.
- HAKOMORI, S.-I. 1989. Aberrant glycosylation in tumors and tumor-associated carbohydrate antigens. *Advances in cancer research*. Elsevier.
- HANAHAN, D. & WEINBERG, R. A. 2000. The hallmarks of cancer. *cell*, 100, 57-70.
- HANAHAN, D. & WEINBERG, R. A. 2011. Hallmarks of cancer: the next generation. *cell*, 144, 646-674.
- HARDIE, D. G. 2012. Organismal carbohydrate and lipid homeostasis. *Cold Spring Harbor perspectives in biology*, 4, a006031.
- HARRIS, A. L. 2002. Hypoxia—a key regulatory factor in tumour growth. *Nature Reviews Cancer*, 2, 38.
- HARRISON, L. & BLACKWELL, K. 2004. Hypoxia and anemia: factors in decreased sensitivity to radiation therapy and chemotherapy? *The oncologist*, 9, 31-40.

- HELDIN, C.-H., RUBIN, K., PIETRAS, K. & ÖSTMAN, A. 2004. High interstitial fluid pressure—an obstacle in cancer therapy. *Nature Reviews Cancer*, 4, 806.
- HÖCKEL, M., SCHLENGER, K., ARAL, B., MITZE, M., SCHÄFFER, U. & VAUPEL, P. 1996. Association between tumor hypoxia and malignant progression in advanced cancer of the uterine cervix. *Cancer research*, 56, 4509-4515.
- HOLOHAN, C., VAN SCHAEYBROECK, S., LONGLEY, D. B. & JOHNSTON, P. G. 2013. Cancer drug resistance: an evolving paradigm. *Nature Reviews Cancer*, 13, 714.
- HOUSMAN, G., BYLER, S., HEERBOTH, S., LAPINSKA, K., LONGACRE, M., SNYDER, N. & SARKAR, S. 2014. Drug resistance in cancer: an overview. *Cancers*, 6, 1769-1792.
- HSIEH, A. L., WALTON, Z. E., ALTMAN, B. J., STINE, Z. E. & DANG, C. V. MYC and metabolism on the path to cancer. *Seminars in cell & developmental biology*, 2015. NIH Public Access, 11.
- HUANG, C., SEINO, J., WANG, L., HAGA, Y. & SUZUKI, T. 2015. Autophagy regulates the stability of sialin, a lysosomal sialic acid transporter. *Bioscience, biotechnology, and biochemistry*, 79, 553-557.
- HUTTUNEN, K. M., RAUNIO, H. & RAUTIO, J. 2011. Prodrugs—from serendipity to rational design. *Pharmacological reviews*, 63, 750-771.
- JAMESON, M. B., RISCHIN, D., PEGRAM, M., GUTHEIL, J., PATTERSON, A. V., DENNY, W. A. & WILSON, W. R. 2010. A phase I trial of PR-104, a nitrogen mustard prodrug activated by both hypoxia and aldo-keto reductase 1C3, in patients with solid tumors. *Cancer chemotherapy and pharmacology*, 65, 791-801.
- JELLUMA, N., YANG, X., STOKOE, D., EVAN, G. I., DANSEN, T. B. & HAAS-KOGAN, D. A. J. M. C. R. 2006. Glucose withdrawal induces oxidative stress followed by apoptosis in glioblastoma cells but not in normal human astrocytes. 4, 319-330.
- JONES, W. & BIANCHI, K. 2015. Aerobic glycolysis: beyond proliferation. *Frontiers in immunology*, 6, 227.
- KAMEL, P. I., QU, X., GEISZLER, A. M., NAGRATH, D., HARMANCEY, R., TAEGTMEYER, H. & GRANDE-ALLEN, K. J. 2014. Metabolic regulation of collagen gel contraction by porcine aortic valvular interstitial cells. *Journal of The Royal Society Interface*, 11, 20140852.
- KAMPHORST, J. J., CHUNG, M. K., FAN, J. & RABINOWITZ, J. D. 2014. Quantitative analysis of acetyl-CoA production in hypoxic cancer cells reveals substantial contribution from acetate. *Cancer & metabolism*, 2, 23.
- KAUFMANN, P., ENGELSTAD, K., WEI, Y., JHUNG, S., SANO, M., SHUNGU, D., MILLAR, W., HONG, X., GOOCH, C. & MAO, X. 2006. Dichloroacetate causes toxic neuropathy in MELAS A randomized, controlled clinical trial. *Neurology*, 66, 324-330.
- KAWAUCHI, K., ARAKI, K., TOBIUME, K. & TANAKA, N. 2008. p53 regulates glucose metabolism through an IKK-NF- κ B pathway and inhibits cell transformation. *Nature cell biology*, 10, 611.

- KIM, J.-W. & DANG, C. V. 2006. Cancer's molecular sweet tooth and the Warburg effect. *Cancer research*, 66, 8927-8930.
- KIM, J.-W., TCHERNYSHYOV, I., SEMENZA, G. L. & DANG, C. V. 2006. HIF-1-mediated expression of pyruvate dehydrogenase kinase: a metabolic switch required for cellular adaptation to hypoxia. *Cell metabolism*, 3, 177-185.
- KLAASSEN, I., VAN NOORDEN, C. J. & SCHLINGEMANN, R. O. 2013. Molecular basis of the inner blood-retinal barrier and its breakdown in diabetic macular edema and other pathological conditions. *Progress in retinal and eye research*, 34, 19-48.
- KO, C. H., SHEN, S. C., YANG, L. Y., LIN, C. W. & CHEN, Y. C. 2007. Gossypol reduction of tumor growth through ROS-dependent mitochondria pathway in human colorectal carcinoma cells. *International journal of cancer*, 121, 1670-1679.
- KO, Y. H., PEDERSEN, P. L. & GESCHWIND, J. 2001. Glucose catabolism in the rabbit VX2 tumor model for liver cancer: characterization and targeting hexokinase. *Cancer letters*, 173, 83-91.
- KOHN, A. D., SUMMERS, S. A., BIRNBAUM, M. J. & ROTH, R. A. 1996. Expression of a constitutively active Akt Ser/Thr kinase in 3T3-L1 adipocytes stimulates glucose uptake and glucose transporter 4 translocation. *Journal of Biological Chemistry*, 271, 31372-31378.
- KOIRI, R. K., TRIGUN, S. K., DUBEY, S. K., SINGH, S. & MISHRA, L. 2008. Metal Cu (II) and Zn (II) bipyridyls as inhibitors of lactate dehydrogenase. *Biometals*, 21, 117-126.
- KONOPLEVA, M., THALL, P. F., YI, C. A., BORTHAKUR, G., COVELER, A., BUESO-RAMOS, C., BENITO, J., KONOPLEV, S., GU, Y. & RAVANDI, F. 2015. Phase I/II study of the hypoxia-activated prodrug PR104 in refractory/relapsed acute myeloid leukemia and acute lymphoblastic leukemia. *Haematologica*, haematol. 2014.118455.
- KOUKOURAKIS, M., GIATROMANOLAKI, A., SIVRIDIS, E., BOUGIOUKAS, G., DIDILIS, V., GATTER, K. & HARRIS, A. 2003. Lactate dehydrogenase-5 (LDH-5) overexpression in non-small-cell lung cancer tissues is linked to tumour hypoxia, angiogenic factor production and poor prognosis. *British journal of cancer*, 89, 877.
- KROEMER, G. & POUYSSEGUR, J. 2008. Tumor cell metabolism: cancer's Achilles' heel. *Cancer cell*, 13, 472-482.
- LANE, D. 1992. Cancer. p53, guardian of the genome.
- LAUZIER, M., MICHAUD, M., DERY, M. & RICHARD, D. 2006. HIF-1 activation during tumor progression: implications and consequences. *Bulletin du cancer*, 93, 349-356.
- LE, A., COOPER, C. R., GOUW, A. M., DINAHAHI, R., MAITRA, A., DECK, L. M., ROYER, R. E., VANDER JAGT, D. L., SEMENZA, G. L. & DANG, C. V. 2010. Inhibition of lactate dehydrogenase A induces oxidative stress and inhibits tumor progression. *Proceedings of the National Academy of Sciences*, 107, 2037-2042.
- LEDOUX, S., YANG, R., FRIEDLANDER, G. & LAOUARI, D. 2003. Glucose depletion enhances P-glycoprotein expression in hepatoma cells: role of

- endoplasmic reticulum stress response. *Cancer research*, 63, 7284-7290.
- LI, P. F., DIETZ, R. & VON HARSDORF, R. 1999. p53 regulates mitochondrial membrane potential through reactive oxygen species and induces cytochrome c-independent apoptosis blocked by Bcl-2. *The EMBO journal*, 18, 6027-6036.
- LI, T., YANG, Y., CHENG, C., TIWARI, A. K., SODANI, K., ZHAO, Y., ABRAHAM, I. & CHEN, Z.-S. 2012. Design, synthesis and biological evaluation of N-arylphenyl-2, 2-dichloroacetamide analogues as anti-cancer agents. *Bioorganic & medicinal chemistry letters*, 22, 7268-7271.
- MAFTOUH, M., AVAN, A., SCIARRILLO, R., GRANCHI, C., LEON, L. G., RANI, R., FUNEL, N., SMID, K., HONEYWELL, R. & BOGGI, U. 2014. Synergistic interaction of novel lactate dehydrogenase inhibitors with gemcitabine against pancreatic cancer cells in hypoxia. *British journal of cancer*, 110, 172.
- MAHER, J. C., KRISHAN, A. & LAMPIDIS, T. J. 2004. Greater cell cycle inhibition and cytotoxicity induced by 2-deoxy-D-glucose in tumor cells treated under hypoxic vs aerobic conditions. *Cancer chemotherapy and pharmacology*, 53, 116-122.
- MAHER, J. C., WANGPAICHITR, M., SAVARAJ, N., KURTOGLU, M. & LAMPIDIS, T. J. 2007. Hypoxia-inducible factor-1 confers resistance to the glycolytic inhibitor 2-deoxy-D-glucose. *Molecular cancer therapeutics*, 6, 732-741.
- MAJMUNDAR, A. J., WONG, W. J. & SIMON, M. C. 2010. Hypoxia-inducible factors and the response to hypoxic stress. *Molecular cell*, 40, 294-309.
- MARKERT, C. L. & URSPRUNG, H. 1962. The ontogeny of isozyme patterns of lactate dehydrogenase in the mouse. *Developmental Biology*, 5, 363-381.
- MARSHALL, N., GOODWIN, C. & HOLT, S. 1995. A critical assessment of the use of microculture tetrazolium assays to measure cell growth and function. *Growth regulation*, 5, 69-84.
- MARTIN, F., LINDEN, T., KATSCHINSKI, D. M., OEHME, F., FLAMME, I., MUKHOPADHYAY, C. K., ECKHARDT, K., TRÖGER, J., BARTH, S. & CAMENISCH, G. 2005. Copper-dependent activation of hypoxia-inducible factor (HIF)-1: implications for ceruloplasmin regulation. *Blood*, 105, 4613-4619.
- MATOBA, S., KANG, J.-G., PATINO, W. D., WRAGG, A., BOEHM, M., GAVRILOVA, O., HURLEY, P. J., BUNZ, F. & HWANG, P. M. 2006. p53 regulates mitochondrial respiration. *Science*, 312, 1650-1653.
- MAXWELL, P. H., WIESENER, M. S., CHANG, G.-W., CLIFFORD, S. C., VAUX, E. C., COCKMAN, M. E., WYKOFF, C. C., PUGH, C. W., MAHER, E. R. & RATCLIFFE, P. J. J. N. 1999. The tumour suppressor protein VHL targets hypoxia-inducible factors for oxygen-dependent proteolysis. 399, 271.
- MCFATE, T., MOHYELDIN, A., LU, H., THAKAR, J., HENRIQUES, J., HALIM, N. D., WU, H., SCHELL, M. J., TSANG, T. M. & TEAHAN, O. 2008. Pyruvate dehydrogenase complex activity controls metabolic and malignant phenotype in cancer cells. *Journal of Biological Chemistry*, 283, 22700-22708.

- MCKEOWN, S. 2014. Defining normoxia, physoxia and hypoxia in tumours—implications for treatment response. *The British journal of radiology*, 87, 20130676.
- MICHELAKIS, E., WEBSTER, L. & MACKEY, J. 2008. Dichloroacetate (DCA) as a potential metabolic-targeting therapy for cancer. *British journal of cancer*, 99, 989.
- MORENO-SÁNCHEZ, R., MARÍN-HERNÁNDEZ, Á., DEL MAZO-MONSALVO, I., SAAVEDRA, E. & RODRÍGUEZ-ENRÍQUEZ, S. 2017. Assessment of the low inhibitory specificity of oxamate, aminooxyacetate and dichloroacetate on cancer energy metabolism. *Biochimica et Biophysica Acta (BBA)-General Subjects*, 1861, 3221-3236.
- NAKANO, A., TSUJI, D., MIKI, H., CUI, Q., EL SAYED, S. M., IKEGAME, A., ODA, A., AMOU, H., NAKAMURA, S. & HARADA, T. 2011. Glycolysis inhibition inactivates ABC transporters to restore drug sensitivity in malignant cells. *PLoS one*, 6, e27222.
- NORDSMARK, M., ALSNER, J., KELLER, J., NIELSEN, O. S., JENSEN, O., HORSMAN, M. & OVERGAARD, J. 2001. Hypoxia in human soft tissue sarcomas: adverse impact on survival and no association with p53 mutations. *British Journal of Cancer*, 84, 1070.
- O'CONNOR, L. J., CAZARES-KÖRNER, C., SAHA, J., EVANS, C. N., STRATFORD, M. R., HAMMOND, E. M. & CONWAY, S. J. 2015. Efficient synthesis of 2-nitroimidazole derivatives and the bioreductive clinical candidate Evofosfamide (TH-302). *Organic Chemistry Frontiers*, 2, 1026-1029.
- OBACH, M., NAVARRO-SABATÉ, À., CARO, J., KONG, X., DURAN, J., GÓMEZ, M., PERALES, J. C., VENTURA, F., ROSA, J. L. & BARTRONS, R. 2004. 6-Phosphofructo-2-kinase (pfkfb3) gene promoter contains hypoxia-inducible factor-1 binding sites necessary for transactivation in response to hypoxia. *Journal of Biological Chemistry*, 279, 53562-53570.
- OLIVEIRA-FERRER, L., LEGLER, K. & MILDE-LANGOSCH, K. Role of protein glycosylation in cancer metastasis. *Seminars in cancer biology*, 2017. Elsevier, 141-152.
- OVERGAARD, J. 2011. Hypoxic modification of radiotherapy in squamous cell carcinoma of the head and neck—a systematic review and meta-analysis. *Radiotherapy and Oncology*, 100, 22-32.
- PEDERSEN, P. L. 2007. Warburg, me and Hexokinase 2: Multiple discoveries of key molecular events underlying one of cancers' most common phenotypes, the “Warburg Effect”, ie, elevated glycolysis in the presence of oxygen. Springer.
- PEDERSEN, P. L. 2012. 3-Bromopyruvate (3BP) a fast acting, promising, powerful, specific, and effective “small molecule” anti-cancer agent taken from labside to bedside: introduction to a special issue. Springer.
- PELICANO, H., MARTIN, D., XU, R., AND & HUANG, P. 2006. Glycolysis inhibition for anticancer treatment. *Oncogene*, 25, 4633.
- PHILLIPS, R. M. 2016. Targeting the hypoxic fraction of tumours using hypoxia-activated prodrugs. *Cancer chemotherapy and pharmacology*, 77, 441-457.

- PISTOLLATO, F., ABBADI, S., RAMPAZZO, E., VIOLA, G., DELLA PUPPA, A., CAVALLINI, L., FRASSON, C., PERSANO, L., PANCHISION, D. M. & BASSO, G. J. B. P. 2010. Hypoxia and succinate antagonize 2-deoxyglucose effects on glioblastoma. *80*, 1517-1527.
- POPOV, K. M., HAWES, J. W. & HARRIS, R. A. 1997. Mitochondrial alpha-ketoacid dehydrogenase kinases: a new family of protein kinases. *Advances in second messenger and phosphoprotein research*, *31*, 105-111.
- POYYA, J., JOSHI, C. G., KUMAR, D. J. & NAGENDRA, H. 2017. Sequence Analysis and Phylogenetic Studies of Hypoxia-Inducible Factor-1 α . *Cancer informatics*, *16*, 1176935117712242.
- QUAIL, D. & JOYCE, J. 2013. Microenvironmental regulation of tumor progression and metastasis. *Nature medicine*, *19*, 1423.
- QUEIRÓS, O., PRETO, A., PACHECO, A., PINHEIRO, C., AZEVEDO-SILVA, J., MOREIRA, R., PEDRO, M., KO, Y. H., PEDERSEN, P. L. & BALTAZAR, F. 2012. Butyrate activates the monocarboxylate transporter MCT4 expression in breast cancer cells and enhances the antitumor activity of 3-bromopyruvate. *Journal of bioenergetics and biomembranes*, *44*, 141-153.
- RANKIN, E. B. & GIACCIA, A. J. 2016. Hypoxic control of metastasis. *Science*, *352*, 175-180.
- RARDIN, M. J., WILEY, S. E., NAVIAUX, R. K., MURPHY, A. N. & DIXON, J. E. 2009. Monitoring phosphorylation of the pyruvate dehydrogenase complex. *Analytical biochemistry*, *389*, 157-164.
- REITZER, L. J., WICE, B. M. & KENNEL, D. 1979. Evidence that glutamine, not sugar, is the major energy source for cultured HeLa cells. *Journal of Biological Chemistry*, *254*, 2669-2676.
- RIEMENSCHNEIDER, M. J., BETENSKY, R. A., PASEDAG, S. M. & LOUIS, D. N. 2006. AKT activation in human glioblastomas enhances proliferation via TSC2 and S6 kinase signaling. *Cancer research*, *66*, 5618-5623.
- RISCHIN, D., PETERS, L., O'SULLIVAN, B., GIRALT, J., FISHER, R., YUEN, K., TROTTI, A., BERNIER, J., BOURHIS, J. & RINGASH, J. 2010. Tirapazamine, cisplatin, and radiation versus cisplatin and radiation for advanced squamous cell carcinoma of the head and neck (TROG 02.02, HeadSTART): a phase III trial of the Trans-Tasman Radiation Oncology Group. *Journal of clinical oncology: official journal of the American Society of Clinical Oncology*, *28*, 2989.
- RISS, T. L., MORAVEC, R. A., NILES, A. L., DUELLMAN, S., BENINK, H. A., WORZELLA, T. J. & MINOR, L. 2016. Cell viability assays.
- RUBBIANI, R., KITANOVIC, I., ALBORZINIA, H., CAN, S., KITANOVIC, A., ONAMBELE, L. A., STEFANOPOULOU, M., GELDMACHER, Y., SHELDRIK, W. S. & WOLBER, G. 2010. Benzimidazol-2-ylidene gold (I) complexes are thioredoxin reductase inhibitors with multiple antitumor properties. *Journal of medicinal chemistry*, *53*, 8608-8618.
- SAELENS, X., FESTJENS, N., WALLE, L. V., VAN GURP, M., VAN LOO, G. & VANDENABEELE, P. 2004. Toxic proteins released from mitochondria in cell death. *Oncogene*, *23*, 2861.

- SANCHEZ, W., MCGEE, S., CONNOR, T., MOTTRAM, B., WILKINSON, A., WHITEHEAD, J., VUCKOVIC, S. & CATLEY, L. 2013. Dichloroacetate inhibits aerobic glycolysis in multiple myeloma cells and increases sensitivity to bortezomib. *British journal of cancer*, 108, 1624.
- SCHWARTZENBERG-BAR-YOSEPH, F., ARMONI, M. & KARNIELI, E. 2004. The tumor suppressor p53 down-regulates glucose transporters GLUT1 and GLUT4 gene expression. *Cancer research*, 64, 2627-2633.
- SEMENZA, G. L. 2011. Hypoxia-inducible factor 1: regulator of mitochondrial metabolism and mediator of ischemic preconditioning. *Biochimica et Biophysica Acta (BBA)-Molecular Cell Research*, 1813, 1263-1268.
- SEMENZA, G. L., JIANG, B.-H., LEUNG, S. W., PASSANTINO, R., CONCORDET, J.-P., MAIRE, P. & GIALONGO, A. 1996. Hypoxia response elements in the aldolase A, enolase 1, and lactate dehydrogenase A gene promoters contain essential binding sites for hypoxia-inducible factor 1. *Journal of Biological Chemistry*, 271, 32529-32537.
- SHAHRZAD, S., LACOMBE, K., ADAMCIC, U., MINHAS, K. & COOMBER, B. L. 2010. Sodium dichloroacetate (DCA) reduces apoptosis in colorectal tumor hypoxia. *Cancer Letters*, 297, 75-83.
- SHANNON, A. M., BOUCHIER-HAYES, D. J., CONDRON, C. M. & TOOMEY, D. 2003. Tumour hypoxia, chemotherapeutic resistance and hypoxia-related therapies. *Cancer treatment reviews*, 29, 297-307.
- SHARMA, V. & FREEZE, H. H. 2011. Mannose Efflux from the Cells A POTENTIAL SOURCE OF MANNOSE IN BLOOD. *Journal of Biological Chemistry*, 286, 10193-10200.
- SHARMA, V., ICHIKAWA, M. & FREEZE, H. H. 2014. Mannose metabolism: more than meets the eye. *Biochemical and biophysical research communications*, 453, 220-228.
- SHIM, H., DOLDE, C., LEWIS, B. C., WU, C.-S., DANG, G., JUNGMANN, R. A., DALLA-FAVERA, R. & DANG, C. V. 1997. c-Myc transactivation of LDH-A: implications for tumor metabolism and growth. *Proceedings of the National Academy of Sciences*, 94, 6658-6663.
- SHIMIZU, S., EGUCHI, Y., KOSAKA, H., KAMIKE, W., MATSUDA, H. & TSUJIMOTO, Y. 1995. Prevention of hypoxia-induced cell death by Bcl-2 and Bcl-xL. *Nature*, 374, 811-813.
- SHIMOBAYASHI, M. & HALL, M. N. 2014. Making new contacts: the mTOR network in metabolism and signalling crosstalk. *Nature reviews Molecular cell biology*, 15, 155.
- SHIRATO, K., NAKAJIMA, K., KOREKANE, H., TAKAMATSU, S., GAO, C., ANGATA, T., OHTSUBO, K. & TANIGUCHI, N. 2010. Hypoxic regulation of glycosylation via the N-acetylglucosamine cycle. *Journal of clinical biochemistry and nutrition*, 48, 20-25.
- SHOSHAN, M. C. 2012. 3-Bromopyruvate: targets and outcomes. *Journal of bioenergetics and biomembranes*, 44, 7-15.
- SIKIC, B. 1986. Biochemical and cellular determinants of bleomycin cytotoxicity. *Cancer surveys*, 5, 81-91.
- SIKORA, M. J., BAUER, J. A., VERHAEGEN, MONIQUE, BELBIN, T. J., PRYSTOWSKY, M. B., TAYLOR, J. C., BRENNER, J. C., WANG, S.,

- SOENGAS, M. S., BRADFORD, C. R. J. C. B. & THERAPY 2008. Anti-oxidant treatment enhances anti-tumor cytotoxicity of (-)-gossypol. *7*, 767-776.
- SIMONS, A. L., AHMAD, I. M., MATTSON, D. M., DORNFELD, K. J. & SPITZ, D. R. 2007. 2-Deoxy-D-glucose combined with cisplatin enhances cytotoxicity via metabolic oxidative stress in human head and neck cancer cells. *Cancer research*, *67*, 3364-3370.
- SINGH, D., BANERJI, A. K., DWARAKANATH, B. S., TRIPATHI, R. P., GUPTA, J. P., MATHEW, T. L., RAVINDRANATH, T. & JAIN, V. 2005. Optimizing cancer radiotherapy with 2-deoxy-D-glucose. *Strahlentherapie und Onkologie*, *181*, 507-514.
- SONG, E. & MECHREF, Y. 2015. Defining glycoprotein cancer biomarkers by MS in conjunction with glycoprotein enrichment. *Biomarkers in medicine*, *9*, 835-844.
- SONG, Y. R., YOU, S. J., LEE, Y.-M., CHIN, H. J., CHAE, D.-W., OH, Y. K., JOO, K. W., HAN, J. S. & NA, K. Y. 2009. Activation of hypoxia-inducible factor attenuates renal injury in rat remnant kidney. *Nephrology Dialysis Transplantation*, *25*, 77-85.
- SONVEAUX, P., COPETTI, T., DE SAEDELEER, C. J., VÉGRAN, F., VERRAX, J., KENNEDY, K. M., MOON, E. J., DHUP, S., DANHIER, P. & FRÉRART, F. 2012. Targeting the lactate transporter MCT1 in endothelial cells inhibits lactate-induced HIF-1 activation and tumor angiogenesis. *PloS one*, *7*, e33418.
- SONVEAUX, P., VÉGRAN, F., SCHROEDER, T., WERGIN, M. C., VERRAX, J., RABBANI, Z. N., DE SAEDELEER, C. J., KENNEDY, K. M., DIEPART, C. & JORDAN, B. F. 2008. Targeting lactate-fueled respiration selectively kills hypoxic tumor cells in mice. *The Journal of clinical investigation*, *118*, 3930.
- SOSA, V., MOLINÉ, T., SOMOZA, R., PACIUCCI, R., KONDOH, H. & LLEONART, M. E. 2013. Oxidative stress and cancer: an overview. *Ageing research reviews*, *12*, 376-390.
- SRADHANJALI, S., TRIPATHY, D., RATH, S., MITTAL, R. & REDDY, M. M. 2017. Overexpression of pyruvate dehydrogenase kinase 1 in retinoblastoma: A potential therapeutic opportunity for targeting vitreous seeds and hypoxic regions. *PloS one*, *12*, e0177744.
- STACPOOLE, P. W., HENDERSON, G. N., YAN, Z., CORNETT, R. & JAMES, M. O. 1998. Pharmacokinetics, metabolism, and toxicology of dichloroacetate. *Drug metabolism reviews*, *30*, 499-539.
- STACPOOLE, P. W., KURTZ, T. L., HAN, Z. & LANGAEE, T. 2008. Role of dichloroacetate in the treatment of genetic mitochondrial diseases. *Advanced drug delivery reviews*, *60*, 1478-1487.
- STANDER, X. X., STANDER, B. A., JOUBERT, A. M. J. C. P. & BIOCHEMISTRY 2015. Synergistic anticancer potential of dichloroacetate and estradiol analogue exerting their effect via ROS-JNK-Bcl-2-mediated signalling pathways. *35*, 1499-1526.
- SUN, R. C. & DENKO, N. C. 2014. Hypoxic regulation of glutamine metabolism through HIF1 and SIAH2 supports lipid synthesis that is necessary for

- tumor growth. *Cell metabolism*, 19, 285-292.
- SUTENDRA, G., DROMPARIS, P., KINNAIRD, A., STENSON, T., HAROMY, A., PARKER, J., MCMURTRY, M. & MICHELAKIS, E. J. O. 2013. Mitochondrial activation by inhibition of PDKII suppresses HIF1a signaling and angiogenesis in cancer. 32, 1638.
- TAKASAWA, M., MOUSTAFA, R. R. & BARON, J.-C. 2008. Applications of nitroimidazole in vivo hypoxia imaging in ischemic stroke. *Stroke*, 39, 1629-1637.
- THOMLINSON, R. & GRAY, L. 1955. The histological structure of some human lung cancers and the possible implications for radiotherapy. *British journal of cancer*, 9, 539.
- THORNBURG, J. M., NELSON, K. K., CLEM, B. F., LANE, A. N., ARUMUGAM, S., SIMMONS, A., EATON, J. W., TELANG, S. & CHESNEY, J. 2008. Targeting aspartate aminotransferase in breast cancer. *Breast Cancer Research*, 10, R84.
- VALVONA, C. J. & FILLMORE, H. L. J. B. S. 2018. Oxamate, but not selective targeting of LDH-A, inhibits medulloblastoma cell glycolysis, growth and motility. 8, 56.
- VAN CUTSEM, E., LENZ, H.-J., FURUSE, J., TABERNERO, J., HEINEMANN, V., IOKA, T., BAZIN, I., UENO, M., CSŐSZI, T. & WASAN, H. 2016. Evofosfamide (TH-302) in combination with gemcitabine in previously untreated patients with metastatic or locally advanced unresectable pancreatic ductal adenocarcinoma: Primary analysis of the randomized, double-blind phase III MAESTRO study. American Society of Clinical Oncology.
- VANDER HEIDEN, M. G., CANTLEY, L. C. & THOMPSON, C. B. 2009. Understanding the Warburg effect: the metabolic requirements of cell proliferation. *science*, 324, 1029-1033.
- VAUPEL, P. & HARRISON, L. 2004. Tumor hypoxia: causative factors, compensatory mechanisms, and cellular response. *The oncologist*, 9, 4-9.
- VAUPEL, P., KALLINOWSKI, F. & OKUNIEFF, P. 1989. Blood flow, oxygen and nutrient supply, and metabolic microenvironment of human tumors: a review. *Cancer research*, 49, 6449-6465.
- VAUPEL, P. & MAYER, A. 2007. Hypoxia in cancer: significance and impact on clinical outcome. *Cancer and Metastasis Reviews*, 26, 225-239.
- VOLATE, S. R., KAWASAKI, B. T., HURT, E. M., MILNER, J. A., KIM, Y. S., WHITE, J. & FARRAR, W. L. J. M. C. T. 2010. Gossypol induces apoptosis by activating p53 in prostate cancer cells and prostate tumor-initiating cells. 9, 461.
- WALSH, J. C., LEBEDEV, A., ATEN, E., MADSEN, K., MARCIANO, L. & KOLB, H. C. 2014. The clinical importance of assessing tumor hypoxia: relationship of tumor hypoxia to prognosis and therapeutic opportunities. *Antioxidants & redox signaling*, 21, 1516-1554.
- WISE, D. R., DEBERARDINIS, R. J., MANCUSO, A., SAYED, N., ZHANG, X.-Y.,

- PFEIFFER, H. K., NISSIM, I., DAIKHIN, E., YUDKOFF, M. & MCMAHON, S. B. 2008. Myc regulates a transcriptional program that stimulates mitochondrial glutaminolysis and leads to glutamine addiction. *Proceedings of the National Academy of Sciences*, 105, 18782-18787.
- Wise, D. R. and C. B. J. T. i. b. s. Thompson (2010). "Glutamine addiction: a new therapeutic target in cancer." 35(8): 427-433.
- WOLF, A., AGNIHOTRI, S., MICALLEF, J., MUKHERJEE, J., SABHA, N., CAIRNS, R., HAWKINS, C. & GUHA, A. 2011. Hexokinase 2 is a key mediator of aerobic glycolysis and promotes tumor growth in human glioblastoma multiforme. *Journal of Experimental Medicine*, jem. 20101470.
- XINTAROPOULOU, C., WARD, C., WISE, A., MARSTON, H., TURNBULL, A. & LANGDON, S. P. J. O. 2015. A comparative analysis of inhibitors of the glycolysis pathway in breast and ovarian cancer cell line models. 6, 25677.
- XI, H., KURTOGLU, M. & LAMPIDIS, T. J. 2014. The wonders of 2-deoxy-d-glucose. *IUBMB life*, 66, 110-121.
- XIAO, H., LI, S., ZHANG, D., LIU, T., YU, M. & WANG, F. 2013. Separate and concurrent use of 2-deoxy-D-glucose and 3-bromopyruvate in pancreatic cancer cells. *Oncology reports*, 29, 329-334.
- XU, R.-H., PELICANO, H., ZHOU, Y., CAREW, J. S., FENG, L., BHALLA, K. N., KEATING, M. J. & HUANG, P. 2005. Inhibition of glycolysis in cancer cells: a novel strategy to overcome drug resistance associated with mitochondrial respiratory defect and hypoxia. *Cancer research*, 65, 613-621.
- YEUNG, S., PAN, J. & LEE, M.-H. 2008. Roles of p53, MYC and HIF-1 in regulating glycolysis—the seventh hallmark of cancer. *Cellular and Molecular Life Sciences*, 65, 3981.
- YOSHIDA, G. J. 2015. Metabolic reprogramming: the emerging concept and associated therapeutic strategies. *Journal of experimental & clinical cancer research*, 34, 111.
- YOSHIMURA, H., DHAR, D. K., KOHNO, H., KUBOTA, H., FUJII, T., UEDA, S., KINUGASA, S., TACHIBANA, M. & NAGASUE, N. 2004. Prognostic impact of hypoxia-inducible factors 1 α and 2 α in colorectal cancer patients: correlation with tumor angiogenesis and cyclooxygenase-2 expression. *Clinical Cancer Research*, 10, 8554-8560.
- YOUNG, D. D. The Effects of 2-Deoxyglucose on the ATP Consumption in Cell Cultures. *Proceedings of the Iowa Academy of Science*, 1972. 41-43.
- ZAPATA-MORALES, J. R., GALICIA-CRUZ, O. G., FRANCO, M. & Y MORALES, F. M. 2014. Hypoxia-inducible factor-1 α (HIF-1 α) protein diminishes sodium glucose transport 1 (SGLT1) and SGLT2 protein expression in renal epithelial tubular cells (LLC-PK1) under hypoxia. *Journal of Biological Chemistry*, 289, 346-357.
- ZHANG, X. D., DESLANDES, E., VILLEDIEU, M., POULAIN, L., DUVAL, M., GAUDUCHON, P., SCHWARTZ, L. & ICARD, P. 2006. Effect of 2-deoxy-D-

- glucose on various malignant cell lines in vitro. *Anticancer research*, 26, 3561-3566.
- ZHENG, M.-F. & SHEN, S.-Y. 2013. DCA increases the antitumor effects of capecitabine in a mouse B16 melanoma allograft and a human non-small cell lung cancer A549 xenograft. *Cancer chemotherapy and pharmacology*, 72, 1031-1041.
- ZHOU, M., ZHAO, Y., DING, Y., LIU, H., LIU, Z., FODSTAD, O., RIKER, A. I., KAMARAJUGADDA, S., LU, J. & OWEN, L. B. 2010. Warburg effect in chemosensitivity: targeting lactate dehydrogenase-A re-sensitizes taxol-resistant cancer cells to taxol. *Molecular cancer*, 9, 33.